

Variability of parameters for modelling soil moisture conditions

501291



CENTRALE LANDBOUWCATALOGUS

0000 0352 3426

Promotoren: dr.ir. W.H. van der Molen
emeritus hoogleraar in de agrohydrologie
dr. J.H.J. Terwindt
hoogleraar in de fysische geografie, in het
bijzonder de fysisch-geografische proceskunde,
Rijksuniversiteit Utrecht

NN08 201,1308

J.A. van den Berg

Variability of parameters for modelling soil moisture conditions

Studies on loamy to silty soils on marly bedrock in the Ardèche drainage basin (France)

Proefschrift
ter verkrijging van de graad van
doctor in de landbouwwetenschappen
op gezag van de rector magnificus,
dr. H.C. van der Plas,
in het openbaar te verdedigen
op dinsdag 24 oktober 1989
des namiddags te vier uur in de aula
van de Landbouwniversiteit te Wageningen

BIBLIOTHEEK
LANDBOUWUNIVERSITEIT
WAGENINGEN

CIP-GEGEVENS KONINKLIJKE BIBLIOTHEEK, DEN HAAG

Berg, Jan A., Van den

Variability of parameters for modelling soil moisture conditions; studies on loamy to silty soils on marly bedrock in the Ardèche drainage basin (France) / Jan A. van den Berg.

— Proefschrift Landbouwniversiteit Wageningen. Utrecht: Geografisch Instituut, Rijksuniversiteit Utrecht — Ill. Met lit. opg. —

(Ook verschenen in Nederlandse Geografische Studies, 93, Koninklijk Nederlands Aardrijkskundig Genootschap, Amsterdam, 1989.)

Met samenvatting in het Nederlands, Engels en Frans.

ISBN 90-6266-071-1 (Thesis)

ISBN 90-6809-103-4 (NGS)

SISO eu-fran 565 UDC 631.42(448/449)

Trefw.: bodemvochthuishouding; verdamping, Ardèche.

Copyright © 1989 Geografisch Instituut, Rijksuniversiteit Utrecht, Nederland

Niets uit deze uitgave mag worden vermenigvuldigd en/of openbaar gemaakt door middel van druk, fotokopie of op welke andere wijze ook zonder voorafgaande schriftelijke toestemming van de uitgever.

All rights reserved. No part of this publication may be reproduced in any form by print or photoprint, microfilm or any other means, without written permission from the publisher.

Gedrukt in Nederland door Elinkwijk b.v., Utrecht

STELLINGEN

1. Formulae for estimating hydraulic conductivity of a soil from its textural properties are mainly based on a concept formulated by engineers for oil bearing rock layers that have a high level of entropy. However, it has to be expected that such a concept does not apply to the soil in the unsaturated zone that is far from a condition of maximum disorder and where receipt and expenditure of power and material result into "structure through fluctuations" (*Prigogine and Stengers, 1985. Order out of chaos, chapter 6*).
Dit proefschrift.

2. Milieuvoorschriften die gekoppeld zijn aan een bepaalde grondwaterstand (langjarig gemiddelde, gemiddeld hoogste, gemiddeld laagste e.d.) zijn niet eenduidig wanneer deze worden toegepast op gebieden met een door de mens ingestelde en beheerste grondwaterstand (bijv. een polder); al naar de inzichten veranderen, kan het streefpeil immers worden verlaagd of verhoogd.
Richtlijn gecontroleerd storten. Uitvoeringsvoorschrift C IV-5 afvalstoffenwet. VROM, 1985. Uitg. Kon. Vermande BV, Lelystad.

3. Bij het nemen, verpakken, transporteren en bewerken van watermonsters voor laboratoriumonderzoek wordt dikwijls onvoldoende aandacht besteed aan het voorkómen van mogelijke verandering in de gehalten van de te bepalen componenten tengevolge van andere atmosferische en fysische omstandigheden in de verpakking, in het transportmiddel en in het laboratorium dan die op de plaats waar werd bemonsterd.

4. Bij onderzoek naar verontreiniging van het grondwater moeten de analyses, indien het grondwater bodemdeeltjes en/of organisch materiaal bevat, zowel aan gefiltreerd als aan ongefiltreerd water plaats vinden. Indien het onderzoek wordt beperkt tot gefiltreerd grondwater dan kan dit een onvolledig beeld geven van de emissie van verontreinigende stoffen door een vervuiliingsbron.

D.H.V. Raadgevend Ingenieursbureau in opdracht van Ministerie van VROM, 1986. Voorlopige Praktijk Richtlijnen voor bemonstering en analyse bij bodemverontreinigingsonderzoek. S.D.U., 's Gravenhage. Overleggroep Kwaliteitsstandaard Bodemonderzoek, 1988. Aangepaste voorlopige Praktijkrichtlijnen voor bemonstering en analyse bij bodemverontreiniging. DHV Raadgevend Ingenieursbureau, Amersfoort.

5. Er dient in Nederland jaarlijks een balans te worden gemaakt van de door verontreiniging definitief verloren gegane hoeveelheid en de nog beschikbare hoeveelheid zoet grondwater naar analogie van bijvoorbeeld de balans voor verbruikte en nog winbare aardgasvoorkomens.

6. Voor de besluitvorming inzake landinrichtingsprojecten voor gebieden met bijzondere natuurwaarden waaronder eco-hydrologische aspecten, zou milieu-effect-rapportage (m.e.r.) verplicht gesteld moeten worden. Dit omdat m.e.r. de voorbereiding van de besluitvorming verlangt over een aantal uitvoeringsalternatieven die passen binnen de doelstelling van het project.

7. Bij de karakterisering van het ontwikkelingspeil van landen over langere tijd zouden de toestand van het milieu en het milieubeleid een volwaardige plaats moeten krijgen naast de gebruikelijke sociaal-economische indicatoren. Dit zou mede kunnen gebeuren door toepassing van het principe van de milieubeleidslevenscyclus van Winsemius.

World Commission on Environment and Development, 1987. Our common future. Oxford University Press.

P. Winsemius, 1986. Gast in eigen huis, beschouwingen over milieumanagement. Alphen aan de Rijn, Samson H.D. Tjeenk Willink.

8. Bij de opstelling van het Besluit milieu-effect-rapportage (m.e.r.) is er onvoldoende rekening mee gehouden dat m.e.r. voor onderdelen van ruimtelijke plannen aan deze onderdelen een onevenredig groot gewicht kan geven in vergelijking met de overige bestanddelen waarvoor geen m.e.r. behoeft te worden uitgevoerd.

Besluit van 20 mei 1987, Stb. 278, houdende de uitvoering van de Wet algemene bepalingen milieuhygiëne.

9. Het Veluwemassief bestaat uit los zand.

Jan A. van den Berg,

Variability of parameters for modelling soil moisture conditions; studies on loamy to silty soils on marly bedrock in the Ardèche drainage basin (France).

Wageningen, 24 oktober 1989.

J' ai cherché une goutte d' eau,
de miel, de sang: tout
en pierre s' est transmué,
en pierre pure:
larme ou pluie, l' eau
circule toujours dans la pierre:
sang ou miel ont pris le chemin
de l' agate.

Pablo Neruda

(L' eau en poésie. Gallimard, 1979)

Dedicated to the memory of my father

CONTENTS

Abstract	9
Preface	11
1. The Ardèche research	13
2. Towards representing soil moisture conditions of catchments	35
3. An algorithm for computing the relationship between diffusivity and soil moisture content from the hot air method	59
4. The variability of soil moisture diffusivity of loamy to silty soils on marl, determined by the hot air method	73
5. Water retention and water movement in a loess soil subject to volume change	91
6. Hydraulic conductivity under saturated and near-saturated conditions, and infiltration capacity: their variability in silt loam soils	103
7. Towards the regionalization of hydraulic and plant-soil parameters for modelling soil moisture conditions of a catchment	129
8. Samenvatting	153
Résumé	157
Appendices	
A Elektronische datenerfassung zur Modellierung des Bodenfeuchtigkeitsregimes unter Verwendung eines Netzunabhängigen Dataloggers und schnellreagierenden Tensiometers	159
B HOFAIR optimizing the D- θ relationship from hot air data	171

C	Textural analysis of samples of loamy to silty soils on marly bedrock	201
D	The impact of ponded infiltration on the instability of macropores (modelled by an electrical analogue)	203
E	The influence of gypsum on the infiltration experiments on crusted soil columns	207
	Curriculum Vitae	208

ABSTRACT

Van den Berg, J. A., 1989.

Variability of parameters for modelling soil moisture conditions (studies on loamy to silty soils on marly bedrock in the Ardèche drainage basin). Doctoral thesis.

Agricultural University Wageningen, Wageningen, The Netherlands.

Field experiments and additional measurements on undisturbed soil samples in the laboratory were done to investigate the variability of the parameters used in modelling soil moisture conditions. The conditions of soil water control the amount of moisture available for the plant cover, crop production, transport of contamination in the unsaturated zone, and are thus of interest for the study of processes of soil erosion and mass movement and for land evaluation. Attention was paid to hydraulic soil characteristics as well as to plant-soil parameters for determining actual evapotranspiration, which is an essential term of the soil moisture balance.

The research mainly concerned loamy and silty soils in the Ardèche drainage basin. Here, nine experimental sites were located where marly bedrock outcrops. As regards the hydraulic properties the textural range found in these soils was extended by including a loess soil from the Netherlands and - for the sake of contrast - two sandy loam soils in the Ardèche basin.

Soil moisture diffusivity was determined with the hot air method. First, an algorithm was developed that enabled the diffusivity to be computed unambiguously and quickly from the collected data.

Concepts about hydraulic soil properties and soil texture, usually based on experiments with artificially packed soils, are discussed. A theory is developed to explain how the change in saturated conductivity under subsequent, ponded conditions is caused by local instability of the macropore walls. This theory could be sustained by computations with an electrical analogue (RC model).

The results obtained were compared with those reported in the literature. It appeared that even for intermediate moisture contents, when most of the pores that still retain soil water are the primary ones, soil texture alone cannot explain differences in soil moisture diffusivity and that other physiographic features are also involved. For example, a micromorphological analysis of the loess soil showed the presence of many voids (vughs).

For high moisture contents and saturated conditions hydraulic properties were investigated on soil columns *in situ*. Such large samples (0.2 m diameter and 0.3 to 0.55 m long) enable the effects of macropores to be studied. The study of these effects was restricted to "closed" soils in which macropores do not reach the soil surface and therefore cannot be filled directly with water from the soil surface.

Under wet conditions the relationship between soil texture and hydraulic properties became weak, because of the involvement of the secondary pores. The impact of these pores could be demonstrated in a very pronounced way by their effect on hydraulic conductivity at the transition from nearly saturated to fully saturated conditions. The conductivity decreases with increasing soil depth. This appeared to cause the capillary pressure head in the transmission zone to become posi-

tive during ponded infiltration and the corresponding hydraulic conductivity to attain the value for saturated conditions. Consequently, the infiltration capacity under ponded conditions can reach much higher values than could be expected from the soil texture only. The results demonstrate the need for models in which the variability of the hydraulic characteristics can be reduced to basic parameters. For land evaluation it is important for such parameters to be related to physiographic properties that can be mapped easily. For a period of mainly dry weather the main terms of the reduced water balance (evapotranspiration and change in moisture storage) were determined at three sites. Application of the one-dimensional SWATRE model to these data sets shows that the simulation of such a simplified water balance provides valuable information about the extension of the soil compartments of the system to be modelled.

Additional index words: regionalization, Green & Ampt infiltration parameters, capillary pressure head of the wetting front, non-rigid soil, canopy or surface resistance to evapotranspiration, crusting of bare soil.

PREFACE

This thesis resulted from a study based on fieldwork done in the fascinating basin of the Ardèche river (southern France). Many people were involved in the realization of my ambitious programme of measurements. I would like to thank everyone who contributed.

I am most grateful to my promotors Prof. dr. ir. W.H. van der Molen and Prof. dr. J.H.J. Terwindt; they stimulated me and improved the content of this thesis by their critical comments. I highly appreciate Professor Van der Molen's continuing interest in my work after his retirement in October 1987; the station buffet of Driebergen-Zeist will always remind me of our discussions, that were so encouraging for me.

Special thanks to Teunis Louters. We started our collaboration when, during his undergraduate study, he chose to do field training in soil physics in the Ardèche, and we finished it as colleagues and authors of three chapters of this thesis. It was a pleasure to collaborate. Furthermore I am grateful to Pieter Ullersma (Dept. of Physics, Utrecht University) for his help in applying a physics solution to a soil physics problem. His ability to put himself in the coarse-material world of soils and soil water made his advice so valuable for me.

I am also indebted to Jaap Hofstee and Chris Visscher, former colleagues of the Soil Research Laboratory of the former IJsselmeerpolders Development Authority. Several times they helped me to get round the traps that the calcareous, silty soils set for a simple hydrologist.

Furthermore I thank Dr. T.A. Buishand (Royal Netherlands Meteorological Institute, De Bilt) for discussing rainfall statistics, Dr. R.A. Feddes (Institute for Land and Water Management Research, Wageningen) for his constructive remarks on Chapter 1, Bart van der Kolk for his three wonderful drawings (on the cover and two in chapter 1) and Dr. H.J. Mûcher (Laboratory of Physical Geography of the University of Amsterdam) for making and analysing thin sections of the loess soil.

I thank all my colleagues of the Department of Physical Geography (Utrecht University) for enabling me to do the research and to publish it in the Nederlandse Geografische Studies. More particularly, I wish to thank Pieter Augustinus who so kindly introduced me to the Ardèche research programme of the department, Theo van Asch and Jan Nieuwenhuis for their soil mechanics support, Jaap van Barneveld for making so much useful equipment, Peter Haringhuizen for his help with the HOTAIR computer program, Kees Klaver and Ton Warmenhoven for their support in the laboratory, Teun Lekkerkerker and Gerard van Betlehem for the photographic work, Gerrit van Omme and his staff for all the excellent drawings, Mr. A. Romein for the X-ray analyses, Celia Roovers for the lay-out and the typing of the manuscript, Henk van Steijn for his comments on the geomorphological paragraphs of chapters 1 and 4 and Theo Tiemissen for his valuable help with electronic measuring devices and data processing.

I am also grateful to all the students who participated in the field measurements and data processing: Steef de Jonge, Bert van der Ploeg, Coen Ritsema, Jan Jens, Hein Kraanen, Jan van de Meene, Harry Pronk (who computerized over ninety thousand meteorological data), Chris van de Meene, Bart Kessels, René van Dongen and Jan Gunning.

Finally, I would like to thank Lotty and Juultje for their warm support during the hard moments that can be recognized only by best friends.

1. THE ARDÈCHE RESEARCH

L'Ardèche, aussi petite qu'elle soit, est aussi grande,
à un autre point de vue, que la terre entière,
puisque elle en reproduit, ou peu s'en faut,
toutes les faces et tous les problèmes;
elle a sa proportion de terres, d'eaux ,
tout comme le globe lui-même: c'est un vrai microcosme.

Docteur Plancus
Voyage le long de la rivière d'Ardèche
1828-1908

1. THE ARDÈCHE RESEARCH

Introduction

The water in the soil is an essential aspect of many environmental issues. Conditions of soil moisture influence geomorphological processes such as soil erosion, gullying and mass movement, and also the transport of chemical constituents over and in the soil. Landuse is often constrained by the amount of soil water that is available during the growing season and, conversely, the soil moisture regime is affected by the vegetation cover. However, the need for information about soil moisture conditions has not given rise to the establishment of a global network of measuring stations as has been done in meteorology.

For many years attempts have been made to simulate the flow and regime of soil water using computational models. Measured meteorological variables are used as independent input. Each simulation model is based on the continuity equation. The transport and storage of water through and in the soil and the delivery of soil water to the vegetation or directly to the atmosphere are simulated by physical or mathematical submodels (such as Darcy's law for laminar flow through the soil matrix, expressions for the retention of water in the soil matrix with or without hysteresis and a sink term for water extraction by roots). The models can be extended with other subroutines such as a shrinkage characteristic for modelling the swelling of the solid particles of a non-rigid soil, or another sink term for flow of water through macropores (FEDDES et al. 1988).

At best, the meteorological data that are used as input represent regional variability on a mesoscale. For modelling soil moisture, the local variation in the behaviour of the water in the soil and in the related geomorphological and environmental processes can only be simulated by varying the input data and the parameters and characteristics in the submodels.

The principal aim of the research reported in this thesis was to study the regionalization of the parameters in models for simulating changes in soil moisture. In this context regionalization is defined as the process of attaching a value to a parameter at different points in space, taking into account its spatial variability. Therefore, most effort was focused on the question of which field measurements have to be done in order to achieve an adequate description of the model parameters. This part of the research was in principle restricted to soils on marly bedrock with a loam, silt loam or silty clay loam texture. Its

results are discussed in Chapters 2, 4, 6.

Chronologically, regionalization is the second of the three phases which can be distinguished in modelling soil moisture. The first step is the identification of the system or prototype. According to the glossary of terms used in modelling hydraulic phenomena (ASCE Task Committee 1982) a system or prototype is "the full-sized structure or phenomenon being modelled". The first phase was carried out in the beginning of the research and is described in Chapter 2. The third phase is the modification, calibration and verification of the model and the simulation with the model. Whereas for a specific problem the simulation of the moisture conditions is the most interesting part, the third phase is beyond the scope of this study. Yet, for two sites where the actual evapotranspiration was measured, an attempt was made to simulate the change of soil moisture and evapotranspiration during the period of the field measurements with the SWATRE model (FEDDES et al. 1978, BELMANS et al. 1983). Because SWATRE is spatially an one-dimensional model, the simulation has to be considered as a test of the simulation of the plant-soil properties of the system, rather than as a test of the simulation of the spatial variation in soil moisture regime; the results are discussed in the last section of this chapter.

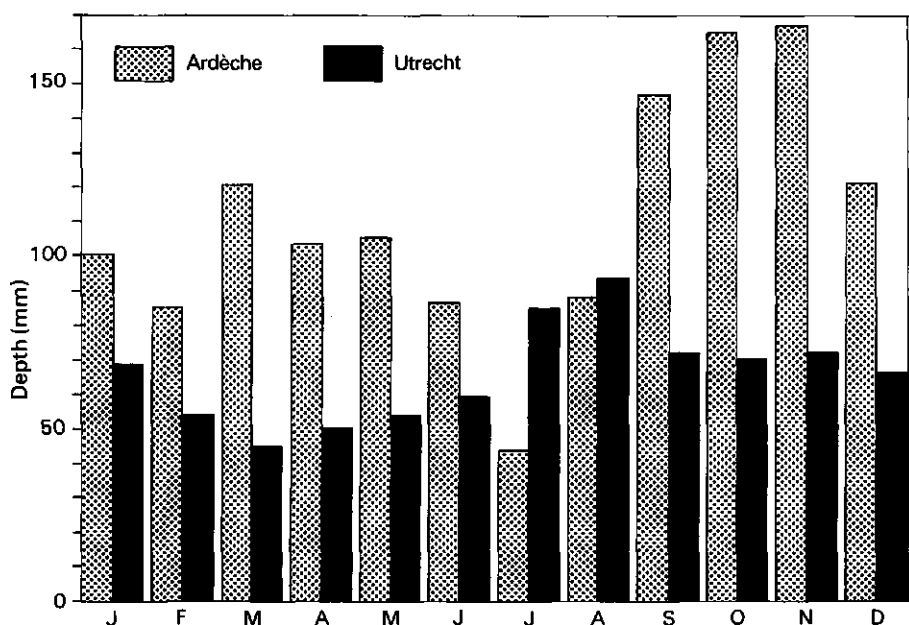


Fig. 1. Mean monthly rainfall in the Ardèche (spatial mean of five stations) and in the Netherlands (De Bilt).

Chapter 7 is a synthesis of all results obtained from the measurements and observations in the field and the data from the laboratory. The remaining Chapters (3 and 5), and the appendices, deal with supplementary parts of the research. In Chapter 3 an algorithm is introduced for objectively calculating an important soil physical parameter, soil moisture diffusivity, at intermediate moisture contents. Chapter 5 reports about the results of experiments with a swelling loess soil that was included in order to extend the range of silt loam soils found in the study areas A and B.

The mapping and field experiments were done during the period of 1980-1985 with the assistance of ten students.

Materials and physiography of the study areas

To be relevant, the research must be done in an area where at least two environmental problems related to soil moisture are topical viz. soil erosion and limited available soil moisture during the growing season. The drainage basin of the Ardèche river meets these conditions. Here erodible soils occur in combination with a submediterranean climate that can be characterized by a warm and dry summer but high rainfall and intensive rainstorms during spring and autumn (Fig. 1).

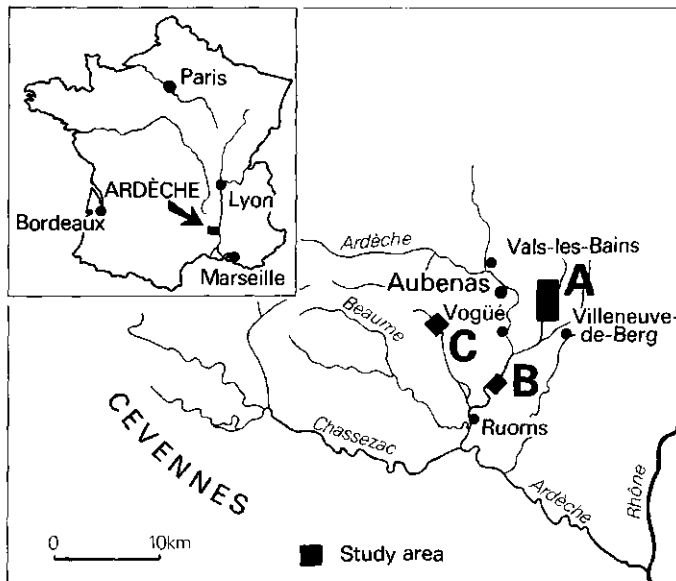


Fig. 2. Location of the study areas within the Ardèche drainage basin, southern France.

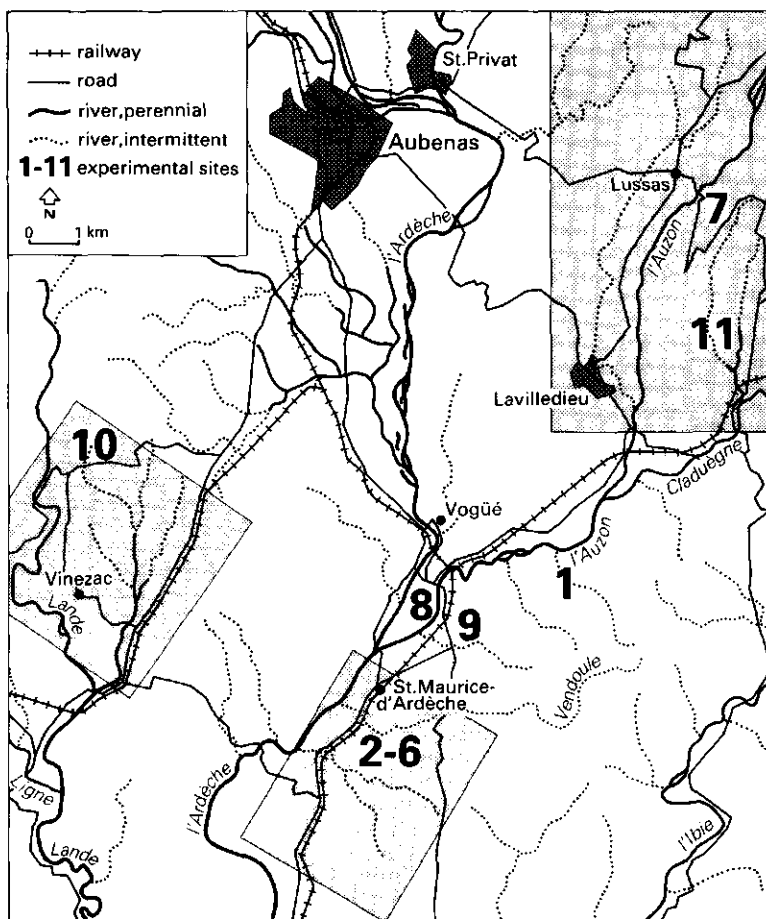
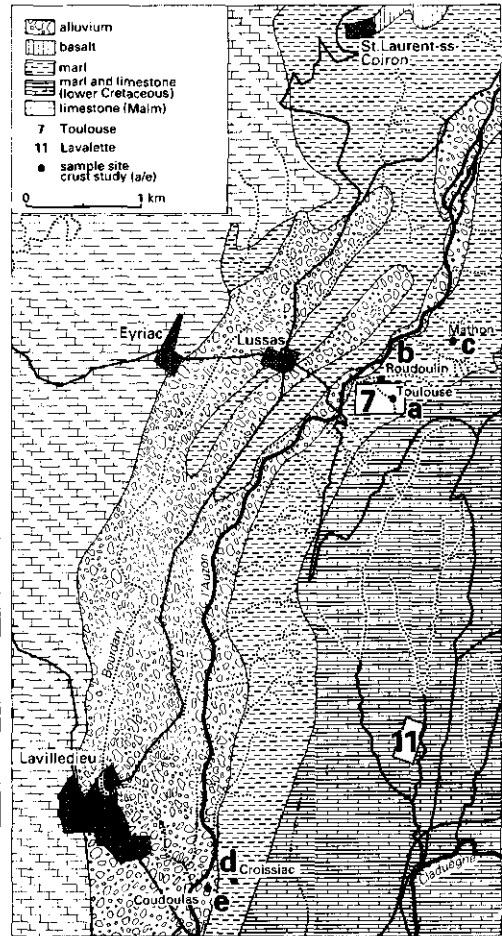
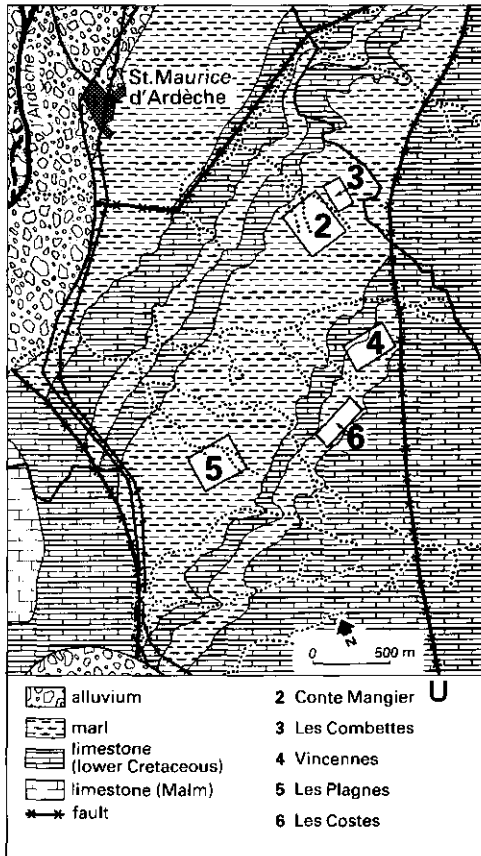


Fig. 3. a. Location of the experimental sites in the drainage basin of the Ardèche river and its tributaries Auzon and Lande.

The experimental sites (nos 1 - 11) were in three study areas (A, B and C) in the midstream part of the Ardèche basin, at an elevation between 150 and 300 m above M. S. L. (Figs 2 and 3a). Here, as a consequence of the uplift of the crystalline basement of the Cévennes mountains during the Alpine orogenesis the rock strata dip to the southeast and, therefore, the age of the outcropping strata increases from east to west.



b

c

Fig. 3. b. Lithology of study area B and location of sites 2-6.
 Fig. 3. c. Lithology of study area A and location of sites 7 and 11.

The Lower-Triassic sandstone at site 10 lies at a distance of 5 km east from where the metamorphic, crystalline rock outcrops; the marly bedrock found at sites 1-7, 9 and 11 is of Lower-Cretaceous age (Valangien). The lithology of the three study areas is shown in Figs 3b, 3c and 3d.

On the marly bedrock brown calcareous soils are found (haploxerolls to xerochrepts); their texture varies between loam, silt loam and silty clay loam. The range of these loamy to silty soils was extended with a loess soil. For the sake of contrast two sites with a sandy loam soil were added: one on an alluvial deposit of the Ardèche river (site 8, north of area B) and another on a deeply weathered sandstone (site 10 in area C).

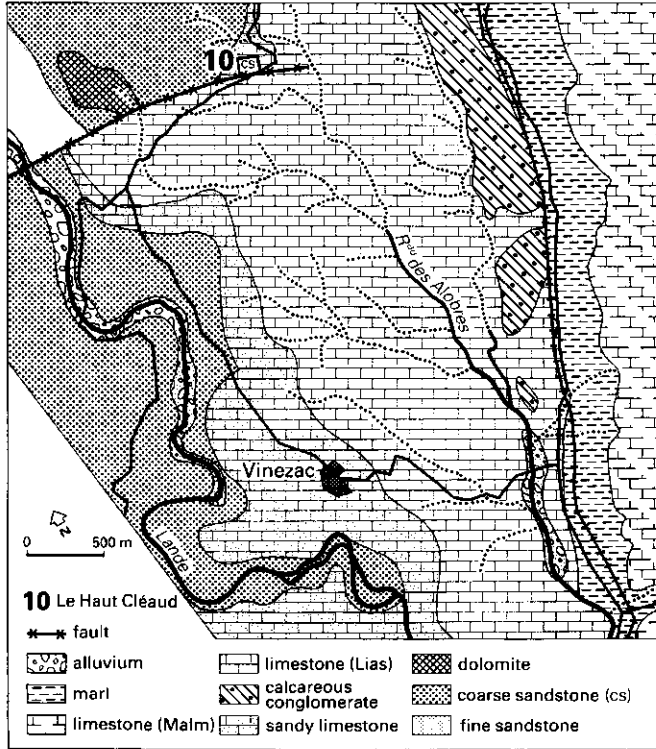


Fig. 3.d. Lithology of study area C and location of site 10.

The soils on marly bedrock largely consist of carbonates; on mass basis the carbonate content varies between 30 and 55 per cent. The carbonates have been found in considerable amounts in all size fractions and they thus form an essential part of the entire soil matrix. This makes it difficult to classify these soils by texture in accordance with the USDA classification in which carbonates are assumed to have been removed from the soil samples before the percentages of clay, silt and sand are determined. In this study, therefore, the soils on marly bedrock were classified inclusive the carbonates. This is discussed in more detail in Appendix C.

The loess soil was sampled at a depth of 3.5 m in the "Belvédère" loess pit near Maastricht in the southeast of the Netherlands (Chapter 5). The soil depth of 3.5 m was chosen because we hoped to sample the "pristine" C-horizon. The loess contains about 15% carbonates. These were removed before the texture was determined.

The man-made terraces and the pediments, in many places intersected by rills and gullies are characteristic landforms of the study areas (Fig. 4). The pediments are found in a ssw-nne orientated belt in which layers of marly and calcareous bedrock of Cretaceous age outcrop (see also Chapter 4). Strictly speaking, this landform should probably be named a glacis, because the flatter part was formed in the softer, marly rock and the steeper part in the harder rock of Cretaceous limestone (ZONNEVELD 1981) but in this study "pediment" refers to landform only, not to its genesis.

The Malm limestone west of the zone with pediments shows many karst phenomena. Along the transition of the Malm to the Cretaceous rock the Ardèche river is deeply incised in places ("Gorges de l'Ardèche"). Such environments, with fertile soils on gentle slopes and many caves near a river valley, provided an attractive habitat for hominids. Several archaeological sites have been found, proving that this area has been settled and cultivated for many millennia (BOYER 1988, BOZON 1974). From Roman times onwards, the farmers constructed terraces, an activity that culminated in the middle of the nineteenth century (BLANC 1984). Since then, many terraces have been abandoned and reverted to rangelands, especially in the area underlain by Cretaceous bedrock. During the last decade, however, the area of vineyards has been increasing again. On the Triassic sandstone most terraces are still cultivated. Most of the experimental sites are situated in extensively grazed rangelands; sites 1 and 8 are in a vineyard and site 10 is under forest. From the foregoing it is clear that the settlement and landuse in the Ardèche can be held responsible for at least some land degradation (BLAIKIE & BROOKFIELD 1987). Furthermore, one should be cautious when classifying an area into eroded or not eroded parts and, therefore, when correlating hydraulic properties of soils on the same rock formation with a single characteristic like soil texture (Chapters 4 to 7). The soil erosion on rangelands in the Ardèche basin has been described by ROELS (1984) who studied erosion processes on plots at site 11 in study area A.

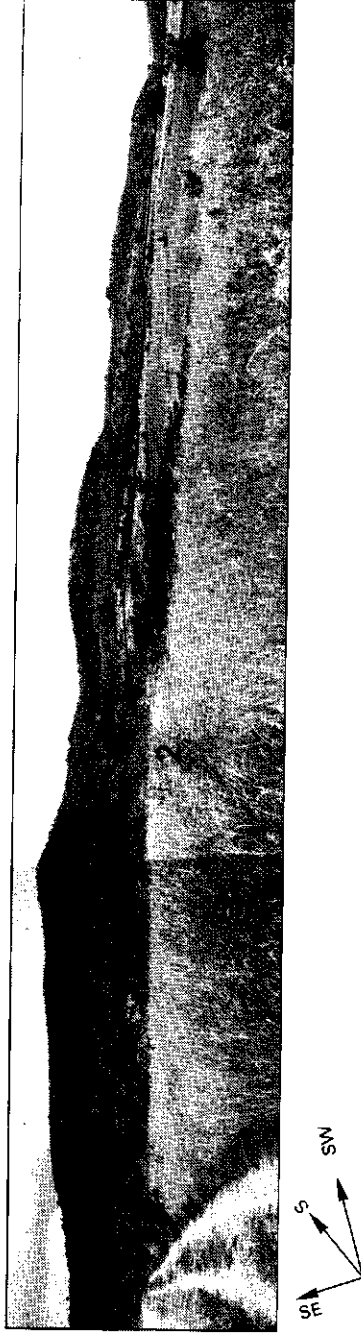


Fig. 4. The landscape at Les Costes (site 6); view to the south (Photos Harry Pronk).
1. Ridge of resistant, Cretaceous limestone;
2. The pediment has been formed in marly bedrock and is incised by n-s orientated gullies. The upslope parts of the interfluvies have a natural vegetation cover and are used as rangeland. The rest of the pediment is in agricultural use, mostly as vineyards.

Methods and equipment

To identify the system to be modelled it was attempted to measure all relevant variables of the soil moisture balance at three sites during spring or autumn. These sites were at Sauveplantade (site 9), where a preliminary investigation was done during the late summer and autumn of 1980, at Conte Mangier (site 2; spring 1983) and at Les Costes (site 6; spring 1985). Sites 6 and 9 were on a pediment. Site 2 was chosen because

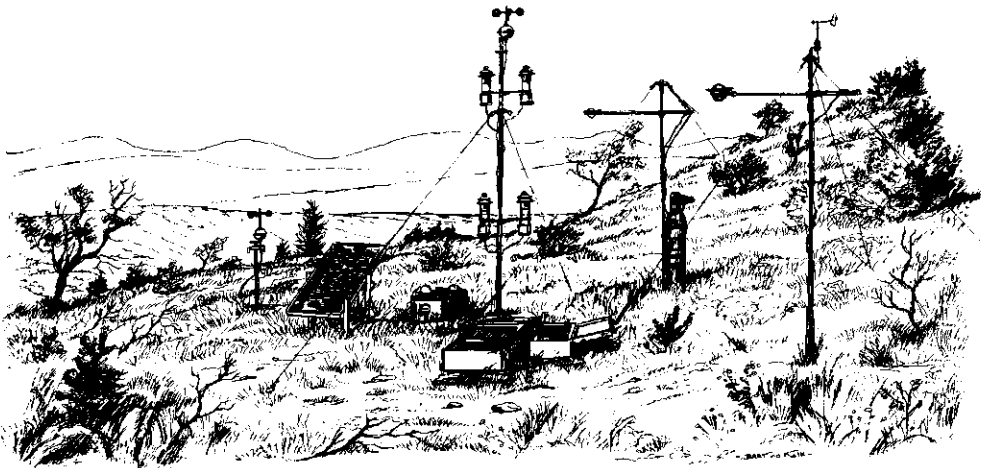


Fig. 5. Meteorological measurements for calculating the evapotranspiration; power supply by battery and solar panel.

of two reasons: here deeper soil layers could be included in the measurements and lateral flow - if any - was limited because the site was on the slope of a single hill. The rainfall, certain meteorological variables for determining actual evapotranspiration (Bowen ratio method) and potential evapotranspiration (methods of Priestly-Taylor and Penman-Monteith-Rijtema) (see Fig. 5), moisture content in the soil (gravimetrically) and

capillary pressure head in deeper layers of weathered marl (tensiometers; at key area Conte Mangier only) were measured.

The "crust method" on soil columns *in situ* was applied to determine unsaturated conductivity at small, negative pressure heads and to find - during ponded infiltration - the saturated conductivity, the hydraulic conductivity of the transmission zone and the pressure head at the wetting front in an infiltration profile (Figs 6 and 7).

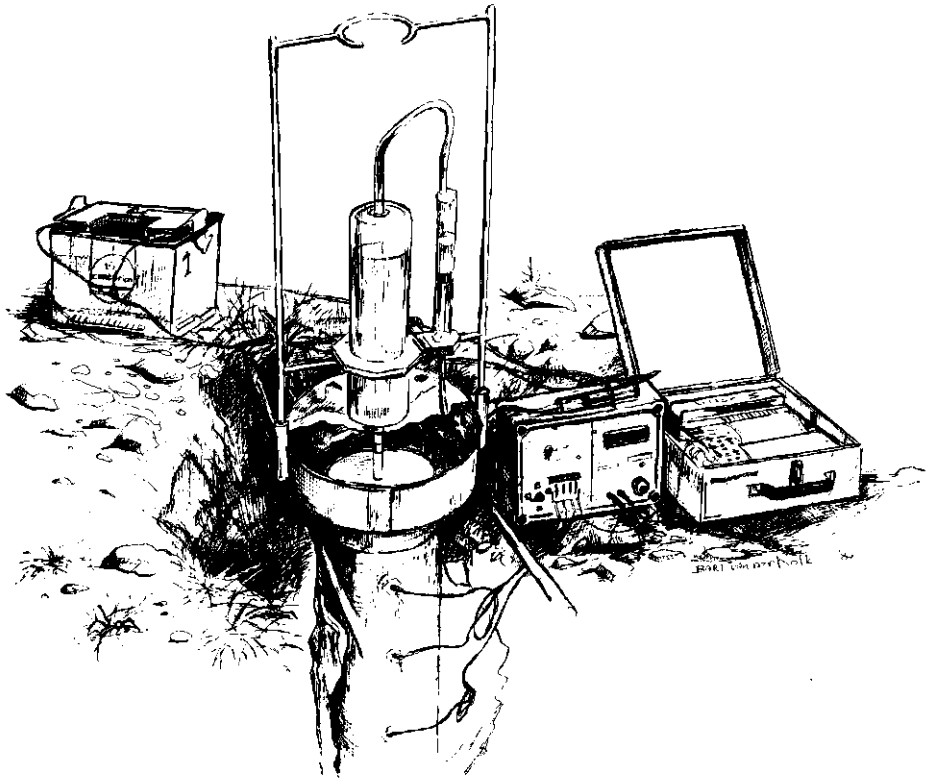


Fig. 6. Ponded infiltration experiment on a soil column *in situ* with an artificial crust.

The soil moisture diffusivity at intermediate moisture contents was obtained with the "hot air" method applied to undisturbed soil cores of 0.1 m length and 0.05 m diameter. The graphical procedure for calculating the diffusivity from the measured moisture distribution that had been generated in the sample appeared to be time-consuming and subjective. Therefore, first an algorithm was evolved, to enable the diffusivity

values to be computed reproducibly and rapidly. The algorithm is described in Chapter 3. The computation can be achieved with the "HOTAIR" computer program; Appendix B contains a flow chart, a manual and a complete listing of this programme.

At each site and at different depths soil samples were taken for determining the carbonate content and the texture and for X-ray analysis. The microscopic structures of undisturbed loess samples were inspected micro-morphologically by Dr Múcher (University of Amsterdam). The retention curves were determined on undisturbed soil samples (in fivefold on sandbox and kaolin box) and on mixed samples (membrane pressure apparatus).

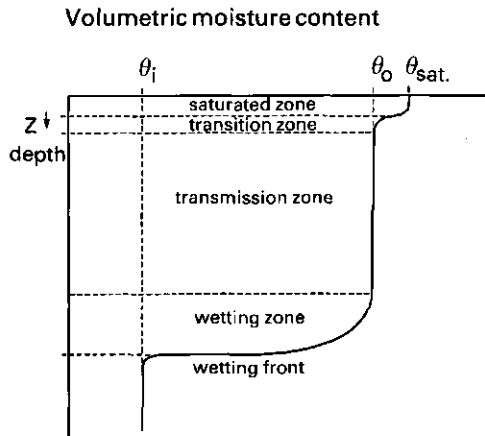


Fig. 7. The infiltration moisture profile in a uniform soil, after Bodman and Colman.

Results and conclusions

Topics A to F below have been arranged according to terms of the water budget (infiltration and soil water flow, including the algorithm for the determination of soil moisture diffusivity, and evapotranspiration) and the degree to which the voids in the soil are filled with water. Each topic starts with a short introduction in which the context is given. (The full discussion can be found in the appropriate chapters.)

- A. The impact of the change of hydraulic properties with soil depth and soil horizon on the infiltration process.

In 1944 BODMAN & COLMAN introduced an infiltration concept based on experiments with infiltration in homogeneous soils under ponded conditions. The soils used were a Yolo silt loam and a Yolo sandy loam which

belong to the same texture classes as those that were investigated in this study. A crucial difference is that Bodman and Colman examined the soils in an artificial arrangement of the soil particles after careful mixing, whereas the loess and Ardèche soils were kept in their natural packing. In an initially dry, uniform soil Bodman and Colman found the well-known infiltration profile shown in Fig. 7. An important feature is the transmission zone in which they found a constant hydraulic conductivity, k_0 , at a small, negative, capillary pressure head (h_0). For the soil matrix (i.e. the soil without macropores of secondary origin) k_0 equals the near-saturation value of the hydraulic conductivity. The Ardèche experiments showed that during ponded infiltration on soil columns *in situ* the pressure head in the transmission zone became slightly positive because the permeability of the Ardèche soils decreases with soil depth. This resulted in a transmission zone that, *de facto*, became an extended saturated zone in which k_0 equalled saturated conductivity (Chapter 6). This means that macroporosity can increase the infiltration capacity to a rate that is many times higher than could be expected on basis of soil texture only. This proved to be valid even for a "closed soil" in which macropores do not reach the soil surface (cf. Table 1 of Chapter 6).

B. Macroporosity and soil water flow

Voids, of biological origin and often of considerable width and length, form the macroporosity of the Ardèche soils; for the loamy to silty soils structural voids caused by shrinkage can also contribute. The effect of macropores on soil water flow has been extensively reported in the literature. For reviews see BEVEN & GERMANN (1982) and, especially for throughflow, GILMAN & NELSON (1980).

Most of the soils studied in the Ardèche, show a distinct discontinuity between the hydraulic conductivity at a small, negative, capillary pressure head (when macropores cannot be filled with water) and the saturated conductivity, the latter being 5 to 80 times larger. GERMANN & BEVEN (1981) found similar factors (4.3 and 18) for two large, undisturbed soil samples.

The possible effect of macroporosity on the infiltration rate under ponded conditions was described under A. During the short time between the end of ponding and the development of a negative pressure head, some of the water in the soil matrix drains to quickly emptying macropores. Where air is encapsulated in the soil matrix near a macropore, the water flow to this macropore can produce a seepage pressure that is large enough to exceed the shear strength between the soil particles and to cause local collapse of the pore wall. This process could explain why a second ponded infiltration usually showed a lower infiltration rate and a lower hydraulic conductivity even if the initial conditions were drier than those at the first ponding (Chapter 6). The conditions under which this process can occur and the procedure for calculating the local, maximum hydraulic gradient have been briefly described in Appendix D. For determining the unsaturated conductivity in a soil column *in situ* the column was capped with a crust of a mixture of gypsum and fine sand. Gypsum, dissolving from this crust may have physico-chemical influences on the soil properties. In these soils in which calcium and sulphate are prevalent ions such influence is not to be expected (Appendix E).

C. Variability of hydraulic characteristics of loamy to silty soils

The advanced facilities for a computerized simulation of the flow and storage of water in the soil with a two- or three-dimensional, numerical model has emphasized the need for local values for the hydraulic parameters at each nodal point of the grid used in the problem domain. Also, a one-dimensional simulation of the changes in the soil moisture storage with time (e.g. the SWATRE model) requires realistic values of the hydraulic parameters as a function of soil moisture content (θ) or capillary pressure head (h_p). Therefore, many researchers have attempted to correlate the retention curve ($-h_p, \theta$) and the characteristics of hydraulic conductivity ($k-\theta$ or $k-h_p$) or diffusivity ($D-\theta$ or $D-h_p$) with soil properties that are much easier to determine. In particular, they have explored the relationship with soil texture, sometimes with additional information about porosity or bulk density and indices of the pore size distribution such as "air entry value", "residual water content" and "effective" and "residual saturation" (Chapter 4).

In this study the $D-\theta$ characteristic for intermediate moisture contents was determined with the hot air method for samples from loamy to silty soils at 11 sites in the Ardèche and from the loess near Maastricht. Analysis of variance showed that samples of soils from different textural classes in the range of loam, silt loam and silty clay loam could be clustered in three groups with significantly different $D-\theta$ characteristics. These groups, however, could not be related to differences in texture (Chapters 4, 5 and 7). Apparently, not only soil texture but other physiographic features such as micro structure of the soil, petrofabric and particle orientation are also involved in the hydraulic properties of these soils. It has to be emphasized that this result was found for intermediate values of θ , when the water is retained in soil pores of intermediate dimensions and where a correlation with soil texture would be most likely.

For wet conditions, when the water in the larger pores comes into play, the impact of soil texture on hydraulic properties becomes minimal because many of the pores now involved, are of secondary origin. This conclusion for loamy to silty soils agrees with the findings of Viville (VIVILLE 1985, VIVILLE et al. 1986) for sandy soils on granite (Vosges) that the areal and vertical differentiation of the saturated conductivity is very weak because of the strong, local variation of this parameter. Furthermore, Viville concluded that neither saturated conductivity nor the retention curve could be correlated with particle size distribution. It would be worth applying the concept of fractals (MANDELROT 1983) and the ideas of PRIGOGINE & STENGERS (1985) about structure arising from disorder to these problems. Future research should investigate if the occurrence and dimensions of large pores and especially of macropores, can be based on stochastic probability functions and whether these functions can be related to factors like landuse, vegetation, clay fabric, antecedent moisture conditions, etc. (Chapter 7).

D. The HOTAIR algorithm for computing $D-\theta$ from hot air data

The procedure of the hot air method is fully described in Chapter 3. The essential part is that rapid drying of the soil sample generates a typical moisture distribution which is established by quickly cutting the

sample into thin slices. For each slice the moisture content (θ) and the distance (x) between its centre and the evaporating surface is determined. All pairs of (x, θ) data together produce a discrete representation of the moisture distribution $\theta(x)$. For computing the diffusivity $D(\theta)$, the derivative and the integral of $\theta(x)$ have to be determined for different x . Therefore, a curve has to be fitted through the measured pairs of (x, θ).

The usual method consists of drawing a monotonically rising curve through the plotted (x, θ) points, followed by graphical differentiation and integration. This procedure is laborious and its results are subjective and not very reproducible (Chapter 3).

With the HOTAIR algorithm an algebraic expression for $\theta(x)$ is fitted through the (x, θ) data. In fact, this expression has four degrees of freedom; two of them are determined by the two boundary conditions that are inherent in the hot air method (Chapter 3). The two remaining parameters, n and b , are obtained by an optimization procedure from NAGFLIB (1983). In this way, θ can be expressed as a differentiable function of the distance x , from which pairs of (D, θ) can be computed for all $\theta < \theta_1$.

The variance resulting from both the hot air method and the algorithm appeared to be less than 25% of the mean diffusivity (cf. Chapter 4). If a set of (x, θ) data contains one or more deviating values the $\theta(x)$ curve can easily be adapted so that most weight is given to the most reliable data.

One of the boundary conditions is that the moisture content at the bottom of the sample must remain unaffected during the evaporation induced by blowing hot air over the top of the sample. In the algorithm the consequence of this boundary condition is that $\theta(x)$ tends asymptotically to θ_1 . The real moisture content in the bottom part of the sample probably varies in a similar way. Anyway, a small difference of the tangent in this part of the $\theta(x)$ curve results in a large change of the derivative of x with respect to θ . Hence, if θ has been taken close to θ_1 in some cases there is a risk that an unrealistic value is calculated for the corresponding diffusivity.

Though the derivative of $x(\theta)$ can be expressed as an analytical function of x and the parameters θ_1 , θ_0 , n and b , a pure mathematical analysis by varying n and b independently from each other does not seem worthwhile, because practice has shown only a restricted number of combinations of n and b . It appears that an overestimation of $D(\theta)$ is prevented by taking $(\theta_1 - \theta) \geq 0.02$. Moreover, the range of moisture contents allowed is restricted by the value of θ that is obtained by substituting the length of the soil core for x in the equation of $\theta(x)$.

E. Soil moisture balance

Periods in which evapotranspiration and decreasing storage of soil moisture are the only substantial terms of the soil moisture balance, are suitable for finding the depth to which plant roots may extract soil moisture. This depth is needed so that the active strata of the system and the lower boundary of the model can be formulated. In the Ardèche research, the soil moisture content and the meteorological variables for calculating the actual evapotranspiration were mostly measured during such periods, i. e. late summer and early autumn 1980 at site 9, spring

1983 at site 2 and spring 1985 at site 6.

The measurements done in 1980 were part of a preliminary study. They showed that 50% or less of the evapotranspiration could be supplied from the upper 0.2 m of the soil; apparently, the rest came from the subsoil that consists of alternating strata of weathered marl and limestone (VAN DEN BERG 1983). At this site (no 9) two profile pits 0.5 and 0.7 m deep respectively, were dug. They showed that the roots of herbs form a dense system in the upper soil layer (between 0 and 0.2 to 0.3 m) and that the subsoil is rooted to the depth of the first stony layer. The main roots of shrubs often penetrate such a layer via joints and spread out in a deeper stratum of weathered marl (cf. Fig. 3a of Chapter 2). From the gravimetrically determined moisture content in combination with the retention curve data it was found that the submediterranean vegetation could dry the upper soil up to pF 5.

In 1983 a comparable study was done at site 2, but here measurements of the pressure head of the moisture in the subsoil were added. In an exposed face on a gully side and in a borehole several metres upslope, tensiometers were placed in three strata of weathered marl that were intercalated in limestone layers. From the initial, nearly saturated conditions, the pressure head became increasingly more negative, especially when the potential evapotranspiration increased under the influence of the mistral wind. The measurements also show that the desiccation took place from the top downwards (cf. Fig. 6 of Chapter 2). Apparently, the moisture in these marly layers was closely related to the moisture status of the plant canopy. The pressure head showed a daily variation that could be correlated with the diurnal change of atmospheric water demand: in the afternoon the pressure head was usually more negative than early in the morning (cf. Fig. 7 of Appendix A). The actual evapotranspiration could be calculated for a few days only, because of a malfunction of the datalogger, and therefore, a soil moisture balance over a longer term could not be made. Nevertheless, the other measurements are still useful for testing the SWATRE model under the prevailing conditions of soil and bedrock.

The third series of measurements on the soil moisture balance was done at site 6, which is located on a pediment. Soil moisture content was determined gravimetrically in the first 0.4 m of the soil. These data were also applied to test the SWATRE model (cf. part F of results and conclusions in this chapter).

For all days for which the available data allowed the actual as well the potential evapotranspiration to be calculated, the internal resistance of the plant canopy (r_c) from the Penman-Monteith-Rijtema equation was computed (Chapter 7). Under conditions of potential evapotranspiration the r_c of the natural Ardèche vegetation is about 60 s.m^{-1} which is the same as for grassland in the Netherlands (DE BRUIN 1982). When during spring the available moisture content in the soil-rock layers becomes too low for potential evapotranspiration, r_c increased gradually to 150 s.m^{-1} . The r_c values that were calculated for late summer and early autumn at site 9 were within the range of r_c values measured in spring.

In 1981 it was tried to examine the variability of the actual evapotranspiration within and between two areas of about 5 hectares, one at site 2 and the other at site 11. It was intended to determine the potential evapotranspiration from measurements at one permanent station at each site, and the actual evapotranspiration during 3 to 4 days at 7 plots in succession (4 in site 11 and 3 in site 2) under stable weather conditions. Then the ratios between actual and potential evapotranspiration were to be analysed in combination with the variation in local soil moisture content.

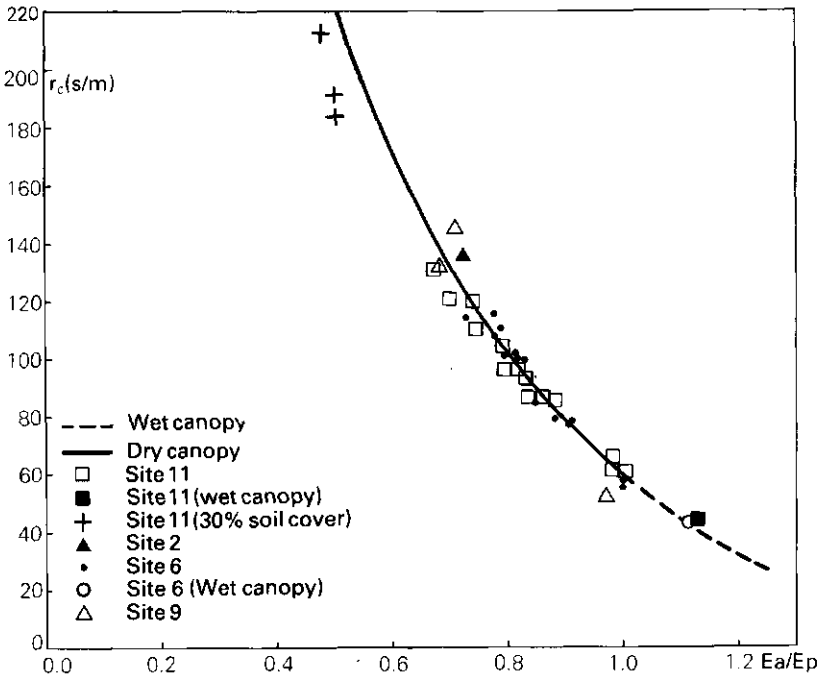


Fig. 8. Measured values of the canopy or surface resistance r_c as a function of the ratio between actual and potential evapotranspiration.

During the experiments, the constant weather type of the mistral continued for one week only. From then on the Ardèche spring of 1981 was characterized by variable weather (very variable net daily radiation; wind from variable directions resulting in problems with fetch) which prevented us from obtaining suitable data. However, the data could be used to calculate r_c values for seven more plots, two of which had an agricultural canopy (cereals and hay land, both as part of crop rotation on vineyards); the results are shown in Fig. 8.

F. Simulation tests with the SWATRE model

The periods that have been described as suitable for calculating the simplified soil moisture budget were also appropriate for testing a one-dimensional (z,t) model such as the SWATRE model.

For site 2 (Conte Mangier) five soil layers were defined in the SWATRE model (cf Fig. 9).

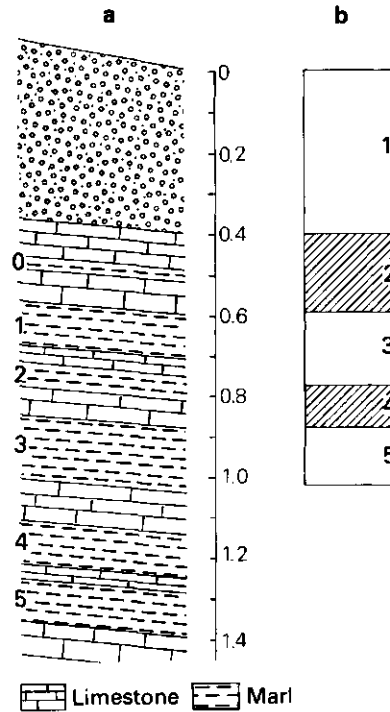


Fig. 9. Schematic representation of the soil profile of site 2.

No. 1 is the soil up to the first limestone layer (at 0.4 m), no. 3 represents marl layers 1 plus 2 (0.60-0.80 m; the intervening fine limestone layer of 0.04 m was ignored) and no. 5 is marl layer 3

(0.87-1.10 m); nos 2 and 4 are intercalated limestone layers. In Fig. 10 the simulated and measured moisture contents are shown for three weeks. For this period SWATRE computed an actual evapotranspiration $E_a = 72$ mm and a ratio of 0.74 between actual and potential evapotranspiration. It can be concluded that the SWATRE model can be calibrated reasonably well for the local conditions and for a period of decreasing moisture content. The model could only reproduce the soil moisture distribution closely if the two intercalated limestone layers were represented as strata with a very low hydraulic conductivity (between 10^{-9} and 10^{-10} m.day $^{-1}$, near saturation) and a small storage capacity (cf. assumed moisture retention curve of inset in Fig. 10).

Under wet conditions, when percolation of soil moisture is important, such a representation of a limestone layer will be insufficient because the limestone is intensively jointed. These joints can produce a high saturated permeability. In the model such a duality can probably be realized by assigning a conditional hydraulic conductivity to the limestone. When the overlying soil layer is saturated then the conductivity of the limestone should be high, but under all other moisture conditions it should be as low as was assumed in this simulation.

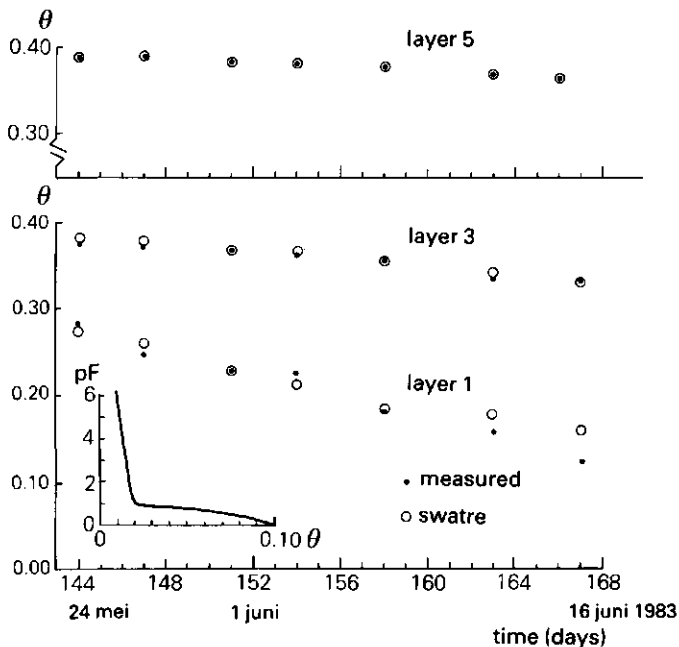


Fig. 10. Measured and computed soil moisture content in three soil layers at site 2 as a function of time. Inset: hypothetical moisture retention curve of a limestone layer (as used for the simulation at site 2).

It also appeared that the capacity of roots for water uptake has to be assumed to decrease with soil depth. If it is assumed to be constant with soil depth, then the upper layer dries too slowly and, consequently, the lower layers too quickly.

The soil at site 6 (Les Costes) was simulated by a two-layer system. The upper soil (0-0.25 m) is intensively rooted. The subsoil contains few roots; its hydraulic properties were assumed to be equal to those of the marly layers of site 2.

A remarkable result of the simulation is that according to the SWATRE model the subsoil should dry faster than it really did. There was probably still an unsaturated, lateral flow of soil moisture from the calcareous mountain ridge to the pediment plain. The one-dimensional SWATRE model could closely simulate the moisture content in the subsoil by assuming a positive seepage of 2 mm day^{-1} at the lower boundary, though such an assumption is not realistic. In both cases the application of the SWATRE model was useful. For site 2 it made clear how deeper rock layers were involved in the moisture supply of the vegetation; for site 6 it indicated that a term of the water balance was missing.

REFERENCES

- ASCE Task Committee on Glossary of hydraulic modelling terms modelling hydraulic phenomena (1982), A glossary of terms. J. Hydraulic Div. 108 (7), pp. 845-852.
- BELMANS, C., WESSELLING, J.G & FEDES, R.A. (1983), Simulation model of the water balance of a cropped soil: SWATRE. J. Hydrol. 63, pp. 271-286.
- BEVEN, K.J. & GERMANN, P. (1982), Macropores and water flow in soils. Water Resour. Res., 18 (2), pp. 1311-1325.
- BLAIKIE, P. & BROOKFIELD, H. (1987), Land degradation and society. Methuen, London.
- BLANC, J.-P. (1984), Paysages et paysans des terrasses de l'Ardèche. L'Imp. du Vivarais, Annonay.
- BODMAN, G.B. & COLMAN, E.A. (1944), Moisture and energy conditions during downward entry of water into soils. Soil Sci. Soc. Am. Proc. 8, pp. 116-122.
- BOYER, M. (1988), Les premiers hommes. In Choloy, G. (Ed.), Histoire du Vivarais. Editions Privat, Toulouse.
- BOZON, P. (1974), Histoire du peuple Vivarais. Imp. Réunies, Valence.
- DE BRUIN, H.A.R. (1982), The energy balance of the earth's surface: a practical approach. Thesis. Scientific Report 82-1, K.N.M.I., De Bilt, NL.
- FEDES, R.A., KOWALIK, P.J. & ZARADNY, H. (1978), Simulation of field water use and crop yield. Pudoc, Wageningen, NL.
- FEDES, R.A., KABAT, P., VAN BAKEL, P.J.T., BRONSWIJK, J.J.B. & HALBERTSMA, J. (1988), Modelling soil dynamics in the unsaturated zone - state of the art. J. Hydrol., 100, pp. 69-111.
- GILMAN, K. & NEWSON, M.D. (1980), Soil pipes and pipeflow - a hydrological study in upland Wales. Geo Books (Geo Abstracts), Norwich.
- GERMANN, P. & BEVEN, K. (1981), Water flow in soil macropores. I. An experimental approach. J. Soil Sci., 32, pp. 1-39.
- MANDELBROT, B.B. (1983), The fractal geometry of nature. W.H. Freeman, New York.
- NAGFLIB (Numerical Algorithms Group) (1983), Fortran Library Manual Mark 11, Vol. 3, E04, JAF. Mayfield House, Oxford.
- PRIGOGINE, I. & STENGERS, I. (1985), Order out of chaos. Fontana Paperbacks, London.
- ROELS, J.M. (1984), Studies of soil erosion on rangelands in the Ardèche drainage basin (France). Thesis. Utrecht University, NL.
- VAN DEN BERG, J.A. (1983), Les aspects hydrogéologiques de l'érosion dans la région limonueuse autour de Villeneuve de Berg. Revue de la Société des Enfants et Amis de Villeneuve de Berg, 38, pp. 11-19.
- VIVILLE, D. (1985), Variabilité spatiale des propriétés physiques et hydriques des sols dans le bassin versant du Ringelbach (Vosges granitiques). Thèse. L'Université Louis Pasteur, Strasbourg.
- VIVILLE, D., AMBROISE, B. & KOROSSEC, B. (1986), Variabilité spatiale des propriétés texturales et hydrodynamiques de sols dans le bassin versant de Ringelbach (Vosges, France). Z. Geomorph. N.F. Suppl. Bd 60, pp. 21-40.
- ZONNEVELD, J.I.S. (1981), Vormen in het landschap (Dutch). Aula, Utrecht, NL.

2. TOWARDS REPRESENTING SOIL MOISTURE CONDITIONS OF CATCHMENTS

Published in: Beiträge zur Hydrologie, Sonderheft 5.2 (1985)
749-774.
Permission for reproduction, 17 July 1989.

2. TOWARDS REPRESENTING SOIL MOISTURE CONDITIONS OF CATCHMENTS

Jan A. van den Berg and Teunis Louters

Abstract

To be successful, a model of soil moisture must have a reliable structure and valid soil parameters. Four erodible catchments in the Ardèche basin were investigated, to ascertain how the information required for such models can be obtained.

For the compilation of the model structure, the water budget of the soil and of the upper layers of bedrock (alternating layers of marl and limestone) was measured. Changes in the moisture content of the marl layers were ascertained by measuring the soil moisture tension daily. Meteorological data were also collected so that potential and actual evapotranspiration could be calculated according to the methods of PRIESTLEY & TAYLOR and of BOWEN. Data on soil parameters were obtained from soil columns *in situ*, and supplemented by measurements on undisturbed soil samples.

Where the soil is thin, the upper, weathered, marly layers appear to be important to the soil moisture regime. Consequently, the root-soil-rock system should be modelled as if it were a multi-layered soil. The hydraulic properties of the soil determined from small undisturbed samples were very variable. Therefore, measurements from soil columns seem to be preferable, as they deliver averaged values of nearly all fundamental hydraulic properties of the soil, including parameters for an infiltration equation that takes account of initial soil moisture conditions.

Zusammenfassung

Ein Beitrag zur Ermittlung der Bodenfeuchte

Ein einsatzfähiges Bodenwassermodell erfordert einen zuverlässigen Modellaufbau und geeignete Bodenkennwerte. In vier Untersuchungsgebieten im Einzugsgebiet der Ardèche wurde überprüft, wie die notwendigen Informationen gewonnen werden können.

Als Modellparameter wurden der Wasserhaushalt des Bodens und der obersten Gesteinsschichten, die aus einer Wechsellage von Mergel und Kalk bestehen, gemessen. Die Feuchteänderungen der Mergelschichten wurden als tägliche Wasserspannungen erfaßt. Meteorologische Werte wurden erhoben, um die potentielle und tatsächliche Verdunstung nach PRIESTLEY & TAYLOR und BOWEN zu berechnen. Die Bodenkennwerte wurden *in situ* und aus ungestörten Bodenproben ermittelt. Wenn die Bodenschicht wenig mächtig ist, kommt der obersten, verwitterten Mergelschicht eine große Bedeutung für den Bodenwasserhaushalt zu. Diese Wurzelzone muß daher im Modell wie ein mehrschichtiges Bodenkompartiment behandelt werden. Da die hydraulischen Eigenschaften, die aus Bodenproben ermittelt werden, unterschiedliche Werte annehmen, war es sinnvoller, die aus den Bodensäulen gewonnenen Werte zu verwenden. Dadurch konnten die mittleren hydraulischen Eigenschaften des Bodens besser erfaßt werden. Dies traf

besonders für die Parameter der Infiltrationsgleichung zu, die die anfänglichen Bodenfeuchteverhältnisse berücksichtigen.

Résumé

Essai de représentation de l'humidité du sol dans les bassins versants

Si on veut étudier efficacement les variations de l'humidité dans le sol avec un modèle informatique, il convient d'introduire dans ce modèle des paramètres valables et une représentation fidèle de la structure du sol étudié. L'étude de quatre sous-bassins du bassin versant de l'Arèche présentant un risque d'érosion a permis de déterminer comment les éléments nécessaires à l'établissement d'un tel modèle peuvent être obtenus.

Pour cela, on a mesuré chaque jour la rétention et ses variations dans le sol et les couches supérieures de la roche-mère, formée d'alternances de calcaires et de marnes. Les données météorologiques ont permis à l'aide des méthodes de PRIESTLEY & TAYLOR et de BOWEN de calculer les évapotranspirations potentielle et réelle. Les paramètres du sol furent déterminées par l'observation de colonnes de sol, *in situ*, complétée par des mesures effectuées en laboratoire sur des carottes de sol intactes.

Là où le sol est peu épais, le rôle des couches supérieures de marnes déjà altérées apparaît comme jouant un rôle essentiel dans le régime hydrique du sol. Par conséquent, le système racines-sol-roche devrait être considéré comme un sol à strates multiples. Les propriétés hydrauliques du sol, déterminées à partir de petits échantillons de sols intacts, se sont révélées très variables et ont donné des résultats trop peu fiables. De ce fait, les mesures à partir de colonnes de sol faites *in situ* apparaissent préférables parce qu'elles fournissent les valeurs moyennes de la quasi totalité des propriétés hydrauliques du sol, y compris les paramètres de la formule d'infiltration tenant compte des conditions initiales d'humidité.

(Revue de Géomorphologie Dynamique, XXXVI (2), pp. 56-57, 1987).

2.1 Introduction

Modelling of soil moisture can be a valuable tool for prediction in land evaluation studies or when mapping the risk of soil erosion. Although several models and modelling techniques of differing sophistication are available, the utility of the output depends strongly upon the validity of the model structure and of the physical parameters of the soil.

Both the complexity of the model structure and the variability of the physical parameters of the soil can be limiting factors, as they depend upon the physiography of the catchment. Therefore, we investigated the problems involved in formulating such a model for simulating the soil moisture regime for the purpose of practical goals. The research was done in a hilly region, where generally a thin soil is found on sedimentary bedrock of alternating layers with differing hydraulic properties.

The research can be subdivided into three phases:

- identification of the system that has to be modelled;
- determination of the main physical parameters of the soil, e. g. the saturated and unsaturated hydraulic conductivity, soil moisture diffusivity and infiltration capacity;
- adaptation of the model and simulation.

The paper is concerned with the first two phases. The identification of the system to be modelled was based on in situ measurements of the terms of the soil moisture budget. During a dry spell, terms other than evaporation and changes in storage of soil moisture become negligible. Thus the required measurements can be restricted to evapotranspiration and soil moisture content. From previous studies it is known that the spatial variability of physical parameters of the soil is generally large (NIELSEN et al. 1973, 1980 and 1983).

This variability is probably enhanced when the parameters are ascertained from undisturbed but small soil samples. Moreover, the presence of chains of large pores such as burrows, cracks or other cavities (e. g. from decayed plant roots) may considerably change the value of physical parameters of the soil, making the data from small soil samples unreliable.

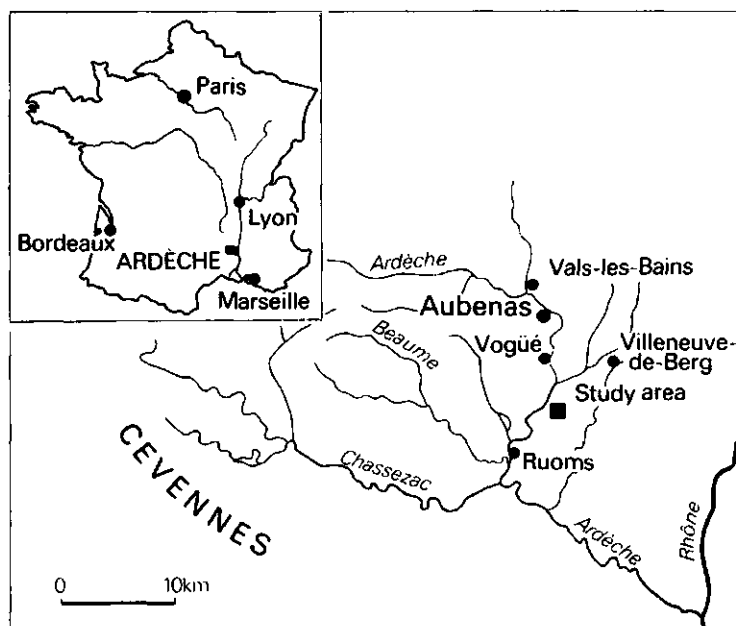


Fig. 2.1 Location of the study area within the Ardèche basin, southern France.

Therefore in this study, we relied mostly on results obtained from columns of soil *in situ* (BOUMA et al. 1971, 1981). These columns have much greater dimensions than ordinary soil samples and this should mean that the values of the parameters obtained in this way more closely approach the average. Moreover, in such columns the influence of macropores can be studied separately.

2.2 Physiography of the catchments

The research was carried out in some small, low-ordered subcatchments within the Ardèche basin (Fig. 2.1). Here the bedrock is banded and consists of alternating layers of Cretaceous marl and limestone, dipping slightly to the south-east. The thickness of the layers ranges from several centimetres to some decimetres, and the rock composition varies between predominantly marl and a sequence of thick layers of limestone, intercalated with bands of marl. Along hill slopes, where the marl predominates, pediments that are at least Pleistocene in age are found (ARCHAMBAULT 1966, TRICART & USSELMANN 1968).

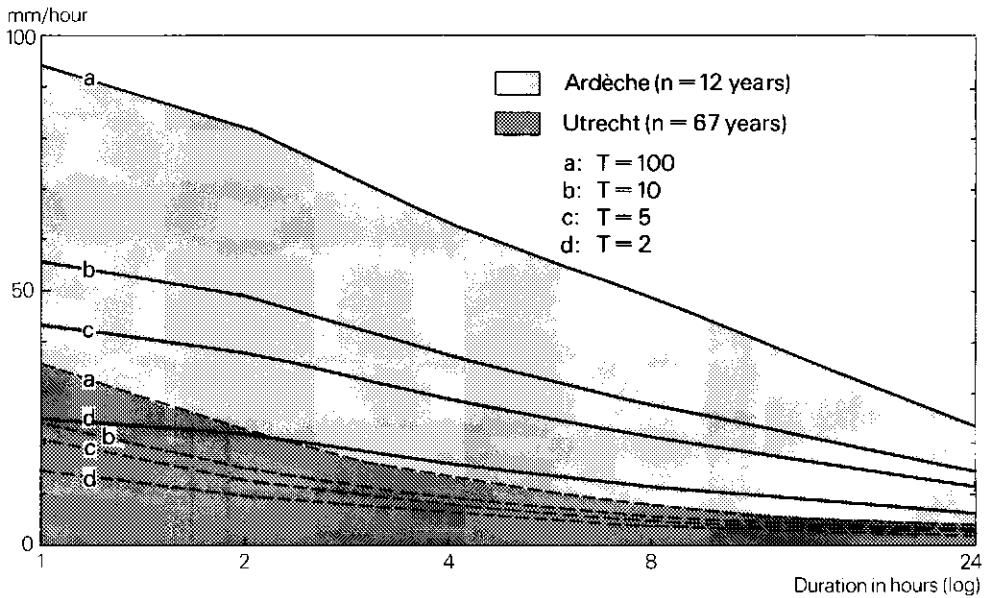


Fig. 2.2 Frequency of rainfall rates at different return periods T for the Ardèche basin as compared with figures for The Netherlands.

The Ardèche basin has a submediterranean climate; its precipitation regime differs from the moderate, maritime climate of Western Europe, having a much higher frequency of high rainfall rates (Fig. 2.2), especially during autumn and spring. The mean annual rainfall amounts to about 1200 mm, but the summer is warm and dry, resulting in sequences of a daily potential evapotranspiration of 6 mm/day or more (section 2.7.2).

The natural vegetation is *Quercus pubescens*, which has to be considered as the vegetational climax under the submediterranean climate. Man has revealed his presence by clear-cutting to promote grazing and agriculture. The deforestation reached its maximum (85 per cent) during the first part of the nineteenth century. The simultaneous occurrence of a number of disasters in agriculture in mid-nineteenth century triggered off a rapid rural depopulation, resulting in the abandonment of fields, many of which were terraced and had been intensively cultivated: from thenceforth these were only used extensively as rangelands.

Given the rainfall regime and lithology, agriculture gave rise to features of intensive soil erosion such as rills and gullies, the presence of thin soils of the rendoll type and small-scale mass movements, including shallow soil slips of the topmost, vegetated horizon. Most soils have a A-C profile in which the A horizon usually consists of a silty loam with stones. Extended systems of deep gullies were formed where the geomorphological and lithological conditions were favourable i. e. in pediments and in deeply weathered marly rock.

2.3 Choice of sample sites

Four sample sites were selected on lithological and geomorphological representativity and on practical considerations; all sites were located on range lands.

Site 2, Conte Mangier: A rendoll soil (0.4 cm thick) overlies bedrock of alternating layers of limestone and marl (Fig. 2.3a). The slope has been terraced almost entirely (Ap/C profile). This site was chosen to be the control site for the identification of the model structure, because the soil moisture regime of the layered subsoil could be studied here two-dimensionally in an exposed face on the gully side and in a borehole some metres upslope.

In addition, the main soil moisture parameters were determined. At the beginning of the research on spatial variation three sample sites whose lithology closely resembled the control site were added. These three sites were located where a thick layer of soil has been preserved but where the erodibility of the soil is very evident from features of soil erosion nearby.

Site 3, Les Combettes: a 0.8 m deep soil on a bedrock of the same chronostratigraphical stage as that at Conte Mangier. Incipient rills and shallow soil slips provide evidence of the erodibility of this soil.

Sites 4 and 5, Vincennes and Les Plagnes: both at the edge of an inter-fluve (soil depth 1.2 m or more) within an extended gully system formed in a pediment on marly bedrock.

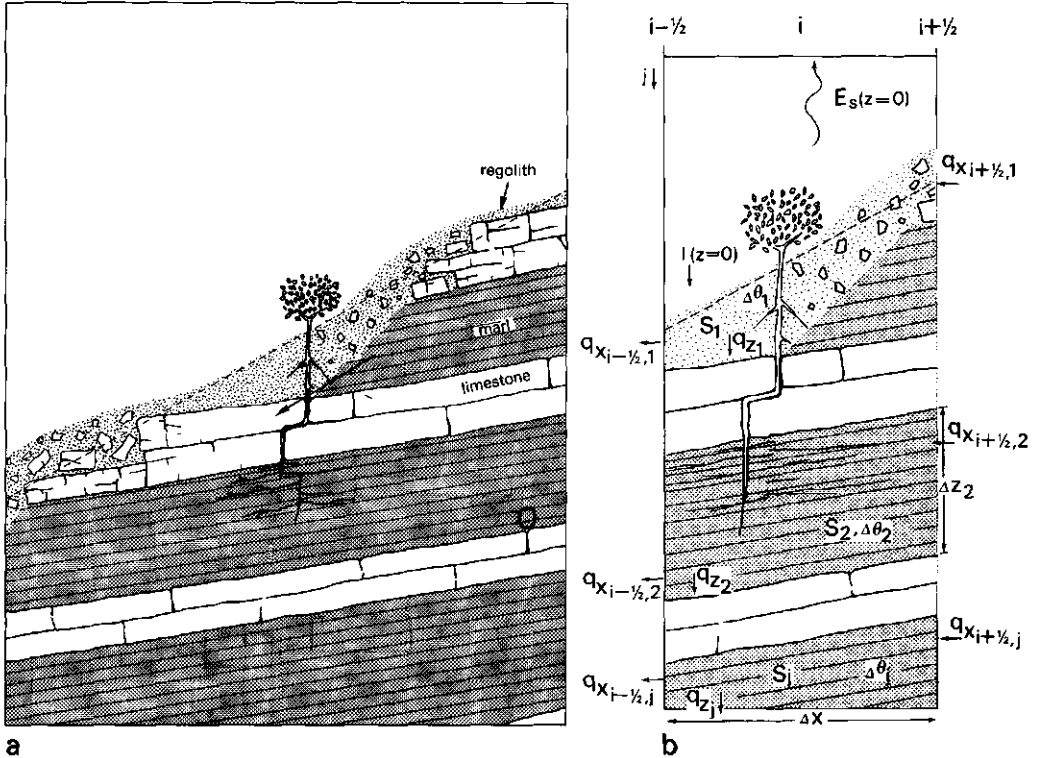


Fig. 2.3. a Hypothetical vertical profile of a slope, schematized with respect to soil moisture
 b. Verified model structure.

2.4 Methods and equipment

At the "Conte Mangier" site two important terms of the soil water budget viz. the evapotranspiration (actual and potential) and the decrease in moisture in the soil and in the upper layers of marl were measured during a drying period in spring.

The actual evapotranspiration was calculated according to the Bowen-ratio method. Net radiation, soil heat flux and the dry and wet bulb temperatures at heights of 0.5 m and 1.5 m above displacement height were measured every 20 seconds and the mean values of every ten minutes were stored on a cassette by means of a datalogger. The potential evapotranspiration was calculated according to the equation of PRIESTLEY & TAYLOR (1972):

$$E_p = \alpha \frac{\Delta \cdot R_{net}}{(\Delta + \gamma) \cdot L} \quad (2.1)$$

which needs only conventional meteorological data on sunshine, wind-speed and temperature and humidity in a screen. In accordance with STRICKER (1981) α was assumed to be 1.34.

Changes in soil moisture storage were determined gravimetrically (soil) or from duplicate measurements of soil moisture tension obtained by electronic pressure transducers, and from retention curves (4 upper layers of marl). The sensor for moisture tension consists of a porous cup; the tension is transduced into an electronic signal with a sensitivity of 0.5 mbar.

The low suction part of the k-psi relationship as well as the parameters of ponded infiltration were calculated from *in situ* measurements. Five columns of soil with a diameter of about 0.2 m and a height of 0.4 m to 0.6 m were made by digging away the surrounding soil. Each column was fitted out with an infiltrometer ring and small cup-tensiometers at two or three depths; a constant head of infiltrating water was maintained with an improved Mariotte bottle (photo 2.1).



Photo 2.1 Measurements during infiltration on two soil columns (Vincennes site).

The infiltration rate was read from the calibrated bottle and the pressure head was recorded: from the latter both the initial moisture suction and the time of the passage of the wetting front were obtained. A commonly used infiltration equation is that developed by PHILIP (1969):

$$I = S \cdot \sqrt{t} + A \cdot t \quad (2.2)$$

Parameters S (sorptivity) and A (gravity) can be optimized from the measured infiltration data, but the disadvantage of this formula is that S and A may vary in an unknown way with the initial soil moisture content.

Therefore, we preferred to use the infiltration equation according to the conditions specified by Green and Ampt. This enables an equation that is identical to equation 2 to be derived, as now

$$S = \sqrt{-2k_0 \cdot \psi_f \cdot (\theta_0 - \theta_n)} \quad (2.3a)$$

$$\text{and } A = \frac{2}{3} k_0 \quad (2.3b)$$

where θ_n and θ_0 are the initial and final moisture content and ψ_f is the pressure head (soil moisture tension) at the wetting front (KOORE-VAAR et al. 1983). However, this is an approximation which holds only as long as the depth L of the wetting front is smaller than the absolute value of ψ_f . Therefore, this formula is only of use for soils whose ψ_f values are not too small: these values appeared to be very small at the sample sites we investigated. Finally, we analysed the infiltration data with the unapproximated equations for cumulative infiltration I and time of infiltration t

$$I = L \cdot (\theta_0 - \theta_n) \quad (2.4a)$$

$$t = \frac{\theta_0 - \theta_n}{k_0} \left(L + \psi_f \cdot \ln \left(\frac{L - \psi_f}{-\psi_f} \right) \right) \quad (2.4b)$$

The disadvantage that in this way the infiltration cannot be expressed explicitly as a function of time can easily be overcome by using of a calculator.

The moisture tension at the wetting front ψ_f was determined in two different ways. Based on a graphic procedure developed by BROOKS & COREY (1964) a method was applied as described by BRAKENSIEK (1977), by which the ψ_f can be calculated with parameters from a double logarithmic plot of rearranged desorption curve data. As well, ψ_f was determined by fitting equations (2.4a and 2.4b) to the infiltration data by trial and error with the minimization of the variance of parameter k_0 as optimization criterion.

Both methods resulted in similar values for ψ_f , e.g. - 3.3 and -3.5 to -4.0 mbar for Conte Mangler and -7.6 and -7.5 to -8.0 mbar for Les Combettes.

In this study k_0 is defined as the hydraulic conductivity of the soil when all pores excluding macropores ($\psi > 1$ mm) are saturated. The notion of k_0 follows the infiltration model of BODMAN & COLMAN (1944)

in which a distinction is made between conductivity near saturation and conductivity at saturation, represented by the symbols k_0 and k_{sat} respectively. Though this distinction was not proposed explicitly for this purpose it nevertheless enabled us to distinguish between the conductivity of a saturated soil matrix and that augmented by transport through chains of macropores such as cracks, burrows or other cavities (for example decayed roots) (BOUMA 1980). Indeed, except in the case of inflow from a ponded surface, the moistening of macropores and their contribution to conductivity will be impeded as soon as the pressure head of soil moisture becomes negative. This will be illustrated by the difference between k_0 and k_{sat} as measured on the soil column at Les Combettes (section 2.7.4).

Likewise, adopting the assumptions of Green and Ampt, the following equation holds for the depth L of the wetting front:

$$L \cdot dL = k_0 \cdot \frac{\psi_0 - \psi_n}{\theta_0 - \theta_n} \cdot dt \quad (2.5)$$

with an effective diffusivity $D = k_0 \cdot \frac{\psi_0 - \psi_n}{\theta_0 - \theta_n}$ (2.6)

Integration of equation (2.5) yields:

$$L^2 = 2 \cdot \tilde{D} \cdot t \quad (2.7)$$

By monitoring the pressure head during the infiltration, the time of passage of the wetting front could be read and the effective diffusivity could be calculated (Fig. 2.4). As the values for ψ and θ of equation (2.6) were also known, k_0 could be determined.

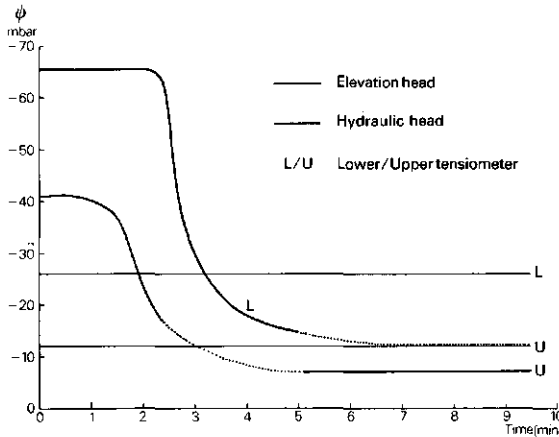


Fig. 2.4 Course of the hydraulic head at two depths in a soil column during infiltration.

Values of unsaturated conductivity at different moisture tensions were obtained by creating different hydraulic resistances at the top of the columns by means of capping them with crusts of different mixtures of sand and gypsum (BOUMA et al. 1971).

For intermediate moisture contents the k-psi relationship was determined in the laboratory with the so-called hot air method, as used by ARYA et al. (1975). First, a space-invariant moisture content is established in undisturbed soil samples 0.1 m long. By briefly drying one side of the soil a distinct soil moisture distribution is achieved, from which the relationship between diffusivity and content of soil moisture ($D - \theta$) can be calculated. To improve the comparability of the results from different soil samples, an algorithm for an unambiguous description of the soil moisture distribution in the sample was introduced (VAN DEN BERG & LOUTERS, in prep.).

The acquired $D-\theta$ relationship can simply be transformed into a k-psi relationship by means of the desorption curve of the soil. This curve was also determined in the laboratory as mean value of data from several undisturbed samples.

2.5 Accuracy

We attempted to ensure the accuracy of the meteorological data by calibrating the sensors and by frequent sampling. However, the accuracy of the calculated evaporation is not only determined by the reliability of the measurements but also by the validity and the appropriateness of the model.

For example, for the Bowen ratio method, the coefficients of turbulent diffusion of sensible and latent heat varied according to the instability of the boundary layer. The overall relative error was estimated to be ca. 10 per cent.

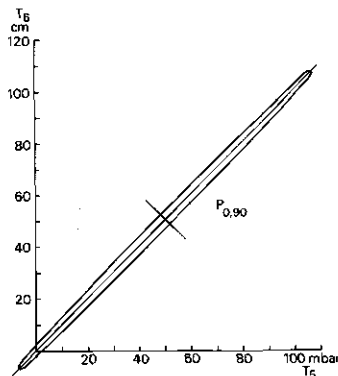


Fig. 2.5 Variation in duplicate measurements of pressure head.

In equation (2.1) for the potential evapotranspiration according to Priestley and Taylor, the value of the constant α in the literature ranges from 1.26 (PRIESTLEY & TAYLOR 1972) to 1.38 (BRUTSAERT 1982), which in itself results in a margin of error of 10 per cent. The soil moisture tensiometers were calibrated frequently during the measurements. The duplicate measurements in the soil-rock profiles at Conte Mangier clearly show that accurate data could be obtained (Fig. 2.5). The margin of error was 2 per cent.

The accuracy of the determination of infiltration parameters, conductivity, diffusivity and desorption curves of soil moisture in situ on a soil column or on undisturbed soil samples cannot yet be quantified, because the variation in the measured data inherent in the method cannot be separated from the variation caused by inhomogeneities of soil and rock.

2.6 Using the water budget to verify the modelling of soil moisture

In order to find the relationship between the spatial variability of soil moisture parameters and the risk of soil erosion processes, the simulation of the soil moisture regime has to produce the probability of situations that are critical to soil erosion, for example local saturation (concentrated throughflow) or positive pore water pressure (decrease of shear strength).

The most suitable models are those that are physically based on the differential equation for flow of soil moisture, for instance the SWATRE model that includes the effect of vegetation (FEDDES et al. 1978). The water budget of such a model consists of infiltration as input, with percolation, net throughflow and evaporation as output, and transpiration as a sink term. The differential equation for two-dimensional flow can now be written as:

$$\frac{\partial}{\partial x} \left(k \frac{\partial \psi}{\partial x} \right) + \frac{\partial}{\partial z} \left(k \frac{\partial \psi}{\partial z} \right) + \frac{\partial k}{\partial z} = S + \frac{\partial \theta}{\partial t} \quad (2.8)$$

or in discrete form:

$$I(z=0) = E_g(z=0) + \sum q_{th \text{ net}}(x_{i+\frac{1}{2}}; x_{i-\frac{1}{2}}) + q_p(z) + \sum S_j \cdot \Delta z + \sum \frac{\Delta \theta_j}{\Delta t} \cdot \Delta z \quad (2.9)$$

where S is the decrease of the volumetric moisture content per unit of time as a consequence of the moisture withdrawal by vegetation (Fig. 2.3b). Consequently, the actual evapotranspiration E_a equals the sum of S and E_g (E_g being the evaporation from the soil); E_g is negligible except during and shortly after rainfall. For the sake of completeness it should be mentioned that the cited model does not include pipe flow, which is generally accepted as one of the factors that can initiate rill and gully formation. Indeed, a reconnaissance tracer study -

simply performed by detecting the spatial distribution of calcium chloride from a point injection during a rainstorm also suggested that in this study area, as well as a downslope matrix flow there were, during periods with high moisture conditions, deviating preferential pathways to a gully. However, the results reported here mainly concern matrix flow, as modelling the occurrence of pipes from soil-rock parameters has not yet succeeded.

2.7 Results

2.7.1 Compilation of system

During the late spring of 1983 the soil moisture regime was determined at the sample site of Conte Mangier. The antecedent moisture conditions were very wet, and over 20 mm of rain was recorded just before the beginning of the measurements on 19 May, so that soil and rock were nearly saturated. During the measuring period, which ended on 20 June, the soil moisture fell continuously, because the weather became dry and sunny and on 12 June the mistral wind started to blow.

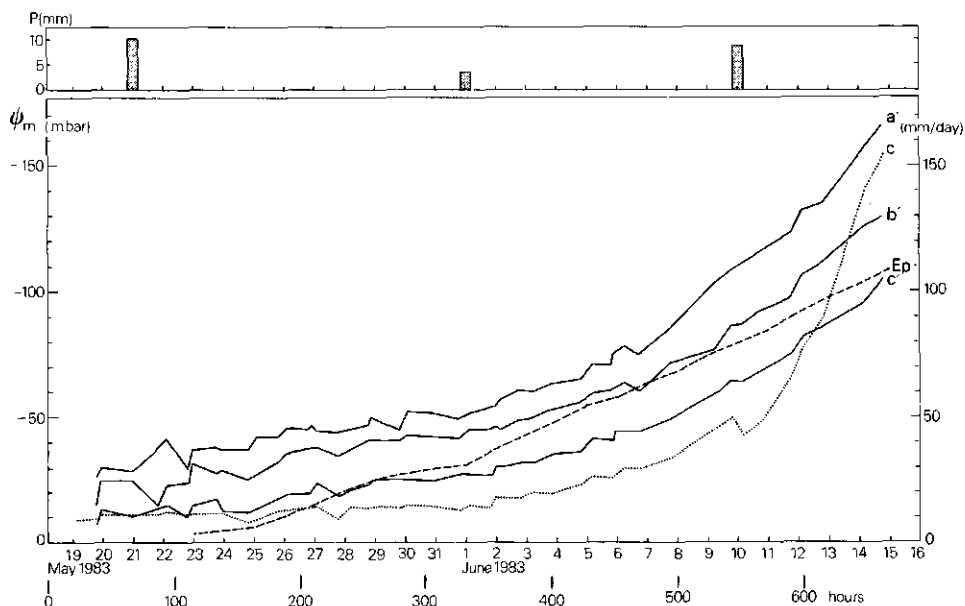


Fig. 2.6 Actual course of the potential evapotranspiration and the pressure head (mean value of two tensiometers) in different marl layers in the borehole (a', b', c') and two-dimensionally in layer 3 (c and c').

Figure 2.6 shows the course of the pressure head in the three upper layers of marl in the borehole and also in layer no. 3 in the free face. The measurements in the different layers in the borehole show that even at the start of the experiment there were small differences in pressure head and that these increased downwards from the top layer. During the following period of depletion the differences in pressure head increased gradually. This supports the assumptions made in root zone modelling and laboratory experiments that plant roots desiccate soil from the top to the bottom of the root zone (FEDDES 1981). The cumulative potential evapotranspiration, which is also presented in Figure 2.6, shows the intervals of low and high atmospheric water demand.

Figure 2.6 shows the course of the pressure head at two places in the same layer of marl (no. 3). Here, three intervals can be distinguished. The interval between 380 and 520 hours shows a difference between both pressure heads equal to the difference in elevation head. Consequently, the difference in hydraulic head is zero, which means no flow of soil moisture. Before this interval the difference in hydraulic head between the borehole and the free face is positive, which means a small downward flow of about 1 mm/day. From time 540 hours the pressure head at the free face decreased much faster than that in the borehole, probably because there was less available moisture in the thinner soil at the free face site.

At the increased hydraulic gradient at 640 hours the flow of moisture was reduced to about 0.4 mm/day.

For the period June 1 to 10, when the hydraulic gradient was negligible in all of the three upper layers of marl, equation (2.9) of the soil moisture budget is very simple:

$$E_a = E_s (z = 0) + \sum S_j \cdot \Delta z = -\sum \frac{\Delta \theta_j}{\Delta t} \cdot \Delta z \quad (2.10)$$

For the upper three layers of marl at the borehole site the decrease in moisture content was 2.2%, 2.0% and 1.0%, which confirms that desiccation proceeds down the soil profile. Figure 2.7 shows the contribution of the soil and the four upper layers of marl to the evapotranspiration. The actual evapotranspiration on the 12 and 13 June (6.4 mm/day) was very similar to the potential evapotranspiration (6.7 and 6.1 mm/day), and therefore the actual and potential evapotranspiration were assumed to have been equal before that date.

This assumption was justified by the data on daily energy budget of the soil surface as shown in figure 2.8: nearly all available energy dissipated as latent heat.

From the analysis of the data on the simplified soil moisture budget it can be concluded that several upper layers of marl play an important role in the soil moisture regime; consequently the root-soil-rock system has to be modelled as a multi-layered soil.

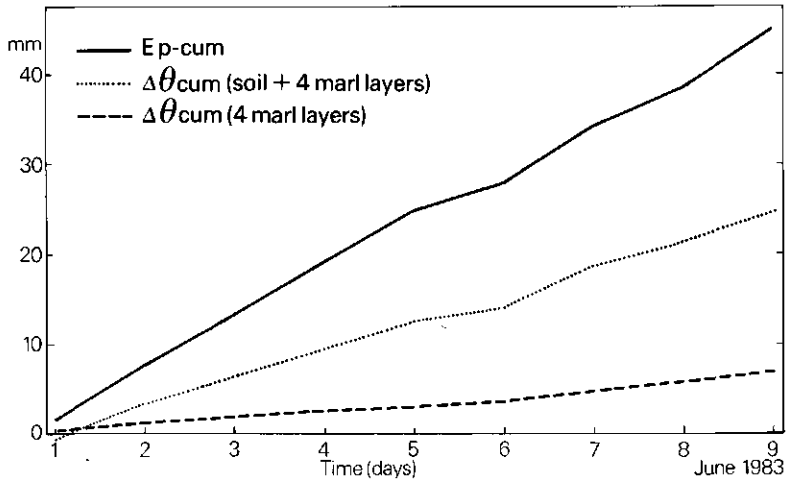


Fig. 2.7 Cumulative course of potential evapotranspiration and of moisture withdrawal from soil and four upper layers of marl.

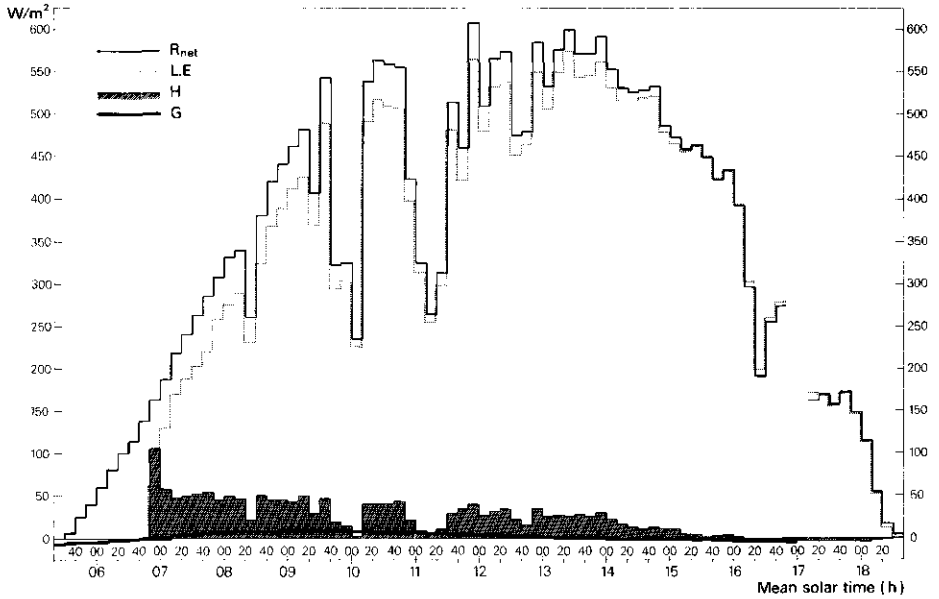


Fig. 2.8 Daily course of net radiation (R_{net}) and the distribution over sensible (H) and latent (L.E) heat flux and soil heat flux (G) during June 13, 1983.

Table 2.1 Mean value and standard deviation of density, porosity, saturated conductivity and pore content for drainage at four sample sites in the Ardèche basin.

Site Depth (m) Orientation	Soil hor.	Density ($\text{kg/m}^3 \cdot 10^{-3}$)		Porosity (volumetric fraction)			Sat. conductivity ¹⁾ (m/day)			Vol. frac. 2)		
		n	$\bar{\rho}$	s	n	\bar{p}	s_p	n	k_{sat}		$s_{k\text{-sat}}$	
												θ
Comte Manquier												
0.01 - 0.06	⊥	Ap ³⁾	16	1.31	0.07	11	0.44	0.04	11	1.48	0.70	---
0.04 - 0.09	⊥	Ap	6	1.30	0.08	6	0.46	0.03	6	5.73	3.57	0.18
0.34 - 0.40	⊥	Ap	6	1.39	0.08	6	0.41	0.02	6	1.04	0.44	---
ma 2	0.66	//	5	1.59	0.14	1	0.41	---	1	0.04	---	0.12
ma 3	0.96	//	6	1.59	0.02	1	0.40	---	2	0.05	---	0.09
ma 4	1.34	//	4	1.64	0.07	4	0.36	0.02	4	0.24	0.10	0.11
Les Combettes												
0.20 - 0.26	⊥	A/C	9	1.54	0.06	14	0.37	0.02	9	0.60	0.85	0.10
0.20 - 0.26	//	A/C	5	1.56	0.22	5	0.36	0.01	5	0.75	0.70	---
0.65 - 0.71	⊥	C	10	1.69	0.10	16	0.34	0.04	10	0.49 ⁴⁾	1.48	0.08
0.65 - 0.71	//	C	9	1.66	0.08	9	0.34	0.04	10	0.25	0.47	---
Vincennes												
0.15 - 0.21	⊥	A/C	10	1.47	0.07	3	0.45	0.02	10	0.32	0.14	0.15
0.40 - 0.46	⊥	C	-	---	---	-	---	---	3	0.28	0.26	---
0.55 - 0.61	⊥	C	4	1.51	0.04	4	0.42	0.02	-	---	---	0.12
Les Plagnes												
0.05 - 0.11	⊥	A	-	---	---	4	0.40	0.02	-	---	---	---
0.10 - 0.16	⊥	A	15	1.42	0.07	-	---	---	-	---	---	---
0.20 - 0.30	⊥	A/C	7	1.50	0.07	5	0.40	0.09	6	0.10	0.08	0.13
0.50 - 0.56	⊥	C	2	1.59	---	-	---	---	-	---	---	---
0.75 - 0.81	⊥	C	4	1.56	0.08	4	0.36	0.02	-	---	---	0.08
0.90 - 0.96	⊥	C	4	1.56	0.06	-	---	---	-	---	---	---

- 1) determined on Kopecki rings (h and ϕ 0.05 m)
 - 2) volumetric pore water content between saturation and pF 2.7
 - 3) Ap: soil layer on a slope with partly disintegrated terraces
 - 4) including an outlier of 4.7 m/day
- n number of replicates
 ⊥ vertical orientated
 // parallel to stratification or horizontal
 ma 2: layer of marl number 2, at given depth

2.7.2 Physical properties of the soil

The mean and variance of bulk density, porosity, saturated conductivity and difference in pore water content between saturation and soil moisture tension of pF 2.7 (water-conducting pores) for the four sample sites are shown in table 2.1. For most properties the laboriousness of the measurements has so far prevented us from obtaining a sufficient number of replicates per site for a valid statistical analysis. However, the number of data on porosity and density are assumed to be sufficient ($n = 25$ and 22 replicates) to allow a tentative analysis. This analysis shows that the frequency distributions of these two parameters have negative skewness which cannot be eliminated by one of the standard transformations.

Nevertheless, analysis of variance was applied to the data of corresponding shallow soil layers between 0.15 m and 0.4 m depth. The analysis indicated that porosity at the four sites belongs to the same population; the bulk density at Conte Mangier should be significantly smaller than at the other three sample sites.

2.7.3 Ponded infiltration

Ponded infiltration was measured on soil columns on which no artificial hydraulic resistance had been introduced by means of a crust. As soon as the pressure head in the column and the infiltration rate had become constant, the saturated hydraulic conductivity k_{sat} , was calculated. k_{sat} amounted to 2.9 m/day for Conte Mangier (and 1.2 m/day on another column in 1982), 2-4 m/day for Les Combettes, and 0.4 m/day for Vincennes.

A first estimate of the hydraulic conductivity near saturation k_0 was tried to obtain by applying equations (2.4a and 2.4b) to the data on infiltrated water versus time. Such an analysis of an experiment starting with an initial saturation rate of 80 to 90 per cent yielded a k_0 of 3.1 m/day for Conte Mangier, of 3.6 m/day for Les Combettes and 0.4 m/day for Vincennes. The correspondence of these k_0 values with those of k_{sat} will be discussed below.

From the recorded course of the pressure head at different depths in a soil column the effective diffusivity \bar{D} and a second estimate of k_0 (equation 2.6) were calculated. These results are also discussed below.

Table 2.2 Hydraulic conductivity in m/day near and at saturation as determined by different methods. The figures in brackets relate to the equation applied.

Sample site	Kopecki (mean) k_{sat}	Ponded infiltration			
		k_{sat}	(2.4a + 2.4b) k_0	(2.6) k_0	($\psi=0$) k_{unsat}
Conte Mangier	2.5	2.9	3.1	2.8	0.65
Les Combettes	0.5	2-4	3.6	2-3	0.24
Vincennes	0.3	0.4	0.4	-	-

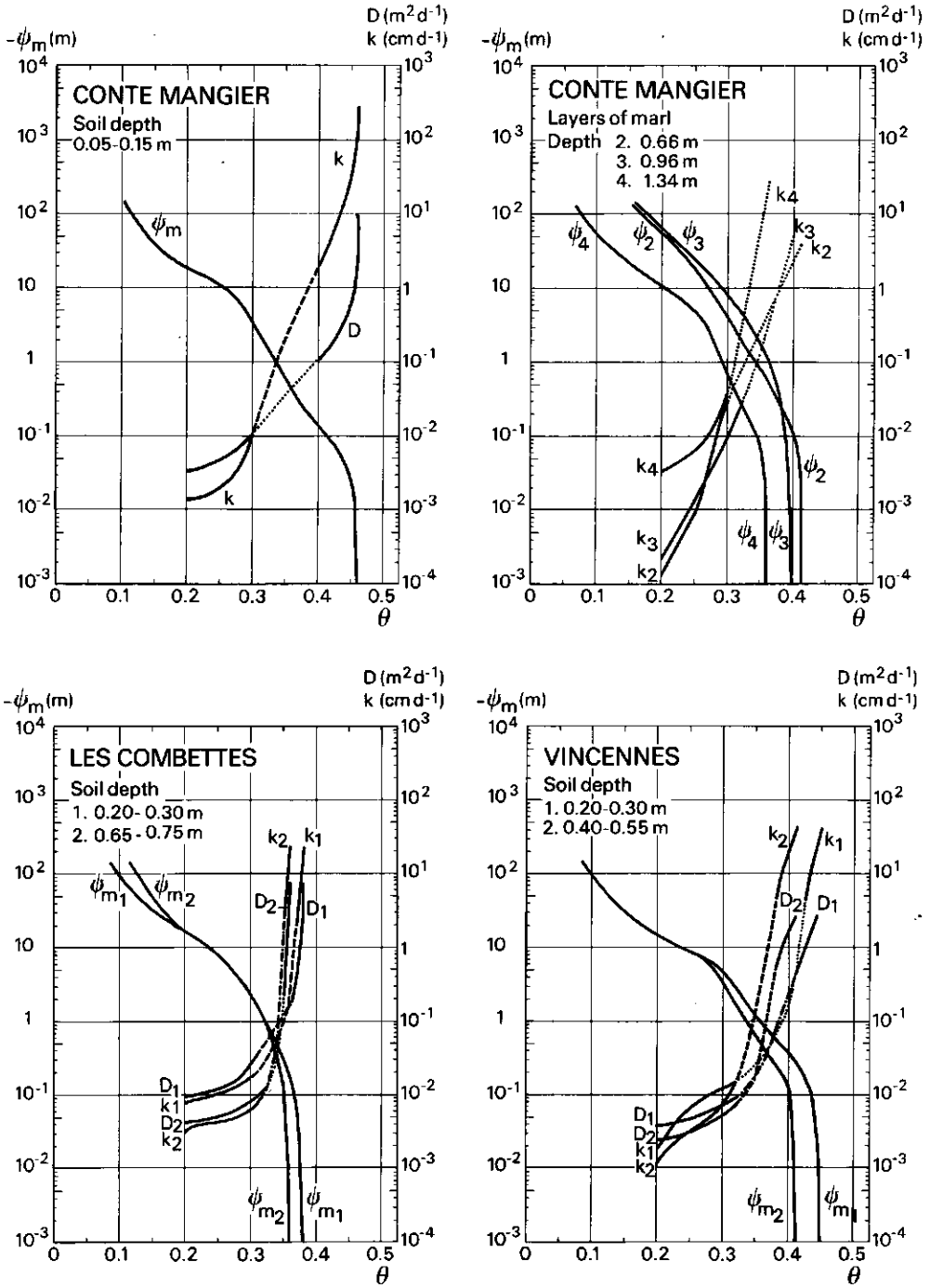


Fig. 2.9 Relationship between soil moisture content and diffusivity, conductivity and pressure head for soil and rock at three sites.

The results of the different methods of determining k_{sat} and k_0 are summarized in table 2.2. The figures for Les Combettes are particularly instructive: the factor of ten between k_{unsat} at $\psi = 0$ and k_{sat} at this site clearly illustrates why conductivity near saturation had to be differentiated from conductivity at saturation.

When the soil column was dissected at the end of the fieldwork, an earthworm burrow was found to be running through nearly the entire length of the soil column. Such a chain of macropores could drain rapidly during saturation and ponded infiltration. Hence, determination of k_0 from the infiltration data (eq. 2.4a and 2.4b) or based on the wetting front method (eq. 2.6) is not applicable to experiments with ponded infiltration without an artificial hydraulic resistance as in this way both methods deliver values of k_0 that approximate to k_{sat} . However, the infiltration experiment under application of a crust with low resistance generates a very small moisture tension ($\psi \approx 0$) that impedes soil water from entering macropores. The pertaining value of k_{unsat} seems a good estimation of k_0 .

The data on k_{sat} (table 2.2, column 2) agree with the corresponding values obtained on Kopecki rings (column 1), if one keeps in mind that extreme (high) values of conductivity from Kopecki rings are unlikely, as any burrows or plant roots are avoided during sampling.

2.7.4 Parameters of soil water flow

In figures 2.9a/d the desorption curves and the relationships between diffusivity and between hydraulic conductivity and soil moisture content are shown for three sample sites. Each retention curve represents the arithmetic mean of 4 or more samples.

For intermediate moisture contents the D-theta relationship is represented by the median of the values calculated with the hot air method. The median was taken because the different samples from the same soil layer often gave diffusivity values whose extremes varied by a factor of 2 to 4. The corresponding k-theta values were obtained by multiplying the D values by the slope of the desorption curve. For pressure heads between 0 and -30 mbar the procedure was precisely the opposite: measurements on a soil column capped by crusts of different hydraulic resistance gave different values of k at different pressure heads. Dividing the k values by the slope of the desorption curve yielded the corresponding diffusivity values. The data obtained from soil columns were considered to be smoothed, as the measurements had been obtained from a much larger soil sample than in the case of the hot air method and the desorption curves.

The parts of the D-theta and k-theta relationships near saturation were obtained from measurements of ponded infiltration on soil columns, i.e. the effective diffusivity D and k_0 (section 2.7.3).

2.8 Conclusions, evaluation and applications

- For the modelling of soil moisture, the model structure of a physiographic unit can be identified from the soil moisture budget. During a period with no flow of soil moisture, measure-

- ments can be restricted to actual evapotranspiration and changes in content or tension of moisture in soil or rock layers with storage capacity.
- Where relatively thin soils are found on rock that consists of alternating layers, e.g. of solid limestone and weathered marl, the upper layers of marl play a very active role in the soil moisture regime (VAN DEN BERG 1983). Such a soil-rock system has to be modelled analogously to multi-layered soils.
 - Our results indicate that desiccation of a root-soil-rock system takes place from the top downwards; this supports practice in root zone modelling.
 - If the general infiltration equation (2. 4a and 2. 4b) is to be applied according to the Green & Ampt assumptions, the moisture tension ψ_f at the wetting front must be known. The method described by BRAKENSIEK (1977) and that of fitting equation (2. 4a and 2. 4b) to measured infiltration data yield ψ_f values, that closely correspond. When ψ_f is known, equations (2. 4a and 2. 4b) give an infiltration formula that takes account of the initial soil moisture condition.
 - Measurements from a soil column in situ can provide nearly all the fundamental hydraulic properties of the soil:
 - .. during ponded infiltration:
 - three different ways of determining saturated hydraulic conductivity: according to Darcy's law, the measured infiltration data (eq. 2. 4a and 2. 4b) and the observations of the movement of the wetting front (eq. 2. 6);
 - .. during infiltration, controlled by an artificial crust:
 - hydraulic conductivity near saturation k_0 i. e. k_{unsat} at a negative pressure head close to zero by use of a low, artificial hydraulic resistance;
 - the wet part of the k-psi and D-psi relationships, which can be supplemented by results for intermediate moisture contents from the hot air method.
 - When macropores are present, k_{sat} and k_0 according to eq. 2. 4a and 2. 4b or to eq. 2. 6 will differ considerably from k_{unsat} at $\psi = 0$.
 - For the measurement of soil moisture tension, small cup tensiometers with an electronic pressure transducer appear to be a cheap but quick and reliable tool, as long as moisture tension does not fall below - 500 mbar.
 - At several places, even near the top of slopes, shallow soil slips were found. Such slips were probably caused by temporarily positive pore water pressure such as had been measured at the equilibrium stage during an infiltration experiment on a soil column (Fig. 2. 4). According to Coulomb's law for shear strength, when pore water pressure is positive the shear strength of clayey and silty soils decreases considerably, thereby affecting slope stability. Where this more or less coincides with an abrupt decrease in root density and consequently with a decrease in cohesive soil strength by roots (GRAY & MEGAHAN 1981) shallow soil slips may result.

Acknowledgements

We are greatly indebted to Prof. dr. P. A. Burrough and Prof. dr. J. H. J. Terwindt for their valuable comments, Mr. T. G. M. Tiemissen for his help with electronic measuring devices and data processing and the students Hein Kraanen, Jan van de Meene and Harry Pronk for their efforts during field work.

LIST OF SYMBOLS

symbol	description	dimension
D	diffusivity of soil moisture	l^2/t
\tilde{D}	effective diffusivity	l^2/t
E_a	actual evapotranspiration	l/t
E_p	potential evapotranspiration	l/t
E_s	actual evaporation from the soil	l/t
I	flux density of moisture at the soil surface	l/t
L	latent heat of evaporation	E/m
L	depth of the wetting front	l
k	hydraulic conductivity of unsaturated soil	l/t
k_0	saturated conductivity excluding large pores	l/t
k_{sat}	saturated conductivity	l/t
n	number of items in a sample	-
p	soil porosity	-
q_p	flux density of percolation or capillary rise	l/t
q_{th}	flux density of throughflow	l/t
R_{net}	net radiation	$E/l^2 \cdot t$
s	standard deviation	-
S	sorptivity	l/t
S	volume of water taken up by plant roots per unit bulk volume of soil in unit time	l/t
t	time	t
x, z	coordinates of space	l
α	empirical constant	-
γ	psychrometer constant	p/T
Δ	slope of the temperature-saturation vapour pressure curve	p/T
θ	volumetric soil moisture content	-
ψ	head; without index pressure head	$l(p)$
ρ	bulk density of soil	m/l^3
indices		
o	saturated	
n	initial	
f	wetting front	
H	hydraulic	
net	net value	

REFERENCES

- ARCHAMBAULT, M. (1966), Essai sur le génèse des glacis d'érosion dans le Sud et le Sud-Est de la France. Mémoires et Documents du Centre de Recherches et Documentation Cartographiques et Géographiques. C. N. R. S. 2, pp. 101-143.
- ARYA, L. M., D. A. FARELL & G. R. BLAKE (1975), A field study of soil water depletion patterns in presence of growing soybean roots. Part I: Determination of hydraulic properties of the soil. Soil. Sci. Soc. Amer. J. 39, pp. 424-430.
- BROOMAN, G. B. & E. A. COLMAN (1944), Moisture and energy conditions during downward entry of water into soils. Soil Sci. Soc. Amer. Proc. 8, pp. 116-122.
- BOUMA, J., D. I. HILLEL, F. D. HOLE & C. R. AMERMAN (1971), Field measurements of unsaturated hydraulic conductivity by infiltration through artificial crusts. Soil Sci. Soc. Amer. Proc. 35, pp. 362-364.
- BOUMA, J. (1980), Field measurement of soil hydraulic properties characterizing water movement through swelling clay soils. J. Hydrology 45, pp. 149-158.
- BOUMA, J. & P. J. M. DE LAAT (1981), Estimation of the moisture supply capacity of some swelling clay soils in the Netherlands. J. Hydrology 49, pp. 247-259.
- BRAKENSTIEK, D. L. (1977), Estimating the effective capillary pressure in the Green and Ampt infiltration equation. Water Res. Res. 13 (3), pp. 680-682.
- BROOKS, R. H. & A. T. COREY (1964), Hydraulic properties of porous media, Agr. Eng. Dep., Colorado State Univ., Fort Collins, Hydrol. Pap. 3, 27 pp.
- BRUTSAERT, W. H. (1982), Evaporation into the atmosphere: theory, history and applications. Reidel Publ. Comp., Dordrecht, Boston, London.
- FEDDES, R. A., P. J. KOWALIK & H. ZARADNY (1978), Simulation of field water use and crop yield. Centre Agricult. Publ. and Documentation, Wageningen.
- FEDDES, R. A. (1981), Water use models for assessing rootzone modification. In: G. F. Arkin & H. M. Taylor, Eds., A. S. A. E. monograph: Modifying the root environment to reduce crop stress. Amer. Soc. Agricult. Eng.
- GRAY, D. H. & W. F. MEGAHAN (1981), Forest vegetation removal and slope stability in the Idaho Batholith; U. S. D. A. Research Paper INT-271.
- KOOREVAAR, P., G. MENELIK & C. DIRKSEN (1983), Elements of soil physics. Elsevier, Amsterdam, Oxford, New York.
- NIELSEN, D. R., J. W. BIGGAR & K. T. ERH (1973), Spatial variability of field measured soil water movement. Hilgardia 42, pp. 215-259.
- NIELSEN, D. R. & A. W. WARRICK (1980), Spatial variability of soil physical properties in the field. In: D. Hillel, Ed., Applications of soil physics. Academic Press, New York.
- NIELSEN, D. R., S. R. VIEIRA, J. L. HATFIELD & J. W. BIGGAR (1983), Geostatistical theory and application to variability of some agronomical properties. Hilgardia 51, 3, pp. 1-75.
- PHILIP, J. R. (1969), Theory of infiltration. Adv. Hydrosol. 5, pp. 215-290.
- PRIESTLEY, C. H. B. & R. J. TAYLOR (1972), On the assessment of surface heat flux and evaporation using large-scale parameters. Month. Weather Rev. 100, pp. 81-92.
- STRICKER, J. N. M. (1981), Methods of estimating evapotranspiration from meteorological data and their applicability in hydrology. In: Evaporation in relation to hydrology; Comm. Hydrol. Research T. N. O. The Hague, Proceed. and Informations, 28, pp. 59-77.
- TRICART, J. & P. USSELMANN (1968), Feuille Géomorphologique Privas 7-8; 1:25.000 - Notice C. N. R. S. R. C. P. 77. Extrait de la Revue de Géomorphologie Dynamique 19 (3) pp. 114-128 (1969/1970).
- VAN DEN BERG, J. A. (1983), Aspects hydrogéologiques de l'érosion dans la région limoneuse autour de Villeneuve-de-Berg. Revue de la Société des Enfants et Amis de Villeneuve-de-Berg, 38, pp. 11-19.
- VAN DEN BERG, J. A. & T. LOUIERS (1986), An algorithm computing the relationship between diffusivity and soil moisture content from the hot air method. J. Hydrol. 83, pp. 149-159.

3. AN ALGORITHM FOR COMPUTING THE RELATIONSHIP BETWEEN DIFFUSIVITY AND SOIL MOISTURE CONTENT FROM THE HOT AIR METHOD

Published in: Journal of Hydrology 83 (1986), 149-159.
Permission for reproduction, 14 July 1989.

[5] 0022-1694/86/\$03.50 © 1986 Elsevier Science Publishers B.V.

AN ALGORITHM FOR COMPUTING THE RELATIONSHIP BETWEEN DIFFUSIVITY AND SOIL MOISTURE CONTENT FROM THE HOT AIR METHOD

JAN A. VAN DEN BERG and TEUNIS LOUTERS

Department of Physical Geography, Geographical Institute, State University of Utrecht, Heidelberglaan 2, 3508 TC Utrecht (The Netherlands)

(Received July 14, 1985; accepted for publication September 4, 1985)

ABSTRACT

Van den Berg, J.A. and Louters, T., 1986. An algorithm for computing the relationship between diffusivity and soil moisture content from the hot air method. *J. Hydrol.*, 83: 149-159.

The hot air method proposed by Arya et al. to determine the relationship between diffusivity and soil moisture content uses a graphical procedure which is time-consuming and subjective. The results obtained by different observers vary greatly.

In this paper, an algorithm is proposed by which the diffusivity values can be computed reproducibly. An empirical function with four parameters is used. Two of them are ascertained by the boundary conditions, the other two have been optimized by a standard procedure. The computation is rapid and unambiguous.

The algorithm also enables an analytical expression for the evaporation that is generated by the drying of a sample by hot air and in this way it gives a reliable judgement of the appropriateness of the data obtained.

The method has been tested on samples obtained from residual, silty soils from the Ardèche Basin, France.

INTRODUCTION

Soil moisture diffusivity is defined as $D(\theta) = k \cdot \frac{d\psi}{d\theta}$ (see the list of symbols). The relationship between D and θ is widely used in models simulating the soil moisture regime. The hot air method (Arya et al., 1975) enables us to determine part of this relationship on undisturbed soil samples. Although this method requires only simple laboratory equipment, the graphical method of transforming the measured data into a D - θ relationship is laborious and its results vary considerably between investigators. Therefore this method should be standardized in order to eliminate this subjective variation. Then the remaining natural variance, which is still considerable (e.g., Nielsen et al., 1973; Bouma et al., 1979), would become suitable for further analysis.

In this paper we propose an algorithm to find the D - θ relationship from the moisture content distribution generated in the soil sample.

The algorithm is easily programmable. Results from forty samples of weathered marl and silty-loam soils in the Ardèche Basin are discussed.

THEORY

According to Bruce and Klute (1956) the diffusivity of soil moisture $D(\theta)$ during moistening of a semi-infinite column can be obtained from:

$$D(\theta) = \frac{1}{2t} \cdot \left(\frac{dx}{d\theta} \right) \cdot \int_{\theta_x}^{\theta_i} x d\theta \tag{1}$$

where θ is the volumetric moisture content and t is time of moisture diffusion. The index i refers to the initial value of θ which has to be constant throughout the soil at the beginning: $\theta = \theta_i$ at $t = 0$ and all $x > 0$.

Gardner (1959) developed a slightly different analysis and applied it to the process of evaporation.

Arya et al. (1975) applied this solution to the desiccation of a cylindrical soil sample of short length. By briefly drying one side of the soil sample a distinct distribution of soil moisture $\theta(x)$ is achieved as a function of the distance x from the evaporating surface (Fig. 1).

Arya formulated as second boundary condition: $\theta = \theta_0$ at $x = 0$ and $t > 0$, which means that the surface of the soil sample dries immediately to the air-dry value of θ_0 . As eqn. (1) is only valid for a semi-infinite soil column, the drying has to be stopped before the initial soil moisture content starts to decline near the base of the soil sample.

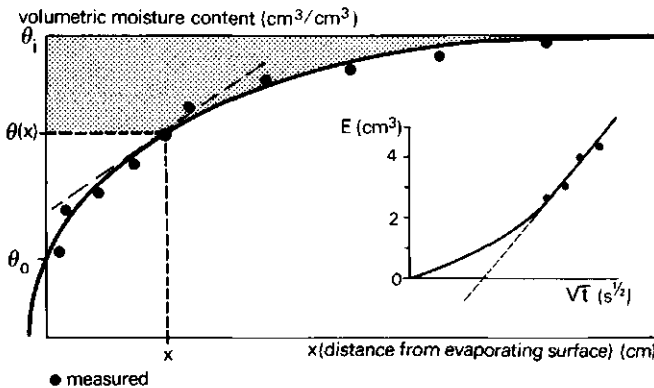


Fig. 1. Schematic distribution of soil moisture after brief drying. The dotted line represents the tangent on the distribution curve at x_j , the shaded area represents the integral of $x(\theta)$ from $\theta(x_j)$ to θ_i . The insert shows the relationship between cumulative evaporation and the square root of drying time.

As Bruce and Klute used the Boltzmann transformation, a linear relationship is implied between the cumulative evaporation E and the square root of the drying time t in the case of horizontal flow:

$$E = p\sqrt{t} + q \quad (2)$$

A similar relationship should also be a sufficient approximation for the vertical flow that occurs while the hot air method is being carried out, as this method is applied at moisture contents where the contribution of gravity to flow is negligible.

PROCEDURE FOLLOWED FOR THE HOT AIR METHOD

After an initial soil moisture content has been achieved by putting the soil cores on a sandbox with a moisture suction between pF 1.7 and 2.0, a distinct moisture distribution is attained by blowing hot air over one side of the core for a short time t . Conduction of heat through the surrounding steel cylinder is minimized by means of a water-cooled heat shield around its top (Fig. 2). More details about the laboratory procedure are given by Arya et al. (1975).

The moisture distribution generated is determined by measuring the moisture content within the thin slices into which the soil core is divided. These data are plotted and a monotonously rising curve is drawn through the measured data (Fig. 1). Then the tangent and the area between the θ_i

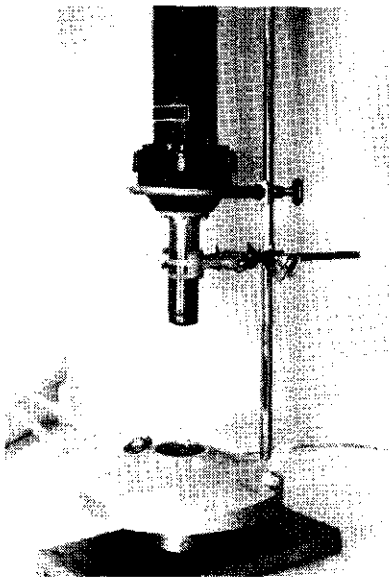


Fig. 2. A distinct distribution of soil moisture is generated in a cylindrical soil sample by blowing hot air over one side of the sample. A water-cooled shield around the top of the cylinder prevents conduction of heat along the steel jacket.

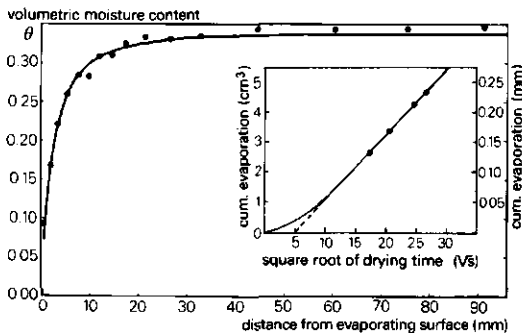


Fig. 3. Measured and computed distribution of soil moisture throughout a sample of weathered marl. Insert: Cumulative evaporation as a function of the square root of drying time.

asymptote and the curve until $\theta(x)$ are determined graphically for points (x, θ) of the distribution curve at regular increments of θ . Inserting these data, together with the drying time t , into eqn. (1), the diffusivity can be calculated as a function of the moisture content for all $\theta_0 < \theta < \theta_i$.

The relationship of eqn. (2) is applied as a check for the drying procedure. While the soil is being dried, its decrease in weight is measured 4–5 times and plotted as a function of the square root of t . In practice, the linear relationship is found from about 2 min on (Figs. 1 and 3).

In our experiments forty soil cores 100 mm long and with a diameter of 50 mm were taken from silty loam, rendoll-type soils on layered marl or alternating marl and limestone in the Ardèche catchment. On a sand box, the samples were brought at pF 2 and subsequently dried with a blower at an air temperature of 180°C near their surface (Fig. 2). The drying time varied between 12 and 15 min. Figure 3 shows the measured moisture distribution in one of the samples as well as the measured increase of evaporated moisture during drying. For $t > 2$ min, the latter closely obeys eqn. (2).

PROBLEMS ARISING IN PRACTICE

Two parts of the graphical procedure, i.e. drawing the best-fitting curve through the measured points of the moisture distribution and calculating the tangent and the area between θ_i and the curve, make the hot air method laborious and subjective. Graphical differentiation especially introduces inaccuracies. As a consequence, the results obtained by different investigators are very difficult to compare.

Therefore, we have developed a standardized algorithm for calculating the diffusivity from the measured moisture distribution, observed after a certain drying time t .

ALGORITHM

Because the main source of errors lies in the graphical differentiation and integration (and mainly in the former), we propose to fit an empirical function to the data. The requirements for such a function are: (1) a monotonous increase of θ with x ; (2) for $x = 0$, $\theta = \theta_0$ (i.e. the first boundary condition; θ_0 is air dry moisture content); (3) for $x \rightarrow \infty$, $\theta = \theta_i$ (i.e. the second boundary condition); and (4) allowing easy differentiation and integration.

The following four-parameter function has been chosen:

$$\theta = a - \frac{c}{(x + b)^n} \quad (3)$$

Substituting the boundary conditions, two parameters can be eliminated and eqn. (3) can be written as:

$$\theta = \theta_i - \frac{(\theta_i - \theta_0) \cdot b^n}{(x + b)^n} \quad \text{or} \quad x = b \sqrt[n]{\frac{\theta_i - \theta}{\theta_i - \theta_0}} - b \quad (4a, b)$$

For positive values of b and n , it fulfills all the requirements mentioned above. An alternative form of eqn. (4a), using the relative moisture deficit Θ (being zero for soil at pF 2 and unity for air-dry soil), is:

$$\Theta = \frac{\theta_i - \theta}{\theta_i - \theta_0} = \left(\frac{b}{x + b} \right)^n \quad (4c)$$

The tangent and the area needed in eqn. (1) are:

$$\frac{dx}{d\theta} = \frac{(x + b)^{n+1}}{n(\theta_i - \theta_0) \cdot b^n} \quad (5)$$

and:

$$\int_{\theta}^{\theta_i} x d\theta = \frac{b \cdot n}{n-1} (\theta_i - \theta_0) \cdot \Theta^{\frac{n-1}{n}} - b(\theta_i - \theta) \quad (6)$$

Substituting eqns. (5) and (6) into (1) yields:

$$D(\theta) = \frac{1}{2t} \cdot \frac{nx + b}{n(n-1)} \cdot \frac{(x + b)^{n+1}}{b^n} \cdot \Theta \quad (7)$$

Parameter b represents a translation; it has the dimension of length and is expressed in the same unit as x . Parameter n is dimensionless; it influences the deflecting rate of the curve. Both parameters are not constant as they depend on the drying time t . D must depend on $\lambda = x \cdot t^{-1/2}$ only ("Boltzmann similarity"), but eqn. (7) does not show this relation unless n and b change with time, probably in a quite complicated way.

Moreover, the amount of evaporated water can be expressed as a function of the parameters by substituting $\theta = \theta_0$ into eqn. (6):

$$E = \frac{b}{n-1} \cdot (\theta_i - \theta_0) \quad (8)$$

which should equal the measured evaporation after the blowing of hot air has been stopped. Hence, eqn. (8) can be used to check the appropriateness of data obtained for $\theta(x)$.

DETERMINING THE PARAMETERS

Measurements on a sample that had not been air-dried indicated that θ_i was reproducible for the Ardèche soils: The standard error of the mean initial moisture content throughout a whole core was 0.0015. However, in replicates that had been treated by hot air, the moisture content near the base of each sample usually showed greater variability. For practical reasons the value of θ_i was obtained as the average of the moisture content belonging to all m slices for which the distance x to the evaporating surface exceeds a given threshold value ϵ :

$$\theta_i = \frac{1}{m} \sum_{p=1}^m \theta_p(x) \quad (x \geq \epsilon)$$

For the silty soils and drying times used, a threshold $\epsilon = 25$ mm appeared to be appropriate; then for each sample, the relative dispersion of measured moisture contents $\theta(x \geq \epsilon)$ remained less than five per cent:

$$\frac{s[\theta(x \geq \epsilon)]}{\theta_i - \theta_0} \leq 0.05$$

where $s(\theta)$ is the standard deviation.

A value of 0.02 seems appropriate for the air-dry value, θ_0 , of the moisture content. The sensitivity of the algorithm to θ_0 was tested for a computed soil moisture distribution with realistic parameters ($\theta_i = 0.331$; $n = 4.161$; $b = 16.1$ mm and $t = 15$ min). The value assigned to θ_0 does not have much influence on the results of the diffusivity computation, except for moisture contents within the range of $0.8 \theta_i$ to θ_i (Fig. 4).

With these values for θ_i and θ_0 , the parameters n and b in eqns. (4) are optimized by means of the least squares method. The sum of squares S of the deviations between the logarithm of the measured values (θ_m) and the computed ones (θ_c) can be expressed as:

$$S = (\ln \Theta_m - \ln \Theta_c)^2$$

$$\text{where } \Theta_m = \frac{\theta_i - \theta_m}{\theta_i - \theta_0} \text{ and } \Theta_c = \frac{\theta_i - \theta_c}{\theta_i - \theta_0} = \left(\frac{b}{x + b} \right)^n$$

Therefore:

$$S = \sum \left[\ln(\theta_i - \theta) - \ln(\theta_i - \theta_0) + n \cdot \ln \left(\frac{x + b}{b} \right) \right]^2 \quad (9)$$

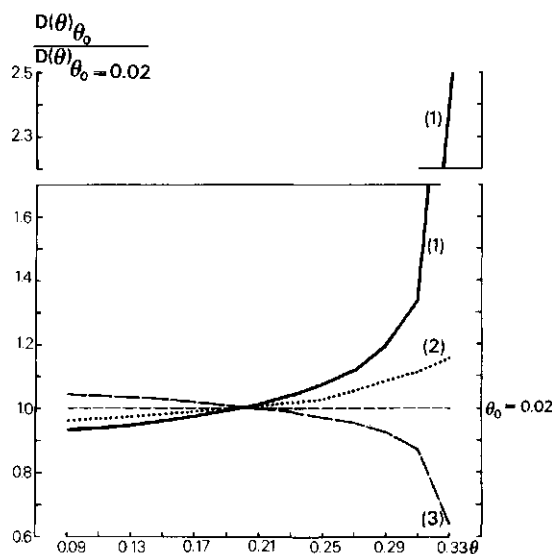


Fig. 4. Relative sensitivity of the algorithm to the value assigned to the air-dry moisture content θ_0 is expressed as ratio between the diffusivity calculated with $\theta_0 = 0.00$ (1), 0.01 (2) or 0.03 (3) and that with $\theta_0 = 0.02$.

Basically, S is minimized by equalizing the first partial derivatives of S to zero, but in practice, parameters n and b are calculated by a subroutine consisting of a quasi-Newton algorithm for finding the minimum of S , subject to fixed upper and lower limits to n and b (NAGFLIB, 1983). The lower limits are chosen as $n \geq 0.5$ and $b \geq 0$. The upper limits are arbitrarily fixed as $n \leq 24.0$ and $b \leq 24.0$.

TESTING THE VALIDITY OF THE ALGORITHM

The algorithm has been tested on forty samples of weathered marl and silty-loam soils from the Ardèche Basin as part of a research on how the variability of soil physical parameters has to be incorporated in the modelling of the soil moisture regime (Van den Berg and Louters, 1985). Two stoney samples showed an unsuitable soil moisture distribution. Statistical analysis of the data from the remaining 38 samples showed close agreement between the measured and calculated evaporation. The null hypothesis that the differences between the measured and calculated evaporation come from a population with mean (median) of zero was not rejected either by Student's test or by the rank correlation test.

The algorithm-based computation was compared with the graphical computation (with increments of θ equal to 0.02), taking into consideration the ratio between the resulting diffusivities at different moisture contents. Seven investigators were provided with the same data set on the moisture

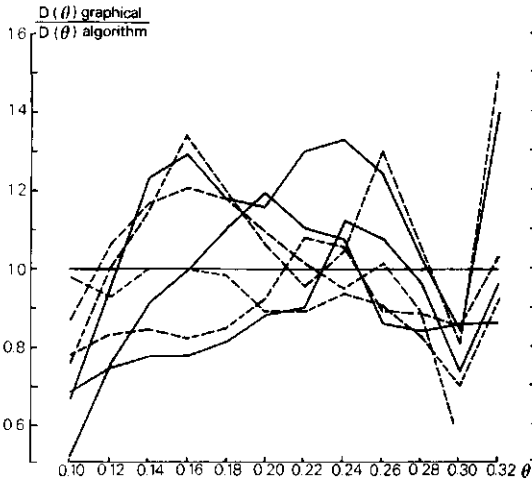


Fig. 5. Ratio between the diffusivity computed graphically and that computed using the algorithm.

distribution of two samples: A real one (Test 1) and one computed according to eqn. (4a), with fictitious but common values for t , θ_i , b and n (Test 2). The results for Test 1 are shown in Fig. 5, where the ratio between the individually calculated diffusivity and that computed according to the standardized calculation is plotted. Test 2 gave a comparable picture.

Figure 5 shows that the diffusivity can vary by a factor 2 or 3 as a result of subjective interpretation. Such a variation will considerably reduce the comparability of the results obtained by different investigators. In order to quantify the results of both tests, the median (M) as well as the half of the interquartile range (K) were calculated and plotted in Fig. 6. It seems that the variance between individually calculated diffusivities decreases with increasing regularity of the moisture distribution data, which are evidently optimal in Test 2; the mean of all halves of interquartile ranges of Test 2 is 0.047 against 0.094 for Test 1.

APPLICATION: THE D - θ RELATIONSHIP FOR SOILS IN THE ARDÈCHE BASIN

Using the algorithm, diffusivity values were obtained for θ -values below about 0.30–0.35 (pF over 2.0). For higher moisture contents (corresponding to pF < 2.0) the hot air method is unsuitable. Instead, use was made of the "crust method" as described by Bouma et al. (1971). A combination of these two methods leads to diffusivity values over the entire range. In combination with the ψ - θ curve (desorption curve) the unsaturated hydraulic conductivity, k , can be obtained by using the definition of D . As an illustration, Fig. 7 gives these relationships for a typical sample from the Ardèche Basin (Van den Berg and Louters, 1985).

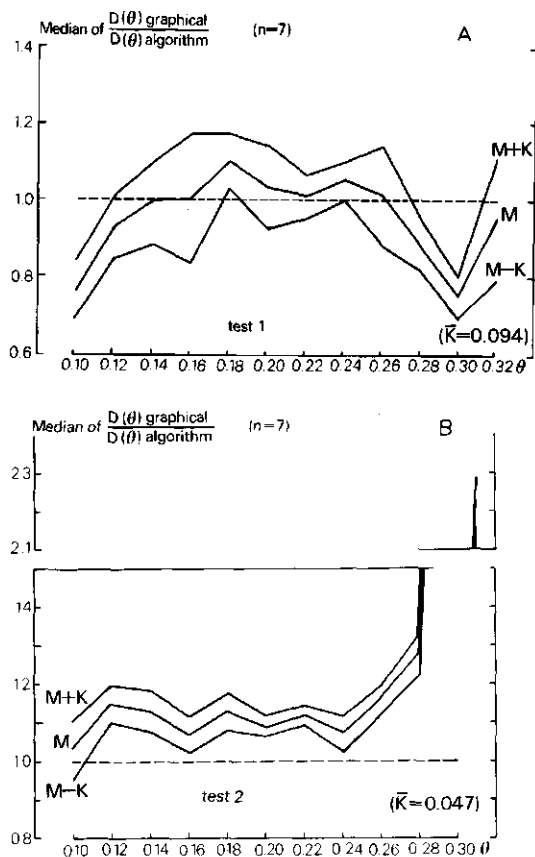


Fig. 6. Median, first quartile (= median M minus half of interquartile range K) and third quartile ($M + K$) of the ratio between the diffusivity computed graphically and that computed using the algorithm. The graphical calculation was performed independently by seven individuals ($n = 7$). Test 1 (A) used measured data from a sample of weathered marl; Test 2 (B) used a computed moisture distribution.

SYNOPSIS

(1) The hot air method, although a suitable tool for obtaining the diffusivity at moisture contents for pF 2 and upwards, is rather time-consuming with regard to the determination of the tangent and area factors in the basic eqn. (1).

(2) Graphical interpretation of a given moisture distribution by different investigators results in diffusivity values that may differ greatly from each other. This variation increases with the irregularity of the measured moisture distribution data.

(3) The proposed algorithm enables reproducible diffusivity values that are suitable for further analysis, such as statistical analysis on spatial variability.

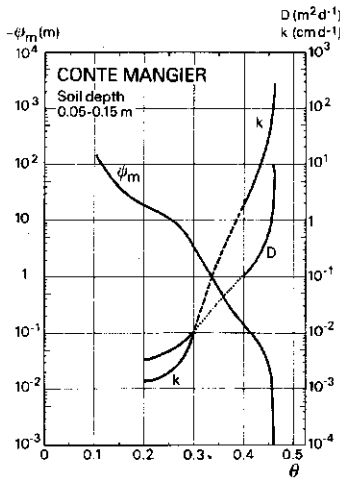


Fig. 7. Relationship between soil moisture content and diffusivity, conductivity and pressure head for a silty loam soil. The diffusivity and conductivity curves result from a combination of two methods: The hot air method (part 1) for the lower moisture contents and the crust method (part 2) for the higher moisture contents.

(4) From the algorithm an expression is derived by which the total evaporation at the end of the drying time can be calculated. By comparing this result to the measured total evaporation the appropriateness of the obtained data can be checked.

(5) As the algorithm is easily programmable, the hot air method also becomes less cumbersome. A programme in FORTRAN 77 is available upon request.

ACKNOWLEDGEMENTS

The authors are greatly indebted to prof. W.H. van der Molen for his valuable comment, to Mrs. Joy Burrough-Boenisch for correcting and editing the English and to Mr. P.J. Haringhuizen and Mr. J.S. Jens for their assistance with the computer and in the laboratory.

LIST OF SYMBOLS

Symbol	Description	Dimension
b	parameter of moisture distribution curve	L
$D(\theta)$	diffusivity of soil moisture	$L^2 T^{-1}$
E	depth of evaporated moisture	L
k	hydraulic conductivity	$L T^{-1}$
K	half of interquartile range	—
M	median	—

n	parameter of moisture distribution curve	—
s	standard deviation	—
S	sum of squares of residuals	—
t	time of moisture diffusion	T
x	distance from the evaporating surface	L
θ	volumetric moisture content per unit volume of soil	—
$\Theta = \frac{\theta_i - \theta}{\theta_i - \theta_0}$	relative moisture deficit	—
λ	Boltzmann parameter	L T ^{-1/2}
ψ	pressure head (negative in unsaturated soil)	L
<i>indices</i>		
i	initial condition	
0	air-dry value	
c	computed value	
m	measured value	

REFERENCES

- Arya, L.M., Farrell, D.A. and Blake, G.R., 1975. A field study of soil water depletion patterns in presence of growing soybean roots: part I: Determination of hydraulic properties of the soil. *Soil Sci. Soc. Am. J.*, 39: 424-430.
- Bouma, J., Hillel, D.I., Hole, F.D. and Amerman, C.R., 1971. Field measurements of unsaturated hydraulic conductivity by infiltration through artificial crusts. *Soil Sci. Soc. Am. Proc.*, 35: 362-364.
- Bouma, J., De Gruijter J. and Stoffelsen, G.H., 1979. The variability of the k - ψ relationship for sandy loam and heavy clay soils, measured by means of the hot air method. (De variabiliteit van de k - ψ relatie in lichte zavel en zware klei, gemeten met behulp van de hete lucht methode.) *Cultuurtech. Tijdschr.*, 19(3): 121-131 (in Dutch).
- Bruce, R.R. and Klute, A., 1956. The measurement of soil moisture diffusivity. *Soil Sci. Soc. Am. J.*, 20(4): 458-462.
- Gardner, W.R., 1959. Solutions of flow equations for the drying of soils and other porous media. *Soil Sci. Soc. Am., Proc.*, 23: 183-187.
- NAGFLIB (Numerical Algorithms Group), 1983. Fortran Library Manual Mark 11, Vol. 3, E04, JAF, Mayfield House, Oxford.
- Nielsen, D.R., Bigger, J.W. and Erh, K.T., 1973. Spatial variability of field measured soil water movement. *Hilgardia*, 42: 215-259.
- Van den Berg, J.A. and Louters, T., 1985. Towards representing soil moisture conditions of catchments. In: *Problems of Regional Hydrology. Proc. Freiburg Symp. Beiträge zur Hydrologie*, Sonderh. no. 5-1 and 5-2.

4. **THE VARIABILITY OF SOIL MOISTURE DIFFUSIVITY OF LOAMY TO SILTY SOILS ON MARL, DETERMINED BY THE HOT AIR METHOD**

Published in: Journal of Hydrology 97 (1988), 235-250.
Permission for publication 14 July 1989.

[5] 0022-1694/88/\$03.50 © 1988 Elsevier Science Publishers B.V.

THE VARIABILITY OF SOIL MOISTURE DIFFUSIVITY OF LOAMY TO SILTY SOILS ON MARL, DETERMINED BY THE HOT AIR METHOD

JAN A. VAN DEN BERG and TEUNIS LOUTERS*

Department of Physical Geography, Geographical Institute, University of Utrecht, Heidelberglaan 2, 3508 TC Utrecht (The Netherlands)

(Received June 1, 1987; accepted for publication June 10, 1987)

ABSTRACT

Van den Berg, J.A. and Louters, T., 1988. The variability of soil moisture diffusivity of loamy to silty soils on marl, determined by the hot air method. *J. Hydrol.*, 97: 235-250.

Various attempts have been made to estimate hydraulic characteristics from textural soil properties, often by testing models on materials with artificial packing. The latter approach prevented soil structure and the arrangement and orientation of soil particles from being taken into account.

In this paper the moisture diffusivity (in short "diffusivity") characteristics of loamy to silty soils with intermediate soil moisture contents are examined. The relationship between diffusivity and soil moisture content was determined by the hot air method on undistributed soil cores from eight different sites in the Ardeche Basin, France.

Our objectives were: (1) to obtain reproducible diffusivity values; (2) to distinguish between the natural and procedural variability; (3) to examine the spatial variability; and (4) to discuss whether soil texture can be used to distinguish between the diffusivities of different loamy soils.

As for problems of regionalization, it was found that the diffusivity of these soils can be related to the physiographic diversity of the area, rather than to soil texture.

INTRODUCTION

Loamy to silty soils have drawn man's attention because of their fertility and good storage capacity for available soil water as well as because of their erodibility and vulnerability to human activity. Simulation of the moisture regime by means of a computer model would be a valuable tool for gaining a comprehensive view of the suitability and erodibility of these soils with regard to their use for agriculture or as nature reserves under the prevailing, local conditions (e.g. climate and slope).

The reliability of the numerical modelling of soil water largely depends on the validity of the hydraulic relations employed. Among these, the relationship between soil moisture and diffusivity is of special importance.

* Present address: Ministry of Transport and Public Works, Tidal Waters Division, Van Alkemade-laan 400, 2500 EX Den Haag (The Netherlands).

NOTATION

Symbol	Description	Dimension
b	parameter of moisture distribution curve	L
$D(\theta)$	diffusivity of soil moisture	$L^2 T^{-1}$
E	total evaporation	L
h	pressure head	L
n	parameter of moisture distribution curve	—
$S = \frac{(\theta - \theta_r)}{(\theta_s - \theta_r)}$	relative saturation	—
t	time of moisture diffusion	T
x	distance from the evaporating surface	L
θ	volumetric moisture content per unit volume of soil	—
<i>indices</i>		
i	initial condition	
o	air-dry value	
r	residual value	
s	saturated value	

The following brief review of the literature shows that different efforts have been made to estimate unsaturated hydraulic conductivity and other hydraulic characteristics from textural soil properties. The first step was sixty years ago, when the relationship between intrinsic saturated permeability and particle size was investigated; Kozeny's formula is an example of this development. Later, Childs and Collis-George (1950) and Marshall (1958) related permeability to the pore-size distribution. This relation became usable in practice after a pore-size distribution index which could be related to the measured soil-moisture retention curve was introduced (Brooks and Corey, 1964; Brutsaert, 1966). The development of techniques enabling the soil moisture regime to be simulated with the help of the computer led to a proliferation of similar concepts e.g.: Hillel (1971), Campbell (1974), Mualem (1976), Haverkamp et al. (1977), Clapp and Hornberger (1978), D'Hollander (1979), Van Genuchten (1980) and Rawls et al. (1983).

Some authors classified the parameters according to the textural triangle of the U.S. Department of Agriculture (Clapp and Hornberger, 1978; Rawls et al., 1983). This provoked a trend to relate all physical and hydraulic properties to soil texture (Clapp and Hornberger, 1978; Brakensiek et al., 1981; McCuen et al., 1981; Rawls et al., 1983). Grismer (1986) assessed the dependence of infiltration rate on changes in pore-size distribution of soils. The determination of the soil moisture characteristic from soil texture and bulk density received particular attention (Hillel, 1971; Gupta and Larson, 1979; Ghosh, 1980; Arya and Paris, 1981). Soil moisture diffusivity, defined by Childs and Collis-George

(1950) as the product of hydraulic conductivity and the slope of the moisture characteristic, was approximated by mathematical formulae (e.g., Abuja and Schwartzendruber, 1972; Murali et al., 1979; Vauclin and Haverkamp, 1985), or calculated from mathematical or differentiable expressions for conductivity and moisture retention, e.g. Van Genuchten (1980). Various authors put forward methods for measuring diffusivity on soil in-situ or on soil cores, e.g. Gardner (1960), Bruce and Klute (1956), Arya et al. (1975).

In this paper, attention is focused on the regionalization of the diffusivity characteristic of loamy to silty soils (loam, silty loam or silty clay-loam) for intermediate soil moisture contents. In this range of moisture contents, the diffusivity can be determined by the hot air method introduced by Arya (Arya et al., 1975). With respect to the boundary conditions that have to be fulfilled for the hot air method (Van Grinsven et al., 1985) loamy soils are more suitable than other soils. The parameters of soil water flow were studied on several sites with loamy soils on marly bedrock in the Ardeche Basin.

Our objectives were fourfold: (1) to obtain reproducible diffusivity values with an algorithm for the hot air method (Van den Berg and Louters, 1986a); (2) to distinguish between the natural variability and the variability resulting from the hot air method; (3) to examine the spatial variability of the diffusivity characteristics (Nielsen et al., 1973); and (4) to question whether soil texture can be accepted as discriminatory for the diffusivity of different loamy soils.

PROBLEMS OF CONCEPTUALIZATION

In general, the approaches cited above are based on the assumption that the soil particles and pores can be described by their radii and that pore space is distributed randomly. This scant regard for the arrangement of pores and soil structure means that neither heterogeneity nor anisotropy can be taken into account. An X-ray analysis of the soils studied, indicated the presence of 13–20% of clay minerals, of which 50–60% were smectites. The concept of soil water flow through compound pores between spherical soil particles is inadequate to describe the water movement between clay platelets. Moreover, lamellar particles are also supposed to occur in the silt fraction of soils, e.g. because of the ion-exchange capacity of these particles (Wiklander, 1965; Ruellan and Delétange, 1967). Some authors have indeed stipulated that their model should be restricted to sandy soils: "For a nonshrinking material such as sand, the pore-size distribution may be derived satisfactorily from the moisture characteristic" (Childs and Collis-George, 1950, p. 396); "With porous media that are stable in the presence of water, permeability is a function of the geometry of the media" (Brooks and Corey, 1964, V). Marshall (1958, p. 1 and 2) also applied his concept to sand only. Most authors tested their model on artificially packed cores of soil or even of synthetic materials. Artificial packing of natural soil material results in the loss of information about soil structure and the original arrangement and orientation of soil particles.

As for the hot air method, the comparability of the results obtained by

different authors is questionable, because the graphical computation of the diffusivity obtained by this method is subjective (Van den Berg and Louters, 1986a). The use of soil texture or pore-size distribution for modelling hydraulic parameters only yields indirect information about their variability. If the hot air method is correctly applied to undisturbed soil cores, then whether the variability within one texture class or within a group of associated textures is due to natural variability or to the procedures followed, remains an important question. Procedural variability can be caused by sampling (e.g. compressing or fissuring the soil), treatment in the laboratory (Van Grinsven et al., 1985), and the interpretation of the moisture distribution in the cores after superficial drying. The latter source of variability may be minimized by using a suitable algorithm. As the variability in the results obtained from the hot air method cannot be subdivided into a natural and a procedural part, fifteen replicates from an apparently homogeneous soil (a loam at sample site 1, Fig. 1) were taken in our research, in order to minimize the natural variability. The results were compared with 45 samples from ten other sites or horizons of soils classified as loam, silt loam or silty clay-loam. For the sake of contrast four

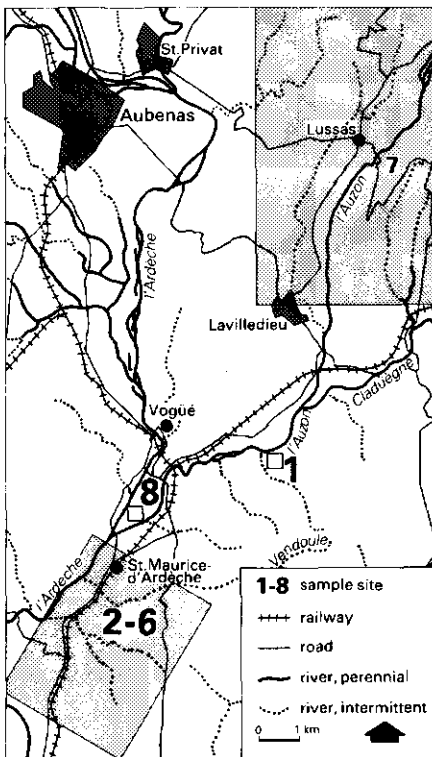


Fig. 1. Location of the eight sample sites within the Ardèche Basin, southern France. Details and lithology of the dotted areas are given in Figs. 2a and b.

samples from a sandy loam (Ardeche alluvium, site 8) were included in the analysis (Table 1).

EDAPHIC AND GEOMORPHOLOGICAL PROPERTIES OF THE SAMPLE SITES

The bedrock of the sample sites 1–7 (Fig. 2) consists of Lower Cretaceous marl, dipping slightly southeast ($12\text{--}18^\circ$). The marl is banded and irregularly intercalated with limestone layers that vary in thickness from a few millimetres to several decimetres. Where gullies have been formed, a layer of fresh limestone acts as a local base level of erosion. Most of the sample sites (Fig. 2, sites 4–7) were on the gently concave lower section of west-facing slopes on marly bedrock with a slope angle of about 6° , at the foot of a steeper ridge of limestone. These slopes can be classified as cryopediments, a periglacial analogue of the pediments or glacis of arid and semiarid regions (Czudek and Demek, 1973; Washburn, 1979). Cryopediments have a slope angle between 3 and 10° and are considered to be denudation surfaces developed by slope processes under periglacial conditions (Czudek and Demek, 1973; French, 1973).

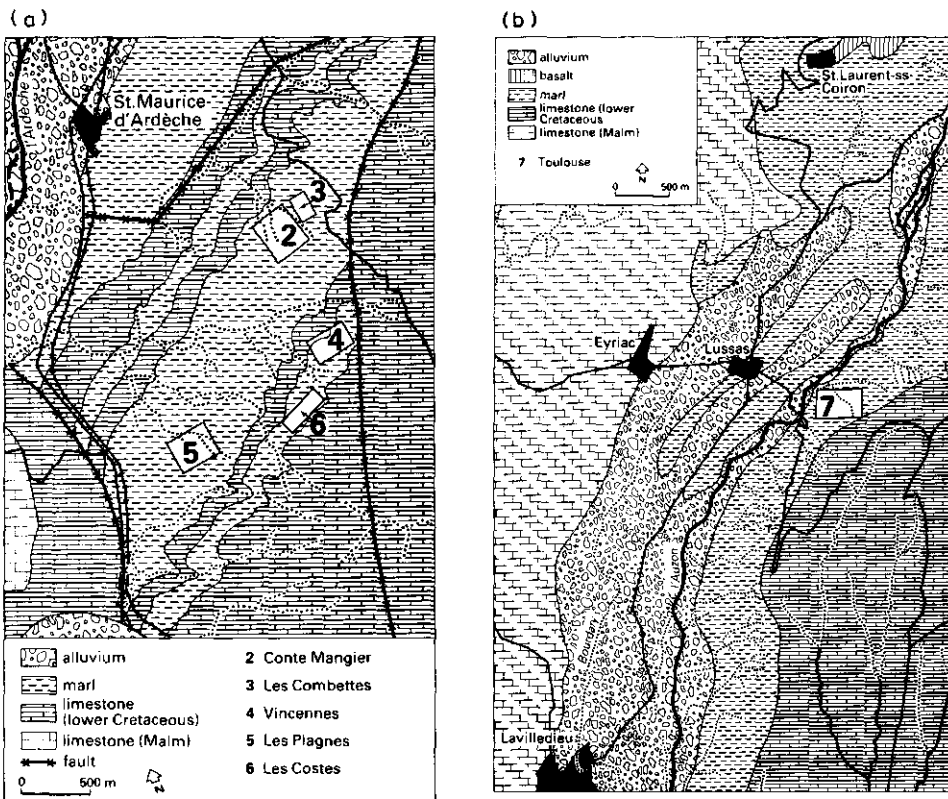


Fig. 2. (a) Lithology and location of sample sites 2–6. (b) Lithology and location of sample site 7.

All sample sites show evidence of former agricultural use, but nowadays sites 2-7 are only extensively grazed; sites 1 and 8 are used for viticulture. Their geological structure and the long period that they have been settled and used for agriculture (evidence of Palaeolithic man has been found in the Ardeche Basin; Bozon, 1974) fostered the erosion of the pediments, which are now intersected by gullies. In the past, terraces were built for erosion control (Blanc, 1984). Mass movements have occurred, for instance at sample site 7. Remnants of slope deposits have been found in only one sample site, in the key area 1 (Fig. 1) beside the Auzon River. Here, the apparently homogeneous deposits of a mudflow are present between two debris flows, all of them probably of Pleistocene origin and undercut by the Auzon River. The surroundings of sample site 3 (Fig. 2a) have been dissected by deep gullies cut in weathered marl. The drainage of the second-order subcatchment of Conte Mangier (site 2) is predominantly joint-controlled. The valley has been terraced almost completely. Sample site 2 is located on the terraced valley slope of this subcatchment. The nature of soils and deposits at the sample sites seems to be related to the lithology of the subsoil and past agricultural practices. According to the USDA Soil Taxonomy classification (Soil Survey Staff, 1975), the marly, loamy soils, which are mostly poorly developed, can be classified as haploxerolls to xerochrepts; the texture varies between loam, silt loam and silty clay-loam (Fig. 3). Table 1 gives certain physical characteristics of the soil of the sample sites, such as the mean and variance of bulk density and of

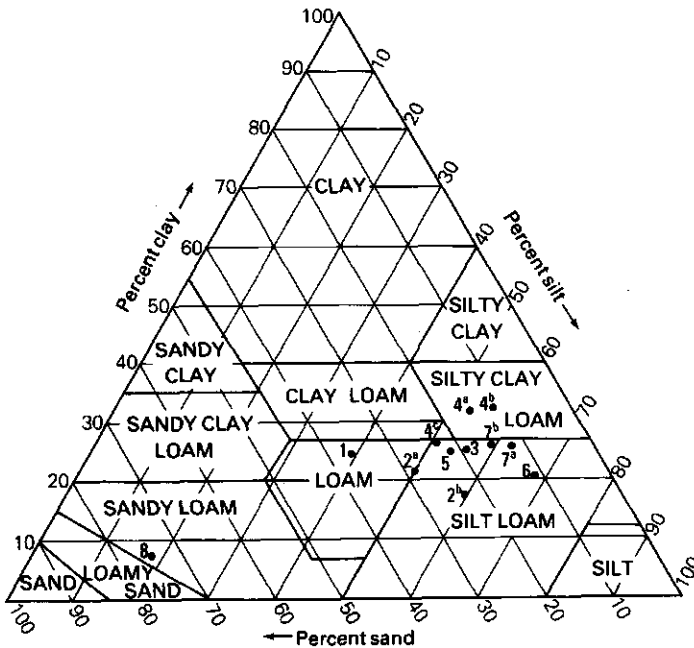


Fig. 3. Soil texture of all plots according to USDA classification.

TABLE 1

Soil physical characteristics of the plots and number of preselected soil cores sampled for $D-\theta$

Plot number	Number of cores	Site	Depth (m)	Soil hor.	Soil texture	Bulk density (d) ($\text{kg m}^{-3} \times 10^{-3}$)			Porosity (p) (volumetric fraction)		Vol. fraction*	
						n	\bar{d}	s_d	n	\bar{p}		s_p
1	15	Auzon	1.9-2.3	C	loam	5	1.45	0.08	5	0.41	0.02	0.23
2a	3	Conte Mangier, soil	0.0-0.4	Ap	loam/silt loam	28	1.33	0.08	23	0.44	0.03	0.27
2b	7	Conte Mangier, marl	0.65-1.4//	R	silt loam	15	1.60	0.09	6	0.38	0.03	0.25
3	7	Combettes	0.6-0.7	C	silt loam/silty clay-loam	10	1.69	0.10	16	0.34	0.04	0.23
4a	8	Vincennes 1	0.0-0.4	A/C	silty clay-loam	23	1.45	0.04	20	0.43	0.17	0.21
4b	2	Vincennes 1	0.4-0.5	C	silty clay-loam	8	1.50	0.05	10	0.42	0.02	0.21
4c	2	Vincennes 2	0.4-0.5	C	silt loam/loam/clay-loam	5	1.54	0.07	5	0.40	0.02	0.22
5	8	Plagnes	0.2-0.45	C	silt loam	30	1.48	0.07	13	0.38	0.05	—
6	2	Costes	0.1-0.3	C	silt loam	35	1.47	0.07	43	0.39	0.03	—
7a	3	Toulouse 1	0.2-0.4	C	silt loam/silty clay-loam	18	1.56	0.03	18	0.38	0.02	0.21
7b	3	Toulouse 2	0.2-0.35	C	silt loam/silty clay-loam	14	1.54	0.06	14	0.38	0.02	0.22
8	4	Ardeche	0.3-0.6	C	sandy loam/(loamy sand)	4	1.28	0.04	1	0.47	—	0.35

* Volumetric soil water content between suction heads of 3.1 and 1554 kPa. n = number of replicates; // = parallel to stratification.

porosity, and the difference in pore water content between soil moisture tensions of 3.1 kPa and 1554 kPa.

THEORY AND PRACTICE OF THE HOT AIR METHOD

The hot air method can be considered as the desorption equivalent of the Bruce and Klute (1956) method for measuring D -theta during adsorption:

$$D(\theta) = \frac{1}{2t} \frac{dx}{d\theta} \int_{\theta_0}^{\theta_i} x d\theta \quad (1)$$

where $D(\theta)$ is the soil moisture diffusivity (L^2T^{-1}), x is the distance from the evaporating surface (L), θ is the volumetric moisture content and t is total drying time (T). The index i refers to the initial boundary conditions of θ , which has to be constant throughout the soil at the beginning: $\theta = \theta_i$ at $t = 0$ and all $x \geq 0$. To solve eqn. (1) a second boundary condition is formulated: $\theta = \theta_0$ at $x = 0$ and $t \geq 0$. This implies that the surface of the soil sample dries immediately to the air-dry value θ_0 . If the θ - x profile is known, the right-hand side of eqn. (1) can be calculated numerically.

As recently proposed by the authors (Van den Berg and Louters, 1986a) the x - θ profile obtained experimentally can be described by:

$$\theta = \theta_i - \frac{(\theta_i - \theta_0) \cdot b^n}{(x + b)^n} \quad (2)$$

where b represents a translation and n influences the deflecting rate of the curve. Parameter b has the dimension of length and n is dimensionless. Both parameters, which can be obtained by the least squares method, are not constant, because they depend on the drying time t .

Calculating the tangent to and the area under eqn. (2), and substituting them in eqn. (1) yields:

$$D(\theta) = \frac{1}{2t} \frac{(nx + b)(x + b)}{n(n - 1)} \quad (3)$$

If the parameters n and b are computed, the measured total evaporation can be checked, because eqn. (2) enables the total evaporation E (L) to be calculated according to:

$$E = \frac{b}{n - 1} (\theta_i - \theta_0) \quad (4)$$

All soil samples were prewetted by saturating them and then putting them on a sandbox at a suction between 3.9 (Ardèche alluvium) and 9.8 kPa for at least one week, during which the water was allowed to equilibrate in the sample.

Then one side of the soil core was heated by a forced hot air stream for a short time t in order to evaporate water from the surface of the core. The air temperature near the evaporating surface was 180°C.

Conduction of heat through the surrounding steel cylinder was minimized by means of a water-cooled heat shield around its top. The drying time in our 64 experiments varied between 12 and 20 min. Loss of weight of the core during evaporation was determined by repeatedly weighing the soil core; the cumulative evaporation appeared to be proportional to the square root of time (Fig. 4). After the drying had been stopped, the moisture distribution was ascertained by measuring the moisture content within the thin slices into which the soil core was divided. Using the algorithm, a monotonously rising curve was calculated through the measured data by optimizing the parameters n and b from eqn. (2) (Fig. 4). This curve was plotted, to check the measured data; unreliable data were discarded. In cases where the optimized curve systematically differed from the x - θ profile, the n and b parameters from eqn. (1) were adjusted slightly. Values of 0.0 to 0.02 were used for the air-dry value θ_0 .

EXPERIMENTAL PROCEDURE AND DATA SELECTION

In this study, soil cores were sampled from eight sites (Figs. 1, 2a and b), seven of which were located in loamy to silty soils developed from marls and one in an alluvial sandy loam. Sites 2, 4 and 7 were subdivided into various plots. At site 2, the soil as well as three underlying layers of weathered marl were sampled; at sites 4 and 7 two adjacent plots were selected (Table 1).

The data on each core were screened to ascertain if there was a regular increase in the moisture content as the distance from the evaporating surface increased (x - θ curve) and if the initial moisture content at the end of this curve was well approximated. An irregular increase of moisture content was usually caused by stones in the soil matrix. Though the HOTAIR algorithm (Van den

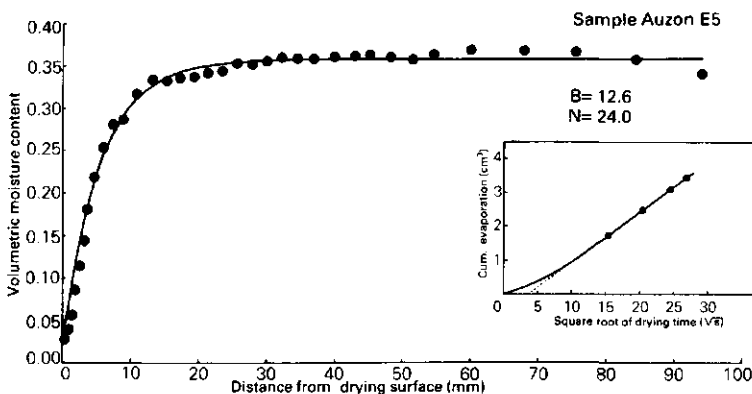


Fig. 4. Measured and computed moisture distribution in a core of loamy soil (site 1) after 12 min of drying time. Insert: cumulative evaporation as a function of the square root of drying time.

Berg and Louters, 1986b) is able to correct for this, it is only meaningful to do so if the stones are small. Large stones may influence the moisture distribution too much. Samples where the moisture content at the bottom of the core did not reach the initial value were also discarded; these cores had probably been heated for too long.

After this screening, the diffusivities for each of the remaining 64 cores were calculated with the HOTAIR algorithm for a range of volumetric moisture contents between 0.1 and 0.3. For the loamy to silty soils this range corresponds with relative saturations of about 24–72%. Three plots (2a, 3 and 4) proved to contain a core whose calculated diffusivities for the whole range of moisture contents had to be considered as outliers. Furthermore, in one core from plot 1, significant deviation was only found at moisture contents above 0.26 (Kolmogorov–Smirnov test). Such outliers disturb analysis of variance, and the data on these four cores were therefore discarded.

As the diffusivities calculated for the cores from sites 5 and 6 matched well, the data on these sites were combined, except for the test on the relationship with texture.

RESULTS AND DISCUSSION

After this selection, we were left with 60 cores from the twelve different plots. The mean, standard error of the mean and the variation coefficient of the calculated diffusivities of these cores are shown in Table 2 for eleven moisture contents between 0.1 and 0.3.

Comparing variability of the diffusivity within each plot, the Auzon site (plot 1) shows the lowest standard error of the mean for each moisture content within the range under consideration. The combined data of Plagnes (plot 5) and Costes (plot 6) also have a low standard error and variation coefficient, which corresponds with the fact that in the field both sites were judged as being rather homogeneous.

The coefficient of variation can only be examined in the five plots with six or more replicates (1, 2b, 3, 4a and 5 + 6), because this coefficient is not a reliable criterion in plots with fewer replicates. The mudflow at plot 1 (Table 2) shows the lowest variability, as well as a very constant coefficient of variation of 25%. Assuming that there is some natural variability, it may be concluded that the procedural variability inherent in the hot air method and in the HOTAIR algorithm amounts to less than 25% of the mean diffusivity.

Four plots have a high standard error of the mean: plots 2b, 3, 4c and 7a. If the standard error is considered to be an index of nonuniformity (Druyan et al., 1986), the high standard error in three of them can be explained by heterogeneity of soil and rock: plot 2b contains soil cores from three consecutive layers of weathered marl that showed different hydraulic behaviour under saturated conditions; at plots 3 and 7a, the soil was formed in a marl that was locally intercalated by platy layers with a higher carbonate content.

The spatial variability of diffusivity was examined by analysis of variance

TABLE 2

Mean, standard error of the mean and variation coefficient of soil moisture diffusivity ($m^2 d^{-1} \times 10^{-4}$)

Plot number	Site	Depth (m)	Selected no. of cores	Volumetric soil moisture content										
				0.10	0.12	0.14	0.16	0.18	0.20	0.22	0.24	0.26	0.28	0.30
1	Auzon	1.9-2.3	14	16.76	17.95	19.27	20.75	22.42	24.35	26.62	29.36	32.81	37.81	44.24
				1.10	1.18	1.26	1.36	1.47	1.61	1.76	1.96	2.21	2.57	3.16
2a	Conte Mangier, soil	0.0-0.4	3	0.244	0.245	0.245	0.245	0.245	0.246	0.247	0.249	0.251	0.256	0.287
				14.87	15.98	17.22	18.63	20.25	22.15	24.45	27.35	31.24	37.15	50.75
2b	Conte Mangier, marl	0.65-1.4	6	0.281	0.281	0.282	0.283	0.284	0.286	0.289	0.293	0.298	0.304	0.406
				21.01	22.28	26.01	29.36	33.58	39.08	46.37	57.41	74.60	106.18	185.91
3	Combettes	0.6-0.7	6	0.576	0.545	0.511	0.474	0.434	0.392	0.352	0.318	0.301	0.311	0.382
				28.34	30.63	33.22	36.19	39.67	43.81	48.90	55.43	64.32	77.84	105.05
4a	Vincennes 1	0.0-0.4	8	0.381	0.388	0.385	0.381	0.377	0.373	0.369	0.364	0.361	0.361	0.392
				23.01	24.56	26.26	28.16	30.30	32.74	35.58	38.94	43.06	48.33	55.57
4b	Vincennes 1	0.4-0.5	2	0.298	0.298	0.299	0.300	0.301	0.303	0.304	0.306	0.308	0.312	0.316
				12.45	13.30	14.25	15.30	16.50	17.88	19.49	21.45	23.93	27.31	32.70
4c	Vincennes 2	0.35-0.45	2	0.343	0.337	0.330	0.322	0.313	0.302	0.289	0.271	0.245	0.203	0.118
				39.70	42.57	45.76	49.35	53.45	58.21	63.85	70.74	79.49	91.32	109.09
5 + 6	Plagnies and Costes	0.1-0.45	10	0.199	0.195	0.191	0.185	0.179	0.172	0.164	0.154	0.142	0.136	0.103
				16.42	17.59	18.89	20.34	21.99	23.90	26.13	28.81	32.16	36.54	42.80
7a	Toulouse 1	0.2-0.4	3	0.311	0.311	0.312	0.313	0.313	0.314	0.315	0.317	0.318	0.318	0.319
				1.62	1.74	1.87	2.01	2.18	2.38	2.61	2.89	3.24	3.69	4.32
7b	Toulouse 2	0.2-0.35	3	0.368	0.368	0.368	0.368	0.368	0.368	0.368	0.368	0.368	0.368	0.368
				20.18	21.54	23.04	24.70	26.57	28.70	31.16	34.08	37.63	42.16	48.33
8	Ardeche	0.3-0.6	3	0.195	0.197	0.199	0.202	0.204	0.208	0.212	0.217	0.224	0.233	0.249
				48.86	57.38	68.38	82.94	102.83	131.08	173.26	240.75	359.87	605.12	1275.9
				8.94	10.70	13.02	16.20	20.71	27.39	37.92	55.94	90.62	171.05	435.3
				0.316	0.322	0.329	0.338	0.348	0.361	0.379	0.402	0.436	0.489	0.590

TABLE 3

F-values of analysis of variance of soil moisture diffusivities for eleven different moisture contents at degrees of freedom d1 and d2, ($\alpha = 0.05$)

Grouping	d1	d2	Volumetric soil moisture content											
			0.10	0.12	0.14	0.16	0.18	0.20	0.22	0.24	0.26	0.28	0.30	
Group 1 with 4a	5	34	2.62	2.57	2.50	2.43	2.36	2.27	2.16	2.03	1.86	1.62	1.27	2.50
Group 1 without 4a	4	27	0.96	0.94	0.92	0.90	0.87	0.84	0.80	0.75	0.68	0.60	0.64	2.74
Group 2 with 4a	4	20	1.79	1.74	1.70	1.67	1.66	1.71	1.88	2.33	3.38	5.61	8.66	2.87
Group 2 without 4a	3	13	1.63	1.52	1.40	1.26	1.10	0.92	0.76	0.72	1.06	2.29	4.47	3.41

between plots for eleven different moisture contents (Table 3). According to this analysis, plots 1, 2a, 4a, 4b, 5 + 6, and 7a (Table 2) can be considered as one group (Group 1) the means of which do not differ significantly for moisture contents from 0.16 upwards. If plot 4a is deleted from this group, the F values for the whole range of θ are low (below unity) and the critical value at the 5% value is 2.74. Plots 2b, 3, 4a, 4c and 7b act as another population (Group 2) for moisture contents up to 0.26, and without plot 4a for the whole range of θ . Group 3 consists of the data on the sandy loam of site 8 (Fig. 5).

What features do each of these groups have in common? The soils sampled in the plots of the first group are all in-situ or have been undisturbed for some time. Plot 1 is on a mudflow of Pleistocene age, and plot 2 has not been cultivated for over fifty years (Van den Berg and Louters, 1985). Site 4 indicates the impact of vegetation. In one location (Vincennes 1, plots 4a and 4b) a substantial decrease in root density occurred at a soil depth between 0.35 and 0.4 m. This may explain the position of plot 4b in group 1 and of plot 4a somewhere in between both groups. In the other location, (Vincennes 2, plot 4c, Group 2) roots penetrated below 0.4 m.

As for group 2, note that the diffusivities of most plots have a higher standard error of the mean than in group 1. For plot 2b, the higher level of the diffusivity may be explained by anisotropy, because the soil cores were sampled parallel to the stratification of the marl and particle orientation. Plot 7b was located where evidence of recent mass movement could be found. At plot 4c a loose soil structure was found to a depth of more than 0.4 m; this might be the result of a superficial landslide (Van den Berg and Louters, 1985).

Within the limited range of loamy to silty soils we studied, neither texture

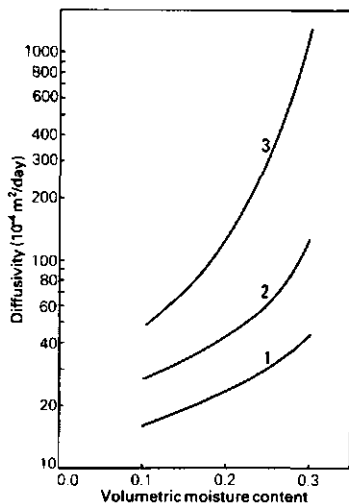


Fig. 5. Soil moisture diffusivity characteristics for the three groups of sample plots distinguished by the analysis of variance. Groups 1 and 2 cover the same textural range of loamy to silty soils; group 3 comprises the sandy loam.

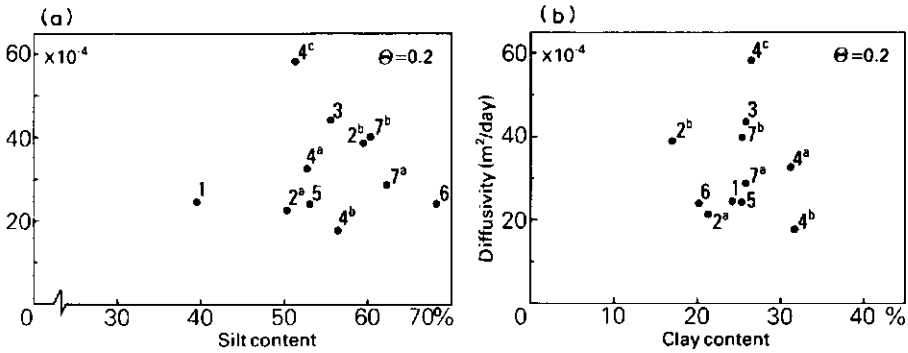


Fig. 6. Correlation between diffusivity (at $\theta = 0.20$) and silt content (a) and clay content (b) for the loamy to silty soils of sites 1-7.

nor bulk density was found to be correlated with diffusivity. For texture, this noncorrelation is shown in Fig. 6 for diffusivities at a moisture content of 0.2. When the soils were grouped into textural categories according to the USDA classification (Fig. 3), the Scheffé test of contrasts (Scheffé, 1959; Dawkins, 1968) gave no significant relationship between diffusivity and texture. It can be concluded that within the range from loam to silt loam and silty clay loam, texture is not discriminating for diffusivity.

Our findings indicate that for regionalization within areas with loamy to silty soils, areal variability of diffusivity should be related to physiographic diversity such as slope instability and heterogeneity of petrofabric and soil structure. Curves 1 and 2 depicted in Fig. 5, cover the same textural range of loamy to silty soils but were distinguished by the analysis of variance. The ratio between both group means of diffusivity increases from 1.5 at $\theta = 0.1$ to about 3.0 at $\theta = 0.3$.

Curve 1 seems an appropriate diffusivity characteristic of loamy to silty soils in a physiographically homogeneous area, and curve 2 seems to be ditto for heterogeneous sites (i.e. group 1 and 2, respectively, in Table 4). Texture is still a differentiating factor between the diffusivities of the loamy to silty soils and a sandy loam of site 8 (Fig 5).

TABLE 4

Mean diffusivity ($m^2 d^{-1} \times 10^{-4}$) of loamy to silty soils grouped according to physiographic diversity of the sample plot

Group	Volumetric soil moisture content										
	0.10	0.12	0.14	0.16	0.18	0.20	0.22	0.24	0.26	0.28	0.30
1	16.5	17.7	19.0	20.4	22.1	24.0	26.2	29.0	32.4	36.9	44.1
2	27.1	29.4	32.0	35.0	38.7	43.2	48.8	56.5	67.6	85.9	127

ACKNOWLEDGEMENTS

The authors are greatly indebted to Prof. W.H. van der Molen for his comments and Mr. A. Romein for X-ray analysis.

REFERENCES

- Ahuja, L.R. and Schwartzendruber, A., 1972. An improved form of soil-water diffusivity function. *Soil Sci. Am., Proc.*, 36: 9-14.
- Arya, L.M. and Paris, J.F., 1981. A physico-empirical model to predict the soil moisture characteristic from particle-size distribution and bulk density data. *Soil Sci. Soc. Am., J.*, 45: 1023-1030.
- Arya, L.M., Farrell, D.A. and Blake, G.R., 1975. A field study of soil water depletion patterns of growing soybean roots; part I: Determination of hydraulic properties of the soil. *Soil Sci. Soc. Am., Proc.*, 35: 362-364.
- Blanc, J.-F., 1984. *Paysages et paysans des terrasses de l'Ardèche. l'Imp. du Vivarais, Annonay*, 321 pp.
- Bozon, P., 1974. *Histoire du peuple Vivarais. Imp. Réunies, Valence*, 278 pp.
- Brakensiek, D.L., Engleman, R.L. and Rawls, W.J., 1981. Variation within texture classes of soil water parameters. *Trans. ASAE*, 24(2): 335-339.
- Brooks, R.H. and Corey, A.R., 1964. Hydraulic properties of porous media. *Colorado State Univ., Fort Collins. Hydrol. Pap. 3*: 27 pp.
- Bruce, R.R. and Klute, A., 1956. The measurement of soil moisture diffusivity. *Soil Sci. Soc. Am., J.*, 20(4): 458-462.
- Brutsaert, W., 1966. Probability laws for pore-size distributions. *Soil Sci.*, 101: 85-92.
- Campbell, G.S., 1974. A simple method for determining unsaturated conductivity from moisture retention data. *Soil Sci.*, 117: 311-314.
- Childs, E.C. and Collis-George, N., 1950. The permeability of porous media. *Proc. R. Soc. London, Ser. A*, 201: 392-405.
- Clapp, R.C. and Hornberger, G.M., 1978. Empirical equations for some soil hydraulic properties. *Water Resour. Res.*, 14(4): 601-604.
- Czudek, T. and Demek, J., 1973. The valley cryopediments in eastern Siberia. *Biul. Peryglacjalny*, 22: 117-130.
- Dawkins, H.C., 1968. *Starforms. Commonw. For. Inst., University of Oxford*.
- D'Hollander, E.H., 1979. Estimation of the pore size distribution from the moisture characteristic. *Water Resour. Res.*, 15(1): 107-112.
- Druyan, L.M., Goldreich, Y. and Mishaeli, Y., 1986. Characteristics of mesoscale precipitation patterns. *Phys. Geogr.*, 7(1): 25-45.
- French, H.M., 1973. Cryopediments on chalk of southern England. *Biul. Peryglacjalny*, 22: 149-156.
- Gardner, W.R., 1960. Measurement of capillary conductivity and diffusivity with a tensiometer. *Trans. 7th Int. Congr. Soil Sci., Madison, Wisc.*, 1 (29): 300-305.
- Ghosh, R.K., 1980. Estimation of soil-moisture characteristics from mechanical properties of soils. *Soil Sci.*, 130(2): 60-63.
- Grismer, M.E., 1986. Pore-size distribution and infiltration. *Soil Sci.*, 141(4): 249-260.
- Gupta, S.C. and Larson, W.E., 1979. Estimating soil water retention characteristics from particle size distribution, organic matter percent and bulk density. *Water Resour. Res.*, 15(6): 1633-1635.
- Haverkamp, R., Vauclin, M., Bouma, J., Wieringa, P.J. and Vachaud, G., 1977. A comparison of numerical simulation models for one-dimensional infiltration. *Soil Sci. Soc. Am., J.*, 41: 286-294.
- Hillel, D., 1971. *Soil and water: Physical principles and processes. Academic Press, New York, N.Y.*, 228 pp.
- Marshall, T.J., 1958. A relation between permeability and size distribution of pores. *J. Soil Sci.*, 9: 1-8.
- McCuen, R.H., Rawls, W.J. and Brakensiek, D.L., 1981. Statistical analysis of the Brooks-Corey and the Green-Ampt parameters across soil textures. *Water Resour. Res.*, 17(4): 1005-1013.

- Mualem, Y., 1976. A new model for predicting the hydraulic conductivity of unsaturated porous media. *Water Resour. Res.*, 12(3): 513-522.
- Murali, V., Krishna Murti, G.S.R. and Sinha, A.K., 1979. Note on the three-parameter functions for soil water diffusivity-water content relationships. *Aust. J. Soil Res.*, 17: 361-366.
- Nielsen, D.R., Biggar, J.W. and Erh, K.T., 1973. Spatial variability of field measured soil water movement. *Hilgardia*, 42: 215-259.
- Rawls, W.J., Brakensiek, D.L. and Miller, N., 1983. Green-Ampt infiltration parameters from soils data. *J. Hydraul. Eng.*, 109(1): 62-70.
- Ruellan, A. and Delétang, J., 1967. Les phénomènes d'échange de cations et d'anions dans les sols. Initiations-doc. Tech. 5, O.R.S.T.O.M., Paris, pp. 11-28.
- Scheffé, H.A., 1959. *The Analysis of Variance*. Wiley, New York, N.Y., 477 pp.
- Service de la Carte Géologique, 1967. Carte géologique de la France. Feuille Privas 1: 80,000 and note explicative. Minist. Ind., Paris.
- Soil Survey Staff, 1975. *Soil Taxonomy*. Agriculture Handbook 436, U.S.D.A., Washington, D.C.
- Vauclin, M. and Haverkamp, R., 1985. Solutions quasi analytiques de l'équation d'absorption de l'eau par les sols non saturés. I. Analyse critique. *Agronomie*, 5(7): 597-606.
- Van den Berg, J.A. and Louters, T., 1985. Towards representing soil moisture conditions of catchments. In: H.E. Müller and K.R. Nippes (Editors), *Problems of Regional Hydrology*. Proc. Freiburg Symp., Beitr. Hydrol., Sonderh. 5-1 and 5-2.
- Van den Berg, J.A. and Louters, T., 1986a. An algorithm for computing the relationship between diffusivity and soil moisture content from the hot air method. *J. Hydrol.*, 83: 149-159.
- Van den Berg, J.A. and Louters, T., 1986b. HOTAIR, optimizing the D -theta relationship from hot air data. Users manual. Dep. Phys. Geogr., University of Utrecht, 28 pp.
- Van Genuchten, M.Th., 1980. A closed-form equation for predicting the hydraulic conductivity of unsaturated soils. *Soil Sci. Soc. Am., J.*, 44: 892-898.
- Van Grinsven, J.J.M., Dirksen, C. and Bouten, W., 1985. Evaluation of the hot air method for measuring soil water diffusivity. *Soil Sci. Soc. Am., J.*, 49(5): 1093-1099.
- Washburn, A.L., 1979. *Geocryology*. Edward Arnold, London, pp. 237-243.
- Wiklander, L., 1965. Cation and anion exchange phenomena. In: F.E. Bear (Editor), *Chemistry of the Soil*. Reinhold, New York, N.Y., pp. 163-205.

5. WATER RETENTION AND WATER MOVEMENT IN A LOESS SOIL SUBJECT TO VOLUME CHANGE

5. WATER RETENTION AND WATER MOVEMENT IN A LOESS SOIL SUBJECT TO VOLUME CHANGE

Abstract

The determination of the water retention capacity and the soil water diffusivity of a loess soil is complicated, because loess acts as a non-rigid soil. This paper shows how the relationship between diffusivity and hydraulic conductivity for rigid soils can also be used for swelling soils by taking into account the change in total volume caused by change in pressure head (eqns. 5.1, 5.2 and 5.3). In order to apply this relationship the retention and shrinkage characteristics must be known - both as functions of the moisture ratio. The computation can be done more simply if a differentiable relationship can be found between vertical expansion and pressure head (eqns. 5.8 and 5.9). The variable bulk volume also has to be taken into account for the calculation of the moisture distribution generated with the hot air method. The diffusivity for intermediate moisture contents was determined using this method. It appeared to be almost as high as that of a sandy loam. Because the diffusivity of loess is relatively high, on loess soils the hot air method has to be applied within a narrow range of test conditions. The high diffusivity also confirms that soil moisture diffusivity should not be related to soil texture only.

5.1 Introduction

The present study arose from an attempt to check if the procedure of relating soil moisture diffusivity solely to soil texture could be applied to loamy and silty soils. This procedure is frequently advocated in the literature and has recently been discussed by VAN DEN BERG & LOUTERS (1988). In order to enlarge the range of soils studied, an almost completely silty soil obtained by sampling a loess deposit, was examined.

The diffusivity of soil moisture for the intermediate range of soil moisture content was determined by applying the hot air method and the HOTAIR algorithm according to Arya (ARYA et al. 1975) and to VAN DEN BERG & LOUTERS (1986a). Some problems arise when calculating the unsaturated conductivity from the diffusivity and the derivative of the retention curve, because the loess is a swelling soil. (Here, the adjective "swelling" implies "subject to volume change if water is added or removed".)

This chapter establishes how the derivative of the soil moisture pressure head with respect to the volumetric moisture content can be calculated from the suction head - moisture ratio curve and the shrinkage characteristic. The diffusivity and unsaturated conductivity of loess at intermediate moisture content are also reported.

5.2 Theory

In a swelling soil, water intake is accompanied by an increase in bulk volume. In cores sampled for laboratory experiments swelling is restrained laterally by the steel jacket and is permitted in one direction only (i.e. vertically, if the soil cores have been taken in this way). In a soil core the vertical expansion is restricted in a different way than in a natural mass of soil: side friction, which may reach large values in long columns, attenuates volume change in soil cores (DOLEZAL 1976). For non-rigid porous materials self-weight and/or surface loading causes a normal stress that constrains vertical expansion (STIRK 1954). Strictly speaking the void ratio e (volume of voids, V_p /volume of solid, V_s) depends on the moisture ratio ϑ (volume of liquid V_l /volume of solid) as well as on the normal stress, but the effect of normal stress is restricted and negligible for soil cores (PHILIP 1971). Under conditions of normal shrinkage the normal stress also produces the overburden component in the soil moisture pressure head; in small soil cores, however, this component is negligible (SMILES & ROSENTHAL 1968, PHILIP 1969 and 1970).

As SMILES (1976b) explains: "though the behaviour of clay/silt-water systems is fundamentally a result of the consequences of the physical chemistry of the interaction of electrolyte-colloid systems we attempt to treat the system, in the first instance, purely in terms of perceived macroscopic interactions between liquid and solid, i.e. we assume for initial simplicity that the void ratio also parameterises the consequences of the physical chemistry of the system". The moisture retention curve of a swelling soil should be represented by the pressure head h or the suction head H as a function of the moisture ratio ϑ , rather than as a function of the volumetric moisture content Θ (volume of liquid/total volume V_t) (see also SMILES & ROSENTHAL 1968, PHILIP 1971). The reciprocal of the derivative of H with respect to Θ can be written as

$$\frac{d\Theta}{dH} = \frac{1}{V_t} \cdot \frac{dV_l}{dH} - \frac{V_l}{V_t^2} \cdot \frac{dV_t}{dH} \quad (5.1)$$

For rigid media the last term of eqn. (5.1) equals zero. Using the void ratio e eqn. (5.1) can be written as

$$\frac{d\Theta}{dH} = \frac{1}{e+1} \cdot \frac{d\vartheta}{dH} - \vartheta \left[\frac{1}{e+1} \right]^2 \cdot \frac{de}{dH} \quad (5.2)$$

Eqn. (5.2) is applicable if a differentiable regression equation between soil expansion and suction head can be found. Using the chain rule for differentiation eqn. (5.2) can be written as

$$\frac{d\Theta}{dH} = \frac{1}{e+1} \cdot \frac{d\vartheta}{dH} - \vartheta \left[\frac{1}{e+1} \right]^2 \cdot \frac{de}{d\vartheta} \cdot \frac{d\vartheta}{dH} \quad (5.3)$$

Having measured the retention curve H - ϑ and the shrinkage characteristic e - ϑ the derivative of Θ to H can be calculated for each value of Θ as

$$\vartheta = (e+1)\theta \quad (5.4)$$

CHILDS & COLLIS-GEORGE (1950) defined soil moisture diffusivity $D(L^2 T^{-1})$ by

$$D = -k \frac{dH}{d\theta} \quad (5.5)$$

so that

$$k = -D \frac{d\theta}{dH} \quad (5.6)$$

where $k(LT^{-1})$ is the unsaturated conductivity. If the diffusivity is determined k can be computed from the $H(\vartheta)$ and $e(\vartheta)$ curves with eqns. (5.3) and (5.6) or with (5.2) and (5.6) from $H(\vartheta)$ and $e(H)$.

By its definition it will be clear that the dry volumetric bulk density ρ_v (mass of solid/total volume) of a swelling soil is not constant but depends on the moisture content. The actual value of ρ_v can be computed by

$$\rho_v = \rho_s \cdot \left[\frac{1}{e+1} \right] \quad (5.7)$$

where ρ_s is density of solid.

In the hot air method for determining $D-\theta$, ρ_v is used for calculating the generated moisture distribution $\theta-x$ from the slices into which the soil core was cut. The distance x from the beginning of the soil core to the centroid of a slice, and the moisture content θ of that slice should be calculated using a variable ρ_v according to eqn. (5.7).

5.3 Material and methods

To determine the moisture retention characteristic and the dependence of soil water diffusivity upon soil moisture content, soil cores (100 and 200 ml volume, height 50 and 100 mm, 9 and 20 replicates, respectively) were collected at a depth between 3.3 and 3.5 m in the "Belvedere" loess pit near Maastricht in the southeast of the Netherlands. The soil cores did not include macropores.

The loess has been dated to be of Late Weichselian age (17,500 years) by the thermoluminescence dating method (HUXTABLE & AITKEN 1985). It was found to contain 15% carbonate and hardly any organic matter (0.3%); it is rich in silt (2 - 53 μ m: 70.5%), medium in clay (< 2 μ m: 16.6%) and low in fine sand (9.8%). The results of X-ray analysis agree well with these data, giving the following composition: carbonate 10-15%, quartz 65%, clay 15%; as to the particles < 2 μ m the analysis shows that over 50% of the clay consists of smectites. Dr. H.J. Múcher (University of Amsterdam) who has studied the macro- and micromorphology of loess deposits (MÚCHER 1986) examined thin sections of two undisturbed soil samples for micromorphological phenomena. In both samples he found vertical craze planes (diameter between 50 and 1300 μ m), many

horizontal, lenticular voids (i.e. vughs; diameter between 10 and 650 μm), argillaceous laminae (locally wavy or as silty cappings developed), biopores with or without excrement, redistribution of carbonates with accumulation around voids (i.e. neocalcitans) and crystals of biogenetic carbonates (Fig. 5.1). The cappings and the wavy or broken laminae indicate that after its primary, aeolian deposition the loess was affected by redeposition and freeze-thaw cycles. This was followed by soil formation (biological activity and redistribution of carbonates).

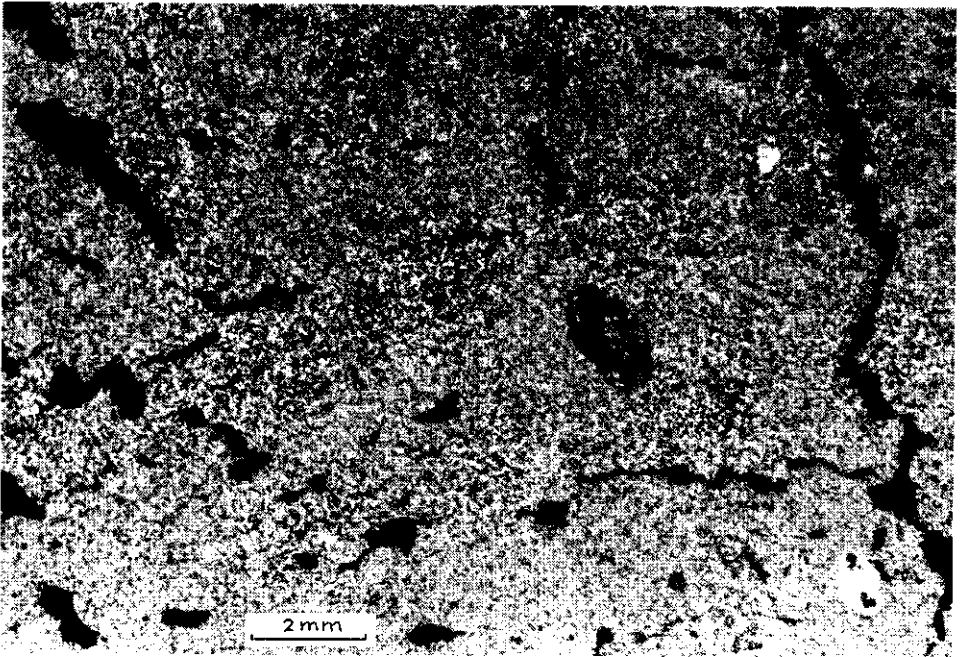


Fig. 5.1. Photomicrograph in crossed polarized light, showing a craze plane (right), vughs, a channel with excrement (central part), an argillaceous lamina (central part, above the channel with excrement) and a neocalcitan (bottom right).

Cores were taken carefully, so that structure was not visibly changed by cracks or horizontal breaks. All cores were prewetted by capillarity for four weeks to a suction head (H) of 0.01 m (pF 0) for the H- θ cores and of 0.025 m (pF 0.4) for the D- θ cores. The higher suction head used for the D- θ cores should prevent reorientation of the particles (SMILES & ROSENTHAL 1968, SMILES 1976a, 1976b). The latter

phenomenon is supposed to have more effect on moisture transport than on moisture capacity. Then, for the determination of the retention curve, the 100 ml soil cores were drained to bring them to equilibrium at a range of suction heads: six points were determined on the sand box (up to 1 m, i.e. pF 2), three points on the kaolin box (suction head between 2 and 5 m, i.e. pF 2.3 and 2.7 respectively) and three other points with the membrane pressure apparatus (suction head between 25 and 160 m, i.e. pF 3.4 and 4.2 respectively). Volume change of the soil was also measured during desorption at suction heads of 0.01 m ("saturated"), 0.17, 0.32, 1.1, 2.0, 3.2 and 5.0 m. During the hot air experiment one side of the soil core is dried by blowing hot air on it and then it is cut into 16 slices to determine the water content distribution $\Theta-x$. Details of the laboratory procedure for determining the diffusivity are described by e.g. ARYA et al. (1975) and VAN DEN BERG & LOUTERS (1986a).

5.4 Results and discussion

Figure 5.2 shows the $e(\vartheta)$ and $H(\vartheta)$ functions of the loess; the almost horizontal part of the retention curve for $.38 < \vartheta < .60$ may be noticed as typical for a well-graded soil of fine texture. It means that for $\Theta > .2$ (i.e. $\vartheta > .38$) high values of $D(\Theta)$ can be expected. The following regression equation was found between vertical expansion and suction head H (in m)

$$\frac{L_a - L_d}{L_{\text{sat}} - L_d} = 1 - 0.329 \log(H) \quad (5.8)$$

with a correlation coefficient $r = 0.98$, where L is length of soil core ($a = \text{actual}$, $d = \text{dried at } 105^\circ\text{C}$ and $\text{sat} = \text{saturated}$, i.e. at a moisture content belonging to $H = 0.01$ m).

Using eqn. (5.8) the differential quotient de/dH in eqn. (5.2) can be calculated analytically as

$$\frac{de}{dH} = -0.143 \cdot \frac{A(L_{\text{sat}} - L_d)}{V_s \cdot H} \quad (5.9)$$

where A is the area of a cross-section of the soil core.

In the search for optimal conditions the hot air procedure was performed for different combinations of initial moisture content Θ_1 , air temperature T (measured at the surface of the soil core) and drying time t (see table 5.1).

The $\Theta-x$ data of each core were screened and a replicate was discarded if one of the following two cases occurred:

- the boundary condition of $\Theta = \Theta_0$ at $x = 0$ and $t > 0$ could not be realized in time because the surface remained partly wet;
- during the test the initial water content Θ_1 could not be maintained unchanged at the bottom of the soil core.

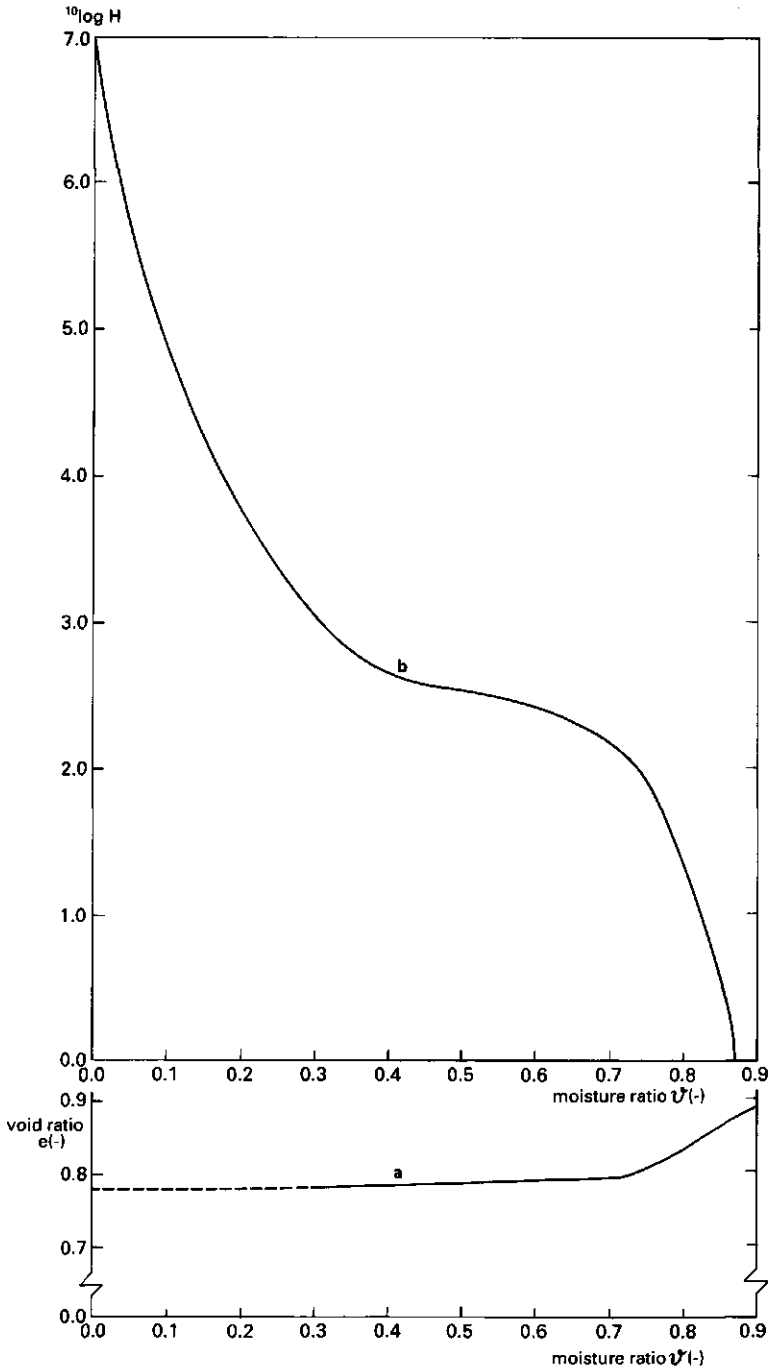


Fig. 5.2. Shrinkage and moisture retention characteristics of loess, both related to the moisture ratio.

Four of the 20 samples were lost: one because of technical failure during the experiment, one because of cracking at the surface of the soil core, and two because of a discontinuity in the moisture content distribution, probably caused by a rupture.

Experience has shown that for the hot air experiment on loess it is essential to find the most suitable test conditions with regard to initial moisture content θ_i , air temperature T and drying time t . In the literature hydraulic properties and their test conditions are mostly related to soil texture only (i. e. VAN GRINSVEN et al 1985). However, this may insufficiently characterize the moisture diffusivity of an undisturbed soil (VAN DEN BERG & LOUTERS 1988). As the test conditions for loess were not known beforehand, only 9 of the 16 samples appeared to be of use for calculating the $D - \theta$ relationship. Most of the selected samples appeared in the lower left-hand corner of Table 5. 1.

Table 5. 1 Ratio of selected to treated samples for different conditions of the hot air method

initial moisture content θ_i (-)	air temp. T (°C)	drying time t (s)				
		360	390	420	480	600
0. 41	180	-	-	-	-	0. 0; a+b
0. 41	210	-	0. 0; a+b	-	-	-
0. 41	260	0. 0; a+b	-	-	0. 0; a+b	-
0. 32	210	-	1. 0	1. 0	-	-
0. 27	210	1. 0	0. 3; b	0. 5; b	-	-

- a the boundary conditions of $\theta = \theta_0$ at $x = 0$ and $t > 0$ could not be realized in time because the surface remained partly wet
 b during the test the initial water content θ_i could not be maintained unchanged at the bottom of the soil core

For these samples the magnitude of D seems independent of the experimental conditions, as it should be.

Figure 5. 3 shows that the diffusivity of loess is almost as high as that of a sandy loam and much higher than that of a group of loamy to silty soils. This emphasizes the conclusion of earlier research that soil texture is insufficient to discriminate for diffusivity (VAN DEN BERG & LOUTERS 1988). Besides, the high diffusivity accounts for the small range of conditions permitted if using the hot air method on loess samples.

For $0. 1 < \theta < . 30$ the unsaturated hydraulic conductivity k was computed with eqn. (5. 6) using the diffusivity as determined with the hot air method (Fig. 5. 3). Between $\theta = . 28$ and saturation D was estimated from an assumed increase in k to saturated conductivity which was measured as $0. 11$ m/day (broken lines).

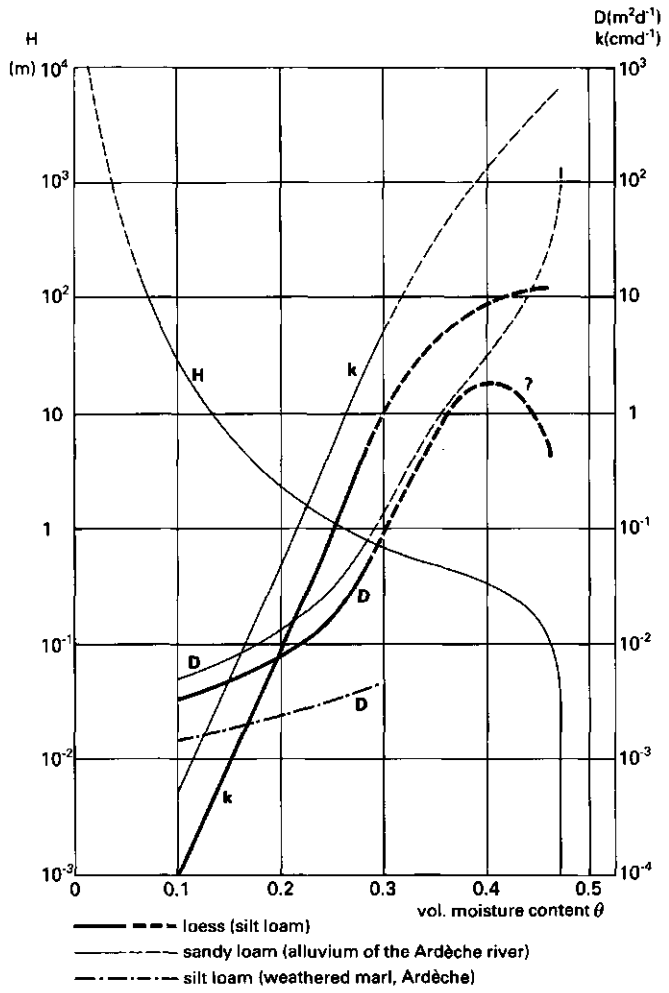


Fig. 5. 3. Soil moisture diffusivity and unsaturated conductivity characteristics for loess; for comparison the characteristics of a sandy loam and a group of loamy to silty soils (VAN DEN BERG & LOUTERS 1988) have been added.

LIST OF SYMBOLS

symbol	description	dimension
A	area of a cross-section of a soil core	L^2
D	diffusivity of soil moisture	L^2t^{-1}
e	void ratio V_p/V_s	-
h	capillary pressure head (potential per unit of weight of soil water)	L
H	capillary suction head ($H = -h$)	L
k	hydraulic conductivity	Lt^{-1}
L	length of a soil core with indices	L
a	actual	
d	dried at 105°C	
sat	"saturated": equilibrium with a pressure head of -0.01 m	
V_l	volume of liquid	L^3
V_p	volume of voids	L^3
V_s	volume of solid	L^3
V_t	total or bulk volume	L^3
x	distance from the drying surface of a soil core	L
ϑ	moisture ratio V_l/V_s	-
Θ	volumetric moisture conten V_l/V_t	-
Θ_i	initial value of Θ	-
Θ_o	air dry value of Θ	-
ρ_s	density of soil solids	mL^{-3}
ρ_v	dry bulk density	mL^{-3}

REFERENCES

- ARYA, L. M., FARELL, D. A. & BLAKE, G. R. (1975), A field study of soil water depletion patterns of growing soybean roots; part I: Determination of hydraulic properties of the soil. *Soil Sci. Soc. Am. Proc.* 35, pp. 362-364.
- CHILDS, E. C. & COLLIS-GEORGE, N. (1950), The permeability of porous media. *Proc. Roy. Soc.*, A201, pp. 392-405.
- DOLEZAL, F. (1976), The measurement of hydrostatic and hydrodynamic parameters of a swelling soil. *Proc. Int. Symp. on Water in heavy soils*, Bratislava, pp. 80-90.
- HUXTABLE, J. & AITKEN, J. (1985), Thermoluminescence dating results for the paleolithic site Maastricht-Belvédère. In: *Maastricht-Belvédère: stratigraphy, paleoenvironment and archaeology of the Middle and Late Pleistocene deposits*. Mededelingen Rijks Geologische Dienst 39-1, pp. 41-44.
- MÜCHER, H. J. (1986), Aspects of loess and loess-derived slope deposits: an experimental and morphological approach. Thesis. *Nederlandse Geografische Studies* 23.
- PARLANGE, J.-Y. (1976), A note on the moisture diffusivity of saturated swelling systems from desorption experiments. *Soil Sci.* 120, pp. 156-158.
- PHILIP, J. R. (1969), Hydrostatics and hydrodynamics in swelling soils. *Water Resour. Res.* 5, pp. 1070-1077.
- PHILIP, J. R. (1970), Reply to comments by E. G. Youngs and G. D. Towne. *Water Resour. Res.* 6, pp. 1248-1251.
- PHILIP, J. R. (1971), Hydrology of swelling soils. In: T. Talsma & J. R. Philip (Eds.) *Salinity and water use*. Mac Millan, London.
- SMILES, D. E. (1976a), On the validity of the theory of flow in saturated swelling materials. *Aust. J. Soil Res.* 14, pp. 389-395.
- SMILES, D. E. (1976b), Theory of liquid flow in saturated swelling materials; some problem areas. *Proc. Int. Symp. on Water in heavy soils*. Bratislava, pp. 32-41.
- SMILES, D. E. & ROSENTHAL, M. J. (1968), The movement of water in swelling materials. *Aust. J. Soil Res.* 6, pp. 237-248.
- STYRK, G. B. (1954), Some aspects of soil shrinkage and the effect of cracking upon water entry into the soil. *Aust. J. Agric. Res.* 5, pp. 279-290.
- VAN DEN BERG, J. A. & LOUTERS, T. (1986a), An algorithm for computing the relationship between diffusivity and soil moisture content from the hot air method. *J. Hydrol.* 83, pp. 149-159.
- VAN DEN BERG, J. A., LOUTERS, T. & HARINGHUIZEN, P. J., (1986b), *HOTAIR*, optimizing the D-theta relationship from hot air data. Users manual. Dept. of Physical Geography, Utrecht University, The Netherlands.
- VAN DEN BERG, J. A. & LOUTERS, T. (1988), The variability of soil moisture diffusivity of loamy to silty soils on marl, determined by the hot air method. *J. Hydrol.* 97, pp. 235-250.
- VAN GRINSVEN, J. J. M., DIRKSEN, C. & BOUTEN, W. (1985), Evaluation of the hot air method for measuring soil water diffusivity. *Soil Sci. Soc. Am. J.* 49, pp. 1093-1099.

6. MEASUREMENTS OF HYDRAULIC CONDUCTIVITY OF SILT LOAM SOILS
USING AN INFILTRATION METHOD

Published in: Journal of Hydrology 110 (1989), 1-22.
Permission for reproduction, 14 July 1989.

6.2 Theoretical considerations

Infiltration concept

BODMAN & COLMAN (1944) schematized the soil moisture profile during ponded infiltration in a way that is still widely used. The five features identified for a uniform soil are the saturated zone, the transition zone, the transmission zone, the wetting zone and the wetting front. These zones were also observed by BOND & COLLIS-GEORGE (1981a and b) in experiments on fine sand from which silt and clay had been removed. According to this concept there are two characteristic conductivities during infiltration: k_{sat} for the saturated zone and k_0 for the transmission zone.

If there is a difference between the conductivity of two consecutive soil layers e.g. between two soil horizons or between the surface crust and the soil below, it is the effective value of the conductivity that is in fact measured (k_s). In the case of a series circuit, k_s can be expressed as a function of the components k_1 and k_2 and the geometry of the percolated soil (Fig. 6.1).

$$k_s = \frac{k_1 \cdot k_2 (d_1 + d_2)}{k_1 \cdot d_2 + k_2 \cdot d_1} \quad (6.1)$$

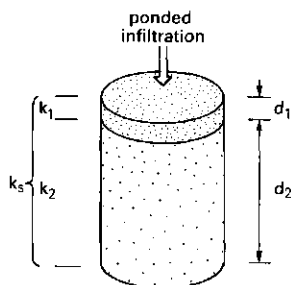


Fig. 1. Schematic representation of a series circuit of two soil layers of different depth (d_1 and d_2) and with different conductivity (k_1 and k_2); k_s is the effective conductivity of both layers.

In the same way the value of k_0 depends on the hydraulic conductivity of the soil layers that the transmission zone has penetrated. If a soil profile can be subdivided into three zones (e.g. zone 1: A-horizon, zone 2: rooted zone and zone 3: subsoil), each with a different but constant value of k_0 (k_1 , k_2 and k_3 in Fig. 6.2a) the effective value, k_s , changes continuously with soil depth in zones 2 and 3 (solid line in Fig. 6.2b). In the case of ponded infiltration, the hydraulic conductivity in the transmission zone, k_0 , will change with time as soon as the wetting front has passed zone 1 (solid line in Fig. 6.2c).

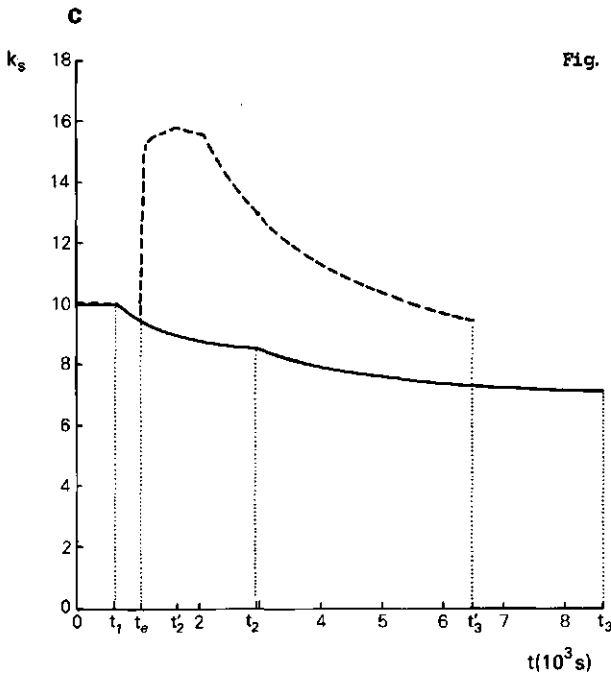
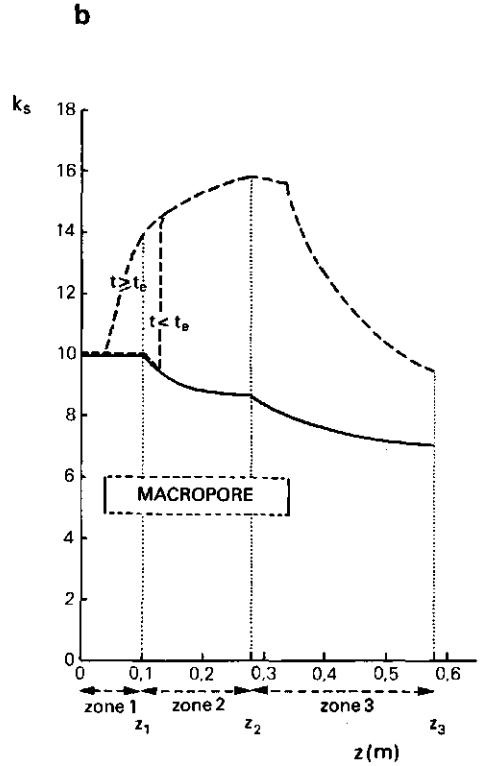
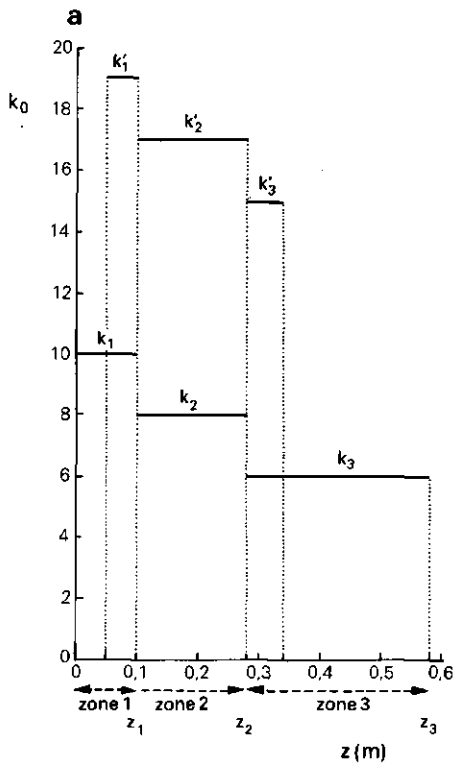


Fig. 2. The hydraulic conductivity of the transmission zone as a function of soil depth (a and b) or time of ponded infiltration (c) for a soil matrix (solid lines) and for a closed soil with a vertical macropore (broken lines). (t_e is time at which the macropore becomes effective for soil water flow; in the calculation the wetting front at $t=t_e$ was taken to be at 10 cm below the top of the macropore).

Whereas in the case of Fig. 6.2 the k_0 value decreased with increasing depth of the soil zone, infiltration into a soil overlain by a thin crust of low conductivity leads to the reverse situation, in which it is the upper zone that has the lowest conductivity. Such a situation gives rise to an unstable wetting front. Therefore, the impact of natural crusts on the infiltration into a bare, crusted soil was determined by measuring the steady-state flux through soil samples.

Infiltration equations of Green and Ampt

For uniform soils with a narrow wetting front and with a constant effective capillary head at this front, ponded infiltration can be described in a simple way (GREEN & AMPT 1911, KOOREVAAR et al. 1983) by

$$I = L(\theta_0 - \theta_i) \quad (6.2a)$$

and

$$t = \frac{\theta_0 - \theta_i}{k_0} \left[L + h_f \left\{ \ln \left(\frac{L - h_f}{-h_f} \right) \right\} \right] \quad (6.2b)$$

where I is cumulative infiltration expressed as a depth of water, θ_i is the initial volumetric moisture content, θ_0 is the moisture content in the transmission zone, L is the depth of the wetting front, t is time since ponded infiltration started, k_0 is the hydraulic conductivity of the soil in the transmission zone and h_f is the effective capillary pressure head at the wetting front.

Complications arise if the wetting front is diffuse, if successive soil layers have different values for the infiltration parameters k_0 and h_f and if these parameters vary with time. Ponded infiltration into a multi-layered soil has been described by several authors such as COLMAN & BODMAN (1945), TAKAGI (1960), BOUWER (1969; 1976), CHILDS & BYBORDI (1969), BYBORDI (1973) AND HACHUM & ALFARO (1980).

Complications by macropores

Ponded infiltration can be strongly influenced by structural macropores such as cracks, or biopores like worm holes and channels of decayed roots, even in "closed soils" (CHAMBERLIN 1972), in which these voids do not come to the soil surface. If the hydraulic conductivity decreases with depth, it is possible for the capillary pressure head to become positive in the transmission zone. For the schematization of Bodman and Colman this means that the saturated zone is extended to the transmission zone. In that case, infiltrating water can enter a hole as soon as the wetting zone has passed the top of the macropore. This process contributes considerably to the conductivity of the transmission zone. The complicated influence of holes and channels of macropores on the hydraulic conductivity was approached by a simple analysis using eqns. 6.2a and 6.2b. The results are shown in Figs 6.2a, b and c in which a vertical macropore has raised the saturated conductivity of the zones 1 to 3 (k_1 , k_2 and k_3 in Fig. 6.2a and the broken lines in

Figs. 6.2b and c). Moreover, such a water-filled channel causes an irregularity in the wetting front (Fig. 6.3).

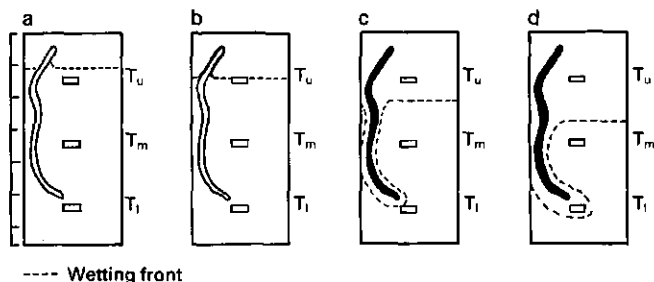


Fig. 3. Infiltration into a soil with a vertical macropore.
 a. The wetting front has passed the top of the macropore that still acts as a barrier.
 b. The bottom of the transmission zone ($h_p > 0$) reaches the top of the macropore, which starts to fill with water.
 c. The water-filled macropore has started to emit a wetting front in all directions.
 d. The perturbed wetting front attains the lower tensiometer (T_l) before the middle one (T_m).

The parameters k_0 and h_f

For a given soil layer, k_0 and h_f can be determined from the series of measured values of I and t during an experiment with ponded infiltration. For different values of h_f , a value of k_0 can be calculated for each pair of I and t data. Optimized values of k_0 and h_f can then be obtained: these latter values have the smallest standard deviation of k_0 (VAN DEN BERG & LOUTERS 1985). Also, h_f can be inferred from retention curve data, for example by using the methods of BROOKS & COREY (1964) and BRAKENSIEK (1977).

The parameters in eq. 6.2a and 6.2b, k_0 and h_f , vary with physiographic factors such as soil texture and soil structure. Many authors have reported values of h_f as a function of texture and soil horizon (MEIN & FARRELL 1974, BRAKENSIEK 1977, BRAKENSIEK et al. 1981, CLAPP & HORNBERGER 1978, McCUEN et al. 1981, RAWLS et al. 1983, RUSSO 1988). The literature suggests that there is a tendency for h_f to increase with the content of fine soil particles. However, in soils containing many macropores the absolute value of h_f is expected to be small. It is usually assumed that h_f is proportional to the air entry value (BOUWER 1966, 1969, WHISLER & BOUWER 1970, BRAKENSIEK 1977) which is likewise small in such soils. CLAPP & HORNBERGER (1978) found that most soils, particularly medium- and fine-textured ones, show a gradual air entry near saturation. If all the soil layers involved contain macropores, h_f may be expected to hardly vary with soil texture and soil depth.

Variance of k_0 with time

For the loamy to silty soils under consideration the hydraulic conductivity at a given moisture content cannot be considered as time-invariant. In the unsaturated zone a continuously changing system of voids exists, in which the cracks are especially subject to change. Most of the processes that cause conductivity to change with time are well-known but there is one feature that needs some explanation. When water flows through the voids of a soil, the total head is dissipated as viscous friction that produces frictional drag on the soil particles in the direction of the flow. The force corresponding to the energy transfer from the water to the soil particles is called the seepage force. The seepage force per unit of volume is called seepage "pressure" and has been defined as

$$j = -\rho_w \cdot g \cdot \frac{\Delta h}{\Delta s} \quad (6.3)$$

in which ρ_w is the density of water, h is total head and s the coordinate in the flow direction. The effective j is obtained by multiplying j by the distance to the level of the saturated soil; the resulting value is a pressure in the physical sense. When during ponded infiltration the capillary pressure head h_p in the transmission zone has become positive so that macropores can contribute to the hydraulic conductivity, it is worth analysing the effect of the seepage pressure on the stability of the wall of a macropore during the time that the macropores are active.

While a macropore is being filled with water during infiltration the effect of the seepage pressure is negligible, because the gradient of h is small. Then, water from the deeper part of the filled macropore may infiltrate laterally and vertically into the surrounding soil matrix; here the seepage pressure has a stabilizing effect on the wall of the macropore. After the ponding has ceased and the macropore has drained, the gradient of the head and, subsequently, the flow direction reverse again; the flow of soil water out of the pore wall has a destabilizing effect. At the moment that the macropore has drained, the total head in the soil matrix remains still nearly unchanged, which causes a finite value of Δh over a small Δs in the wall of the macropore. Where encapsulated air is present in the soil matrix around the macropore, the resulting elasticity permits the soil water to flow nearly instantaneously towards the macropore. According to eq. (6.3) this produces a momentary rise of the seepage pressure that can be large enough to result in the macropore collapsing locally.

6.3 Methods and materials

Methods and instrumentation

For the study of hydraulic properties under wet conditions it is preferable to do experiments on soil columns in situ, because for modelling, many of the phenomena that occur in natural soils are difficult

to reproduce in the laboratory or to envisage beforehand. Small samples of undisturbed soil give spurious results, because their dimensions are less than the scale of biopores and structural voids. The "crust method" as introduced by HILLEL & GARDNER (1969 and 1970 a,b) and modified by BOUMA et al. (1971, 1972) was used for the experiments described below.

Soil water flow and capillary pressure head were measured during ponding infiltration on soil columns which had been carved out of the soil in situ with a diameter of about 0.2 m and a height of 0.30 to 0.55 m. Grasses and herbs were cut off and for each experiment the top surface was provided with an artificial crust of a different hydraulic resistance or, finally, with no crust. The columns were not encased, but macropores ending in the wall of a column were sealed off with a mixture of bentonite and soil material. The advantage of an unencased column is that lateral air escape is unimpeded, which approximates natural conditions.

Each column was provided with an infiltrometer ring and two or three cup-tensiometers at different depths. The tensiometers consisted of a small, porous ceramic cup and an electronic pressure transducer; they are usable for pressure heads in the range of 0 - 500 cm and have a sensitivity of 0.5 cm (VAN DEN BERG & LOUITERS 1984). A constant head between 10 and 30 mm was maintained with an improved Mariotte bottle (ADAMS et al., 1957), able to provide a head constant within 3 mm. The artificial crusts were made from different mixtures of very fine sand ("Blokzijklzand") and gypsum $((\text{CaSO}_4)_2 \cdot \text{H}_2\text{O})$. Because calcium and sulphate ions are common in soils on marl and limestone, adding this electrolyte to the soil solution was assumed not to modify soil properties.

During one experiment on ponding infiltration, the downward movement of the wetting front was observed on the outside of the soil column. The position of the wetting front is sharply defined by a colour change, which was marked by putting pins along four vertical lines at fixed time intervals.

The effective capillary pressure head, h_f , at the wetting front was determined from the desorption curve by a graphical procedure as described by BRAKENSIEK (1977) and BROOKS & COREY (1964). Furthermore, in a homogeneous soil layer, h_f was optimized with eqns. 6.2a and 6.2b by searching for the lowest variance of the conductivity. The saturated conductivity of the natural crust of bare soil was calculated from measuring stationary flow through undisturbed samples (diameter and height 0.05 m). Using a constant head permeameter the saturated conductivity was measured on samples of the crusted soil (k_s) and on samples from which the crust had been carefully scraped off (k_2). The conductivity of the crust, k_1 , could be calculated from eqn. (6.1) as

$$k_1 = \frac{k_2 \cdot k_s \cdot d_1}{k_2 (d_1 + d_2) - k_s \cdot d_2} \quad (6.4)$$

Because k_1 depends on the conductivity of the soil, k_2 , which may have a large spatial variability, a more stable and dimensionless expression was derived by considering both k_1 and k_g relative to k_2

$$\frac{k_2}{k_1} = \frac{f (1 - k_g/k_2) + 1}{k_g/k_2} \quad (6.5)$$

in which the ratio $f = d_2/d_1$ can be considered as a parameter. For $f=10$ and $f=24$ the relationship between k_2/k_1 and k_g/k_2 has been plotted in Fig. 6.4. As to the measurements on natural crusts, data from samples that contained macropores such as worm holes below the crust, were discarded. Any openings between soil and cylinder jacket were carefully sealed with bentonite and all samples were prewetted.

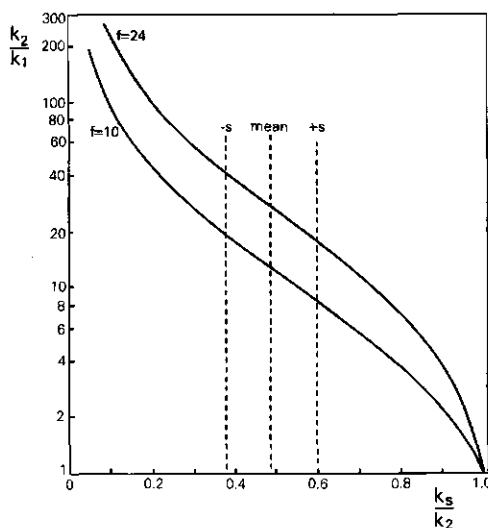


Fig. 4. The relationship between the ratio of both constituent conductivities of a crusted soil (k_1 and k_2) and their effective value (k_g) relative to the conductivity of the underlying soil (k_2) for two ratios of the depth of the crust (d_1) to that of the soil below (d_2); $f=d_2/d_1$.

The dry bulk density of the soil was determined by sampling a known volume of soil; the volume of the soil crusts was determined with the paraffin method. The porosity (n) of the soil and the soil crust was calculated from the measured ρ_b and the density of the solid matter ρ_s .

$$n = 1 - \frac{\rho_b}{\rho_s} \quad (6.6)$$

For ρ_s a value of 2600 kg.m^{-3} was taken, because the organic matter content of the crust and soil was about 3%.

Experimental sites and experimental design

The field experiments on soil columns were done at seven sites (2 to 8) which were selected in three study areas A, B and C in the Ardèche Basin according to erodibility, bedrock and soil type (Fig. 6.5). At all sites environmental evidence of erodibility could be found, but they had not yet been eroded. The lithological information was obtained from geological maps (Bureau de Recherche Géologique et Minières 1966, 1967 and 1974) and augmented by field mapping. All sites are on Mesozoic rock: Cretaceous marl with limestone (2 to 7) or Triassic sandstone (8); lithological maps and the detailed location of sites nos 2-7 have been given elsewhere. Sites 4 to 7 are on the gentle slope of a west-facing cryopediment; sites 2 and 8 are located on a terraced valley slope.

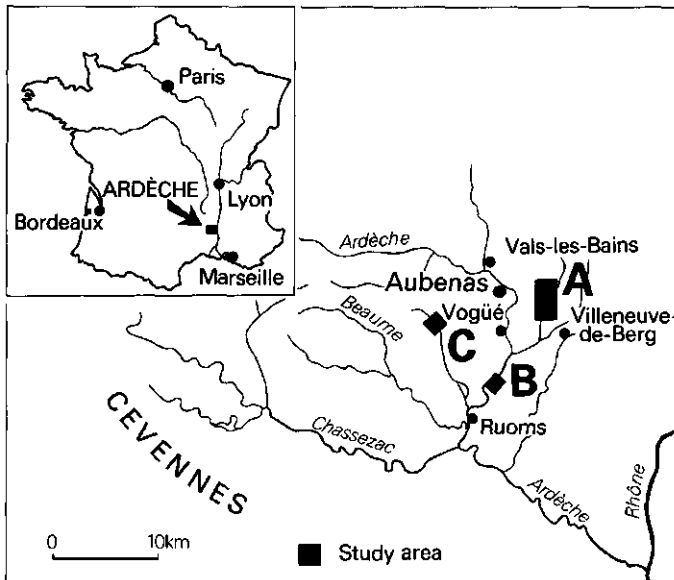


Fig. 5. Location of the study areas within the Ardèche drainage basin, southern France. The exact locations can be ascertained from the author (cf. Fig. 1.3.c.).

All experimental sites show evidence of former agricultural use but nowadays they are only extensively grazed (1 to 7) or under forest (8). Sites 2 to 7 were selected because of similarities in lithology and landuse; they correspond to the plots where soil cores were sampled for the determination of the hydraulic properties for intermediate moisture contents.

On the marly bedrock a brown calcareous soil or pararendzina of moderate to shallow depth is found (haploxeroll to xerochrept); its texture varies between silt loam and silty clay loam. On the deeply weathered sandstone an argillic brown soil has developed (ustult), which has been influenced during the past by the building of terraces. Here the topsoil has a texture of loamy sand and the texture of the subsoil is a sandy loam.

An X-ray analysis indicated the presence of 13 to 20% clay minerals (50-60% of which were smectites) in the soils on marly bedrock, and the presence of 5% clay (40% of which were smectites) in the soil on sandstone.

In total, ten columns were carved out at sites 2 to 7 in loam, silt loam or silty clay loam soils on marl. For the sake of contrast, two other columns in the loamy sand on sandstone (site 8) were included in the analysis. At sites 4 and 8 the measurements were done in duplicate simultaneously on two soil columns (4a and 4b, and 8a and 8b, respectively) and at sites 2 and 3 the measurements were repeated on another column in a subsequent year (2a and 2b, and 3a and 3b, respectively). The soil properties of all the twelve columns have been summarized in Table 6.1.

Each column was carved out where the soil was of the closed type (CHAMBERLIN 1972). At site 5 the uppermost soil layer (0.15 m deep) was removed from the soil column; here the subsoil contained hardly any macropores.

In general, the same sequence of experiments was conducted on each column, by first measuring unsaturated conductivity in a series of decreasing resistances of the artificial crust, and then measuring the saturated conductivity.

For the ponding experiments, only the data obtained before the transmission zone had penetrated to the bottom of the column were analysed. This time was too short to measure any significant effects on conductivity resulting from the swelling of smectites. For three columns an unsaturated conductivity test was repeated after ponded infiltration experiments.

The porosity and saturated conductivity of natural crusts on bare soil were investigated on five plots (a to e) within study area A. Plots a to d were on marly bedrock, with plot a at site 7; plot e was located on an alluvial deposit of the Auzon river. The texture of the crust and of the underlying soil is silt loam at all plots. All the plots, with the exception of plot a, were sampled two or three times; after unreliable samples had been discarded, between 4 and 13 samples remained per plot from each sampling.

Table 6.1 Description of the soil columns and the experimental sites

Site no	Column number	Column height 10 ⁻² m	Texture (USDA)a	Hor.	First soil horizon				Subsequent soil horizons			
					Depth 10 ⁻² m	Organ. matter %	Carbon. content.b) %	Porosity	Hor.	Depth 10 ⁻² m	Carbon. content.b) %	Porosity
2	2a;2b	30-34	l/sl	A _p	0-40	8	36	0.47	-	-	-	-
3	3a	51	sl	A	0-15	4	42	0.46	C	15-50	44	0.40
3	3b	48	sl	A	0-15	4	42	0.44	C	15-50	43	0.43-0.38*
4	4a;4b	50	scl	A	0-15	3	37	0.44	C	15-45	33-43*	0.42
									R	>45	45	0.41
5	5	54 ^{c)}	sl	A	0-20	6	25-42*	0.46	C	20-100	35-40*	0.40
6	6	50	sl	A	0-12	4	28-40*	0.43	C	12-45	38-40*	0.40
7	7a	38	sl/scl	A	0-20	9	45	0.45	C	20-50	46	0.42
7	7b	44 ^{d)}	sl/scl	A _p e)	0-50	10-6*	40-44*	0.45-0.42*	-	-	-	-
8	8a;8b	45	ls	A _p	0-60	5-1*	- f)	0.45	B-Cg)	60-200	-f)	0.44

*) variation measured with soil depth

a) l = loam; sl = silt loam; scl = silty clay loam; ls = loamy sand

b) the carbonate content has been determined as CO₂ and represented as CaCO₃

c) the upper 0.15 m of the soil was removed

d) the upper 0.03 m of the intensively rooted soil was removed

e) soil disturbed by mass movement

f) not relevant; pH 4.5

g) texture of sandy loam

6.4 Results

The capillary pressure head in the transmission zone during ponded infiltration

The tensiometers in the soil columns showed that the capillary pressure head in the transmission zone mostly increased to a small positive value of 2 to 5 cm during ponded infiltration (Fig. 6.6). A final positive pressure head was found both in the silt loam and in the sandy loam soil.

This small positive pressure head in the transmission zone was just sufficient to enable the infiltrating water to enter macropores inside a closed soil. Support for this contention can be derived from the data on h_p-t from soil column 3b, which are shown in Fig. 6.7. Here, the wetting front encountered the tensiometer at 0.40 m depth before the one at 0.22 m (see arrows in Fig. 6.7). This can be explained by short-circuiting via a worm hole that was found to run through the column when at the end of the infiltration experiments the column was inspected for irregularities in soil structure. Fig. 6.3 gives a schematic picture of this case. Nevertheless, water movement out of the soil along the sides of a column remained negligible as long as the transmission zone had not yet reached the bottom of the soil column. Obviously, the outermost soil mantle of the column started with a lower initial moisture content than the rest, and local saturation was retarded in this outermost mantle.

Length of the wetting zone

During the ponding experiments the tensiometers showed the progress of the wetting front. If the transition from the transmission zone to the wetting zone is considered to be where the capillary pressure head becomes positive, the progress of the back of the wetting front can also be shown (Fig. 6.6). In this example, at $t=800$ s the wetting front had passed the middle tensiometer at 0.235 m depth and the transmission zone had just penetrated to the upper tensiometer at 0.075 m depth. Profiles of h_p with depth at a given time reveal that the length of the wetting zone was 0.10 to 0.15 m in the topsoil, increasing with depth. BOND & COLLIS-GEORGE (1981 a) also found a length of 0.15 m in fine sand.

The shape of the wetting front

The results of marking the advance of the wetting front in column 4a are shown in Fig. 6.8, in which the velocity of the wetting front is plotted against its depth as measured at the end of each time interval. The displacement of the wetting front along the outside of the column shows a general retardation with depth but also a spatial and temporal variability caused by macropores inside the column. However, the comparable data measured inside the column with the tensiometers seem to be a good average of the four lines and correspond quite well with those of line 2.

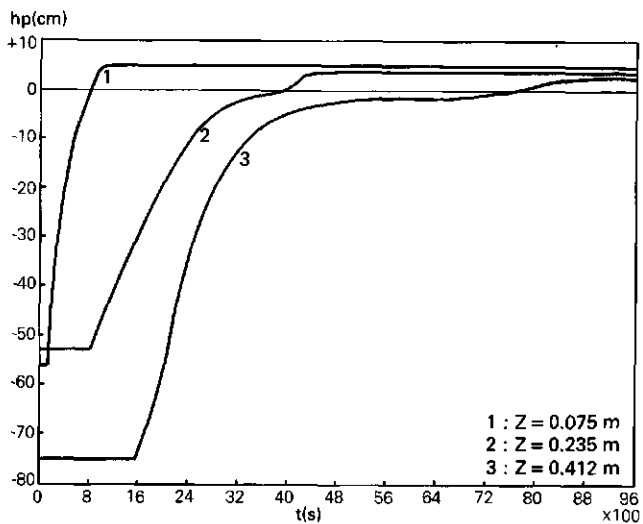


Fig. 6. Curves of the capillary pressure head at three depths in the soil matrix during ponded infiltration (2nd experiment on column 4a).

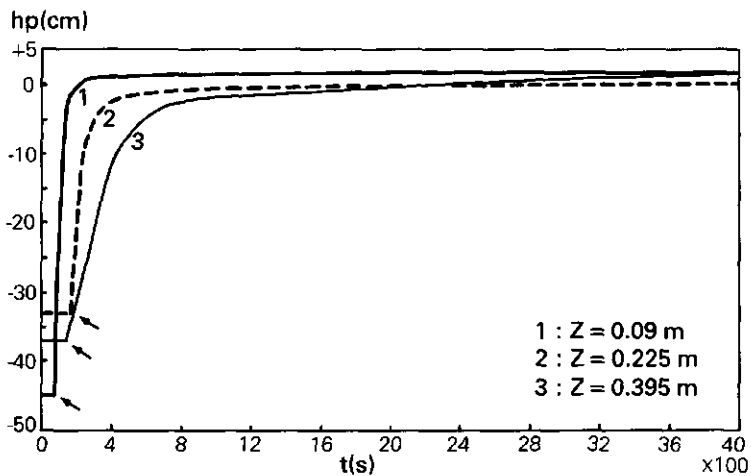


Fig. 7. Curves of the capillary pressure head at three depths in a soil matrix with a vertical macropore during ponded infiltration (1st experiment on soil column 3b).

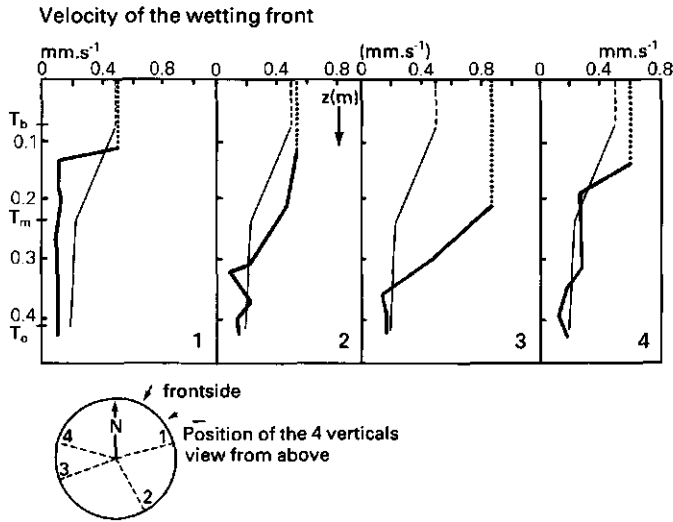


Fig. 8. Velocity of the wetting front inside (fine line) and along four vertical lines on the outside of soil column 4a.

The wetting front pressure head

The pressure head at the wetting front was determined from the desorption curve data and from eq. 6. 2a and 6. 2b by smallest variance of k_0 . The results are summarized in Table 6. 2 and show a fair correspondence.

Table 6. 2 Wetting front pressure head from desorption curve data (I) and from eqns. 1a, 1b and 4 by smallest variance of k_0 in a homogeneous soil layer (II)

h_f (cm)	Column number							
	2a/b	3a/b	4a/b	5	6	7a	7b	8a/b
I	-3.5	-6.5	-4	-23	-7	-6	-7.5	-13
II	-3.5	-5	-4	-20	-4	-4	-4	-6

Variation of k_0 with time during ponded infiltration

For columns 4a, 2b and 3b the value of k_0 as calculated from eqns. 6. 2a and 6. 2b were plotted against ponding time (Fig. 6. 9). Because in each case the pressure head in the transmission zone was positive, the

effective value of the saturated conductivity is measured in this way. Curves a, b and c resemble the solid line of Fig. 6.2c, i.e. a relationship in which k_s decreases asymptotically with time as a consequence of the variation of k_0 with soil depth. The higher level of curve c (site 2, note change of scale) can be explained by this soil having a crumb structure and containing many large pores between the peds throughout the profile. At site 4 (Fig. 6.9 curves a and b) the subsoil has less structure. Curve d of Fig. 6.9 belongs to column 3b, in which a worm hole was found (as shown in Fig. 6.3). The way k_s changes with time in this column is similar to the broken line of Fig. 6.2c and clearly illustrates the effect of such macropores on saturated conductivity.

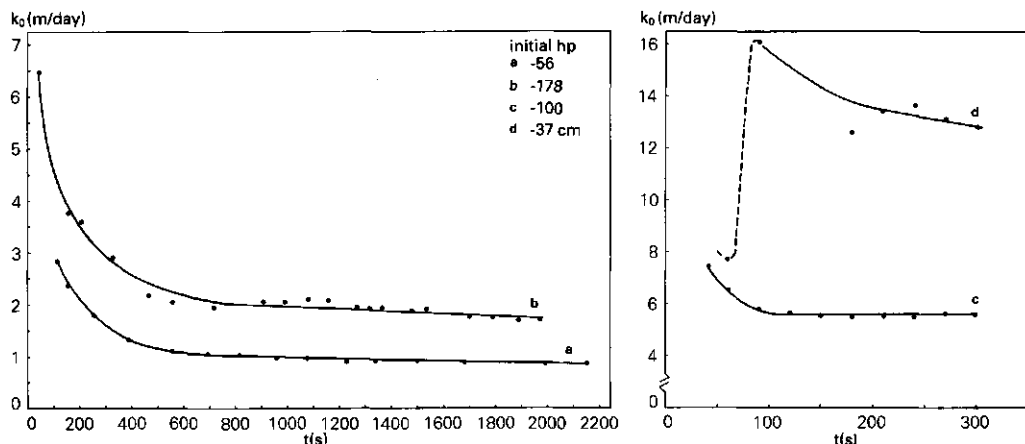


Fig. 9. Change of k_0 with ponding time for two different initial moisture conditions (a and b: 2nd and 3rd ponding experiments on column 4a) and for different soil structure (c: 1st exp. on column 2b; d: 1st exp. on column 3b).

Variation of k_0 (k_g) with antecedent conditions

The effect of antecedent moisture conditions is illustrated by the curves a and b of Fig. 6.9. The experiment plotted as curve b was carried out five days after that of curve a, but started with a more negative pressure head (-178 cm) than that of curve a (-56 cm). In this case, soil structure changed with time between the two ponding experiments because shrinkage caused fine cracks and fissures to form, which contributed to the saturated conductivity.

In most experiments, however, a second ponded infiltration showed a k_s lower than the k_s at the end of the first experiment (Fig. 6.10). Unsaturated infiltration tests done before and after the ponding experiments showed unchanged values for k_{unsat} .

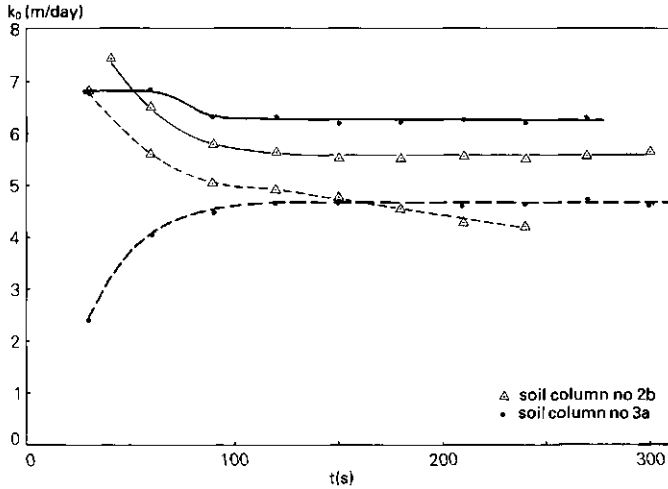


Fig. 10. Change of k_0 during a first (solid lines) and a second (dashed lines) experiment of ponded infiltration

Saturated and unsaturated conductivity

The results of the infiltration tests on soil columns are summarized in Table 6.3. Most of the experimental sites show a distinct discontinuity between the hydraulic conductivity at a small negative capillary pressure head, h_p , and the saturated conductivity k_{sat} , the latter being 5 to 80 times larger.

The effective hydraulic resistance of the artificial crust could not be adjusted beforehand on the basis of the mixture of gypsum and sand. Therefore, capillary pressure heads at which the unsaturated conductivity was measured, vary unsystematically.

Conductivity of natural crusts of bare soil

The porosity and saturated conductivity of natural crusts on bare, silt loam soils were compared with the same properties of the underlying soil. The mean porosity of the crust and of the underlying soil has been plotted in Fig. 6.11 for each sample. Analysis of variance shows a very significant difference between the mean porosity of the crusts (0.30) and that of the soil below (0.45).

The data concerning the saturated conductivity were analysed with eqns. 6.1, 6.4 and 6.5; the terminology used is as shown in Fig. 6.1. The conductivity of the subsoil, k_2 , showed a considerable spatial variability, and therefore the ratios of k_1/k_2 (or of k_2/k_1) and k_s/k_2 were used, so that the results from different plots could be analysed together. The relationship between these ratios given by eqn. 6.5 has

Table 6. 3a Unsaturated conductivity k_{unsat} (10^{-2} m d^{-1}) at h_p (cm) tabulated as (h_p, k_{unsat}) for the different soil columns

Range of h_p	Column number											
	2a	2b	3a	3b	4a	4b	5	6	7a	7b	8a	8b
$-3 < h_p < 0$	-2; 25	-0; 65 -2; 35	*-0; 24	-3; 5					-1; 10 -2; 7			
$-7.5 < h_p < -3$	-4; 20 -7; 14	-4; 10		-7; 4*				-6; 17*		-7; 5	-7; 53	-4; 303
$-11 < h_p < -7.5$			-9; 3	-8; 4	-9; 9*		-11; 3	-8; 8			-10; 36	-8; 77
$-20 < h_p < -15.5^{**}$		-17; 2				-16; 8*	-18; 2				-17; 3	-20; 3
$h_p < -20$					-23; 2	-32; 2		-23; 2			-22; 2	-22; 2 -28; 1

* after an experiment with ponded infiltration

** no data within the class $-15.5 < h_p < -11$

Table 6. 3b Range of the effective value of k_0, k_g (10^{-2} m day^{-1}) for soil depths between 0 and 0.2m below the top of the column and from all experiments with ponded infiltration

k	Column number											
	2a	2b	3a	3b	4a	4b	5	6	7a	7b	8a	8b
-		410	230	800	90	160	5	140	270	400	1000	680
-		740	680	1400	400	280		160	1000	1300	2000	1800

been plotted in Fig. 6.4. From this figure the range of k_2/k_1 can be found for the range of variation of the mean value of the ratio k_s/k_2 (also plotted in Fig. 6.4) and for the best value of $f=d_2/d_1$. Most crusts were 4 to 5 mm thick, which agrees with laboratory experiments done by LE BISSONNAIS (1988) on a silt loam soil. Given the size of the sample, the ratio between the thickness of the underlying soil, d_2 , and that of the crust, d_1 , then becomes $f = 10$ and consequently k_2/k_1 varies between 8 and 20; on average, k_1 is a twelfth of k_2 . Because of the way the samples used for the data analysis were selected, the results of this part of the research apply to the soil matrix only.

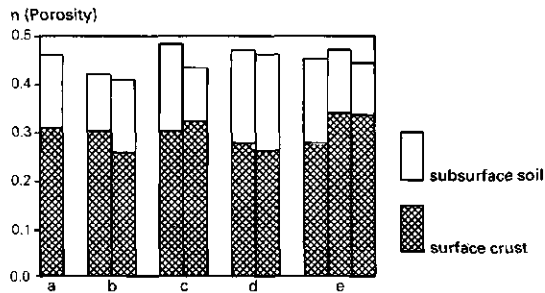


Fig. 11. Porosity of the crust and the subsoil of bare, silt loam soils.

6.5 Discussion and conclusions

The measurements obtained during ponded infiltration on twelve soil columns suggest that water can be conducted through macropores even in a closed soil in which holes do not reach the soil surface. This contention is corroborated directly by measurements of the capillary pressure head in the transmission zone and indirectly by the large difference between the hydraulic conductivity during ponded infiltration and that when a small negative pressure head is maintained by means of an artificial crust (Table 6.3).

Only in the uniform, unstructured soil of column 5 in which hardly any macropores were found, did the final capillary head remain negative (between -1 and -3 cm). BODMAN & COLMAN (1944) found that water did not move sideways out of the soil during their infiltration experiments on columns of homogeneous soil of Yolo silt loam or Yolo sandy loam. From this they concluded that the infiltration could not move into the macropores inside the soil, but they did not measure the capillary head.

In their experiments with infiltration into layered soils, COLMAN & BODMAN (1945) found a positive pressure head in the whole upper soil layer if a coarse-textured soil (Yolo sandy loam) overlay a fine-textured soil.

tured one (Yolo silt loam). For most soils considered here, the texture remained the same but the structure generally weakened with depth or became platy, causing conductivity to decrease with soil depth. It thus seems that the capillary pressure head in the transmission zone of a closed, homogeneous soil without cracks or holes remains negative - as stated by BODMAN & COLMAN (1944) - but that decreasing hydraulic conductivity allows the pressure head to attain a positive value in the wetting zone.

A positive pressure head enables macropores to contribute to the conductivity of the transmission zone. For open soils in which macropores are open to the soil surface, the effect of short-circuiting by macropores on saturated conductivity has been discussed by many authors, such as EDWARDS et al. (1979), BEVEN (1981), BEVEN & GERMANN (1982), BOUMA (1982), BOUMA et al. (1982), DAVIDSON (1984, 1985, 1987), BEVEN & CLARKE (1986), GERMANN & BEVEN (1981) and SMETTEM (1986). For closed soils, however, it has generally been assumed that macropores do not contribute to the transmission of soil moisture. Yet, from Table 6.3 it can be concluded that for high moisture contents corresponding to a $h_p > -20$ cm, the hydraulic conductivity of loamy to silty soils depends mainly on the secondary pores that are created by soil fauna, soil structure and shrinkage. With regard to saturated conductivity, macropores are dominant. The increase in conductivity that occurred when the moisture content increased from nearly saturated to completely saturated conditions must have been caused by the presence of macropores that can transmit soil water even through a closed soil as soon as the h_p has become slightly positive.

No such difference between saturated and unsaturated conductivity was found by BODMAN & COLMAN (1944) or BOND & COLLIS-GEORGE (1981a and b) because they used homogeneous soil material with artificial packing. The measurements at site 5, where the conductivity during ponding in the non-structured silt loam subsoil remained small (Table 6.3), are in line with this. Here, the pressure head in the transmission zone remained negative. These data also agree with the sample mean of the saturated conductivity (k_2) of the soil matrix just below the soil crust; this mean was in the range of 0.25 to 0.65 $\text{m}\cdot\text{day}^{-1}$, with a total mean of 0.42 $\text{m}\cdot\text{day}^{-1}$, which agrees well with the values of k_{unsat} as measured on the soil columns when $h_p = 0$.

Table 6.2 shows the values for the pressure head at the wetting front (h_f), as calculated from the desorption curve (first row) or computed with eqns. 6.2a and 6.2b from the infiltration data (second row). The values of -20 and -23 cm for site 5 are remarkable; here, the subsoil seems to be homogeneous because it has little structure and contains hardly any macropores. The h_f -values of this soil are close to the value of -28 cm found by BODMAN & COLMAN (1944) for a Yolo silt loam without macropores, but are still half of the value of -50 cm given by STROOSNIJDER (1976) for a Dutch silt loam. The effect of macropores obviously lowers the absolute value of h_f . The values given by BRAKEN-SIEK (1977) for a silt loam are similar to the values of -3.5 to -5 cm in Table 6.2, but for a sandy loam he found -20 to -25 cm.

Repeated ponded infiltration mostly showed that the effective value of k_0 (k_s) fall between the end of the first and subsequent experiments with ponded infiltration. Three mechanisms could be responsible for this:

- Decreasing conductivity of cracks as a result of the swelling of colloidal soil particles. However, this mechanism does not explain why a subsequent ponding experiment could show a reduced k_s after a dry interval of up to several days when the initial moisture contents in the column were the same or even lower. Neither does it explain why the same phenomenon was also found in the loamy sand with hardly any smectites.
- Mechanical blocking by movement of the finest particles of non-cemented materials during the flow of infiltrated water; release of dissolved air or other blockage by air in pores. Blocking by fine soil particles could explain the lower level of k_s in later experiments, but not the major decrease in k_s occurring during the dry interval between two experiments when only a slight capillary flow was involved.

Blocking by air entry could explain the fall of k_s observed after a short interruption of ponding during an experiment at site 3 when k_{sat} decreased from 6 to 1.9 m. day^{-1} , but it seems an unlikely explanation for the lower level of k_s found two to five days afterwards.

- Partial collapse of a hole provoked by a momentary rise of the seepage pressure, as explained in the section "Theoretical considerations". Such a blocking of part of a macropore will lower the saturated conductivity. Calculations of the gradient of the head and the shear strength of the soil close to a vertical hole show that encapsulated air can give rise to a seepage pressure that exceeds the shear strength. Unsaturated infiltration tests done before and after the ponding experiments showed unchanged values for k_{unsat} . This supports the contention that the changes in hydraulic conductivity were caused by changes in the macropores.

Acknowledgements

The author is greatly indebted to Prof. W. H. van der Molen for his valuable comments.

NOTATION

symbol	description	dimension
d	height of a soil layer	L
g	gravitational field strength	$L \cdot t^{-2}$
h	hydraulic head of soil moisture	L
h_f	capillary pressure head at wetting front	L
h_p	capillary pressure head of soil moisture	L
I	cumulative infiltration	L
j	seepage pressure	$M \cdot L^{-2} \cdot t^{-2}$
k	hydraulic conductivity	$L \cdot t^{-1}$
L	depth of the wetting front	L
n	porosity	-
s	coordinate in flow direction	L
t	time	t
z	depth below soil surface (pos. downward)	L
θ	volumetric soil moisture content	-
ρ_w	density of water	$M \cdot L^{-3}$
ρ_b	dry bulk density of soil	$M \cdot L^{-3}$
ρ_s	density of solid soil matter	$M \cdot L^{-3}$

subscripts

i	initial
0	belonging to the transmission zone
s	effective
sat	saturated
unsat	unsaturated

REFERENCES

- ADAMS, J. E., KIRKHAM, D. & NIELSEN, D. A. (1957), A portable rainfall-simulator infiltrometer and physical measurements of soil in place. *Soil Sci. Soc. Am. Proc.* 21 (5), pp. 473-477.
- BEVEN, K. J. (1981), Micro-, meso-, macroporosity and channeling flow in soils. *Soil. Sci. Soc. Am. J.* 45, p. 1245.
- BEVEN, K. J. & CLARKE, R. T. (1986), On the variation of infiltration into a homogeneous soil matrix containing a population of macropores. *Water Resour. Res.* 22 (3), pp. 383-388.
- BEVEN, K. J. & GERMAN, P. (1982), Macropores and water flow in soils. *Water Resour. Res.* 18 (2), pp. 1311-1325.
- BODMAN, G. B. & COLMAN, E. A. (1944), Moisture and energy conditions during downward entry of water into soils. *Soil Sci. Soc. Am. Proc.* 8, pp. 116-122.
- BOND, W. J. & COLLIS-GEORGE, M. (1981a), Ponded infiltration into simple soil systems: 1. The saturation and transition zones in the moisture content profiles. *Soil Sci* 131 (4), pp. 202-209.
- BOND, W. J. & COLLIS-GEORGE, M. (1981b), Ponded infiltration into simple soil systems: 3. The behavior of infiltration rate with time. *Soil Sci.* 131 (6), pp. 327-333.
- BOUMA, J., HILLEL, D. I., HOLE, F. D. & AMERMAN, C. R. (1971), Field measurement of unsaturated hydraulic conductivity by infiltration through artificial crusts. *Soil Sci. Soc. Am. Proc.* 35, pp. 362-364.
- BOUMA, J. & DENNING, J. L. (1972), Field measurement of unsaturated hydraulic conductivity by infiltration through gypsum crusts. *Soil. Sci. Soc. Am. Proc.* 36, pp. 846-847.
- BOUMA, J. (1982), Measuring the hydraulic conductivity of soil horizons with continuous macropores. *Soil Sci. Soc. Am. J.* 46, pp. 438-441.
- BOUMA, J., BELMANS, C. F. M. & DEKKER, L. W. (1982), Water infiltration and redistribution in a silt loam subsoil with vertical worm channels. *Soil Sci. Soc. Am. J.* 46, pp. 917-921.
- BOUWER, H. (1966), Rapid field measurement of air entry value and hydraulic conductivity of soil as significant parameters in flow system analysis. *Water Resour. Res.* 2, pp. 729-738.
- BOUWER, H. (1969), Infiltration of water into nonuniform soil. *J. Irrigation Drainage Div., ASCE*, 95 (IR4), pp. 451-462.
- BOUWER, H. (1976), Infiltration into increasingly permeable soils. *J. Irrigation Drainage Div., ASCE*, 102 (IR1), pp. 127-136.
- BRAKENSIK, D. L. (1977), Estimating the effective capillary pressure in the Green and Ampt infiltration equation. *Water Resour. Res.* 13 (3), pp. 680-682.
- BRAKENSIK, D. L., ENGLEMAN, R. L. & RAWLS, W. J. (1981), Variation within texture classes of soil water parameters. *Trans. ASAE*, 24 (2), pp. 335-339.
- Bureau de Recherche Géologiques et Minières (1966), Carte géologique a 1:80.000, Feuille 197, Largentière et notice explicative. Ministère de l'Industrie, Paris.
- Bureau de Recherche Géologiques et Minières (1967), Carte géologique a 1:80.000, Feuille 198, Aubenas et notice explicative. Ministère de l'Industrie, Paris.
- Bureau de Recherche Géologiques et Minières (1974), Carte géologique a 1:50.000, Feuille 864, Largentière et notice explicative. Service Géologique National, Orléans.
- BROOKS, R. H. & COREY, A. T. (1964), Hydraulic properties of porous media. *Hydrol. Pap.* 3. Agr. Eng. Dept. Colorado State Univ., Fort Collins, 27 pp.
- BYBORDI, M. (1973), Infiltration of water into nonuniform soils. In: A. Hadas, Ed., *Physical aspects of soil and water and salts in ecosystems*. Springer Verlag, Berlin, Germany, pp. 91-95.
- CHAMBERLIN, T. W. (1972), Interflow in the mountain forest soils of coastal British Columbia. In: H. O. Slaymaker & H. J. McPherson, Eds., *Mountain geomorphology*, Vancouver, Canada.
- CHILDS, E. C. & BYBORDI, M. (1969), The vertical movement of water in stratified porous material. 1. Infiltration. *Water Resour. Res.* 5 (2), pp. 446-459.
- CLAPP, R. S. & HORNBERGER, G. M. (1978), Empirical equations for some hydraulic properties. *Water Resour. Res.* 14 (4), pp. 601-604.
- COLMAN, E. A. & BODMAN, G. B. (1945), Moisture and energy conditions during downward entry of water into moist and layered soils. *Soil Sci. Soc. Am. Proc.* 9, pp. 3-11.
- DAVIDSON, M. R. (1984), A Green-Ampt model of infiltration in a cracked soil. *Water Resour. Res.* 20 (11), pp. 1685-1690.
- DAVIDSON, M. R. (1985), Asymptotic behavior of infiltration in soils containing cracks or holes. *Water Resour. Res.* 21 (9), pp. 1345-1353.
- DAVIDSON, M. R. (1987), Asymptotic infiltration into a soil which contains cracks or holes but whose surface is otherwise impermeable. *Transport in porous media* 2, pp. 165-176.

- EDWARDS, W.M., VAN DER PLOEG, R.R. & EHLERS, W. (1979), A numerical study of the effects of noncapillary-sized pores upon infiltration. *Soil Sci. Soc. Am. J.* 43, pp. 851-856.
- GERMANN, P. & BEVEN, K. (1981), Water flow in soil macropores. I. An experimental approach. *J. Soil. Sci.* 32, pp. 1-39.
- GREEN, W.H. & AMPT, G.A. (1911), Studies on soil physics: I. Flow of air and water through soils. *J. Agr. Sci.* 4, pp. 1-24.
- HACHUM, A. & ALFARO, J.F. (1980), Rain infiltration into layered soils: prediction. *J. Irrigation Drainage Div.* 106 (IR4), pp. 311-319.
- HILLEL, D.I. & GARDNER, W.R. (1969), Steady infiltration into crust-topped profiles. *Soil Sci.* 107, pp. 137-142.
- HILLEL, D.I. & GARDNER, W.R. (1970a), Transient infiltration into crust-topped profiles. *Soil Sci.* 109, pp. 69-76.
- HILLEL, D.I. & GARDNER, W.R. (1970b), Measurement of unsaturated conductivity and diffusivity by infiltration through an impeding layer. *Soil Sci.* 109, pp. 149-152.
- KOOREVAAR, P., MENELIK, G. & DIRKSEN, C. (1983), *Elements of soil physics*. Elsevier, Amsterdam.
- LE BISSONNAIS, Y. (1988), Analyse des mécanismes de mobilisation et de déplacement des particules à la surface du sol sous l'action des pluies. Thesis, Univ. Orléans, France.
- MCCUEN, R.H., RAWLS, W.J. & BRAKENSIEK, D.L. (1981), Statistical analysis of the Brooks-Corey and the Green-Ampt parameters across soil textures. *Water Resour. Res.* 17 (4), pp. 1005-1013.
- MEIN, R.G. & FARRELL, D.A. (1974), Determination of wetting front suction in the Green-Ampt equation. *Soil Sci. Am. Proc.* 38 (5), pp. 872-876.
- RAWLS, W.J., BRAKENSIEK, D.L. & MILLER, N. (1983), Green-Ampt infiltration parameters from soils data. *J. Hydraul. Eng.* 109 (1), pp. 62-70.
- RUSSO, D. (1988), Determining soil hydraulic properties by parameter estimation: On the selection of a model for the hydraulic properties. *Water Resour. Res.* 24 (3), pp. 453-459.
- SMETTEM, K.R.J. (1986), Analysis of water flow from cylindrical macropores. *Soil Sci. Soc. Am. J.* 50, pp. 1139-1142.
- STROOSNIJDER, L. (1976), Infiltration and redistribution of water in soils. *Agric. Res. Rep.* 847, Pudoc, Wageningen, Netherlands, pp. 119-174.
- TAKAGI, S. (1960), Analysis of vertical downward flow of water through a two-layered soil. *Soil Sci.* 90, pp. 98-103.
- VAN DEN BERG, J.A. & T. LOUTERS (1984), Elektronische Datenerfassung zur Modellierung des Bodenfeuchtigkeitsregimes unter Verwendung eines netzunabhängigen Dataloggers und schnellreagierenden Tensiometers. Dept. of Physical Geography, Utrecht University, The Netherlands, 9 pp.
- VAN DEN BERG, J.A. & T. LOUTERS (1985), Towards representing soil moisture conditions of catchments. In: Müller, H.E. & K.R. Nippes (Eds.) *Problems of regional Hydrology*. Proc. Freiburg Symp. Beitr. Hydrol., Sonderheft 5.2, pp. 749-774.
- VAN DEN BERG, J.A. & T. LOUTERS (1988), The variability of soil moisture diffusivity of loamy to silty soils on marl, determined by the hot air method. *J. Hydrol.* 97, pp. 235-250.
- VAN DEN BERG, J.A. & P. ULLERSMA (in prep.), The impact of ponded infiltration on the stability of macropores (modelled by an electric analogon).
- WHISLER, F.D. & H. BROUWER (1970), Comparison of methods for calculating vertical drainage and infiltration for soils. *J. Hydrology* 10 (1), pp. 1-19.

7. **TOWARDS THE REGIONALIZATION OF HYDRAULIC AND PLANT-SOIL
PARAMETERS FOR MODELLING SOIL MOISTURE CONDITIONS OF A CATCH-
MENT**

Accepted for publication in *Earth Surface Processes and
Landforms*, March 1989.

Permission for reproduction 17 August 1989 of John Wiley &
Sons, Ltd.

7. TOWARDS THE REGIONALIZATION OF HYDRAULIC AND PLANT-SOIL PARAMETERS FOR MODELLING SOIL MOISTURE CONDITIONS OF A CATCHMENT

Abstract

Computational simulation of the moisture regime of the soil is a useful help in studying land potential, ecology and land degradation processes such as soil erosion and mass movement. The utility of modelling soil moisture depends on the validity of the model structure and of the model parameters. Moreover, except for differences in relief and for variation in rainfall and net radiation, such a model will show spatial variability only if the variability of the ecological properties of the soil and the vegetation canopy can be input.

Eight experimental sites on erodible loamy to silty soils in the Ardèche Basin, France, were investigated, to ascertain how the information required for modelling soil moisture can be obtained. Three terms of the soil moisture budget were measured or determined for compiling the model structure: rainfall, soil moisture content (or capillary pressure head) and actual evapotranspiration. The latter was calculated with the Bowen ratio method from the energy balance measured at three sites. These data were also used to calculate the canopy resistance in the evaporation formula based on transport resistances.

To study how to regionalize the hydraulic parameters, the characteristics of unsaturated conductivity and soil moisture diffusivity as a function of moisture content or capillary pressure head were determined by the hot air method for intermediate moisture contents and with the crust method on soil columns *in situ* for high moisture contents. Estimation of the diffusivity from soil texture appeared to be less successful for fine-textured soils. Macropores apparently crucially influenced the capacity of ponding infiltration and the frequency of overland flow.

Key words: soil moisture systems, saturated and unsaturated conductivity, diffusivity, macropores, canopy resistance.

7.1 Introduction

Land degradation is a problem of major order that erodes the basis of civilization (BLAIKIE & BROOKFIELD 1987). Water is a fundamental factor in land degradation processes such as soil erosion and soil mass movement, as well as in ecology or when studying land potential. Therefore it is important to know how the regional soil moisture can be modelled for different forms of land use and a wide range of plant cover. A suitable and common way of understanding the soil moisture regime of an area is its computational simulation. Various models and modelling techniques of differing sophistication are available to do this. But the utility of their output depends strongly on the validity of the model structure (which should be verified by field measurements) and

also on the validity of the parameters applied in the model. Two types of parameters can be distinguished: hydraulic ones for the flow of soil water and plant-soil parameters that determine the response of the vegetation to atmospheric water demand. The main elements in regionalization will be to take account of the impact of different physiographic factors such as geology, geomorphology and pedology on the schematization and the relevant depth of the soil-rock system and on the system characteristics concerning the storage and flow parameters of soil moisture.

This paper describes research done on erodible soils of a loamy to silty texture in the Ardèche Basin, France, to ascertain the spatial and temporal variability of the parameters of such models. In the study area the upper soil is reasonable homogeneous but its thickness varies. The subsoil is banded and consists of alternating layers of two types of bedrock, each with strongly different hydraulic properties: one with storage capacity and Darcian water flow in pores (weathered marl) and the other with storage and water flow in planar voids of fissured rock (limestone). Figure 7.1 is a schematic representation of the system in the study area.

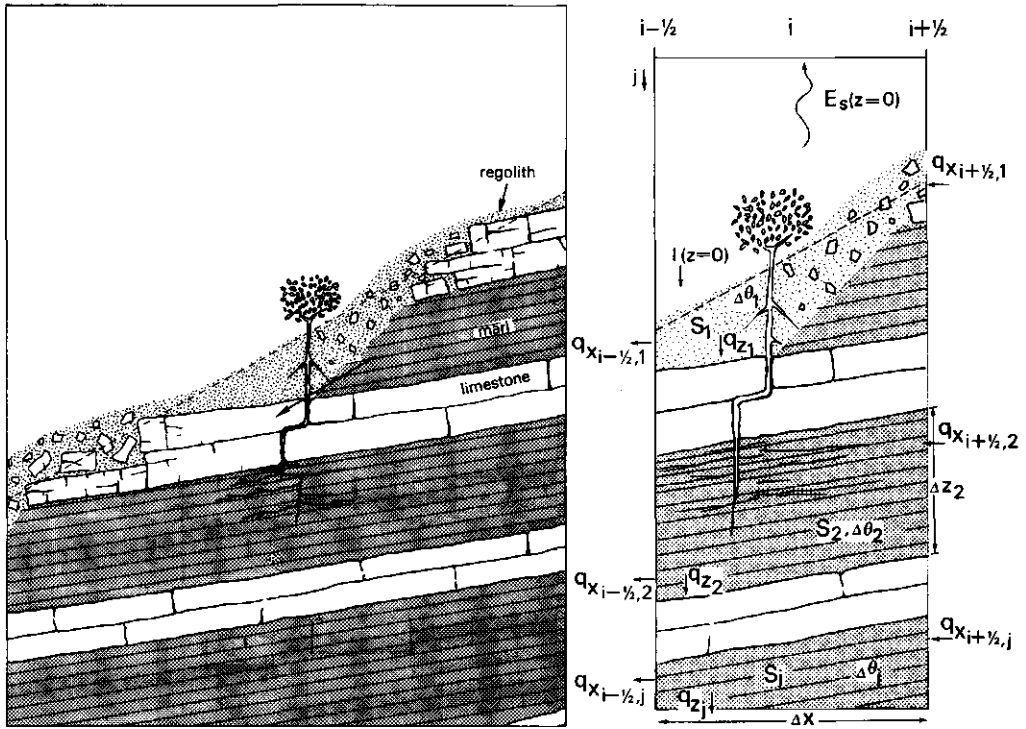


Fig. 7.1. a. Vertical soil profile.

b. Verified model structure.

Three phases can be distinguished. First, the system must be reliably identified, so that the following questions concerning the boundaries and the sectioning of the area to be modelled can be answered:

- to what depth is the soil moisture relevant in the system we wish to model (i. e. at what depth can we place the lower boundary)?
- into how many layers does the soil have to be subdivided with regard to differences in hydraulic properties and sink term strength?

A preliminary investigation of the soil moisture budget showed that at the end of summer up to 90% of the evapotranspiration was extracted from porous layers in the subsoil (VAN DEN BERG 1983). In this paper, therefore, "soil" will include all soil-rock strata within the reach of plant roots.

Aspects of the second phase, the regionalization of the model parameters, are discussed in this chapter. In this context "regionalization" means the process of attaching a value to a parameter at different points (e. g. nodal points) in an area, taking into account the spatial variability of that parameter.

The third phase, which is still in progress, is the modification, calibration and verification of the model and the simulation.

7.2 Theoretical considerations

7.2.1 Flow in the unsaturated zone

Each model for simulating the flow of soil moisture in a porous medium is based on two fundamental hydrological laws: Darcy's law and the continuity equation. Two-dimensional flow of soil moisture can be represented by a linear combination of the flux densities q_x and q_z in the x- and z-direction.

According to Darcy's law these flux densities (in $\text{kg. m}^{-2}. \text{day}^{-1} = \text{mm. day}^{-1}$) can be written as

$$q_x = -k_x(h) \frac{\partial h}{\partial x} \quad \text{and} \quad q_z = -k_z(h) \left(\frac{\partial h}{\partial z} - 1 \right) \quad (7.1)$$

where h is the capillary pressure head (negative in the unsaturated zone) and $k(h)$ is the hydraulic conductivity; z and q are positive downwards.

The continuity equation for the unsaturated zone can be written as

$$-\frac{\partial q_x}{\partial x} - \frac{\partial q_z}{\partial z} = S + \frac{\partial \theta}{\partial t} \quad (\text{day}^{-1}) \quad (7.2)$$

where t is time, θ is the volumetric soil moisture content and S a volumetric sink term. S is the volume of soil water that is taken up by the plant roots per unit bulk volume of soil in unit time and almost all of which is released through the leaves to the atmosphere, only a tiny amount being stored in the growing vegetation.

FEDDES et al. (1978) modelled the sink term S as a function of the absolute value of the capillary pressure head h :

$$S(|h|) = a(|h|). S_{\max} \quad \text{with} \quad 0 \leq a(|h|) \leq 1.$$

As anaerobic soil conditions are not likely to occur in the area investigated, $a(|h|) = 1$ as long as $|h| < |h^*|$; from $|h^*|$ to permanent wilting point $a(|h|)$ decreases from 1 to 0. $|h^*|$ is an important parameter in this model and depends on vegetation and on atmospheric water demand (FEDDES et al. 1988).

Soil moisture diffusivity $D(\theta)$ is a soil property like hydraulic conductivity; it determines soil water flow at a given gradient of θ and is defined as

$$D(\theta) = + k(h) \frac{dh}{d\theta} = k(\theta) \frac{dh}{d\theta} \quad (7.3)$$

With eqn. (7.1) this gives

$$q_x = - D_x(\theta) \frac{\partial \theta}{\partial x} \quad \text{and} \quad q_z = - D_z(\theta) \frac{\partial \theta}{\partial z} + k(\theta) \quad (7.4)$$

In the unsaturated zone $k(\theta)$ and $d(\theta)$ depend on the moisture content. Combining eqns. (7.1) and (7.2) gives us the partial differential equation for isothermic, isobaric two-dimensional flow of water through the unsaturated soil.

$$\frac{\partial}{\partial x} \left(k_x \frac{\partial h}{\partial x} \right) + \frac{\partial}{\partial z} \left(k_z \frac{\partial h}{\partial z} \right) + \frac{\partial k_z}{\partial z} = S + \frac{\partial \theta}{\partial t} \quad (7.5)$$

Figure 7.2 is a schematic representation of an element of a spatial finite difference grid for flow in an x, z -plane; time has to be added as third dimension.

For unsaturated flow eqn. (7.5) is called the Richards equation (SPOTOSITO 1987). Though the mass flow of soil water through the layers of jointed limestone cannot be described by Darcy's law, such layers can be modelled as a theoretically porous medium whose hydraulic properties are comparable with respect to soil moisture budget: low storage capacity and high vertical, saturated permeability.

When eqn. (7.2) is applied to a soil compartment as shown in Fig. 1b this yields a formula for the soil moisture budget over time step Δt (all terms are averages over time and expressed in mm. day^{-1}).

$$I(z=0) = E_s(z=0) + \sum_0^r [q_{x_{i+\frac{1}{2},j}} - q_{x_{i-\frac{1}{2},j}}] \Delta z_j + q_p(z) + \sum_0^r S_j \cdot \Delta z_j + \sum_0^r \frac{\Delta \theta_j}{\Delta t} \cdot \Delta z_j \quad (7.6)$$

in which I (infiltration) and E_s (soil evaporation) are flux densities across the upper boundary, $q_p(z)$ is the flux density across the lower boundary (percolation or capillary rise) and r is rooting depth. During dry weather ($I = 0$) and when throughflow and percolation are negligible, the actual evapotranspiration E_a in the study area is equal to

$$E_a = E_s(z=0) + \sum_0^r S_j \Delta z_j = - \sum_0^r \frac{r \Delta \theta_j}{\Delta t} \Delta z_j \quad (\text{mm. day}^{-1}) \quad (7.7)$$

According to the conditions specified by GREEN & AMPT ponding infiltration can be modelled as follows

$$I_c = L_f \cdot (\theta_0 - \theta_i) \quad (7.8a)$$

$$t = \frac{\theta_0 - \theta_i}{k_0} \cdot L_f + h_f \cdot \ln \left[\frac{L_f - h_f}{-h_f} \right] \quad (7.8b)$$

where I_c is cumulative infiltration depth, t is duration of ponding infiltration, L_f is depth of the wetting front, h_f (negative) is the effective capillary pressure head at this front, k_0 is the hydraulic conductivity in the transmission zone and θ_i and θ_0 are the initial volumetric moisture content and that in the transmission zone (KOORE-VAAR et al. 1983). The principal assumptions of this approach are that a distinct wetting front exists, that h_f remains constant, regardless of time and position and that the soil behind the wetting front is uniformly wet and of constant conductivity (HILLEL 1980). Although

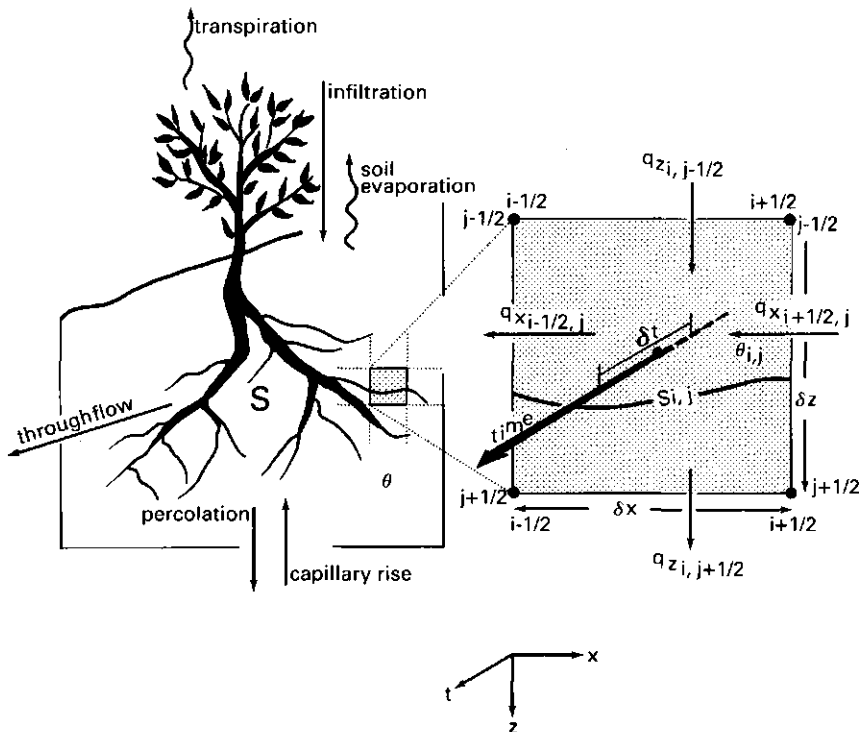


Fig. 7.2. An element from a spatial finite difference grid for two-dimensional flow. All terms are mean values for time step δt .

macropores can cause an irregular wetting front in a fine-textured soil, eqns. (7.8a) and (7.8b) still represent a useful infiltration formula because they contain soil physical parameters that can be adapted to soil conditions.

Measurements of hydraulic parameters such as the unsaturated conductivity $k(h)$ or $k(\theta)$ and the soil moisture diffusivity, $D(\theta)$, both as a function either of capillary pressure head h or of soil moisture content θ are laborious and often cumbersome. Therefore researchers have often attempted to correlate hydraulic characteristics with soil properties that are easier to ascertain. Many relationships between hydraulic parameters and soil texture and porosity have been established in this way. Brief reviews of such relationships have been given recently by RUSSO (1988) and VAN DEN BERG & LOUTERS (1988). Indeed, the storage and flow of water are determined by soil pores, which in turn are related to soil texture. However, this way of estimating hydraulic soil characteristics seems less successful for soils that contain an appreciable proportion of colloids, as do the silt loam and silty-clay loam soils of the study area (VAN DEN BERG & LOUTERS 1988). Moreover, it also results in macropores being overlooked. These pores have such large diameters that they can be kept filled with water only if the capillary pressure head is close to zero. Thus, when the soil is temporarily saturated, macropores appreciably enhance the hydraulic conductivity. In this way the presence of macropores complicates the estimation of the hydraulic properties of a soil. For open soils in which the macropores come to the soil surface, the impact of macropores on the saturated conductivity has been discussed by many authors (e.g. BEVEN & GERMAN 1982, BOUMA 1982). Most macropores are secondary pores and result from mechanical or biological processes such as cracking, shrinkage and the activity of soil fauna and plant roots (SIDLE et al. 1985).

7.2.2 Evapotranspiration

Evaporation is the connecting link between the water budget and the energy budget. The major portion of the incoming total radiation is absorbed near the surface of the earth and transmitted into long-wave back radiation, convection of sensible heat (flux density H), evaporation of water (flux density E_a) and conduction of heat into the soil (flux density G). The energy budget can thus be written as

$$R_n = H + L.E_a + G \quad (W.m^{-2}) \quad (7.9)$$

in which R_n is net incoming radiation and L is latent heat of vaporization. Soil heat flux is often neglected in practical applications. However, as will be shown later, for this area it must be incorporated.

Variation of meteorological model input can be expected, especially concerning rainfall, the net radiation as affected by season and cloudiness and the part of net radiation that is available for evapotranspiration E_a . If the surfaces of plants and soil are dry, E_a consists mainly of transpiration that equals the sink term S of eqn.

(7.2). As the latent heat of vaporization is large (ca. 2.45 MJ.kg⁻¹), the budget of soil moisture is strongly related to the energy budget of eqn. (7.9).

The response of vegetation to atmospheric water demand results in actual or potential transpiration, depending on whether available soil moisture is a restricting factor.

The actual evapotranspiration E_a was calculated with the Bowen ratio method

$$E_a = \frac{(R_n - G)}{L(B + 1)} \text{ (mm day}^{-1}\text{)} \quad (7.10)$$

in which

$$B = \gamma \cdot \frac{k_h}{k_m} \cdot \frac{\Delta T}{\Delta e} \quad (-) \quad (7.11)$$

where γ is the psychrometer constant, k_h and k_m are the eddy diffusivities of sensible heat and of water vapour, respectively; k_h has been taken equal to k_m . ΔT and Δe are the differences in air temperature and water vapour pressure over the vertical distance Δz .

By introducing the canopy resistance r_c for the internal diffusion of water vapour within the canopy, and the aerodynamic resistance, r_a , to the turbulent diffusion of sensible heat and water vapour through the air layer between the plant canopy and z (the height of measurement), the actual evapotranspiration can also be calculated from the Penman-Montheith-Rijtema equation

$$E_a = \frac{s(R_n - G) + \rho_a c_p (1/r_a)(e_s - e)}{L[s + ((r_a + r_c)/r_a)]} \text{ (mm day}^{-1}\text{)} \quad (7.12)$$

where s is the slope of the saturation vapour pressure curve at air temperature, ρ_a is air density, c_p is specific heat at constant pressure and e and e_s are the actual and saturated water vapour pressure (MONTEITH 1965, RIJTEMA 1965). The great advantage of eqn. (9.12) over eqn. (9.10) is that meteorological data measured at standard height will suffice if only r_c is known. When the vegetation canopy is wet, the diffusion resistance r_c becomes zero (KEYMAN 1981).

The aerodynamic resistance r_a can be estimated from canopy height L_c and the wind velocity u at 2 m follows

$$r_a = \frac{[\ln(z/z_0)]^2}{(k_n^2 \cdot u)} \text{ (s. m}^{-1}\text{)} \quad (7.13)$$

in which z_0 is the aerodynamic roughness parameter of the vegetation cover (of order $L_c/9.55$) and k_n is von Kármán's constant (0.41). For the preliminary investigation r_a has been adapted to an unstable atmosphere; in accordance with LETTAU (1949) r_a was multiplied by the stability factor:

$$(1 + R_i)^2 \quad (7.14)$$

in which R_i is the Richardson number; ($R_i = 0$ for neutral conditions, $R_i < 0$ for unstable and $R_i > 0$ for stable conditions). The difference resulting from this correction was so slight that atmospheric instability has been neglected in the subsequent experiments. According to THOM & OLIVER (1977) and using Penman's wind function eqn. (7.13) can be written as

$$r_a = \frac{4.72 [\ln(z/z_0)]^2}{(1 + 0.54 u)} \quad (\text{s. m}^{-1}) \quad (7.15)$$

The potential evapotranspiration of a dry canopy was calculated according to Penman as modified by THOM & OLIVER (1977):

$$E_p = \frac{s(R_n - G)/L + m\gamma \cdot f \cdot (1 + 0.54 u) \cdot (e_s - e)}{s + \gamma \cdot (1 + n)} \quad (\text{mm. day}^{-1}) \quad (7.16)$$

in which $n = r_c/r_a$; r_a was estimated by eqn. (7.15).

$$m = [\ln(z/z_{OP}) / \ln(z/z_0)]^2$$

z_{OP} = value of z_0 in Penman's equation (1.37 mm).

z_0 = local value of z_0 .

$$f = \frac{26640 \cdot n_1}{L}$$

n_1 = duration of the period over which the meteorological variables of eqn. (7.16) were summed or averaged.

If a shortage of available soil moisture has not increased the bulk stomatal resistance, r_c , the evapotranspiration according to eqn. (7.12) equals the potential value; thus, the corresponding value of r_c equals its potential value r_{cp} . In this way, E_p can be calculated with eqn. (7.12) if the potential value r_{cp} is substituted for r_c . E_p , calculated in this way, should give nearly the same value compared to the value computed with eqn. 7.16.

Using eqn. (7.12) as an expression for actual (with r_c) and for the potential (with r_{cp}) evapotranspiration, the actual canopy resistance r_c can be written as a function of the ratio between actual and potential evapotranspiration

$$r_c = \left[1 + \frac{s}{\gamma} \right] \cdot r_a + r_{cp} \cdot \frac{E_p}{E_a} - \left(1 + \frac{s}{\gamma} \right) \cdot r_a \quad (\text{s. m}^{-1}) \quad (7.17)$$

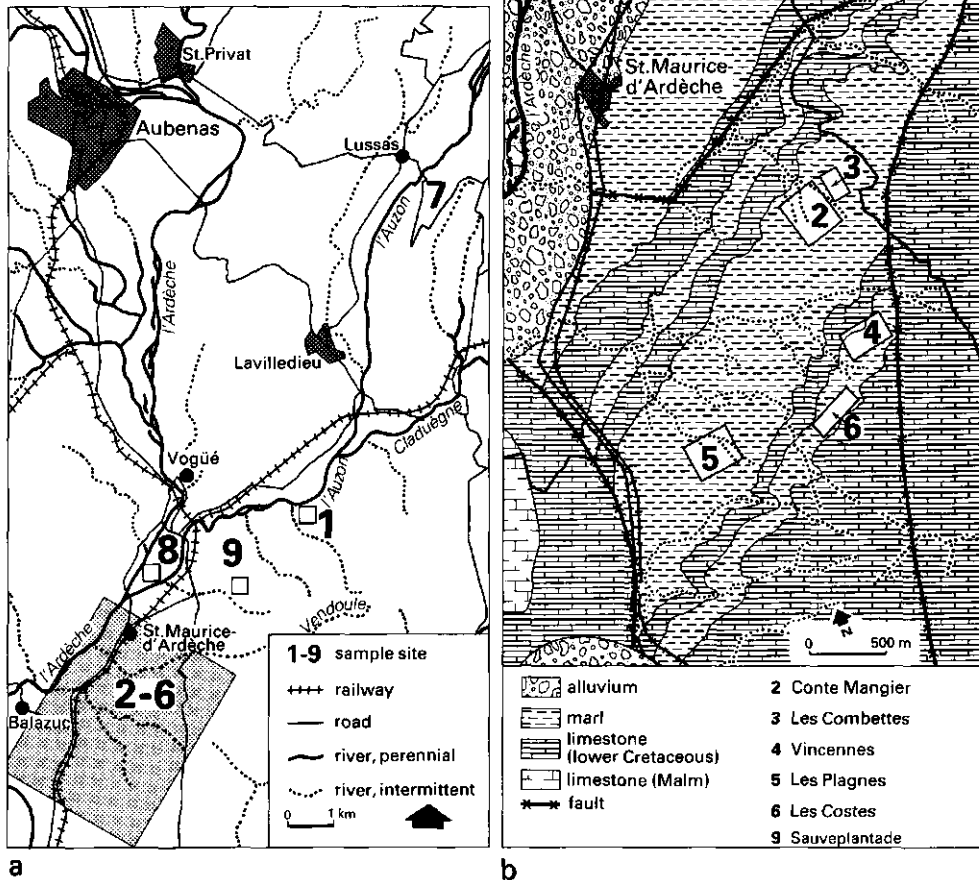


Fig. 7.3. a. Location of the experimental sites within the Ardèche Basin, southern France. For the shaded area: see fig. b.
b. Lithology and location of sites 2-6.

7.3. Site description

To study the effect of local physiographical variability on hydraulic parameters, eight representative experimental sites were selected in parts of the study area with bedrock belonging to the same lithological unit (Fig. 3a: 1-7 and 9). Three of these sites (Conte Mangier, Les Costes and Sauveplantade, Fig. 3b) can be considered as key areas, because evapotranspiration and soil moisture content were measured simultaneously there.

The eight experimental sites are located between 150 and 300 m altitude in the midstream part of the Ardèche Basin, where the bedrock consists of Lower Cretaceous marl irregularly intercalated with limestone. Here, drainage pattern and relief are governed by geological structure (fault lines) and lithology. Steeper slopes are found where Cretaceous limestone outcrops; the landscape is slightly sloping on marly bedrock where, in places, a pediment or glacis that interfingers with river

terraces has been formed. Five of the experimental sites (Fig. 3a and b, nos 4 to 7 and 9) are on such a pediment (VAN DEN BERG & LOUTERS 1988).

In many places, features of present-day soil erosion are found; a soil loss of 0.8 tons/ha upslope to 2.2 tons/ha on the lower part of an eroded slope was measured during winter (ROELS 1984). The gently sloping relief on marl is frequently intersected by gullies up to 50 m deep.

In the study area the upper soil is reasonably uniform and its thickness varies, mainly between 0.1 and 0.8 m. The subsoil is banded and consists of alternating layers of limestone and weathered marl dipping slightly southeast (12-18°). The limestone in the subsoil is hard and dense but very jointed. On the bedrock of marl and limestone brown calcareous soils are found; according to the USDA Soil Taxonomy these soils can be classified as poorly developed haploxerolls to xerochrepts. The texture varies between silt loam, silty-clay loam and loam (see Fig. 4). For the sake of contrast, a site with a sandy loam soil on an alluvial deposit of the Ardèche river (Fig. 3a, site 8) and a site with a loamy sand on a deeply weathered Triassic sandstone were added.

This part of the Ardèche Basin, where numerous natural caves and rock shelters offered a favourable habitat for humans, has a long history of anthropogenic activity. Prehistoric traces dating from the last two glaciations, Riss and Würm, have been found (BOYER 1988). Soil degradation has been occurring since Neolithic times (fourth millennium BC) when human occupation expanded (over 650 dolmens have been found) and people changed from being hunters and gatherers to growing crops and keeping livestock (PIGGOTT 1981, BOYER 1988).

Viticulture was introduced into the area in protohistoric times. The expansion of this type of land use promoted the construction of terraces. Three periods during which terraces were constructed and intensively used, can be distinguished: 1000-1350, 1400-1550 and 1600-1850. During this last period population growth led to new terraces being built, even on unsuitable slopes and far from settlements (BLANC 1984). In between and after these periods many terraces were abandoned and fell into disrepair, thereby becoming prey to soil erosion.

Nowadays, sites 1 and 8 are in use as vineyards; the others (2-7 and 9) are only extensively grazed and have a semi-natural vegetation cover that includes *Quercus pubescens*, *Buxus sempervirens*, *Juniperus oxicedrus*, *Thymus vulgaris*, *Lavendula stoechas*, *Aphyllanthes monspeliensis*, *Linum* and *Carex*. The three sites where the energy budget was measured, had a 95% plant cover consisting of grass and herbs (70%), scrub (20%) and trees (5%).

Natural vegetation is adapted to submediterranean climatic conditions that are characterized in the Ardèche Basin by a dry and warm summer and high rainfall in autumn and spring. Mean annual rainfall is about 1200 mm. Erosive rainfall events occur frequently, although under a cover of *Quercus pubescens* which is considered to be the present climax vegetation, the actual erosion rate is limited (MARTIN 1987). Heavy, local rainstorm events are especially common during September and

October; for example, 280 mm fell in 2 days in 1976, 205 mm in 9 hours in 1970, and 791 and 1060 mm fell in one day in 1827 and 1899 respectively (Ardèche Annales Météorologiques 1980, BOULLE 1986). Such torrential rainstorms cause the river to rise several metres; an increase of more than 20 m was recorded for the Ardèche river in 1890 (BOULLE 1986).

For a good understanding of the present-day erosional processes it would be interesting to know if the formation of the gullies in the Ardèche Basin should also be partly attributed to catastrophic rainfall events during the 14th and 18th centuries, as the Borks have found for loess areas in Central Europe (BORK & BORK, 1987).

7.4. Measurements and methodology

Field measurements done at representative sites and supplemented by laboratory measurements on undisturbed soil cores, were used to identify the system to be modelled and to examine the regionalization of the model parameters. The experimental sites were selected not at random but on the basis of surveys of lithology and soil, physiographic mapping and knowledge of the hydrological system obtained by preliminary research on the soil moisture budget (VAN DEN BERG 1983).

7.4.1. System identification

Three terms of the soil moisture budget were measured to identify the system: rainfall, actual evapotranspiration and change in water content of the soil. The plant canopy intercepts part of the rainfall. Because most rainfall in the Ardèche Basin occurs during spring and autumn, interception is a small term in the water budget; in this study it was omitted. The volumetric moisture content of the upper soil was determined gravimetrically. As well, in the key area Conte Mangier (Fig. 3.b) the pressure head in different marl layers of the subsoil was measured with tensiometers. Their arrangement was two-dimensional in order to be able to account for throughflow.

7.4.2. Evapotranspiration

The actual evapotranspiration rate E_a was calculated with the Bowen ratio method (eqn. 7.10). Net radiation was measured with a net pyroradiometer. The flux density of heat into the soil was measured with soil heat flux plates at 0.05 m depth and corrected for the difference in the specific heat conductivity of plate and soil and for the change in heat storage in the soil layer between 0.00 and 0.05 m, using the soil temperature at a depth of 0.02 m.

The differences in air temperature ΔT and in water vapour pressure Δe over the vertical distance Δz in the atmosphere were measured with psychrometers at 0.5 and 1.5 m above zero displacement height. Wind velocity was measured with two cup anemometers at the same heights as the psychrometers. All variables were measured every 15 seconds by a datalogger (Simac Logmaster MDL 500) and ten-minute averages were recorded on a cassette recorder (VAN DEN BERG & LOUTERS 1984). Furthermore, air temperature and relative humidity were measured in a Steven-

son's screen at 2 m height and recorded every 20 minutes by a Squirrel-Grant electronic recorder. Electric power was supplied by a combination of a solar collector and batteries.

7.4.3. Soil moisture parameters

Soil moisture retention curves were determined on undisturbed soil samples. For high moisture contents up to saturation (corresponding to a capillary pressure head between about -40 hPa and zero) the hydraulic conductivity was measured during ponding infiltration on crusted and uncrusted soil columns *in situ* (BOUMA 1971, VAN DEN BERG 1989). For the range of intermediate moisture contents the soil moisture diffusivity characteristic was determined by applying the hot air method on undisturbed soil cores. These methods have been described in detail elsewhere (VAN DEN BERG & LOUTERS 1986, 1988). If necessary, correction were made for changes in the volume change of the samples caused by swelling and shrinkage.

The cores were sampled from 11 plots at 7 different sites on marly bedrock in the study area (1-7 in Fig. 3), a loess pit near Maastricht (NL) and an alluvial deposit of the Ardèche River (Fig. 3, site 8). The loess was added in order to include a very silty soil, and the sandy loam was added for the sake of contrast. The soil texture of the samples is shown in the USDA texture triangle of Fig. 4.

USDA textural triangle

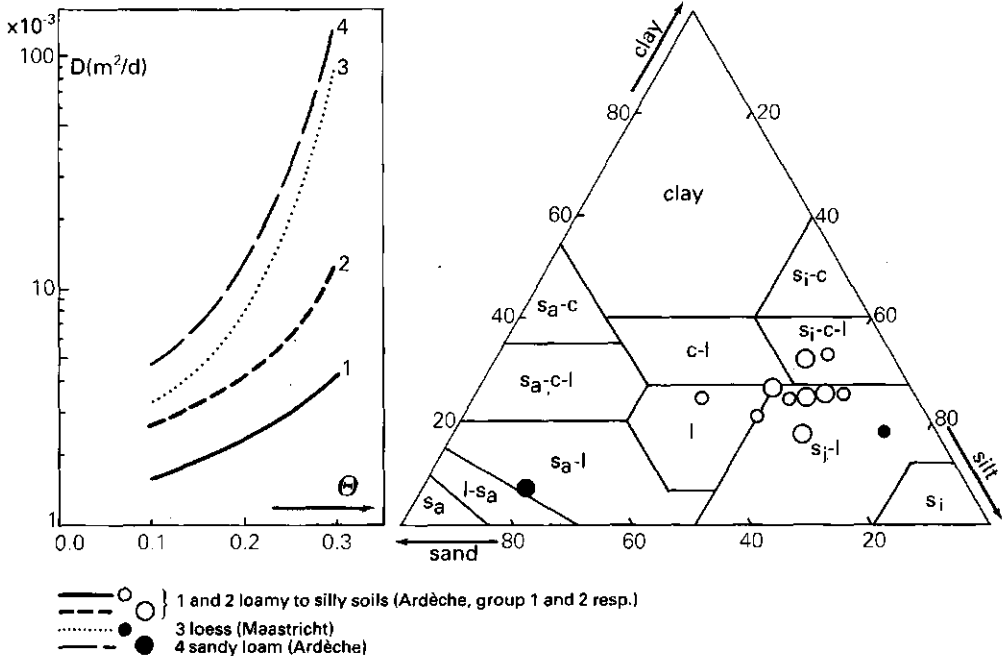


Fig. 7.4. Texture and characteristics of diffusivity at moisture contents between 0.1 and 0.3 for 11 grouped loamy to silty Ardèche soils, a loess and, for contrast, a sandy loam.

7. 4. 4. The canopy resistance

The internal diffusion resistance r_c and its potential value r_{cp} were calculated with eqn. 7.12 under different conditions of atmospheric water demand and soil moisture content. The meteorological measurements were done during spring and autumn only.

7. 5. Results

7. 5. 1. Identification of the system

The structure of the system to be modelled was compiled according to the measurements of the terms of the soil moisture budget as expressed in eqn. 7.7 for the different layers within the rooting zone. It appeared that the soil should be considered to be multi-layered, because several layers of weathered marl, intercalated between fresh limestone, are involved in the soil moisture regime of the plant-soil-rock system. This can be illustrated by the change of pressure head with time as measured in three subsoil layers of weathered marl; each graph could be analysed as a trend line due to moisture extraction and a daily variation caused by the cyclic change in moisture suction that was produced by plants in response to atmospheric water demand (VAN DEN BERG & LOUTERS 1984). This has been discussed in greater detail elsewhere (VAN DEN BERG & LOUTERS 1985).

7. 5. 2. Regionalization of parameters of soil water flow

For intermediate moisture contents the soils were arranged according to their diffusivity. The loamy to silty soils from the Ardèche were divided into two groups: one with a low diffusivity (group 1) and the other with an intermediate diffusivity (group 2). The diffusivity of the loess is much higher and the sandy loam has the highest diffusivity. These findings indicate that for soil moisture diffusivity of loamy to silty soils - even for intermediate moisture contents, when primary pores are mainly involved - texture may sometimes be used as a global differentiating factor, but that it seems to be an insufficient indicator to regionalize diffusivity within an area with fine-textured soils. From the description of the different sites it is concluded that areal variability of diffusivity of such soils can better be related to physiographic diversity, such as the heterogeneity of the petro fabric, clay fabric and soil structure (VAN DEN BERG & LOUTERS 1988).

For moisture contents belonging to values of the capillary pressure head (h) between -40 and 0 hPa, the hydraulic conductivity was plotted against h (Fig. 5). Lines 1 and 2 show the relationship for two silt loam soils. Both soils belong to group 1 with respect to the diffusivity at intermediate moisture contents. The soil represented by curve 1 contains macropores. These allow the hydraulic conductivity to increase very rapidly to the high value of about 3 m. day^{-1} for the saturated conductivity k_s . The other soil, curve 2, has no macropores and has a saturated conductivity of 0.07 m. day^{-1} . Curve 3 represents a loamy sand soil on Triassic sandstone and was added for contrast.

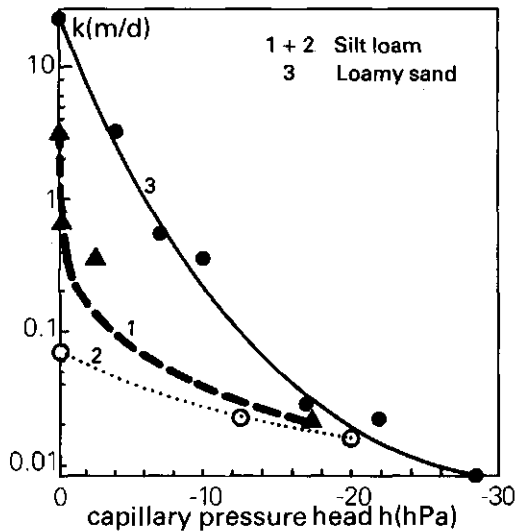


Fig. 7.5. Effect of macropores on hydraulic conductivity for two silt loam soils: 1 = with and 2 = without macropores, 3 = loamy sand soil for contrast.

The saturated conductivities of a silt loam soil with and without macropores (curves 1 and 2 of Fig. 5) were substituted in the formula of Green & Ampt for ponding infiltration (eqns. 7.8a and b). This was repeated for such a soil under conditions in which the effect of macropores on permeability was reduced because the soil had previously been saturated (VAN DEN BERG 1989). The corresponding values of the pressure head at the wetting front were also obtained from measurements on soil columns. Then the effect of macropores on the frequency of Hortonian overland flow was estimated for rainfall in October (for frequency curves of October rainfall see VAN DEN BERG & LOUTERS 1985). Rainstorms lasting one hour and with return periods (T_r) of 10 or 100 years result in overland flows of 42 mm or 82 mm, respectively. Where macropores had raised the saturated conductivity to about 3 m day^{-1} , overland flow did not occur. Some overland flow was calculated if the effectiveness of the macropores had been reduced by a previous saturation, see Table 1.

The impact of macropores on conductivity is considerable, but their effect is still difficult to model, because in silt loam they are mostly temporary (VAN DEN BERG 1989).

7.5.3. Plant-soil parameters

Daily values of r_c , E_a and E_p were calculated with eqns. (7.12, 7.10 and 7.16) for two sites: Les Costes (plant cover 95%, $z_0 = 40 \text{ mm}$) and Conte Mangier (plant cover 95%, $z_0 = 50 \text{ mm}$). Mean values (averaged over 8 to 11 days) were obtained with less accurate equipment for the Sauveplantade site (plant cover 90% and $z_0 = 40 \text{ mm}$). During spring, when the

Table 7.1 The effect of macropores on the cumulative values of ponding infiltration I_C and overland flow O , and on time t at which ponding starts after the beginning of the event, for two rainstorms (P) lasting one hour and with a return period of T_R of 10 years ($P = 56$ mm) or 100 years ($P = 96$ mm). ($\Theta_0 - \Theta_1$) has been taken 0.1.

no.	soil	k_S (m/d)	h_g (hPa)	I_C (mm)	P = 56 mm		P = 96 mm	
					t (min)	O (mm)	t (min)	O (mm)
1	with macropores	2.85	- 3.5	--	no ponding		no ponding	
	macropores previously saturated	0.80	- 4	43	17	13	3	53
2	no macropores	0.07	-25	14	3	42	0.5	82

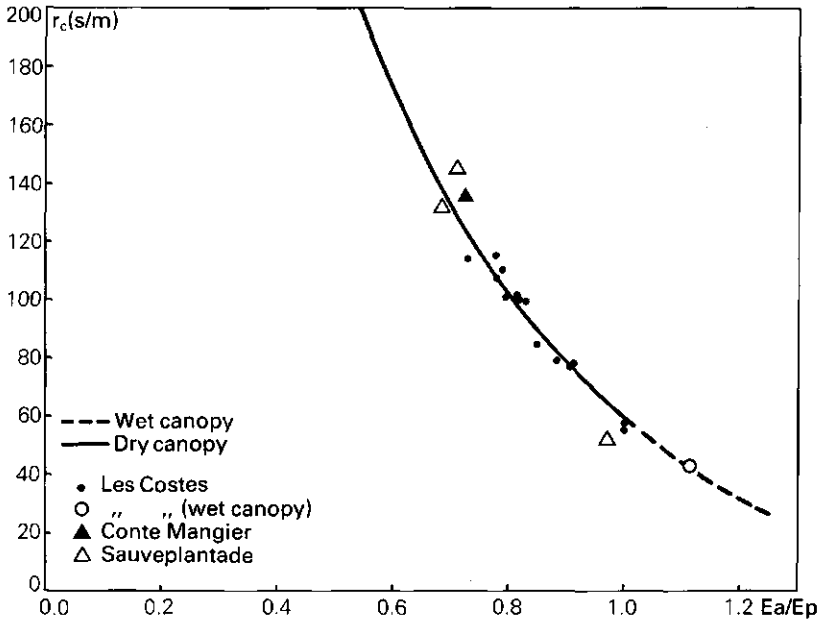


Fig. 7.6. Theoretical (line) and measured (points) values of the canopy or surface resistance r_c as a function of the ratio between actual and potential evapotranspiration.

soil is wet, the flux of latent heat could attain 95% of R_n (VAN DEN BERG & LOUTERS 1985). The differences between E_p , calculated with eqn. 7.12 by taking $r_c = r_{cp}$, and E_p , computed with eqn. 7.16, were smaller than 0.1 mm day^{-1} . The resistances r_c that were ascertained from the three plots, have been plotted in Fig. 6 as a function of the ratio E_a/E_p . The potential value of r_c was found for dry-surface conditions where moisture content did not limit transpiration i. e. where $E_a = E_p$; r_{cp} appeared to be 60 s.m^{-1} . R_c decreased to the lower value of 43 s.m^{-1} during a period with a moist soil and a canopy that was wetted temporarily by rain ($E_a/E_p = 1.13$).

R_c should depend on capillary pressure head of soil moisture as well as on atmospheric water demand. However, the relationship between r_c and pressure head is complicated by the layered soil-rock system. At Conte Mangier r_c was found to be 140 s.m^{-1} at a pressure head of pF 4.2 (near the surface) to 3.4 in the upper soil and pF 2 to 2.1 in the marl layers of the subsoil; E_p was 6.5 mm day^{-1} .

A value of $|h^*|$ for which the sink term S of submediterranean vegetation starts to fall below its maximum can be found by comparing the ratio of E_a/E_p with the absolute value of the capillary pressure head $|h|$, if we assume that $T_a/T_p = E_a/E_p$ ($T =$ transpiration). Then $|h^*|$ is that $|h|$ for which during dry weather E_a/E_p becomes significantly lower than one. However, such an analysis is complicated by the layered structure of the soil-rock system and by the variable rooting depth of the different plants and trees. Only the measurements at Sauveplantade led to unambiguous results. According to these data, $|h^*|$ should vary between 600 and 800 hPa (i. e. pF 2.8 to 2.9) at an atmospheric water demand of about 5 mm day^{-1} .

7.6. Conclusions

1. The system to be modelled can be identified if the components of the soil moisture budget have been measured (eqn. 7.6 or 7.7).
2. Concept by which soil hydraulic properties are determined from soil texture should only be applied with caution to silty and clayey soils. For the range of intermediate moisture contents in silty soils, the diffusivity was found to vary by a factor 2 (at $\theta = 0.1$) to 40 (at $\theta = 0.3$), irrespective of texture.
3. Infiltration measurements on uncrusted soil columns in situ showed that the presence of macropores can increase the saturated conductivity by a factor of 35. GERMANN & BEVEN (1981) found a factor between 4 and 18, depending on the volume of the macropores which was in the range of 0.01 and 0.045. For silt loam soils the effect of the increased saturated permeability due to macropores on the capacity of ponding infiltration and on the frequency of Hortonian overland flow was estimated for rainfall in October. Rainfall events lasting one hour and with return periods of 10 or 100 years give rise to overland flows of 42 mm or 82 mm respectively if the saturated conductivity has not been increased by macropores. For a silt loam with macropores no overland flow was calculated, but a moderate overland flow was computed in the effectiveness of the macropores had been reduced by a previous saturation (see Table

- 7.1). The effect of macropores on the capillary pressure head at the wetting front should also be noted.
4. Repeated ponding infiltration showed that macropores are not stable. Evidently, cracks from shrinkage will disappear during wetting as a consequence of swelling. Other macropores such as those of biological origin (biopores) also appear to be unstable; as soon as saturated conditions have ended, the seepage into the macropores seems to produce the collapse of some macropores (VAN DEN BERG 1989). This behaviour of the soil will reduce the saturated conductivity, k_s , which is represented schematically in fig. 7.7.a. However, during dry periods new macropores may be formed which may raise k_s . In this way k_s may change during a mean meteorological year as shown in fig. 7.7.b.
 5. Progress in modelling of soil moisture can be achieved if we can model the functioning of macropores and their spatial occurrence, for instance by stochastic probability functions that should be related to land use, vegetation, clay fabric, antecedent moisture conditions etc.
 6. The canopy or surface resistance to evapotranspiration was determined during spring and autumn for a semi-natural plant cover. Under conditions of potential evapotranspiration the value of r_c was found to be about 60 s. m^{-1} . A gradual increase of r_c to 140 s. m^{-1} could be ascertained at an actual evapotranspiration equal to 70% of the potential rate.

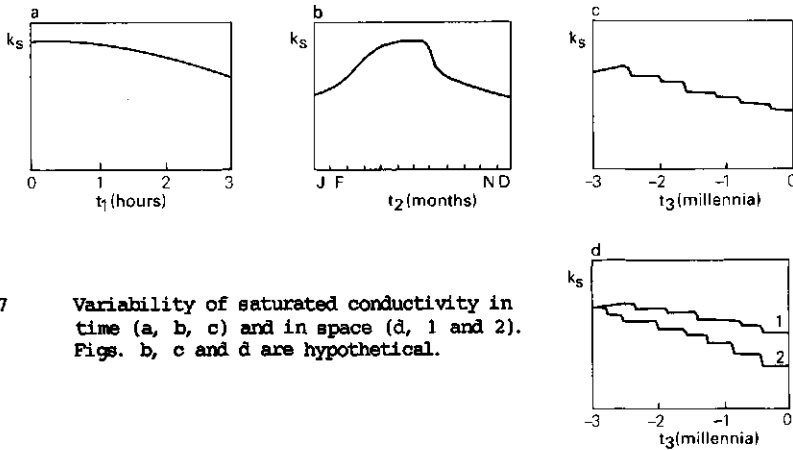


Fig. 7.7 Variability of saturated conductivity in time (a, b, c) and in space (d, 1 and 2). Figs. b, c and d are hypothetical.

7. A drawback when regionalizing soil modelling parameters with the help of properties of soil and bedrock in the Ardèche is that most of the landscape has been exposed to human activities of varying intensity. For the upper soil we assumed that soil formation under a natural vegetation cover will produce an increasing permeability, whereas anthropogenic activity will cause decreasing permeability, because of loss of organic matter, compaction etc. (Fig. 7.7.c). During the tenth millenium BC the Würm glacial was ending and the steppe landscape was becoming reforested. Anthropogenic

S_{\max}	maximum value of S	$1/t$
t	time	t
T	air temperature	T
T_r	mean return period	t
u	wind velocity	$1/t$
x	horizontal distance	l
z	vertical distance, positive if downwards	l
z_0	aerodynamic roughness parameter	l
γ	psychrometer constant	p/T
θ	volumetric moisture content	-
θ_i	initial volumetric moisture content	-
θ_0	volumetric moisture content in the transmission zone	-

REFERENCES

- BEVEN, K. J. & GERMANN, P. (1982), Macropores and water flow in soils. *Water Resour. Res.*, 18 (2), pp. 1311-1325.
- BLAIKIE, P. & BROOKFIELD, H. (1987), *Land degradation and society*. Methuen, London.
- BLANC, J.-F. (1984), Paysages et paysans des terrasses de l'Ardèche. l'Imp. du Vivarais, Annonay.
- BORK, H.-R. & BORK, H. (1987), Extreme jungholozäne hygrische Klimaschwankungen in Mitteleuropa und ihre Folgen. *Eiszeitalter und Gegenwart* 37, pp. 109-118.
- BOULLE, M. (1986), Les rivières d'Ardèche. *Mémoire d'Ardèche Temps Présent* 11/12, pp. 9-13.
- BOUMA, J. (1982), Measuring the hydraulic conductivity of soil horizons with continuous macropores. *Soil Sci. Soc. Am. J.* 46, pp. 438-441.
- BOUMA, J., D. I. HILLEL, F. D. HOLE & C. R. AMERMAN (1971), Field measurements of unsaturated hydraulic conductivity by infiltration through artificial crusts. *Soil Sci. Soc. Amer. Proc.* 35, pp. 362-364.
- BOYER, M. (1988), Les premiers hommes. In: Choly, G. (Ed.) *Histoire du Vivarais*, Editions Privat, Toulouse.
- Commission Météorologique Départementale (1980), *Chroniques météorologiques du Vivarais. Ardèche Annales Météorologiques*.
- FEDES, R. A., P. J. KOWALIK & H. ZARADNY (1978), Simulation of field water use and crop yield. *Centre Agricult. Publ. and Documentation*, Wageningen.
- FEDES, R. A., P. KABAT, P. J. T. VAN BAKEL, J. J. B. BRONSWIJK & J. HALBERTSMA (1988), Modeling soil water dynamics in the unsaturated zone - state of the art. *J. Hydrol.* 100, pp. 69-111.
- HILLEL, D. (1980), *Applications of soil physics*. Academic Press, London.
- KEYMAN, J. Q. (1981), Theoretical background of some methods for the determination of evaporation. In: *Evaporation in relation to hydrology*. Proc. and Info. 28, CHO-TNO, 's Gravenhage.
- KOOREVAAR, P., G. MENELIK & C. DIRKSEN (1983), *Elements of soil physics*. Elsevier, Amsterdam, Oxford, New York.
- LETTAU, H. (1949), Isotropic and non-isotropic turbulence in the atmospheric surface layer. *Geophys. Res. Pap.* 1, Cambridge, Mass.
- MARTIN, C. (1987), *Garrigues en pays languedocien*. Editions Lacour, Nîmes, France.
- MONTIETH, J. L. (1965), Evaporation and environment. *Proc. Symp. Soc. Exp. Biol.* 19, pp. 205-234.
- PIGGOTT, S. (1981), *The agrarian history of England and Wales. Prehistory 1 (1)*. University Press, Cambridge.
- RIJTEMA, P. E. (1965), An analysis of actual evapotranspiration. *Agric. Res. Rep.* 659, Pudoc, Wageningen, The Netherlands.
- ROELS, J. M. (1984), *Studies of soil erosion on rangelands in the Ardèche drainage basin (France)*. Thesis. Utrecht University, The Netherlands.
- RUSSO, D. (1988), Determining soil hydraulic properties by parameter estimation: on the selection of a model for the hydraulic properties. *Water Resour. Res.* 24 (3), pp. 453-459.
- SIDLE, R. D., A. J. PEARCE & C. L. O'LOUGHLIN (1985), *Hillslope stability and land use*. AGU Water Resour. Monograph 11, Washington.
- SPOSITO, G. (1987), The physics of soil water physics. In: Landa, E. R. and S. Ince (Eds.), *The history of hydrology*, AGU Washington, pp. 93-101.
- THOM, A. S. & H. R. OLIVER (1977), On Penman's equation for estimating regional evaporation. *Quart. J. Roy. Met. Soc.* 103, pp. 345-357.
- VAN DEN BERG, J. A. (1983), Les aspects hydrogéologiques de l'érosion dans la région limonaise autour de Villeneuve de Berg. *Revue de la Soc. des Enfants et Amis de Villeneuve de Berg* 38, pp. 11-19.
- VAN DEN BERG, J. A. (1989), Measurements of hydraulic conductivity of silt loam soils using an infiltration method. *J. Hydrol.* 110, pp. 1-22.
- VAN DEN BERG, J. A. & T. LOUTERS (1984), Elektronische Datenerfassung zur Modellierung des Bodenfeuchtigkeitsregimes unter Verwendung eines netzunabhängigen Dataloggers und schnellreagierenden Tensiometers. Dept. of Physical Geography, Utrecht University, The Netherlands, 9 pp.
- VAN DEN BERG, J. A. & T. LOUTERS (1985), Toward representing soil moisture conditions of catchments. In: Müller, H. E. & K. R. Nippes (Eds.) *Problems of regional hydrology*. Proc. Freiburg Symp. Beitr. Hydrol., Sonderheft 5.2, pp. 750-774.

- VAN DEN BERG, J.A. & T. LOUTERS (1986), An algorithm for computing the relationship between diffusivity and soil moisture content from the hot air method. J. Hydrol. 83, pp. 149-159.
- VAN DEN BERG, J.A. & T. LOUTERS (1988), The variability of soil moisture diffusivity of loamy to silty soils on marl, determined by the hot air method. J. Hydrol. 97, pp. 235-250.

"De variabiliteit van de parameters uit modellen waarmee de bodemvochthuishouding kan worden nagebootst; studies verricht aan gronden met een fijne textuur op mergelgesteente in het stroomgebied van de Ardèche".

Het water in de bodem is belangrijk in allerlei aspecten van het milieu. Zo is de vochttoestand van de bodem van invloed op sommige geomorfologische processen zoals bodemerosie en massabeweging en voorts op de verplaatsing van stoffen over en in de bodem. De gebruiksmogelijkheden van land kunnen worden beperkt door de hoeveelheid water die tijdens het groeiseizoen voor de gewassen beschikbaar is, terwijl omgekeerd de begroeiing weer van invloed is op de vochthuishouding van de bodem. Daarom zijn er reeds sinds vele jaren computerprogramma's ontwikkeld waarmee de vochthuishouding van de bodem kan worden gesimuleerd. In deze modellen komen belangrijke bodemfysische en bodem-plant parameters voor zoals de doorlatendheid en de vochtvereffeningscoëfficiënt van de bodem bij verschillende vochtgehalten, de doorlatendheid onder verzadigde omstandigheden, parameters die bepalend zijn voor het infiltratievermogen van de grond, voor de snelheid waarmee plantenwortels bij verschillende vochtgehalten water uit de bodem kunnen opnemen en voor de verdamping van een begroeid oppervlak.

Het is van wezenlijk belang om in elk knooppunt van het netwerk dat bij modellering over een studiegebied wordt gelegd, over de juiste waarde van de modelparameters te beschikken omdat alleen dan de ruimtelijke variatie in vochthuishouding en de hieraan gerelateerde processen kunnen worden nagebootst.

Het hoofddoel van het onderzoek waarover in dit proefschrift wordt gerapporteerd, was om te bestuderen in welke mate de modelparameters voor gronden binnen een bepaalde textuurklasse variëren en hoe die variabiliteit van de parameters kan worden bepaald. Het onderzoek is hoofdzakelijk uitgevoerd op gronden met een fijne textuur (volgens de USDA classificatie loam, silt loam en silty clay loam) op mergelgesteente in negen proefgebieden in het stroomgebied van de Ardèche (Frankrijk). De simulatie van de bodemvochthuishouding van deze sloefrijke gronden is interessant omdat zij een goed productievermogen hebben maar tevens erosiegevoelig zijn. Voor wat betreft het onderzoek naar het verband tussen hydraulische bodemeigenschappen en textuur zijn aan de onderzochte verweringsbodems op mergelgesteente een lössgrond uit de omgeving van Maastricht en -ter wille van het contrast - twee zandige bodems ("sandy loam") uit het stroomgebied van de Ardèche toegevoegd.

Tijdens het voor- of najaar van 1980, 1983 en 1985 is voor steeds een ander proefgebied getracht alle variabelen te meten die van belang zijn voor de bodemvochthuishouding. Hierbij waren de neerslag, de werkelijke verdamping en de verandering in bodemvochtgehalte de essentiële termen uit de bodemvochtbalans. De verdamping werd bepaald volgens de Bowen-verhouding methode. De veranderingen in bodemvochtgehalte werden gravimetrisch bepaald of aan de hand van de gemeten capillaire drukhoogte afgeleid uit de vocht karakteristiek.

De hydraulische bodemeigenschappen bij vochtgehalten uit het middenbereik zijn met de hete luchtmethode bepaald aan ongestoorde grondmonsters. Er werd een algoritme ontwikkeld en getoetst waarmee de vochtvereffeningscoëfficiënt snel en eenduidig met de computer uit de uitkomsten van deze proeven kan worden berekend.

Voor hoge vochtgehalten en voor verzadigde omstandigheden zijn de bodemfysische eigenschappen gemeten met behulp van infiltratieproeven op grondkolommen *in situ*. Deze kolommen werden verkregen door de omringende grond weg te graven. Bij een deel van de infiltratieproeven werd de bovenkant van de grondkolom eerst voorzien van een kunstmatige korst, namelijk een mengsel van fijn zand en gips met een bepaalde hydraulische weerstand waardoor de grond tijdens de proef onverzadigd blijft. In twee proefgebieden werden de metingen gelijktijdig aan twee kolommen vlak naast elkaar verricht, in twee andere proefgebieden werden de waarnemingen in een ander jaar en aan een andere grondkolom herhaald. Voorts werden de vocht karakteristiek, de textuur en het gehalte aan zwellende kleimineralen bepaald. Van de lössgrond werden tevens slijpplaatjes gemaakt en onder de microscoop bestudeerd.

Uit het onderzoek bleek dat de verschillen in hydraulische eigenschappen ook bij vochtgehalten uit het middenbereik waarbij het aanwezige bodemwater vooral in primaire poriën wordt aangetroffen, niet uitsluitend uit verschillen in textuur kunnen worden verklaard. Blijkbaar spelen ook andere fysiografische factoren een rol. Voor löss grond bijvoorbeeld bleek uit micromorfologisch onderzoek aan slijpplaatjes dat zich vrij veel langgerekte, holle ruimten (zogenaamde "vughs" en "planes") in de bodemmatrix bevonden.

Bij hoge vochtgehalten en onder verzadigde omstandigheden was het verband tussen hydraulische eigenschappen en textuur zeer vaag omdat dan vooral secundaire poriën een rol spelen. De invloed van met name de macroporiën kon heel duidelijk worden vastgesteld door de doorlatendheid onder bijna verzadigde omstandigheden te vergelijken met de verzadigde doorlatendheid; deze laatste was 5 tot 80 maal zo groot. Er lijkt daarom behoefte te bestaan aan modellen waarmee de variatie in hydraulische bodemeigenschappen kan worden teruggevoerd op basale parameters. Voor praktische doeleinden is het belangrijk dat zulke parameters zijn af te leiden uit fysiografische eigenschappen die eenvoudig kunnen worden gekarteerd.

De experimenten waarbij er tijdens de infiltratie steeds een dun waterlaagje op de grondkolom stond, toonden aan dat slechts in één proefgebied de capillaire drukhoogte in de transmissie zone van het infiltratieprofiel - overeenkomstig de gangbare beschrijving in de literatuur - negatief bleef. Bij deze kolomproef was de bovenste 0,15 m van de grond verwijderd waarna er een relatief dikke, homogene bodem met weinig macroporiën was overgebleven. In alle andere proefgebieden bereikte de drukhoogte in de transmissie zone een kleine, positieve waarde. Dit werd waarschijnlijk veroorzaakt doordat hier de doorlatendheid van de bodems met de diepte afnam. De positieve drukhoogte had in elk geval tot gevolg dat de verzadigde zone uit het infiltratie profiel zich in feite kon uitbreiden tot de transmissie zone en dat macroporiën het infiltratie vermogen van de grond veel sterker konden verhogen als op grond van alleen de textuur kon worden verwacht. Dit gold ook voor

een zogenaamde "closed soil", dat is een grond waarin de macroporiën niet tot aan het grondoppervlak doorlopen en waarin deze dus ook niet vanaf maaiveld met water kunnen vollopen.

Als een dergelijke infiltratieproef werd herhaald, bleek de verzadigde doorlatendheid dikwijls kleiner te zijn geworden. Berekeningen toonden aan dat dit kan worden verklaard doordat de wand van macroporiën hier en daar inzakt direct nadat aan het einde van de eerste infiltratieproef de macroporie is leeggelopen.

De meting van een vereenvoudigde waterbalans (neerslag, verdamping en verandering in bodemvochtgehalte) was belangrijk om een goed inzicht krijgen tot welke diepte de bodemlagen rechtstreeks zijn betrokken bij de vochtvoorziening van de vegetatie. Dit is belangrijk omdat de onder-rand van een model in elk geval beneden deze diepte moet worden gelegd. Simulatie van de bodemvochthuishouding met het (ruimtelijk ééndimensionale) SWATRE model vergrootte het inzicht in de wijze waarop verschillende bodemlagen hydraulisch functioneren.

De waterbalansmetingen leverden ook getalswaarden voor de plant-bodem parameters onder de omstandigheden in de Ardèche. De verdampingsweerstand r_c van een begroeid oppervlak bedroeg bij hoge vochtgehalten 60 s.m^{-1} , dit is evenveel als voor gras in Nederland is gemeten. Als tijdens voor- of najaar de werkelijke verdamping door het afnemende vochtgehalte in de bodem werd gereduceerd, liep de r_c waarde op tot 200 s.m^{-1} .

RESUME

Van den Berg, Jan A., 1989.

Variabilité de paramètres pour la modélisation du régime hydrique du sol (études sur les sols limoneux et limoneux fins sur assise rocheuse marneuse dans le bassin versant de l'Ardèche). Thèse de doctorat. Université Agronomique Wageningen, Wageningen, Pays-Bas.

Des expériences sur le terrain et des mesures complémentaires sur des carottes de sol intactes en laboratoire ont été réalisées afin d'étudier la variabilité des paramètres utilisés dans le modelage du régime hydrique du sol. Le régime d'eau du sol est intéressant pour la quantité d'humidité disponible pour la couverture en végétaux, la production de récolte, le transport de contamination dans la zone non-saturée, l'étude de processus d'érosion du sol et de mouvements de masse et l'étude de l'évaluation du sol. Une attention toute particulière a été portée aux propriétés hydriques du sol, ainsi qu'aux paramètres végétaux-sol pour la détermination de l'évapotranspiration actuelle, qui est un poste essentiel du bilan hydrique.

L'étude s'est principalement concentrée sur les sols limoneux fins dans le bassin de l'Ardèche. Neuf sites expérimentaux ont été localisés, où une roche marneuse affleure. Comme pour les propriétés hydriques, la série de ces sols a été élargie avec un sol loess des Pays-Bas et - pour contraste - avec deux sols limono-sableux dans le bassin de l'Ardèche.

La diffusivité capillaire a été déterminée au moyen de la méthode à air chaud. Tout d'abord, un algorithme a été mis au point permettant un calcul sans ambiguïté et rapide de la diffusivité à partir des données récoltées.

Les concepts sur les propriétés hydriques et la granulométrie des sols, habituellement basés sur des expériences avec des sols d'un mode d'arrangement artificiel, furent mis en doute. Une théorie fut développée afin d'expliquer le changement dans la conductivité hydraulique saturée sous des conditions subséquentes d'infiltration en retenue par l'instabilité locale des parois macro-intersticielles. Cette théorie a pu être soutenue au moyen de calculs par une analogie électrique (modèle RC).

Les résultats obtenus furent comparés avec ceux rapportés dans la littérature. Il est apparu que même pour des teneurs en eau intermédiaires, lorsque la plupart des pores qui retiennent toujours l'eau du sol sont les pores primaires, la granulométrie du sol ne peut expliquer à elle seule les divergences dans la diffusivité capillaire et que d'autres caractéristiques physiographiques sont également impliquées. Par exemple, une analyse micro-morphologique du sol loess a permis de constater la présence de nombreuses cavités ("vughs" et "planes"). Pour les teneurs en eau élevées et sous les conditions de saturation, les propriétés hydriques ont été étudiées sur des colonnes de sol *in situ*. Des échantillons de cette grandeur (0,2 mètre de diamètre et 0,3 à 0,55 mètre de hauteur) permettent d'inclure des effets de macro-pores. L'étude de ces effets a été limitée aux sols "fermés", dans lesquels les macro-pores n'atteignent pas la surface du sol et qui, pour cette raison, ne peuvent pas directement être remplis d'eau à

partir de la surface du sol.

Dans des conditions humides, la relation entre la granulométrie du sol et les propriétés hydriques devenait faible parce que les pores secondaires étaient également impliqués. L'influence de ces interstices a pu être démontrée d'une façon particulièrement claire par leur effet sur la conductivité hydraulique lors de la transition entre conditions presque saturées et conditions totalement saturées. La conductivité diminue au fur et à mesure de la profondeur grandissante du sol. Il est apparu qu'à cause de cela, durant l'infiltration en retenue, la charge hydraulique dans la zone de transmission devient positive et que la conductivité hydraulique correspondante atteint la valeur pour des conditions saturées. En conséquence, la capacité d'infiltration sous des conditions en retenue peut atteindre des valeurs beaucoup plus élevées que ce à quoi l'on pouvait s'attendre à partir de la granulométrie du sol seule.

Les résultats démontrent le besoin de modèles dans lesquels la variabilité des caractéristiques hydriques peut être réduite à des paramètres de base. En pratique, il est important que de tels paramètres puissent être mis en relation avec des propriétés physiographiques qui peuvent être aisément tracées.

Pour des périodes de temps principalement sec, les postes principaux du bilan hydrique réduit (évapotranspiration et changement dans le stockage d'humidité) ont été déterminés sur trois sites. L'application d'un modèle SWATRE uni-dimensionnel à ces sets de données montre que la simulation d'un bilan hydrique ainsi simplifiée procure des informations de valeur sur l'extension des compartiments du sol du système à modeler.

Mots d'index supplémentaires: régionalisation, paramètres d'infiltration Green & Ampt, charge hydraulique du front d'humidification, sol non-rigide, résistance en surface ou résistance végétale à l'évapotranspiration, incrustation de sol découvert.

(Traduction: Algemeen Ned. Vertaalbureau, Zeist)

APPENDIX A

ELEKTRONISCHE DATENERFASSUNG ZUR MODELLIERUNG DES BODENFEUCHTIGKEITSREGIMES UNTER VERWENDUNG EINES NETZUNABHÄNGIGEN DATALOGGERS UND SCHNELLREAGIERENDEN TENSIO METERS

Jan A. van den Berg & Teunis Louters

(Zusammenfassung eines Vortrages im Rahmen des Jahrestreffen des Arbeitskreises Hydrologie, Seeshaupt, 22-24 November 1984.)

EINLEITUNG

Die Messungen, die in diesem Vortrag besprochen werden sollen, sind durchgeführt worden im Rahmen einer Untersuchung über die Möglichkeiten, das Bodenfeuchtigkeitsregime eines Stromgebiets zu bestimmen und zu simulieren. Die Simulation wird anhand eines auf der Differentialgleichung für die Strömung der Bodenfeuchte basierenden Modells stattfinden. Die Untersuchung ist primär praktisch ausgerichtet: Anwendungen gibt es zum Beispiel auf dem Gebiet der Landschaftskunde und der Landevaluierung wie bei der Verhütung und Bekämpfung der Bodenerosion. Im Verlauf dieser Untersuchung können drei Phasen unterschieden werden:

1. Identifizierung des Systems oder des Prototyps, das von dem Modell simuliert werden soll;
2. Bestimmung wichtiger bodenphysischer Parameter, wie gesättigte und ungesättigte Durchlässigkeit, Bodenfeuchteaustauschkoeffizient und Infiltrationskapazität;
3. Modellanpassung und Simulation.

Die Identifizierung des Prototyps basiert auf der Bodenfeuchtebilanz. In einer Trockenperiode spielen dabei hauptsächlich die Verdunstung und Veränderungen in der Speicherung der Bodenfeuchte eine Rolle. Im ersten Teil dieses Vortrags handelt es sich deshalb um die Bestimmung der realen Verdunstung von Kulturland und halbwüsten Bodens. Der zweite Teil behandelt eine Tensiometer mit kurzer Einstellzeit und dessen Anwendungen bei der Bestimmung der Veränderungen bei der Feuchtespeicherung und der bodenphysischen Parameter *in situ*.

BESTIMMUNG DER REALEN VERDUNSTUNG ALS TERM DER BODENFEUCHTEBILANZ

Bowen-verhältnis-methode

Einige vielfach angewandte Methoden zur Bestimmung der realen Verdunstung basieren auf der Energiebilanz der Erdoberfläche:

$$R_n = H + L \cdot E - G \text{ oder } R_n + G = H + L \cdot E \quad (\text{A. 1})$$

Eine von diesen Methoden ist die Bowen-verhältnis-methode, wobei außer der Nettostrahlung das Verhältnis zwischen den Fluxen fühlbarer und latenter Wärme gemessen wird:

$$\beta = \frac{H}{L \cdot E} = \gamma \cdot \frac{K_H}{K_m} \cdot \frac{\Delta T}{\Delta e} \quad (\text{A. 2})$$

worin β = Bowen-verhältnis
 H = Flux fühlbarer Wärme
 $L \cdot E$ = Flux latenter Wärme
 γ = Psychrometer-konstante
 K_H und K_m = turbulente Austauschkoefizienten für fühlbare, respektive latente Wärme
 ΔT und Δe = vertikale Gradienten respektive der Lufttemperatur und der partiellen Wasserdampfspannung.

N. B.: Der Bodenwärme-flux G ist negativ in negativer z -Richtung. Aus den Vergleichen (A. 1) und (A. 2) können die gesonderten Fluxe errechnet werden:

$$L \cdot E = \frac{R_n + G}{1 + \beta} \quad \text{oder} \quad E = \frac{R_n + G}{L(1 + \beta)} \quad (\text{A. 3})$$

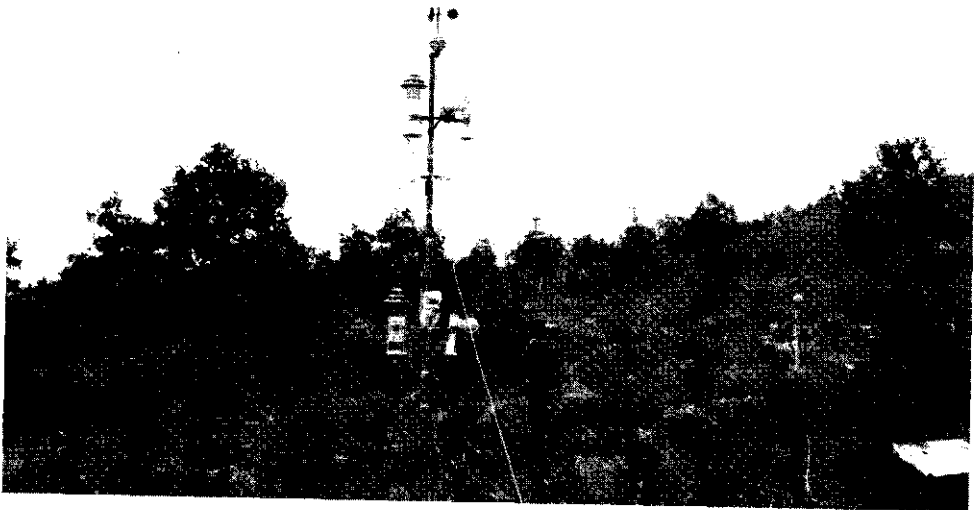


Abb. 1 Messung der realen Verdunstung nach die Bowen-verhältnis-methode in dem Ardèche Gebiet.

Meßfühler

Folgende Messungen sind erforderlich (Abbildungen 1 und 3):

- Nettostrahlung (R_n) mit einem Strahlungsbilanzmesser;
- Bodenwärmeflux mit Bodenwärmestromplättchen (BW) und Bodenthermometer (T_g);
- Lufttemperatur (T_0 und T_2) und partielle Wasserdampfspannung (Feuchttemperatur T_1 und T_3) in mindestens zwei verschiedenen Höhen über der Erdoberfläche. Als Meßfühler sind dafür trockene Platinwiderstände angewandt, resp. solche, die naß gehalten wurden; sie wurden gut ventiliert und waren gegen die direkte Sonnenstrahlung abgeschirmt.

In welcher Höhe messen und wie oft?

Höhe: Es gibt zwei Gründe für Messungen in der untersten Luftschicht (bis zu einer Höhe von 2 bis 3 Metern):

1. hier sind die Gradienten am größten und also ist der Einfluss von Meßfehlern am geringsten;
2. je dichter über der Erdoberfläche gemessen wird, um so kleiner ist die erforderliche Streichlänge (Abbildung 2).

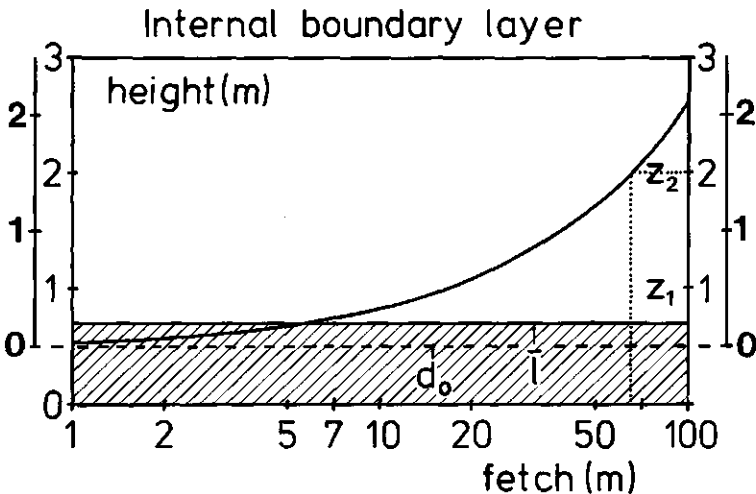


Abb. 2 Die Luft muß eine bestimmte Streichlänge zurückgelegt haben, damit die Eigenschaften der Luft sich der Landoberfläche angepaßt haben.

Meßfrequenz:

Nettostrahlung, Wärmeflux und Bodentemperatur sind verhältnismäßig langsam verändernde Variablen, dagegen variiert die Lufttemperatur schnell. Um einen unnötig großen Datenbestand zu verhindern, wird also vorzugsweise mit einem verschiedenen Meßintervall gemessen werden müssen. Von eventuellen systematischen Fehlern abgesehen haben wir uns zum Ziel gesetzt, die Lufttemperaturen bis zu etwa $0,1^\circ\text{C}$ präzise mit

einer Zuverlässigkeit von 95% zu messen. Mit anderen Worten: $2\sigma \leq 0,1^\circ\text{C}$ worin σ der Standardfehler für den Mittelwert ist.

Aus kontinuierlichen Messungen geht hervor, daß die Lufttemperatur zum Beispiel in einer Höhe von 2 Meter über der Erdoberfläche schnell fluktuiert. Die Standardabweichung kontinuierlicher Messungen während eines kurzen Zeitintervalls beträgt im Sommer in den Niederlanden etwa $0,3^\circ\text{C}$ und in der Ardèche $0,45^\circ\text{C}$. Mit "kurz" wird hier gemeint: kurz in Bezug auf den Tagesablauf, z. B. 10 Minuten. Wenn wir in einer Zeitspanne von 10 Minuten 85 Mal messen, das heißt alle 7 Sekunden, so beträgt der Standardfehler für den Mittelwert:

$$\sigma = \frac{0,45^\circ\text{C}}{85} = 0,049^\circ\text{C}$$

so daß der gestellten Anforderung gerade entsprochen wurde.

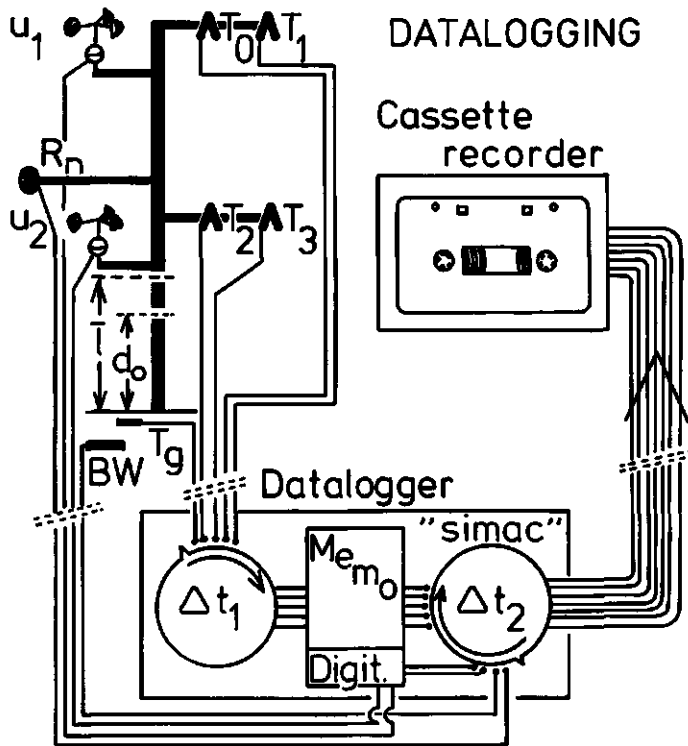


Abb. 3 Schema eines Dataloggers mit zwei verschiedenen Scanintervallen t_1 und t_2 (u : digitaler Windgeschwindigkeitsmesser; l : Bewuchshöhe; d_0 : Nullflachverschiebung).

AN SENSOREN UND RECORDERN GESTELLTE ANFORDERUNGEN

Sensoren/Meßfühler

- kurze Einstellzeit;
- sie sollen ein elektrisch-analoges oder digitales Signal geben.

Recorder

- geeignet für den Gebrauch im Felde:
 - stoßsicher, unempfindlich gegen Schmutz und Staub;
 - unempfindlich gegen Temperaturschwankungen und solche der Luftfeuchtigkeit
 - geeignet für Batteriespannung und vorzugsweise auch für Netzspannung
- gute Synchronisation der Messungen: Zentralmeßsystem mit Abtaster;
- geeignet für die Eingabe analoger und digitaler Signale (digital z. B. in bezug auf einen Windgeschwindigkeitsmesser);
- Vermögen zur Reduzierung definitiv zu speichernder Daten durch Speicherung auf Zeit und Errechnung des Datenmittelwertes;
- digitale Datenregistrierung, sofort geeignet für Computerverarbeitung, da es sich um eine sehr hohe Anzahl von Daten handelt;
- mindestens zwei verschiedene Scanintervalle;
- die Möglichkeit, jeden Kanal laufend zu messen, so daß der Recorder zeitweilig als Meßinstrument fungieren kann (Kontrolle im Feld);
- vorzugsweise sofortige Umrechnung eines elektrischen Signals.

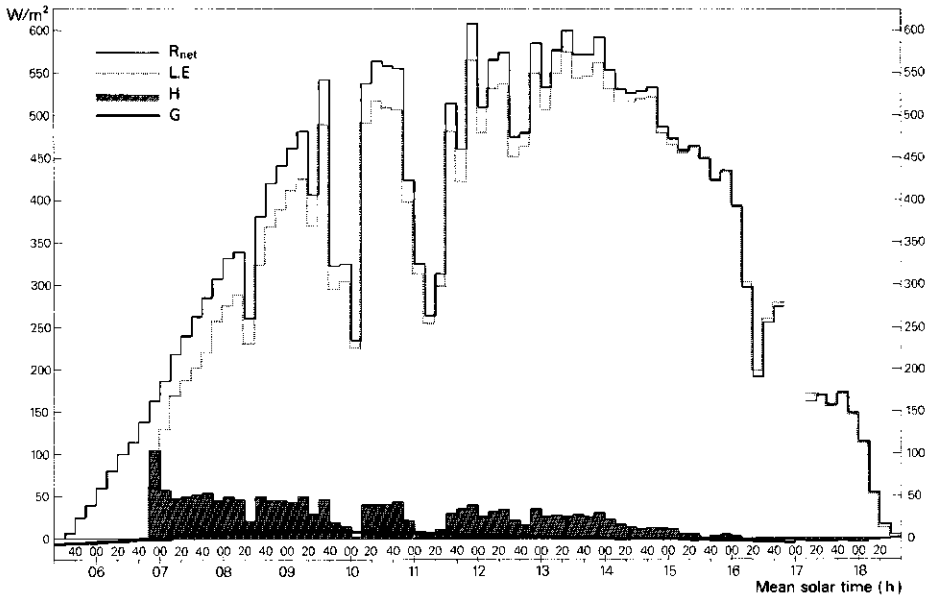


Abb. 4 Die Energiebilanz für den 13. Juni 1983 in der Ardèche; fast alle verfügbare Energie verschwand als latente Wärme.

Allen diesen Anforderungen entsprach der Felddatenspeicher von Simac, Meß- und System-Technik-Typ Logmaster MDL 500 mit dem zugehörigen Kassettenrecorder (Abbildung 3). Dieser Datenspeicher besitzt zwei unabhängig voneinander einstellbare Scanintervalle Δt_1 und Δt_2 . Zum Schluß des ersten Teils möchte ich Ihnen als Ergebnis dieser Messungen die Energiebilanz zeigen, wie wir die für den 13. Juni in der Ardèche registriert haben (Abbildung 4). Er zeigt sich, daß fast alle verfügbare Energie verschwand als latente Wärme, so daß die reale und die potentielle Evapotranspiration einander fast gleich waren. Tatsächlich betrug die wirkliche Verdunstung 6,4 mm pro Tag und die potentielle - errechnet nach Priestley und Taylor - 6,1 mm pro Tag.

TENSIOMETER ZUR ERFASSUNG DER BODENFEUCHTESPEICHERUNG UND BODENPHYSISCHEN PARAMETERN

Im zweiten Teil unseres Vortrages handelt es sich um die Frage, wie die Veränderungen in Bezug auf die Speicherung der Bodenfeuchte - ein wesentlicher Term der Bodenfeuchtebilanz - und die wichtigsten bodenphysischen Parameter, d. h. die gesättigte und die ungesättigte Durchlässigkeit, die 'effective Diffusität' und die Infiltrationskapazität *in situ* gemessen werden können. Im Mittelpunkt steht dabei ein Tensiometersystem, das von Dipl. Ing. Bakker vom Institut für Kulturtechnik und Wasserhaushalt in Holland entwickelt worden ist.

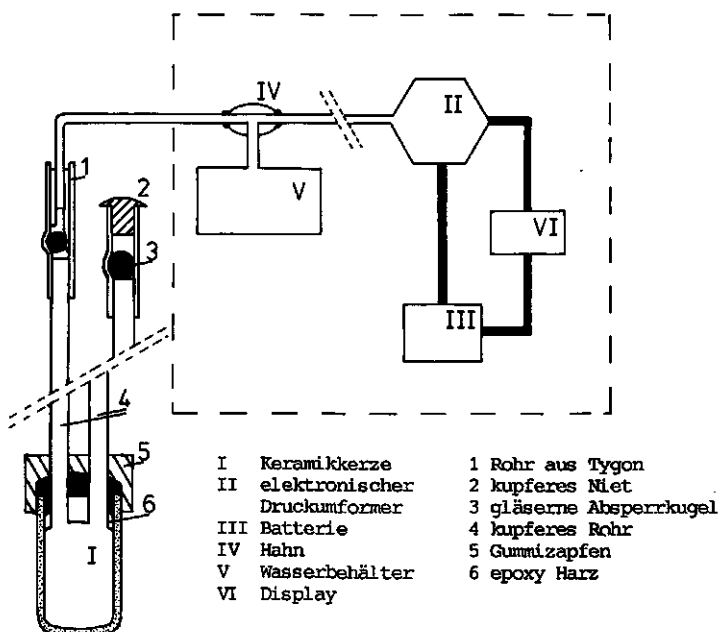


Abb. 5 Schema eines Tensiometers mit einem elektronischen Druckumformer.

Das Tensiometer

Das Tensiometer besteht aus einem kleinen (!), mit Wasser gefüllten Behälter aus feinem, porösem keramischem Material (Abbildung 5). An den Innenraum sind zwei dünne Kupferleitungen angeschlossen (\varnothing 1 mm); eine Leitung verbindet den Behälter mit einem elektronischen Druckumformer, die andere dient dazu, das System entlüften zu können. Weil eine Seite der Membrane in offener Verbindung mit der Luft steht, wird der Druck der Bodenfeuchte also automatisch in Bezug auf den atmosphärischen Druck gemessen. Die verwendeten keramischen Behälter sind bis zu 500 Millibar Unterdruck brauchbar; bei einem höheren Unterdruck leeren sie sich.

Veränderungen im Bodenfeuchtespeicherung

Das beschriebene Tensiometer wurde im Felde unter anderem angewandt, um die Veränderungen im Feuchtigkeitsgehalt in einem Schichtprofil zu bestimmen. Bildet doch - gesetzt den Fall, dass die Desorptionskurven des Bodens bekannt sind - die Messung des Verlaufs der Feuchtigkeitsspannung eine nichtdestruktive Methode zur Bestimmung des Feuchtigkeitsgehalts während einer Periode der Austrocknung (bis zu einer Feuchtigkeitsspannung von pF 2, 7).

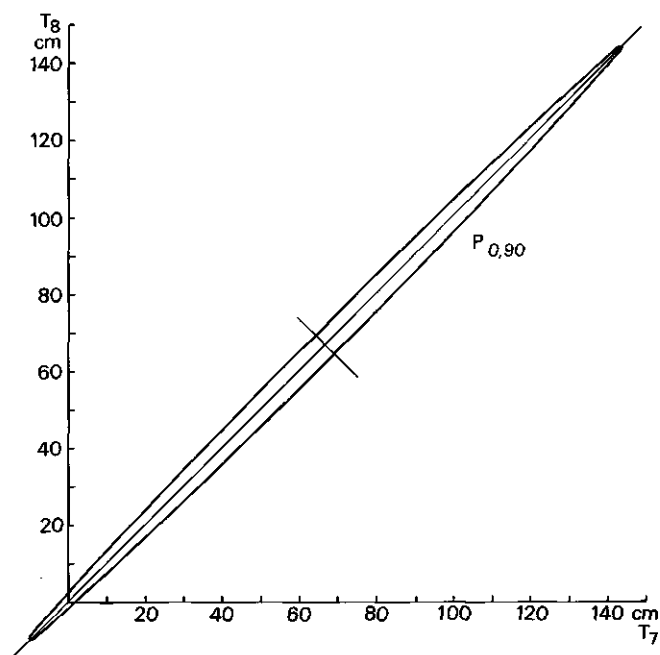


Abb. 6 Beziehung zwischen Doppelmessungen mit zwei Tensiometern im Gelände und das Zuverlässigkeitsintervall von 90%.

Aufgrund Doppelmessungen erweist sich die Reproduzierbarkeit auch unter Feldumständen als sehr gut im Raum von 0 bis pF 2,2. Vgl. dazu Abbildung 6. Die Empfindlichkeit erweist sich als ausreichend, um in den Messungen den durch die Verdunstung in Gang gesetzten täglichen Verlauf in der Feuchtespannung zu erkennen (Abbildung 7). Abbildung 8 zeigt die Ganglinien a', b' und c' der durchschnittlichen Bodenfeuchtespannung für drei aufeinanderfolgende Mergelschichten in einer Tiefe von 66, 78 und 96 cm. Daraus ist für die Periode vom 1.-9. Juni 1983 die Abnahme des Bodenfeuchtheitsgehalts errechnet worden sowohl für den Boden zusammen mit den vier oberen Mergelschichten wie für die vier Mergelschichten gesondert. Der Vergleich mit der realen Verdunstung ergibt, daß die Mergelschichten im Bodenfeuchtereime eine aktive Rolle spielen (weil hypodermischer Abfluss und Durchsickerung in dieser Periode unberücksichtigt bleiben können).

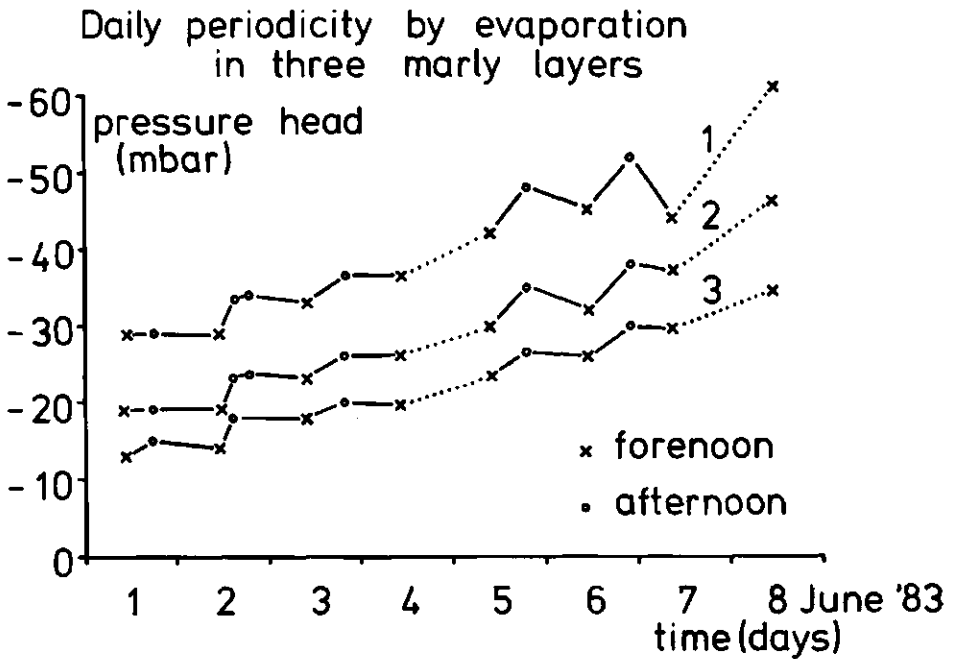


Abb. 7 Der durch die Verdunstung in Gang gesetzte tägliche Verlauf in der Bodenfeuchtespannung.

Bodenphysische Parameter

Durch seine kurze Einstellzeit ist dieses Tensiometer auch sehr geeignet für Messungen der Feuchtespannung während der Bestimmung *in situ* von bodenphysischen Parametern an einer Erdsäule. Dank dem elektrischen Ausgangssignal lässt sich der Verlauf der Feuchtespannung sehr gut auf einem Linie-recorder (mit mehreren Kanälen) aufzeichnen; geeignet für den Feldgebrauch zeigte sich der Linseis-Doppellinien recorder Typ LM 300.

Die Methode zur Bestimmung von bodenphysischen Parametern einer Erdsäule - und zwar namentlich K ungesättigt *in situ* - ist 1969 von Gardner and Hillel eingeführt und 1971 von Bouma modifiziert worden. Es hat sich außerdem herausgestellt, daß sich die Methoden bis zu K gesättigt, zur Bestimmung der 'effektive Diffusität' und von Infiltrationsparametern ausdehnen läßt.

Wasserüberschichtetes Profil

Sobald die mit den Tensiometern gemessenen Feuchtepotentiale und die Infiltrationsgeschwindigkeit konstant geworden sind, kann die gesättigte Durchlässigkeit errechnet werden; sie stimmt praktisch überein mit der Infiltrationsgeschwindigkeit, weil der Gradient des Feuchtepotentials jetzt klein ist. Ausgehend von den Voraussetzungen von Green und Ampt läßt sich aus dem Zeitunterschied zwischen dem Durchgang der Feuchtigkeitsfront an beiden Tensiometern vorbei zu gleicher Zeit die effektive Diffusität errechnen.

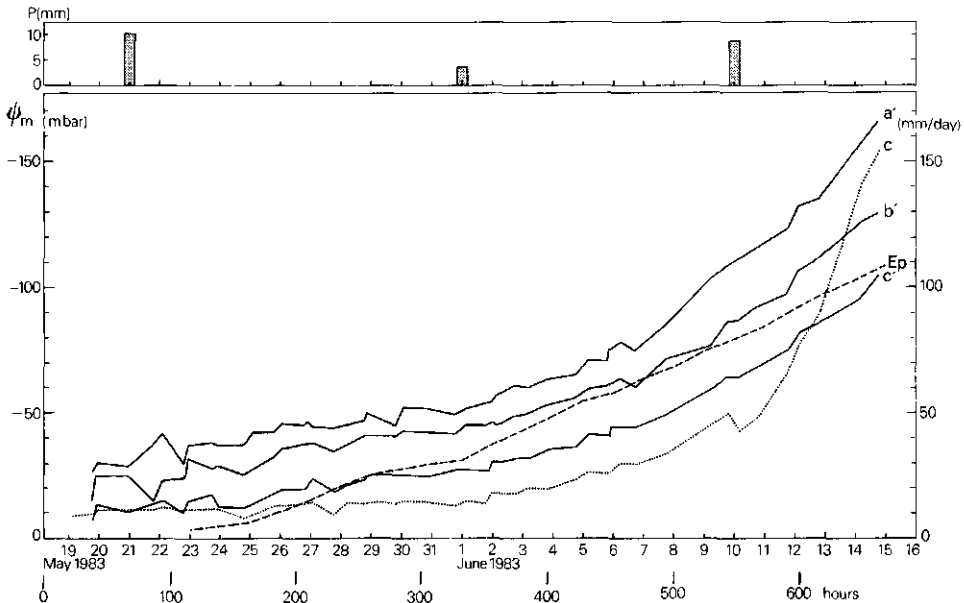


Abb. 8 Die potentielle Verdunstung (E_p) und die Ganглиen der Bodenfeuchtespannung für drei aufeinanderfolgende Mergelschichten in einer Tiefe von 0.66 (a'), 0.78 (b') und 0.96 m (c').

$$L^2 = 2\tilde{D} \Delta t \quad \tilde{D} = \frac{L^2}{2\Delta t}$$

Schließlich können aus dem Infiltrationsverlauf und der Desorptionskurve des Bodens die Parameter aus der Infiltrationsformel von Philip bestimmt werden: die Sorptivität und die hydraulische Durchlässigkeit bis zur Sättigung K_0 .

Ungesättigte Säule

Die Erdsäule kann in unterschiedlichem Ausmaß in ungesättigtem Zustand belassen werden, indem man die Oberfläche der Säule mit sogenannten Krusten ('crusts') versieht, die einen verschiedenen hydraulischen Widerstand haben (Abbildung 9). Jeder andere hydraulische Widerstand ergibt eine andere stationäre Feuchtigkeitsspannung mit der zugehörten ungesättigten Durchlässigkeit. In dieser Weise kann die K - ψ -Relation *in situ* bestimmt werden für die Strecke der kleinen Saugspannungen. Mit Hilfe der Desorptionskurve kann daraus wieder die D - ψ -Relation abgeleitet werden.

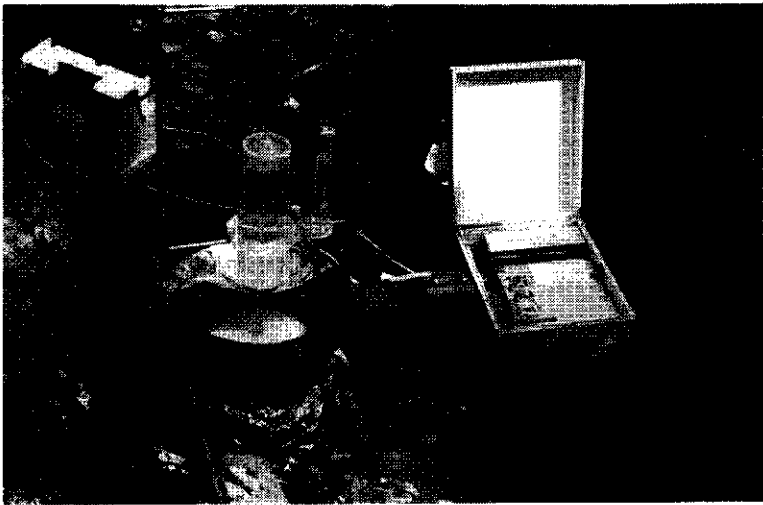


Abb. 9 Eine Erdsäule zur Bestimmung der ungesättigten hydraulischen Durchlässigkeit. Die Oberfläche der Säule ist mit einer Kruste eines bestimmten hydraulischen Widerstandes versehen.

Abbildungen 10a und b zeigen die Ergebnisse für die K- θ und D- θ Relationen. Die Angaben für die Strecke mit den höheren Saugspannungen beruhen auf den Diffusivitätsbestimmungen mit der sogenannten Heißluftmethode nach Arya an ungestörten Probenahmen.

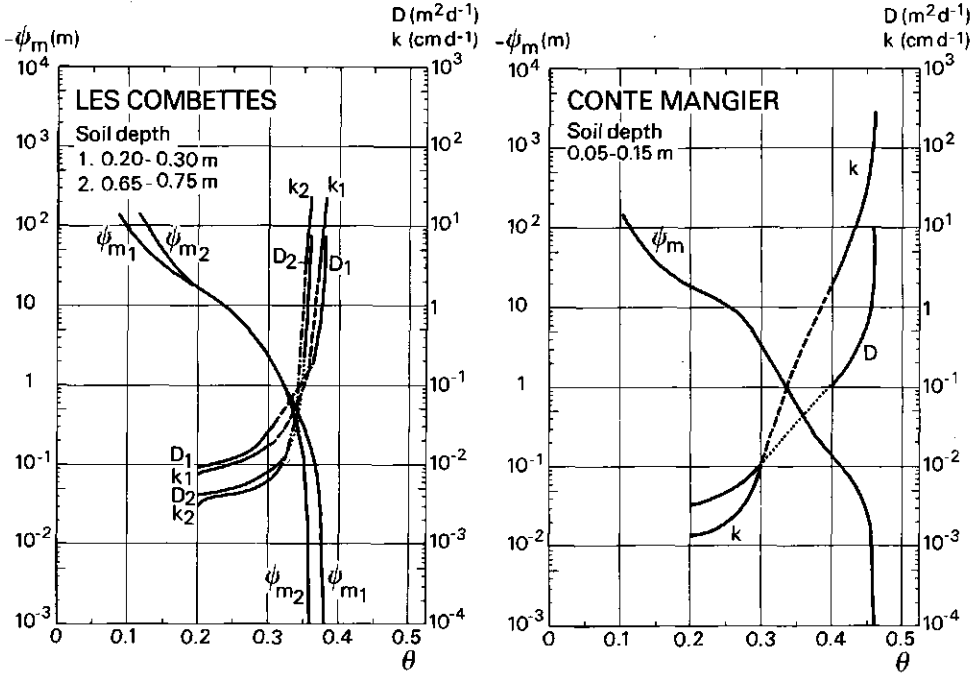


Abb. 10 Die Relationen zwischen Bodenfeuchtegehalt und hydraulischer Durchlässigkeit, Diffusivität und Bodenfeuchtespannung für zwei Untersuchungsgebiete in der Ardèche.

Für die Übersetzung bin ich meinem verstorben Kollegen Drs. G. F. Faber (Fachgruppe Deutsche Sprach- und Literatur Wissenschaft, Universität Groningen) zu Dank verpflichtet.

APPENDIX B

HOTAIR USERS MANUAL OPTIMIZING THE D-THETA RELATIONSHIP FROM HOT AIR DATA

B. 1. Introduction

The HOTAIR computer program primarily calculates the relationship between soil moisture diffusivity (D) and volumetric soil moisture content (θ or theta) from laboratory data obtained with the hot air method (ARYA et al. 1975). If the soil moisture retention curve (pF-curve) can be supplied the relationship between unsaturated conductivity (k) and soil moisture content (theta) can also be computed (option). To do this, the measured points must be supplemented with an adequate number of auxiliary points of the pF-curve, to ensure a well-fitting polynomial:

$$10 \log h = \sum_{i=0} a_i \cdot \theta^i \quad \text{with } h = \text{suction head (cm)}$$

Input data are in free format; they can be given in two ways:

Option 1.

For each slice the following must be given:

- XA: mass of moist soil (after hot air) (grams);
- XB: mass of dry soil (dried at 105°C) (grams);
- XC: mass of stones ($\phi > 2$ mm) (grams);
- XD: volume of stones ($\phi > 2$ mm) (cm³).

Option 2.

All pairs of x and theta are given, x being the distance from the centre of a slice to the evaporating surface and theta the volumetric moisture content after the hot air treatment.

In the first case a pair of x and theta values is calculated for each slice and arranged in a table with an option for plotting. Additional output consists of soil density and, occasionally, the density of the stones.

The program is interactive and is written in Fortran 77. To optimize the curve-fitting parameters b and n the program makes use of the routine E04 JAF from the NAGF-library; however, other optimization routines should be applicable too.

Basically, most output is presented in tables; graphical output is also possible, but this subroutine may need some adaptations as it is based on the KOMPLOT routine which is in use at the ACCU (Academic Computer Centre Utrecht).

N. B. It is emphasized that the option in the HOTAIR program for calculating the unsaturated conductivity (k) is not essential with regard to the algorithm. The subroutine in question makes use of fitting the soil moisture retention curve by a polynomial. As k


```

-----/
/ CALL EO4JAF : / yes / DO YOU KNOW THE VALUES /
/ WARNING: FOR OTHER USERS / :--<--/ OF THE CURVE-FITTING /
/ THAN OF ACADEMIC COMPUTER/ : / PARAMETERS B AND N ? /
/ CENTRE UTRECHT: IF YOU / : /-----/
/ DON'T HAVE SUBROUTINE / : : no
/ EO4JAF AT YOUR DISPOSAL, / : :
/ DO YOU HAVE INSERTED A / : :
/ VALID SUBSTITUTE ? / : :
-----/
: yes : no
V V
-----/
-- CALCULATION OF DIFFUSIVITY -- no :
-- WANTED YES OR NO ? -- -->----- :
: :
: yes :
: :
V :
-----/
( CALL SUBROUTINE ) :
( DIFFIT AND PRINT ) :
( THE CALCULATED ) :
( D-THETA VALUES ) :
: :
: :
V :
-----/
-- CALCULATION OF UNSATURATED -- no :
-- CONDUCTIVITY WANTED -- -->----- :
-- YES OR NO ? -- :
: :
: yes :
V V
-----/
( READ INPUT DATA OF SOIL ) :
( MOISTURE RETENTION CURVE ) :
: :
: :
V V
-----/
( CALL SUBROUTINE POLYD ) :
( AND PRINT THE pF-THETA ) :
( VALUES AND THE POLYNOMIAL ) :
( COEFFICIENT ) :
: :
: :
V V
-----/
( CALL SUBROUTINE CONDOC ) :
( AND PRINT THE K-THETA ) :
( VALUES ) :
-----/

```



```

      :
      V
/-----/
/ DO YOU WANT TO PLOT YES OR NO ? /
/ WARNING: FOR OTHER USERS THAN OF ACADEMIC/
/ CENTRE UTRECHT: IF YOU DON'T HAVE THE /
/ KOMPLOT SUBROUTINE AT YOUR DISPOSAL, DO /
/ YOU HAVE INSERTED A VALID SUBSTITUTE ? /
/-----/
      yes :                               no :
      :                               :
      V                               V
-----
--- PLOT OF X-THETA PAIRS AND --- no :
--- OPTIMIZED X-THETA CURVE --- --> :
--- WANTED YES OR NO ? --- :
-----
      :                               :
      : yes                           no : : no
      V                               : :
-----
( CALL SUBROUTINE )                   :
( PLOTF1 )                               :
-----
      : :                               :
      V V                               V
-----
--- PLOT OF D-THETA CURVE --- no :
--- WANTED YES OR NO ? --- --> :
-----
      :                               :
      : yes                           no : : no
      V                               : :
-----
( CALL SUBROUTINE )                   :
( PLOTF2 )                               :
-----
      : :                               :
      V V                               V
-----
--- PLOT OF K-THETA CURVE --- no :
--- WANTED YES OR NO ? --- --> :
-----
      :                               :
      : yes                           :
      V                               :
-----
( CALL SUBROUTINE )                   :
( PLOTF3 )                               :
-----
      :                               :
      :                               :
      :                               :

```

```

      :
      V
-----
PLOT OF pF- CURVE      --- no
WANTED YES OR NO ?   --->-----
-----
      :
      : yes
      V
-----
( CALL SUBROUTINE )
(   PLOTPF         )
-----
      :
      V
-----
      :
      V
-----
      :
      V
-----
/ END HOTAIR PROGRAM /
-----

```

B. 3. Input data

Input data are in free format: numbers on the same line should be separated by at least one space.

Before starting the program a (local) file must be created with the data arranged as follows.

Option 1.

First line: number of slices;

Subsequent lines: four numbers per slice and per line consisting of:

- mass of moist soil * (XA, grams);
- mass of dry soil * (XB, grams);
- mass of stones (XC, grams);
- volume of stones (XD, cm³).

(In sequence, starting with the data on the slice at the evaporating surface.)

Option 2.

First line: number of pairs of x and theta values;

Subsequent lines: two numbers per line, consisting of x (in cm) and theta respectively. (In sequence, starting with the data on the slice at the evaporating surface, up to a maximum of 100 pairs.)

If the soil moisture retention curve is available, these data must also be accessible on another (local) file as follows:

First line: number of pF-curve values: measured and additional data;

Subsequent lines: two numbers per line, consisting of the moisture suction head (h, in cm) and the corresponding moisture content (theta).

(In sequence, starting with the smallest suction head.)

B. 4. Interactive part of the program

After the program has been started the following questions have to be answered:

1. Name of output file.
2. Title.
3. Computation of x-theta pairs wanted? Type y (yes) if computation is wanted, type n (no) if it not wanted.
If yes: then 3.a. length (XL) of the cylinder (cm)
 3.b. diameter (XDD) of the cylinder (cm).
4. Drying time (XF, in minutes).
5. Theta-zero (YA); the value of 0.02 often seems to be useful.
6. Threshold value of x (X-EPS, in cm) for computing the initial value of theta (theta-i). For silty soils a threshold value of 2.5 cm has proved to be useful; for sandy soils a slightly higher value may be better.
7. Computation of curve-fitting parameters b and n; type in y (yes) if b and n have to be calculated, or n (no) if b and n are already known.

* i.e. soil matrix and stones

- a. If yes, the next question is: default values of b and n? If you type y (yes) then b starts with 0.01 and n with 1.1. If you want to choose the starting values, type n (no) and input the initial values of b (0.01:24) and n (1.1:24). Then give the discriminating value of the sum of least squares:
 - If 0 (zero) is typed in, then the program itself determines the sum of the least squares.
 - If a value unequal to zero is typed in, then the optimizing of b and n ends as soon as the sum of least squares has become smaller than the given value or as b or n has reached the upper bound, fixed in E04 JAF subroutine.
 N.B. In the last case the heading of b and n in the print out consists not of "optimized values" but of "ifail = 5" which is, in fact, an error reference from the E04 JAF procedure.
- b. If no, then put in the values of b and n.
8. Computation of diffusivity (D-theta); type in y (wanted) or n (not wanted).
9. Computation of (unsaturated) conductivity (k-theta); type in y (wanted) or n (not wanted);
If yes, then type in degree of polynomial. Usually a degree of 3 up to 5 fits reasonably, if sufficient auxiliary points have been added to the measured ones.
10. Stepsize of theta (XSTAP). The relationships of D and k with theta are presented in tables for consecutive values of theta; XSTAP enables the interval between the subsequent values of moisture content to be chosen.

Questions 11 up to 14 examine whether output has to be plotted.

11. Plot x-theta curve? y = wanted, n = not wanted.
12. Plot D-theta curve? y = wanted, n = not wanted.
If yes, then fixed lower and upper bound of moisture content? y/n (also valid for plot of k-theta).
If yes, then put in lower and upper bound values.
Fixed bounds of diffusivity? y/n
If yes, then - put in lower bound value
 - put in upper bound value.
13. Plot k-theta curve? y = wanted, n = not wanted.
If yes, then fixed bounds of conductivity? y/n
If yes, then - put in lower bound value
 - put in upper bound value.
14. Plot pF-curve polynomial? y = wanted, n = not wanted.
If yes, then put in the polynomial degree.
15. If question 3 has been answered with yes then type the name of the file with slice data.
If question 3 has been answered with no then type the name of the file with x-theta data.
16. If question 9 has been answered with yes then type the name of the file with pF-curve data (h, theta).

B. 5. Running the program
 (only for users of ACCU-CYBER computer !)

Put ready (local) files	ATTACH, data, ID = xxx.
Put ready HOTAIR program	ATTACH, HOTAIR, ID=FG.
Start of HOTAIR	HOTAIR.
Output on the screen	REWIND, result. COPYBF, result.
Plotting output	CHARON, PEN, FID=plotid.
Printing output	REWIND, result. BATCH, result, PRINT, user.

N. B. Words in CAPITALS have to be copied, words or symbols typed in lower case must be replaced by your own names and symbols. If your run into difficulties, please contact Mr. P.J. Haringhuizen (telephone 030 - 531237, room no. 402).

B. 6. Test run

```

HH  HH  00000  TTTTTTT  AAA      IIIIII  RRRRR
HH  HH  000 000  TTTTTTT  AAAAA  IIIIII  RRRRR
HH  HH  000  000  TT      AAA AAA  II     RR  RR
HHHHHHH 000  000  TT      AAA AAA  II     RR  RR
HHHHHHH 000  000  TT  AAAAAAAAAA  II     RRRRR
HH  HH  000  000  TT  AAA   AAA  III     RR  RR
HH  HH  000 000  TT  AAA   AAA  IIIIII  RR  RR
HH  HH  00000  TT  AAA   AAA  IIIIII  RR  RR

```

OPTIMIZING THE D-THETA RELATIONSHIP FROM HOT AIR DATA.

VERSION 2.0

AUGUST 1986.

PROGRAMMING BY

TEUNIS LOUTERS*

JAN A. VAN DEN BERG*

PETER J. HARINCHUIZEN**

* DEPARTMENT OF PHYSICAL GEOGRAPHY

**FACULTY AUTOMATION SERVICE

GEOGRAPHICAL INSTITUTE, STATE UNIVERSITY OF UTRECHT
P.O.BOX 80,115 3508 TC UTRECHT NL

REFERENCE: BERG, J.A.VAN DEN AND T.LOUTERS:
AN ALGORITHM FOR COMPUTING THE RELATIONSHIP BETWEEN DIFFUSIVITY
AND SOIL MOISTURE CONTENT FROM THE HOT AIR METHOD.
J. HYDROLOGY 83 (1986): 149-159.

INPUT PARAMETERS:

```

-----
SUBJECT NAME:                TEST
CYLINDER LENGTH (CM):       10.00
CYLINDER DIAMETER (CM):     5.10
DRYING TIME:                 12.00
THETA-ZERO:                  .02
THRESHOLD (CM):             2.00
STEPsize THETA :            .01
VALUE 'B':                   .0000
VALUE 'N':                   .0000
SUM OF LEAST SQUARES :      .00000
DESIRED POLYNOMIAL DEGREE : 3
COMPUTATION OF X-THETA :    Y
COMPUTATION OF D-THETA :    Y
COMPUTATION OF K-THETA :    Y
PLOT X-THETA CURVE :        Y
PLOT D-THETA CURVE :        Y
PLOT K-THETA CURVE :        Y
PLOT PF-CURVE POLYNOMIAL:   N
LOWER BOUND MOISTURE :      .00
UPPER BOUND MOISTURE :      .00
LOWER BOUND DIFFUSIVITY :   .0000E+00
UPPER BOUND DIFFUSIVITY :   .0000E+00
LOWER BOUND CONDUCTIVITY :  .0000E+00
UPPER BOUND CONDUCTIVITY :  .0000E+00

```

MEASURED DATA PER SLICE:

 XA : MASS OF WET SOIL
 XB : MASS OF DRY SOIL
 XC : MASS OF STONES
 XD : VOLUME OF STONES

SLICE	XA	XB	XC	XD
1	4.341	4.104	.000	.000
2	5.196	4.705	.000	.000
3	6.844	6.020	.000	.000
4	8.186	7.058	.000	.000
5	8.127	6.918	.000	.000
6	8.482	7.222	.000	.000
7	10.316	8.668	.000	.000
8	8.831	7.410	.000	.000
9	13.812	11.507	.000	.000
10	18.937	15.706	.000	.000
11	21.729	18.042	.000	.000
12	29.189	24.198	.000	.000
13	63.350	52.305	.000	.000
14	65.097	53.734	.000	.000
15	55.333	45.655	.000	.000
16	70.175	57.761	.000	.000

CALCULATED SOIL PHYSICAL DATA:

DENSITY OF SOIL MATRIX: 1.62037
 DENSITY OF STONES: .00000

NUMBER OF PF-PAIRS: 19

H	LOG(H)	THETA
1.0000	.0000	.3920
3.1620	.5000	.3910
10.0000	1.0000	.3890
31.6200	1.5000	.3810
100.0000	2.0000	.3640
199.5300	2.3000	.3510
251.1900	2.4000	.3450
316.2300	2.5000	.3380
501.1900	2.7000	.3150
398.1100	2.6000	.3320
630.9600	2.8000	.3130
794.3300	2.9000	.3030
1000.0000	3.0000	.2950
1584.8900	3.2000	.2750
2511.8900	3.4000	.2580
3981.0700	3.6000	.2270
6309.5700	3.8000	.1870
10000.0000	4.0000	.1730
15848.9300	4.2000	.1470

COMPUTED POLYNOMIAL-COEFFICIENTS:

A0: 13.6647
 A1: -119.7861
 A2: 480.5158
 A3: -663.0815

X-THETA PAIRS:

X	THETA
.06199152	.09357413
.19505276	.16909730
.35705546	.22179183
.55460057	.25896571
.76571011	.28317868
.97929689	.28270135
1.21931767	.30807263
1.46217822	.31073537
1.74792229	.32458140
2.15897865	.33333904
2.66874715	.33113362
3.30678856	.33421267
4.46237761	.34216638
6.06411229	.34265625
7.56539773	.34348841
9.12751161	.34825058
THETA-I:	.33932099

OPTIMISED VALUES:

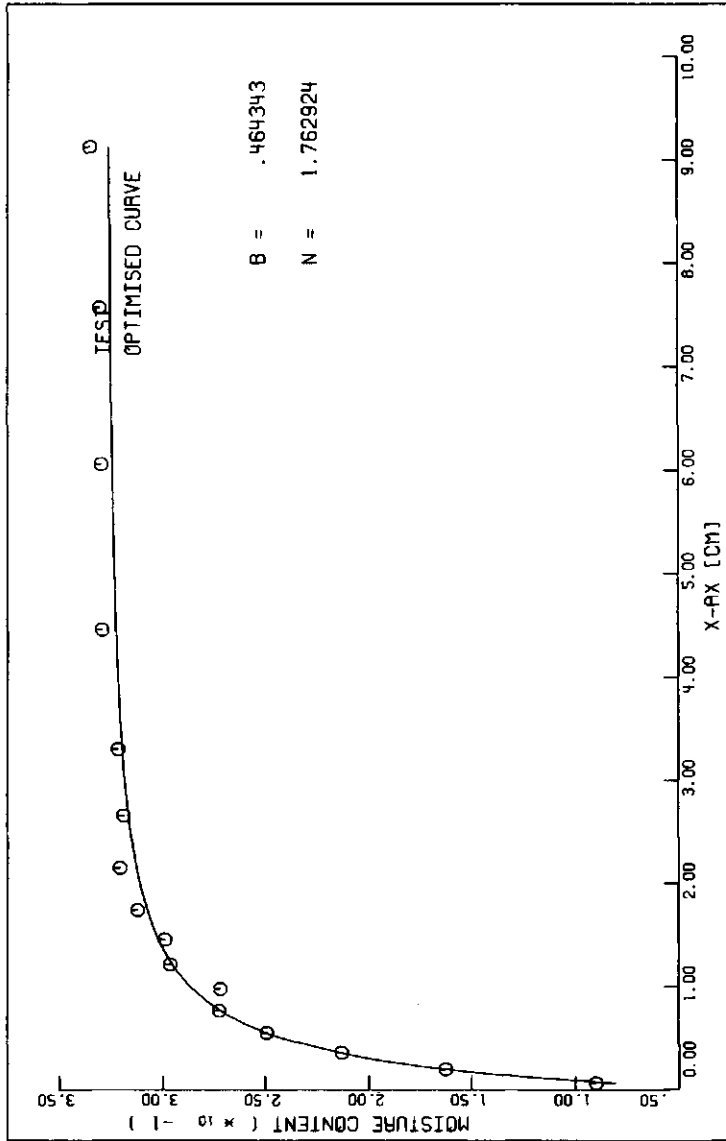
B: .476571
 N: 1.814949
 FSUMQ: .000670

DIFFUSIVITY (M2/DAY):

THETA	D
.01	.00087811
.02	.00092132
.03	.00096771
.04	.00101762
.05	.00107142
.06	.00112959
.07	.00119263
.08	.00126114
.09	.00133585
.10	.00141756
.11	.00150727
.12	.00160614
.13	.00171558
.14	.00183728
.15	.00197331
.16	.00212623
.17	.00229923
.18	.00249632
.19	.00272267
.20	.00298495
.21	.00329204
.22	.00365589
.23	.00409305
.24	.00462699
.25	.00529219
.26	.00614131
.27	.00725871
.28	.00878826
.29	.01099595
.30	.01443135
.31	.02043214
.32	.03326427
.33	.07687235

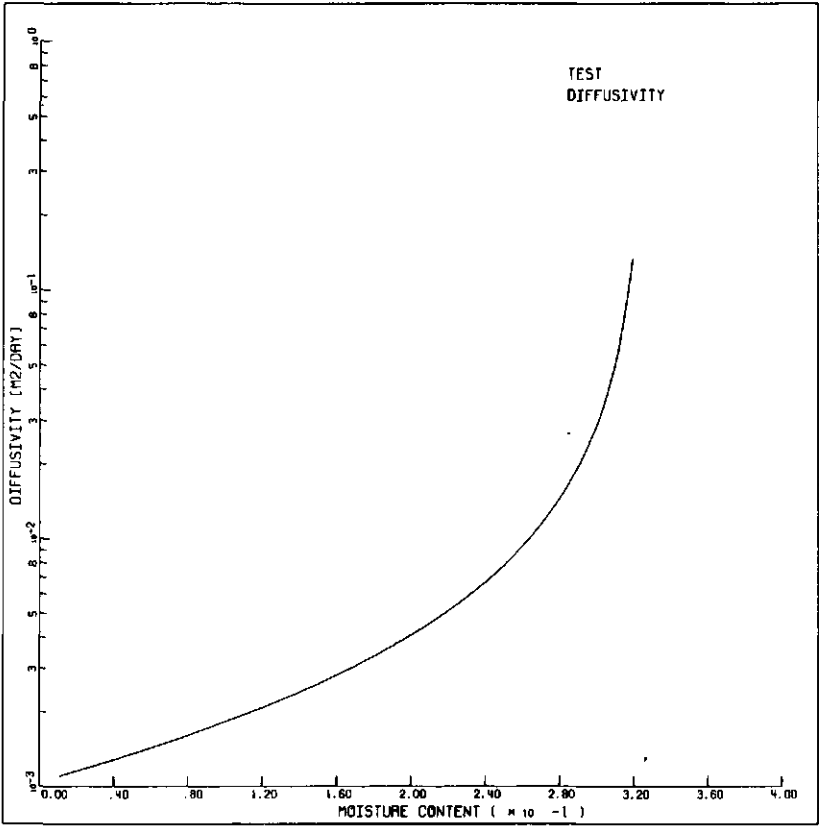
CONDUCTIVITY (M/DAY):

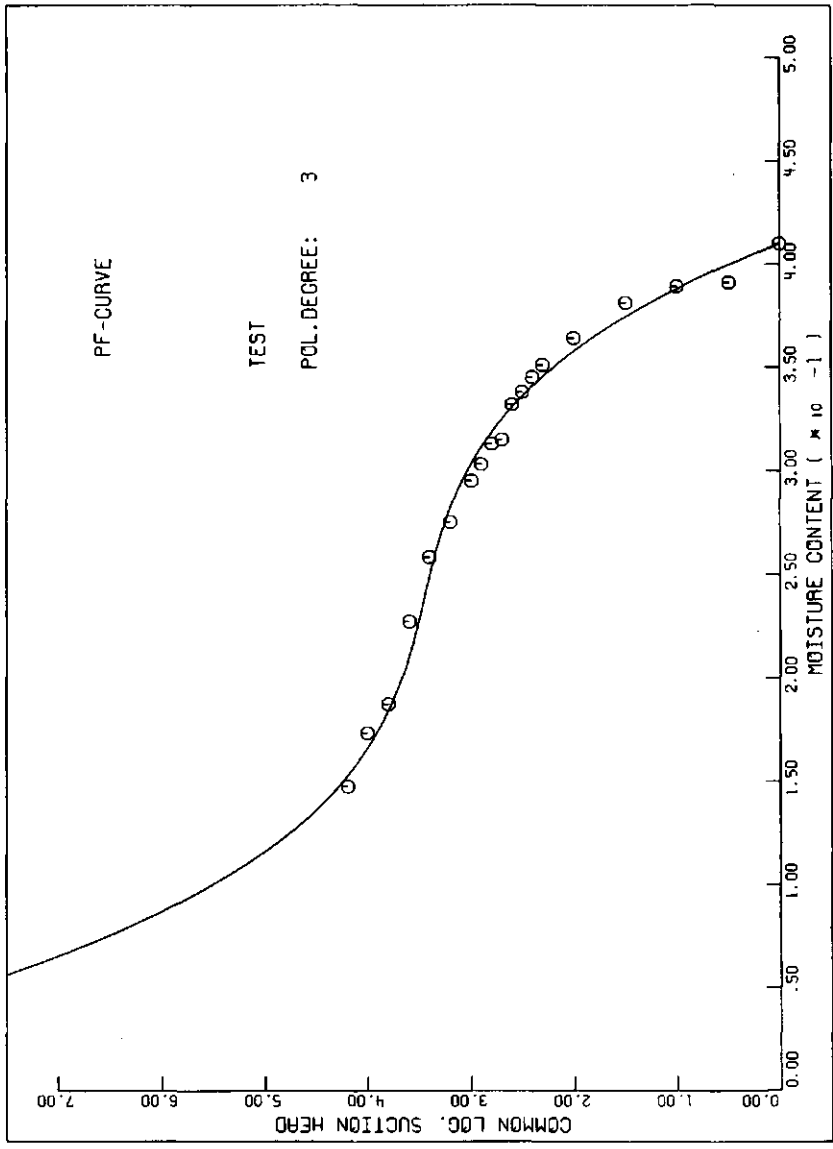
THETA	K
.01	.1057E-15
.02	.1382E-14
.03	.1481E-13
.04	.1314E-12
.05	.9751E-12
.06	.6107E-11
.07	.3260E-10
.08	.1498E-09
.09	.5984E-09
.10	.2098E-08
.11	.6526E-08
.12	.1818E-07
.13	.4585E-07
.14	.1058E-06
.15	.2254E-06
.16	.4489E-06
.17	.8435E-06
.18	.1510E-05
.19	.2597E-05
.20	.4315E-05
.21	.6921E-05
.22	.1062E-04
.23	.1529E-04
.24	.2020E-04
.25	.2429E-04
.26	.2720E-04
.27	.2963E-04
.28	.3292E-04
.29	.3885E-04
.30	.5051E-04
.31	.7556E-04
.32	.1402E-03
.33	.4020E-03



3/86 10:01:17 FC=SF

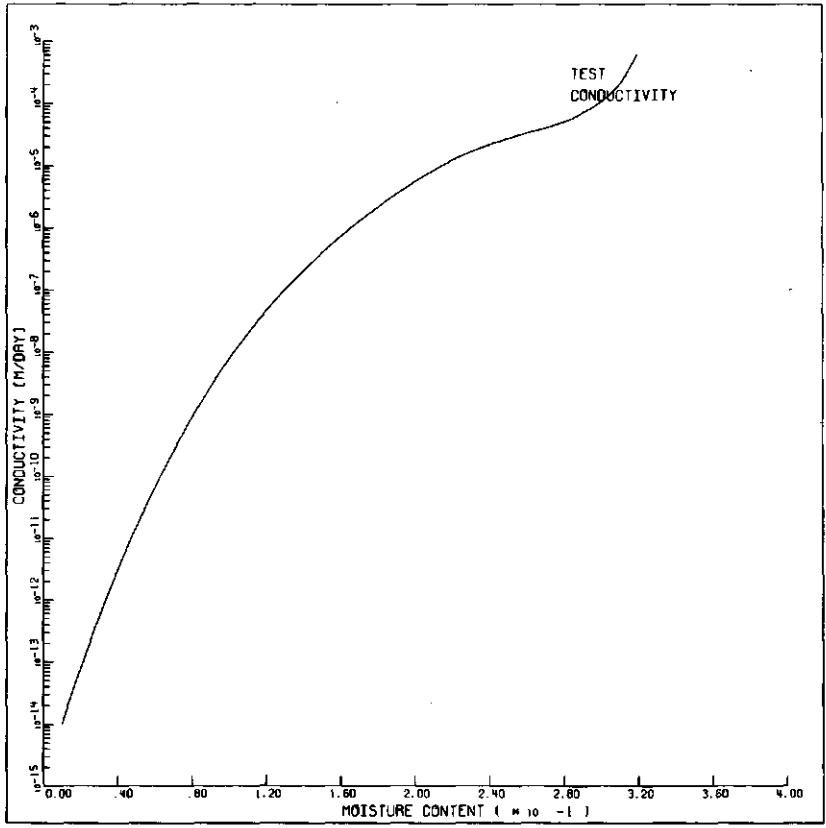
IZ 0 03/09/86 09:58:43 FC=SF





/09/86 10:00:23 FC=SF

JZ 1 03/09/86 09:59:26 FC=SF



B. 7. Program listing

```

PROGRAM HOTAIR (PLFILE=0, TAPE98=PLFILE, OUTPUT, TAPE5=OUTPUT)
REAL YA, YB, XL, XF, XDD, LOWMOIS, LOWDIF, LOWCON, INIB, ININ
REAL XSTAP, XA(100), XB(100), XC(100), XD(100), W(100), ZA(100)
REAL X(2), BL(2), BU(2), IW(4), FSUMQ, C(20), XPA(100), XPB(100)
INTEGER IFAIL, LIW, LW
CHARACTER*10 SLICEF, PFCURF, OUTF, XTHETAF
CHARACTER SUBJECT*31, STRING*30
CHARACTER*1 IPAR0, IPAR1, IPAR2, IPAR3, ITEKO, ITEK1, ITEK2, ITEK3, IPARTI
CHARACTER*1 IBOMO, IBOCON, IBODIF, ANS
LOGICAL STEP
COMMON/STAP/STEP(100)
COMMON M, YA, YB, T(100), Y(100)
COMMON/NAME/SUBJECT
COMMON/TEK/ITEKO, ITEK1, ITEK2, ITEK3
COMMON/IBOUNDS/IBOMO, IBOCON, IBODIF
COMMON/VBOUNDS/LOWMOIS, UPMOIS, LOWCON, UPCON, LOWDIF, UPDIF
COMMON/DIST/ DISTMIN, BU, SUM2
COMMON/POL/ IORD
C *****
C XL=CYLINDER LENGTH (CM)
C XDD=CYLINDER DIAMETER (CM)
C XF=DRYING TIME (MIN)
C YA=THETA-ZERO
C XEPS=THRESHOLD VALUE OF X FOR COMPUTING INITIAL VALUE OF THETA (CM)
C X(1)=X1=OPTIMISED VALUE OF B
C X(2)=X2=OPTIMISED VALUE OF N
C IPAR0=OPTIMISATION OF 'B' AND 'N'
C IPAR1=COMPUTATION PAIRS OF X-THETA (MOISTURE CONTENT)
C IPAR2=COMPUTATION PAIRS OF D-THETA (DIFFUSIVITY)
C IPAR3=COMPUTATION PAIRS OF K-THETA (CONDUCTIVITY)
C XSTAP=STEPSIZE OF THETA
C ITEK1= PLOT X-THETA CURVE
C ITEK2= PLOT D-THETA CURVE
C ITEK3= PLOT K-THETA CURVE
C M = NUMBER OF SLICES
C XA = MASS OF WET SOIL
C XB = MASS OF DRY SOIL
C XC = MASS OF STONES
C XD = VOLUME OF STONES
C IORD= DESIRED DEGREE OF THE POLYNOMIAL
C NTEL= NUMBER OF PF-PAIRS
C XPA = SUCTION HEAD OF PF-CURVE (CM)
C XPB = THETA-VALUE OF PF-CURVE (MOISTURE CONTENT CM3/CM3)
C *****
5 FORMAT (A1)
ITEKO=' N'
ITEK1=' N'
ITEK2=' N'
ITEK3=' N'
XL=0
YB=0

```

```

INIB=0.01
ININ=1.1
EPS=0
XDD=0
SUM2=0
IORD=0
DISTMIN=0
LOWMOIS=0
UPMOIS=0
LOWDIF=0
UPDIF=0
LOWCON=0
UPCON=0
  CALL HEADER (5)
  PRINT *, 'ENTER NAME OF THE OUTPUTFILE: '
  READ (*, '(A10)') OUTF
  OPEN (UNIT=7, FILE=OUTF)
  REWIND 7
  CALL HEADER (7)
  PRINT *, 'HOTAIR PARAMETER INPUT'
  PRINT *, '-----'
  PRINT *, 'SUBJECT NAME: '
  READ (*, '(A20)') STRING
  WRITE (SUBJECT, '(A20,A1)') STRING, ';'
  PRINT *, 'COMPUTATION OF X-THETA PAIRS (Y/N) ?'
  READ (*, 5) IPARI
  IF (IPARI.EQ.'Y') THEN
    PRINT *, 'CYLINDER LENGTH: '
    READ *, XL
    PRINT *, 'CYLINDER DIAMETER: '
    READ *, XDD
  ENDIF
  PRINT *, 'DRYING TIME: '
  READ *, XF
  PRINT *, 'THETA-ZERO: '
  READ *, YA
  PRINT *, 'COMPUTATION OF THETA-I (Y/N) ?'
  READ (*, 5) IPARTI
  IF (IPARTI.NE.'Y') THEN
    PRINT *, 'VALUE OF THETA-I: '
    READ *, YB
  ELSE
    PRINT *, 'THRESHOLD: '
    READ *, EPS
  ENDIF
  PRINT *, 'COMPUTATION OF ''B'' AND ''N'' (Y/N) ?'
  READ (*, 5) IPARO
  IF (IPARO.EQ.'Y') THEN
    X1=0
    X2=0
    PRINT *, 'DEFAULT INITIAL VALUES (Y/N) ?'
    READ (*, 5) ANS
    IF (ANS.NE.'Y') THEN

```

```

        PRINT *, ' INITIAL B-VALUE [0. 01: 24] : '
        READ *, INIB
        PRINT *, ' INITIAL N-VALUE [1. 1: 24] : '
        READ *, ININ
    ENDIF
    PRINT *, ' SUM OF LEAST SQUARES: '
    READ *, DISTMIN
ELSE
    PRINT *, ' FIXED B-VALUE [0. 01: 24] : '
    READ *, X1
    PRINT *, ' FIXED N-VALUE [1. 1: 24] : '
    READ *, X2
ENDIF
PRINT *, ' COMPUTATION OF DIFFUSIVITY (Y/N) ? '
READ (*, 5) IPAR2
PRINT *, ' COMPUTATION OF CONDUCTIVITY (Y/N) ? '
READ (*, 5) IPAR3
PRINT *, ' STEPSIZE OF THETA: '
READ *, XSTAP
IF (IPAR3.EQ.' Y '.AND. IPAR2.NE.' Y ') THEN
    IPAR2=' Y '
    PRINT *, ' WARNING: DIFFUSIVITY HAS TO BE COMPUTED ! '
ENDIF
PRINT *, ' PLOT X-THETA CURVE (Y/N) ? '
READ (*, 5) ITEK1
IF (IPAR2.EQ.' Y ') THEN
    PRINT *, ' PLOT D-THETA CURVE (Y/N) ? '
    READ (*, 5) ITEK2
    IF (ITEK2.EQ.' Y ') THEN
        PRINT *, ' FIXED BOUNDS MOISTURE CONTENT (Y/N) ? '
        READ (*, 5) IBOMO
        IF (IBOMO.EQ.' Y ') THEN
            PRINT *, ' LOWER BOUND VALUE: '
            READ *, LOWMOIS
            PRINT *, ' UPPER BOUND VALUE: '
            READ *, UPMOIS
        ENDIF
        PRINT *, ' FIXED BOUNDS DIFFUSIVITY (Y/N) ? '
        READ (*, 5) IBODIF
        IF (IBODIF.EQ.' Y ') THEN
            PRINT *, ' LOWER BOUND VALUE: '
            READ *, LOWDIF
            PRINT *, ' UPPER BOUND VALUE: '
            READ *, UPDIF
        ENDIF
    ENDIF
ENDIF
ENDIF
10 IF (IPAR3.EQ.' Y ') THEN
    PRINT *, ' DESIRED DEGREE OF POLYNOMIAL: '
    READ *, IORD
    IF (IORD.GT. 19) THEN
        PRINT *, ' WARNING: MAXIMUM DEGREE SHOULD BE LESS THAN 20 '
        GOTO 10
    
```



```

ENDIF
PRINT *, ' PLOT K-THETA CURVE (Y/N) ?'
READ (*, 5) ITEK3
IF (ITEK3.EQ.'Y') THEN
  PRINT *, ' FIXED BOUNDS CONDUCTIVITY (Y/N) ?'
  READ (*, 5) IBODIF
  IF (IBODIF.EQ.'Y') THEN
    PRINT *, ' LOWER BOUND VALUE:'
    READ *, LOWCON
    PRINT *, ' UPPER BOUND VALUE:'
    READ *, UPCON
  ENDIF
  PRINT *, ' PLOT PF-CURVE POLYNOMIAL (Y/N) ?'
  READ (*, 5) ITEKO
ENDIF

```

```

ENDIF
WRITE(7, ' (" OINPUT PARAMETERS: ")' )
WRITE(7, ' (" -----" )' )
WRITE(7, ' (" OSUBJECT NAME:                ", A20)' ) STRING
WRITE(7, ' (" CYLINDER LENGTH (CM):         ", F10. 2)' ) XL
WRITE(7, ' (" CYLINDER DIAMETER (CM):         ", F10. 2)' ) XDD
WRITE(7, ' (" DRYING TIME:                       ", F10. 2)' ) XF
WRITE(7, ' (" THETA-ZERO:                          ", F10. 2)' ) YA
WRITE(7, ' (" THETA-I:                             ", F10. 2)' ) YB
WRITE(7, ' (" THRESHOLD (CM):                      ", F10. 2)' ) EPS
WRITE(7, ' (" STEPSIZE THETA :                     ", F10. 2)' ) XSTAP
WRITE(7, ' (" (FIXED) B-VALUE:                     ", F10. 4)' ) X1
WRITE(7, ' (" (FIXED) N-VALUE:                     ", F10. 4)' ) X2
WRITE(7, ' (" INITIAL B-VALUE:                     ", F10. 4)' ) INIB
WRITE(7, ' (" INITIAL N-VALUE:                     ", F10. 4)' ) ININ
WRITE(7, ' (" SUM OF LEAST SQUARES :                 ", F10. 5)' ) DISTMIN
WRITE(7, ' (" DESIRED POLYNOMIAL DEGREE :          ", I10)' ) IORD
WRITE(7, ' (" COMPUTATION OF X-THETA :              ", A10)' ) IPAR1
WRITE(7, ' (" COMPUTATION OF D-THETA :              ", A10)' ) IPAR2
WRITE(7, ' (" COMPUTATION OF K-THETA :              ", A10)' ) IPAR3
WRITE(7, ' (" PLOT X-THETA CURVE :                  ", A10)' ) ITEK1
WRITE(7, ' (" PLOT D-THETA CURVE :                  ", A10)' ) ITEK2
WRITE(7, ' (" PLOT K-THETA CURVE :                  ", A10)' ) ITEK3
WRITE(7, ' (" PLOT PF-CURVE POLYNOMIAL:            ", A10)' ) ITEKO
WRITE(7, ' (" LOWER BOUND MOISTURE :                 ", F10. 2)' ) LOWMOIS
WRITE(7, ' (" UPPER BOUND MOISTURE :                 ", F10. 2)' ) UPMOIS
WRITE(7, ' (" LOWER BOUND DIFFUSIVITY :             ", E10. 4)' ) LOWDIF
WRITE(7, ' (" UPPER BOUND DIFFUSIVITY :             ", E10. 4)' ) UPDIF
WRITE(7, ' (" LOWER BOUND CONDUCTIVITY :           ", E10. 4)' ) LOWCON
WRITE(7, ' (" UPPER BOUND CONDUCTIVITY :           ", E10. 4)' ) UPCON
XSUM1=0.0
XSUM2=0.0
XSUM3=0.0
XSUM4=0.0

```

```

C ----- COMPUTATION OF PI -----
PI=4.0*ATAN(1.0)

```

```

C -----
C

```

C ---- COMPUTATION OF THE TOTAL CYLINDER VOLUME ----
 XVOL=0.25*PI*XL*(XDD**2)

C -----

```

IF (IPAR1.EQ.'Y') THEN
  WRITE(7,(' OMEASURED DATA PER SLICE: '))
  WRITE(7,(' -----'//))
18  PRINT *,' NAME OF FILE WITH SLICE-DATA: '
  READ (*,' (A10)') SLICEF
  IF (SLICEF.EQ.'NONE') STOP ' NO SLICES'
  OPEN (UNIT=2, FILE=SLICEF)
  REWIND 2
  WRITE(7,(' XA :   MASS OF WET SOIL"'))
  WRITE(7,(' XB :   MASS OF DRY SOIL"'))
  WRITE(7,(' XC :   MASS OF STONES"'))
  WRITE(7,(' XD :   VOLUME OF STONES"'))
  WRITE(7,(' OSLICE      XA      XB      XC      XD'//))
  READ(2,*,END=18) M
  DO 20 I=1,M
    READ(2,*) XA(I),XB(I),XC(I),XD(I)
    XSUM1=XA(I)+XSUM1
    XSUM2=XB(I)+XSUM2
    XSUM3=XC(I)+XSUM3
    XSUM4=XD(I)+XSUM4
    WRITE(7,(' (I6,4F8.3)') I,XA(I),XB(I),XC(I),XD(I)
20  CONTINUE

```

C ----- COMPUTATION OF DENSITY -----

```

  XMATR=(XSUM2-XSUM3)/(XVOL-XSUM4)
  IF(XSUM4.EQ.0.0) XSUM4=1.0
  XGR=XSUM3/XSUM4
  WRITE (7,(' OCALCULATED SOIL PHYSICAL DATA: '))
  WRITE (7,(' ODENSITY OF SOIL MATRIX: ",F12.5)') XMATR
  WRITE (7,(' " DENSITY OF STONES: ",F17.5)') XGR
ELSE
52  PRINT *,' NAME OF FILE WITH X-THETA DATA ?'
  READ (*,' (A10)') XTHETA F
  IF (XTHETA F.EQ.'NONE') STOP ' NO X-THETA'
  OPEN (UNIT=2, FILE=XTHETA F)
  REWIND 2
  READ (2,*,END=52) M
  WRITE(7,(' IX-THETA PAIRS:  ",//,14X," X      THETA"'))
  DO 55 I=1,M
    READ (2,*) T(I), Y(I)
    WRITE (7,(' (2F15.8)') T(I), Y(I)
55  CONTINUE
ENDIF

```

```

IF (IPAR3.EQ.'Y') THEN
35  PRINT *,' NAME OF FILE WITH PF-CURVE DATA: '
  READ(*,' (A10)') PFCURF
  IF (PFCURF.EQ.'NONE') STOP ' NO PFCURVE'
  OPEN (UNIT=3, FILE=PFCURF)
  REWIND 3
  READ (3,*,END=35) NTEL
  WRITE(7,(' ONUMBER OF PF-PAIRS:  ",I5)') NTEL

```

```

WRITE(7,('0          H    10LOG(H)      THETA'))
DO 40 I=1,NTEL
  READ(3,*) XPA(I),XPB(I)
  XPA0=XPA(I)
  XPA(I)=ALOG10(XPA(I))
  WRITE(7,(3F12.4)) XPA0, XPA(I), XPB(I)
40  CONTINUE
C --- COMPUTATION OF THE DESIRED POLYNOMIAL ---
CALL POLYD(XPB,XPA,NTEL,IORD,C)
WRITE(7,('0COMPUTED POLYNOMIAL-COEFFICIENTS:  "//,
*      ("      A",I1,":",F20.4/))' ) (I-1,C(I),I=1,IORD+1)
ENDIF
IF (IPAR1.EQ.'Y') THEN
C -- COMPUTATION OF DISTANCE DELTA X TO SURFACE --
  XHULP=0.0
  XHULPP=0.0
  XHULPA=0.0
  WRITE(7,('1X-THETA PAIRS:  ",//,14X,"X      THETA'))
  DO 60 I=1,M
    XHULP=(XB(I)-XC(I))/(0.25*XMATR*PI*(XDD**2))
    IF(XGR.GE.0.0) XHULPP=XC(I)/(0.25*XGR*PI*(XDD**2))
    XHULP=XHULP+XHULPP
    T(I)=XHULPA+0.5*XHULP
    XHULPA=XHULP+XHULPA
C
C -- COMPUTATION OF MOISTURE CONTENT THETA PER SLICE --
C
    Y(I)=((XA(I)-XB(I))/(XB(I)-XC(I)))*XMATR
    WRITE(7,(2F15.8)) T(I), Y(I)
60  CONTINUE
ENDIF
IF (IPAR11.EQ.'Y') THEN
C --- COMPUTATION OF THETA-I ---
  YSUM=0
  NY=0
  DO 65 I=1,M
    IF (T(I).GE.EPS) THEN
      YSUM=YSUM+Y(I)
      NY=NY+1
    ENDIF
65  CONTINUE
  YB=YSUM/NY
  WRITE (7,('0THETA-I:",F21.8)) YB
ENDIF
C --- STEP SELECTION
DO 66 I=1,100
66  STEP(I)=.FALSE.
  K=YB*100
  L=XSTAP*100
  DO 67 I=1,K,L
67  STEP(I)=.TRUE.
  STEP(K)=.TRUE.
C

```

```

C --- OPTIMISATION OF N AND B WITH SUBROUTINE E04JAF ---
70   X(1)=X1
      X(2)=X2
      N=2
      IFAIL=0
      FSUMQ=0.00
      IF(X(1).NE.0.0.AND.X(2).NE.0.0) THEN
          CALL FUNCT1 (N, X, SUM2)
          GOTO 500
      ENDIF
      X(1)=1.0
      X(2)=1.0
      LIW=4
      LW=25
      BL(1)=INIB
      BU(1)=24.0
      BL(2)=ININ
      BU(2)=24.0
      IFAIL=1
      IBOUND=0
      CALL E04JAF(N, IBOUND, BL, BU, X, FSUMQ, IW, LIW, W, LW, IFAIL)
500  IF (IFAIL.EQ.0) THEN
      WRITE (7, ' (" OPTIMISED VALUES:  "/" )' )
    ELSE
      WRITE (7, ' (" OIFAIL = ", I5)' ) IFAIL
    ENDIF
      WRITE (7, ' (" B: ", F15.6)' ) X(1)
      WRITE (7, ' (" N: ", F15.6)' ) X(2)
      WRITE (7, ' (" FSUMQ: ", F11.6)' ) SUM2
C ----- COMPUTATION OF D-THETA
      IF(IPAR2.EQ.'Y') CALL DIFFIT(X, N, XF, W, ZA)
C ----- COMPUTATION OF K-THETA
      IF(IPAR3.EQ.'Y') CALL CONDOC(X, N, C, IORD, W, ZA, XPA, XPB, NTEL)
C ---- PLOT X-THETA ----
      IF(ITEK1.EQ.'Y') CALL PLOTF1(N, X)
      WRITE (5, ' (" 1COMPUTATION RESULTS READY ON FILE ", A10)' ) OUTF
      STOP ' END OF HOTAIR'
      END
C -----
C          SUBROUTINES
C -----
C
C
C          SUBROUTINE POLYD (XPB, XPA, NTEL, IORD, C)
      REAL XPB(100), XPA(100), C(20)
C
C ACCULIB
C
      REAL XPW(100), AA(20), BB(20), CC(20), GG(20), VV(20), DD(20)
      DO 10 I=1, NTEL
10   XPW(I)=1.0
C 70107
      POLF = POLFIW (NTEL, XPB, XPA, XPW, IORD, AA, BB, CC, GG, VV)

```

```

      SIGMA=SQRT(POLF/FLOAT(NTEL-IORD-1))
C 71301
      CALL TRFORD (IORD, AA, BB, CC, C, SIGMA, DD, GG)
      RETURN
      END

C
C *****
C
      SUBROUTINE FUNCT1(N, X, FC)
      COMMON/DIST/ DISTMIN, BU(2), SUM2
      REAL X(N)
      COMMON M, YA, YB, T(100), Y(100)
      REAL FC, F
      FC=0
      DO 20 I=1, M
          F=YB-((YB-YA)*(X(1)**X(2)))/((T(I)+X(1))**X(2))-Y(I)
          FC=FC+F*F
20      CONTINUE
      SUM2=FC
      IF (FC. LT. DISTMIN) FC=0
      RETURN
      END

C
C *****
C
      SUBROUTINE DIFFIT(X, N, XF, W, ZA)
      CHARACTER*1 ITEKO, ITEK1, ITEK2, ITEK3
      COMMON/TEK/ITEKO, ITEK1, ITEK2, ITEK3
      REAL X(N), W(100), ZA(100)
      LOGICAL STEP
      COMMON/STAP/STEP(100)
      COMMON M, YA, YB, T(100), Y(100)
      WRITE(7, ' ("1DIFFUSIVITY (M2/DAY): " //, "      THETA      D' )' )
      K=YB*100
      DO 20 J=1, K
          Z=J/100.0
          B=X(1)*(((YB-YA)/(YB-Z))**(1/X(2)))-1
          S=((B+X(1))**(X(2)+1))/(X(2)*(YB-YA)*X(1)**X(2))
          A=((YB-Z)/(YB-YA))**(X(2)-1)/X(2)
          R=X(1)*(YB-YA)*(X(2)/(X(2)-1))*A-X(1)*(YB-Z)
          W(J)=R*S*0.072/XF
          ZA(J)=Z
          IF (STEP(J)) WRITE(7, ' (F10.2, F12.8)' ) ZA(J), W(J)
20      CONTINUE
C ---- PLOT D-THETA ----
      IF (ITEK2.EQ. 'Y' ) CALL PLOTF2 (K, ZA, W)
      RETURN
      END

C
C *****
C
      SUBROUTINE PLOTFF(NTEL, XPA, XPB, K, ZA, POL)
      COMMON/POL/IORD

```

```

COMMON/NAME/SUBJECT
REAL XPA(100),XPB(100),ZA(100),POL(100)
ORD=IORD
CALL FRAME (20.0,0.0,0.0,14.0,0.0,7.0,
* ' MOISTURE CONTENT;' , ' COMMON LOG. SUCTION HEAD;' )
CALL GRAPH (NFEL,XPB,XPA,0.0,0.2,' ; ' )
CALL GRAPH (K,ZA,POL,0.0,2,0,' PF-CURVE ; ' )
CALL GRAPH (-1,14.0,10.0,0.0,113,0,SUBJECT)
CALL GRAPH (-1,14.0,9.0,ORD,114,300,' POL. DEGREE; ; ' )
RETURN
END

```

```

C
C *****
C

```

```

SUBROUTINE PLOTF1(N,X)
REAL F(100),X(N)
COMMON/NAME/SUBJECT
COMMON M,YA,YB,T(100),Y(100)
DO 10 I=1,M
  F(I)=YB-((YB-YA)*(X(1)**X(2))/((T(I)+X(1))**X(2)))
10 CONTINUE
CALL FRAME (20.0,0.0,10.,12.0,0.0,0.0,' X-AX [CM]; ' ,
* ' MOISTURE CONTENT;' , SUBJECT)
CALL GRAPH (M,T,Y,0.0,0.2,' ; ' )
CALL GRAPH (M,T,F,0.0,2,0,' OPTIMISED CURVE ; ' )
CALL GRAPH (-1,16.0,8.0,X(1),114,306,' B =;' )
CALL GRAPH (-1,16.0,7.0,X(2),114,306,' N =;' )
RETURN
END

```

```

C
C *****
C

```

```

SUBROUTINE PLOTF2(K,ZA,W)
REAL LOWMOIS,LOWDIF,LOWCON
CHARACTER*1 IBOMO,IBOCON,IBODIF
COMMON/IBOUNDS/IBOMO,IBOCON,IBODIF
COMMON/VBOUNDS/LOWMOIS,UPMOIS,LOWCON,UPCON,LOWDIF,UPDIF
REAL ZA(100),W(100)
COMMON/NAME/SUBJECT
CALL FRAME (20.0,LOWMOIS,UPMOIS,-20.0,LOWDIF,UPDIF,
*' MOISTURE CONTENT;' , ' DIFFUSIVITY [M2/DAY]; ' , SUBJECT)
CALL GRAPH(K,ZA,W,0.0,2,0,' DIFFUSIVITY;' )
RETURN
END

```

```

C
C *****
C

```

```

SUBROUTINE PLOTF3(K,ZA,XCON)
REAL LOWMOIS,LOWDIF,LOWCON
CHARACTER*1 IBOMO,IBOCON,IBODIF
COMMON/IBOUNDS/IBOMO,IBOCON,IBODIF
COMMON/VBOUNDS/LOWMOIS,UPMOIS,LOWCON,UPCON,LOWDIF,UPDIF

```

```

REAL ZA(100), XCON(100)
COMMON/NAME/SUBJECT
DO 10 I=1, K
10 CONTINUE
CALL FRAME (20. 0, LOWMOIS, UPMOIS, -20. 0, LOWCON, UPCON,
*' MOISTURE CONTENT;', ' CONDUCTIVITY [M/DAY];', ' SUBJECT')
CALL GRAPH(K, ZA, XCON, 0. 0, 2, 0, ' CONDUCTIVITY ;' )
RETURN
END

C
C
C *****
C
SUBROUTINE CONDUCT(X, N, C, IORD, W, ZA, XPA, XPB, NTEL)
CHARACTER*1 ITEKO, ITEK1, ITEK2, ITEK3
COMMON/TEK/ITEKO, ITEK1, ITEK2, ITEK3
COMMON M, YA, YB, T(100), Y(100)
LOGICAL STEP
COMMON/STAP/STEP(100)
REAL X(N), W(100), POL(100), ZA(100), XCON(100), XPA(100), XPB(100)
REAL C(20)
K=YB*100
K1=K
WRITE(7, (' 1CONDUCTIVITY (M/DAY): " //, " THETA K" )' )
IF (XPB(1). GT. YB) K1=XPB(1)*100
DO 20 J=1, K1
Z=J/100. 0
XTOT=0. 0
XTOTA=0. 0
DO 40 N=1, (IORD+1)
XTOT=C(N)*(Z**(N-1))
XTOTA=XTOTA+XTOT
40 CONTINUE
TOT=0. 0
XTOT=0. 0
DO 50 L=2, (IORD+1)
TOT=FLOAT((L-1))*C(L)*(Z**(L-2))
XTOT=XTOT+TOT
50 CONTINUE
ZA(J)=Z
IF (J. GT. YB*100) GOTO 60
E=0. 01*(10**(XTOTA))*ALOG(10. )
H=-E*(XTOT)
XCON(J)=W(J)/H
IF (STEP(J)) WRITE(7, ' (F10. 2, E14. 4)' ) ZA(J), XCON(J)
60 POL(J)=XTOTA
20 CONTINUE
C ---- PLOT K-THETA ----
IF (ITEK3. EQ. ' Y' ) CALL PLOTF3 (K, ZA, XCON)
IF (ITEKO. EQ. ' Y' ) CALL PLOTPF (NTEL, XPA, XPB, K1, ZA, POL)
RETURN
END

```

C

C *****

C

SUBROUTINE HEADER (M)

WRITE(M,' (

```

** 1 HH HH      OOOO      TTTTTTTT      AAA      IIIIII      RRRRR"/
**  HH HH      OO OOO      TTTTTTTT      AAAAA      IIIIII      RRRRR"/
**  HH HH      OO  OOO      TT      AAA AAA      II      RR RR"/
**  HHHHHH      OO  OOO      TT      AAA AAA      II      RR RR"/
**  HHHHHH      OO  OOO      TT      AAAAAAAAAA      II      RRRRR"/
**  HH HH      OO  OOO      TT      AAA      AAA      II      RR RR"/
**  HH HH      OO OOO      TT      AAA      AAA      IIIIII      RR RR"/
**  HH HH      OOOO      TT      AAA      AAA      IIIIII      RR  RR" )' )

```

WRITE (M,' (////

```

** OPTIMIZING THE D-THETA RELATIONSHIP FROM HOT AIR DATA. "//
** VERSION 2.2                                NOVEMBER 1986. "//
** PROGRAMMING BY                             TEUNIS LOUTERS**/
**                                             JAN A. VAN DEN BERG**/
**                                             PETER J. HARINGHUIZEN**/
** * DEPARTMENT OF PHYSICAL GEOGRAPHY"/
** **FACULTY AUTOMATION SERVICE"//
** GEOGRAPHICAL INSTITUTE, STATE UNIVERSITY OF UTRECHT"/
** P. O. BOX 80, 115                          3508 TC UTRECHT      NL"/
** REFERENCE: BERG, J. A. VAN DEN AND T. LOUTERS: "/
** AN ALGORITHM FOR COMPUTING THE RELATIONSHIP BETWEEN DIFFUSIVITY"
*/" AND SOIL MOISTURE CONTENT FROM THE HOT AIR METHOD. "/
** J. HYDROLOGY 83 (1986): 149-159. "//////)' )

```

RETURN

END

C

C *****

C

REAL FUNCTION POLFIW(N, X, F, W, K, A, B, C, G, V)

C*****

C ACCU (ACADEMIC COMPUTER CENTER UTRECHT)

C THIS SUBPROGRAM IS PORTABLE TO OTHER TYPES OF COMPUTER

C*****

DIMENSION X(N), F(N), W(N), A(20), B(20), C(20), G(20), V(20)

DELTA = 0.

DO 10 J=1, N, 1

DELTA = DELTA + W(J)*F(J)**2

10 CONTINUE

K3 = K + 1

DO 60 I3=1, K3, 1

I = I3 - 1

XS = 0.

FS = 0.

S1 = 0.

S0 = 0.

DO 40 J=1, N, 1

G1 = 1.

G0 = 0.

IF (I.EQ.0) GO TO 30

DO 20 I1=1, I, 1


```

        S = 0.
        IF (I1.NE.1) S = B(I1-1)*GO
        GO = (X(J)-A(I1))*G1 - S
        S = GO
        GO = G1
        G1 = S
20      CONTINUE
30      S1 = S1 + G1**2*W(J)
        FS = FS + G1*F(J)*W(J)
        IF (I.EQ.K) GO TO 40
        S0 = S0 + GO**2*W(J)
        XS = XS + G1**2*X(J)*W(J)
40      CONTINUE
        IF (I.EQ.K) GO TO 50
        A(I+1) = XS/S1
        IF (I.NE.0) B(I) = S1/S0
50      C(I+1) = FS/S1
        G(I+1) = S1
        IF (I.NE.0) V(I+1) = ABS(V(I)-C(I+1)**2*S1)
        IF (I.EQ.0) V(I+1) = ABS(DELTA-C(I+1)**2*S1)
60      CONTINUE
        POLFIW = V(K+1)
        RETURN
        END
C
C
C *****
C
SUBROUTINE TRFORD(K, A, B, C, P, SIGMA, D, G)
DIMENSION A(20), B(20), C(20), P(20), D(20), G(20), S1(20), S0(20)
IF (K.LT.20) GO TO 5
PRINT 900
RETURN
5  CONTINUE
   IF (K.NE.0) GO TO 10
   D(1) = 1.
   P(1) = C(1)
   GO TO 90
10  S0(1) = 1.
     S1(2) = 1.
     S1(1) = -A(1)
     P(1) = -C(2)*A(1) + C(1)
     P(2) = C(2)
     D(1) = A(1)**2/G(2) + 1./G(1)
     D(2) = 1./G(2)
     IF (K.LE.1) GO TO 90
     DO 20 I=2,K,1
       D(I+1) = 0.
       P(I+1) = 0.
20  CONTINUE
     K1 = K - 1
     DO 80 J=1,K1,1
       S0(J+2) = 1.

```

```

SO(J+1) = S1(J) - A(J+1)
IF (J. GT. 1) SO(J) = S1(J-1) - A(J+1)*S1(J) - B( )
IF (J. LT. 3) GO TO 40
J1 = J - 2
DO 30 I1=1, J1, 1
    I = J1 - I1 + 1
    SO(I+1) = S1(I) - A(J+1)*S1(I+1) - B(J)*SO(I+1)
30  CONTINUE
40  SO(1) = -A(J+1)*S1(1) - B(J)*SO(1)
    J1 = J + 2
    DO 70 I=1, J1, 1
        IF (I. EQ. J1) GO TO 50
        H = S1(I)
        S1(I) = SO(I)
        SO(I) = H
        GO TO 60
50  S1(I) = SO(I)
60  P(I) = P(I) + C(J+2)*S1(I)
    D(I) = D(I) + S1(I)**2/G(J+2)
70  CONTINUE
80  CONTINUE
90  K1 = K + 1
    DO 100 I=1, K1, 1
        D(I) = SIGMA*SQRT(D(I))
100 CONTINUE
    RETURN
900 FORMAT(///, " ERRORMESSAGE FROM TRFORD: ", /,
+ " DEGREE MUST BE LESS THAN 20", /)
    END

```

APPENDIX C

TEXTURAL ANALYSIS OF SAMPLES OF LOAMY TO SILTY SOILS ON MARLY BEDROCK

The loamy to silty soils on marly bedrock contain 30 to 55 percent carbonates. For a standard soil textural classification like that of the USDA triangle, carbonates have to be removed from the soil before it is analysed. Thus it is important to know how the carbonates in these soils are distributed over the different textural classes. Therefore, a skilled researcher from a Dutch soil research laboratory has determined the soil texture of four samples with carbonates and after the carbonates had been removed with hydrochloric acid. The samples were taken from site 2 (0.2-0.3 m and marl at 1.3 m), site 3 (0.6-0.7 m) and site 4 (0.2-0.4 m). The results for 3 samples are summarized in Table C.1. The loam of site 2 (0.2-0.3 m) deviated slightly from the other three samples (no carbonates < 2 μ m, and fewer carbonates in the silt fraction).

Table C.1. Distribution of carbonates over the textural classes of loamy to silty soils on marly bedrock

Soil textural class	ratio between quantity of carbonates in texture class and that in all soil < 2 mm	fraction of carbonates in each class
clay (< 2 μ m)	0.03 - 0.15	0.05 - 0.15
silt (2 - 16 μ m)	0.25 - 0.35	0.40 - 0.60
silt (16 - 53 μ m)	0.35 - 0.40	0.70 - 0.75
silt (2 - 53 μ m)	0.65 - 0.70	0.55 - 0.65
sand (53 - 2000 μ m)	0.20 - 0.30	0.85 - 0.90
all particles < 2 mm	(1.00)	0.45 - 0.50

Table C.1 shows that carbonates are found in all textural classes and that their content increases with particle size. Because the hydraulic properties investigated in this research depend on the voids between the soil particles, regardless of their chemistry, it was decided to include the carbonates in the soil texture.

This resulted in a more complicated analysis. Additional steps have to be taken in order to obtain a complete separation of the individual soil particles.

To be sure that the results obtained in relation to soil texture were not affected by spurious textural analyses, eleven soil samples from sites 1-4, 6 and 7 were also analysed in duplicate at the above-mentioned laboratory. These analyses tended to give a somewhat higher clay content and a somewhat lower silt content, but the conclusions of the research as reported in the different chapters remained fully supported.

APPENDIX D

THE IMPACT OF PONDED INFILTRATION ON THE INSTABILITY OF MACROPORES (MODELLED BY AN ELECTRICAL ANALOGUE)

This part of the Ardèche research is done in close collaboration with Dr P. Ullersma, Dept. of Physics, Utrecht University.

1. Introduction

Short-circuiting via macropores (e.g. cracks or channels of biopores such as worm holes) considerably affects the saturated conductivity of soils. For "open" soils (in which such macropores are open to the soil surface) this effect has been discussed by many authors (EDWARDS et al. 1979, BEVEN 1981, BEVEN & GERMANN 1982, BOUMA 1982, BOUMA et al. 1982, DAVIDSON 1984, 1985 and 1987; BEVEN & CLARKE 1986 and SMETTEM 1986). In "closed" soils (CHAMBERLIN 1972), in which these voids do not come to the soil surface, macropores also become conductors of soil water as soon as the pressure head in the transmission zone of the infiltration profile has become positive (e.g. as a consequence of a decreasing conductivity with soil depth). However, the contribution of macropores to saturated conductivity is variable. Measurements with ponded infiltration on columns *in situ* silt loam soils on marl showed that saturated conductivity was reduced after the first ponded infiltration, though the conductivity near saturation was not changed (cf Chapter 6). This decrease in saturated conductivity can be explained by a local collapse of the wall of a macropore.

In this appendix it will be shown that when a macropore is drained - i.e. at the end of ponded infiltration - air that has been locally encapsulated in the soil matrix may give rise to a seepage pressure which is large enough to overcome the cohesion between the soil particles of the wall of the macropore.

2. Flow processes

The stability of macropores is discussed on the basis of a long, vertical macropore within a soil column. When the infiltration ends the macropore will drain more quickly than the pores in the surrounding soil matrix. As long as the pore water has a positive pressure head, it can drain to the macropore. Air entrapped at distance L from the wall of the macropore enables the pore water in between to react quickly to a gradient of the head of the soil water.

3. Models

The behaviour in space and time of the head $h(x, t)$ of the water in the soil matrix can usually be described by a diffusion equation

$$\frac{\partial h}{\partial t} = \frac{k}{\mu} \frac{\partial^2 h}{\partial x^2} \quad (D. 1)$$

in which x is the distance from the pore wall, k the hydraulic conductivity and μ the specific storativity (μ is the ratio of the change of volumetric moisture content, Θ , to the change of head, h , that caused the change of Θ).

Because the relevant quantities for determining the conditions that cause macropore collapse via shear are the overall values for the maximum gradient of h , $\text{grad}_m(h)$, and the corresponding maximum flow of soil moisture, q_m , one is led to a simplified model that describes the behaviour of the system in time only. An RC network seems to be a fruitful electrical analogue; it is described by the following equations

$$R \cdot I(t) + Q_e(t)/C = V(t) \quad (\text{D. 2a})$$

$$I(t) = \frac{dQ_e}{dt} \quad (\text{D. 2b})$$

in which R is electrical resistance, Q_e the charge, C the capacity, $I(t)$ the current and $V(t)$ is the power source. The hydrological equivalents of R , Q_e , C and $V(t)$ are $L/(A \cdot k)$, $L \cdot A \cdot \Theta$, $L \cdot A \cdot \mu$ and $h(t)$ in which A is the area perpendicular to the x -direction and L is the distance between the wall of the macropores and encapsulated air. $I(t)$ corresponds to the product of A and the flux density of soil moisture $q(t)$. The boundary condition at $x = 0$ is determined by the drainage of the macropore; the head in the macropore is described as

$$h(0, t) = h_0 \cdot \exp(-\beta t)$$

with $t = 0$ when the infiltration stops and with $h_0 = h(0, 0)$. In this way one obtains for $q(t)$

$$q(t) = \mu L h_0 / (\mu L^2 / k - 1/\beta) \cdot [\exp(-\beta t) - \exp(-kt/\mu L^2)] \quad (\text{D. 3})$$

From this equation the maximum gradient of h ($\text{grad}_m(h)$) and the corresponding maximum flow of soil water can be calculated.

The electrical analogue gives an "overall" solution over distance L that cannot be described as a function of x ; this can be considered as a disadvantage compared with the solution with the diffusivity equation. However, the advantage of this model is that the specific solution can be derived easily and in a transparent way.

4. Parameters

The value for saturated conditions has to be taken for the conductivity k , because the soil water only drains to the macropore as long as the soil water pressure head remains positive. For the silt loam soils, k values of 0.022 and 0.22 m/day were taken. The presence of macropores that are filled with water and presence of encapsulated air affect μ ; values of μ have been varied between 10^{-3} to 0.1 m^{-1} . β has been taken as 1 s^{-1} .

5. Results

For the given ranges of k and μ and for $0.001 \leq L \leq 0.02$ m the ratio of $\text{grad}_m(h)$ to h_0 is shown in figure 1 (for $t_m > 1$ s). For the silt loam soils under consideration an "area" constrained by realistic values of k , μ and L , can be found where at prevailing values of h_0 $\text{grad}_m(h)$ is large enough to cause macropore collapse via shear.

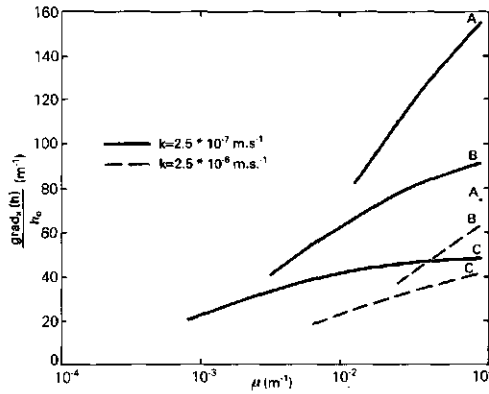


Figure 1. The ratio of $\text{grad}_m(h)$ to h_0 for various values of μ , k and L .
 A: $L = 0.005$ m; B: $L = 0.010$ m; C: $L = 0.020$ m.

References: see chapter 6.

APPENDIX E

THE INFLUENCE OF GYPSUM ON THE INFILTRATION EXPERIMENTS ON CRUSTED SOIL COLUMNS

Measurements showed that there was an excess of calcium and magnesium ions with respect to the probable content of bicarbonate in the soil water, groundwater and rainwater in study areas A and B. Except for the groundwater from site 2, the calcium ions alone exceeded the concentration of bicarbonate. The excess of the calcium ions was balanced by sulphate ions (Table E. 1).

Table E. 1. Ion concentrations in soil water, groundwater and rainwater

site origin and water table below surface level	electr. N _{tot} P _{tot} conduct.			ion concentration in meq per litre							
	μS	ppm	ppm	Ca ⁺⁺	Mg ⁺⁺	Na ⁺	K ⁺	Cl ⁻	SO ₄ ⁻⁻	Ecat	HCO ₃ ⁻
(2) mean of 5 rainfall events	24	0.5	0.05	0.11	0.03	0.02	0.00	0.00	0.12	0.13	0.01
2 spring; flow rate $8 \cdot 10^{-5} \text{ m}^3 \cdot \text{s}^{-1}$	614	0.2	0.02	7.55	0.69	0.15	0.01	0.31	1.22	8.40	6.87
2 groundwater in 130 m well; 3.5 m	648	0.6	0.06	5.10	1.79	1.73	0.04	0.34	2.05	8.66	6.27
11 flow through weathered marl	449	3.7	0.02	4.00	1.74	0.18	0.03	0.17	2.65	5.95	3.13
11 groundwater in well; 2.6 m	666	0.1	0.02	7.50	1.68	0.14	0.02	0.17	3.02	9.34	6.15

N.B. The concentration of bicarbonate ions could not be measured because of the long interval between the sampling and the chemical analysis of the water samples. Therefore, it was estimated by subtracting the chloride and sulphate ions from the sum of the cations.

Because calcium ions and sulphate ions are abundant in soils on marly bedrock a small addition of these ions from the gypsum to the soil solution is assumed not to modify soil properties.

CURRICULUM VITAE

De schrijver van dit proefschrift werd geboren op 27 juli 1937 te Leeuwarden. In 1957 behaalde hij het diploma gymnasium β aan het Gereformeerd Gymnasium te Leeuwarden. Vervolgens vervulde hij de militaire dienstplicht en was hij ondermeer werkzaam op het natuurkundig research laboratorium van de Hollandse Draad- en Kabelfabriek te Amsterdam. In 1962 liet hij zich inschrijven aan de Universiteit van Amsterdam en legde aldaar in 1966 het kandidaatsexamen in de Fysische Geografie af. Capita hydrologie en grondmechanica (in casu grondwaterstroming) gevolgd aan de Technische Hogeschool te Delft vormden met mathematische statistiek de bijvakken voor het doctoraal diploma Fysische Geografie dat in 1970 cum laude werd behaald.

Van 1970 tot 1979 was hij als hydroloog verbonden aan de Afdeling Waterhuishouding van de Wetenschappelijke Afdeling van de Rijksdienst voor de IJsselmeerpolders waar hij onderzoek deed naar de afvoerhydrologie van stedelijke gebieden en naar grondwaterwinning in Oostelijk en Zuidelijk Flevoland. Vanaf 1979 is hij als hydroloog werkzaam bij de Vakgroep Fysische Geografie van de Faculteit Ruimtelijke Wetenschappen van de Universiteit van Utrecht. Sinds 1982 is hij lid van de (tot 1986 voorlopige) Commissie voor de Milieu Effect Rapportage.